Australian National University

Genetic Basis of Natural Variation in Photoprotection in *Arabidopsis*

Author:
Tepsuda RUNGRAT

Supervisors:
Professor Barry POGSON
Professor Justin BOREVITZ
Professor Owen ATKIN
Dr Philippa WILSON

A thesis submitted for the degree of Doctor of Philosophy of The Australian National University.

Submitted February 2017

This thesis was typeset using the LaTeX typesetting system originally developed by Leslie Lamport, based on TeX created by Donald Knuth.

Declaration

This thesis is an original work. None of the work has previously been submitted by me for the purpose of obtaining a degree or diploma in any university or other tertiary institution. To the best of my knowledge this thesis does not contain material previously published by another person, except where due reference is made in the text.

.....

Tepsuda Rungrat
tepsuda.rungrat@anu.edu.au
Submitted February 2017

This thesis is dedicated to the memory of my Dad Chalee Rungrat, who encouraged me into Science. Without his continual support, I don't know if I would have enough strength to achieve this milestone.

Acknowledgements

First of all, I would like to express my sincere appreciation to my main supervisor Prof. Barry Pogson for his guidance and for giving me an opportunity to be his students, which is something I will always be thankful for. Also, I would like thank him for trusting me, someone with no background and no practical experience in plant molecular genetic and photosynthesis. I would like also to thank Prof. Justin Borevitz, one of my supervisory panel, for introducing me to the world of GWAS. A special thanks is also due to Dr. Pip Wilson for her valuable guidance, encouragement and kindly support during my PhD. Pip is an advisor on my supervisory panel who has worked closely with me for the last four years. I would also like to thank for all her helpful suggestions on my project as well as her invaluable comments on my thesis.

My special thanks also must go to all present and past members of the Pogson lab and the Borevitz lab for their support and friendship and for sharing the PhD life experiences. I am also grateful to Dr. Riyan Cheng who helped me with computational analysis for GWAS mapping.

In addition, my grateful thanks are given to the ANU Thai community for sharing the memorable moments and all activities, especially for cooking delicious Thai food. Further thanks go to my lovely partner and his family, who has always been supporting, understanding, and encouraging me to do things that I haven't done before during the past four years. My life here would not have been enjoyable without him.

Finally and most importantly, I want to thank my mum, Wassana Rungrat, my sister and my brother; their love and pray, understanding, and encouragement

have given me motivation to complete this work.

Associated Publications

Brown, T.B., Cheng, R., Sirault, X.R.R., **Rungrat, T**., Murray, K.D., Trtilek, M.,Furbank, R.T., Badger, M., Pogson, B.J. and Borevitz, J.O. (2014), TraitCapture:Genomic and environment modelling of plant phenomic data. *Current Opinion in Plant Biology* 18(1):73-79.

Rungrat, T., Awlia, M., Brown, T., Cheng, R., Sirault, X., Fajkus, J., Trtilek, M., Furbank, B., Badger, M., Tester, M., Pogson, B.j., Borevitz, J.O., and Wilson, P. (2016). Using Phenomic Analysis of Photosynthetic Function for Abiotic Stress Response Gene Discovery. *Arabidopsis book* 14: e0185.

Abstract

Light is a necessary factor for most living organism on Earth; however it can also become one of the most important abiotic environmental stresses limiting plant growth. As natural environments are extremely variable, plant has developed several mechanisms to cope with excess light energy such as adjusting leaf angle, chloroplast position, thermal dissipation, and detoxification of the reactive oxygen species resulting from stress. Among those mechanisms, thermal dissipation or Non-Photochemical Quenching (NPQ) seem to be the most rapid photoprotective response in higher plants. To investigate the natural variation of NPQ, different sets of *Arabidopsis thaliana* (*Arabidopsis*) including a genetically balanced set of natural accessions, Recombinant Inbred Intercross (RIXs), and photoprotective mutants were studied using simulated natural environments.

In natural habitats, natural genetic variation is selected on to result in adaptive allelic variation. The Genome-Wide Association Study (GWAS) has been successful in identifying natural allelic variants underlying natural variation in many traits and in different plant species such as *Arabidopsis*, rice and maize. In order to expand the current knowledge of the genetic basis of NPQ, which may also be affected by environment, two main approaches were taken in this thesis. Firstly, the natural variation in NPQ under simulated natural environments was explored. Secondly, two mapping approaches, RIXs and GWAS, were applied to reveal candidate genes/loci underlying variation in the NPQ trait.

This study investigated the physiological and molecular changes that occur in response to diurnal and seasonal growth conditions which plant experiences in the field. Two dynamic natural environments were simulated: coastal-autumn; which had moderate temperatures and light intensities, and inland-autumn; where plants were exposed to greater temperature variations and higher light intensi-

ties. Inland plants presented evidence of rapid NPQ in response to sudden higher light exposure, a decline of steady state NPQ and a decrease in chlorophyll content, indicating long-term acclimation. In contrast, coastal plants had a slower induction of NPQ followed by a slow increase in NPQ over time. This provides a better understanding on how plants have different NPQ kinetics responses under different environments; furthermore the responses are varied between accessions.

The findings presented in this thesis demonstrated that natural genetic variation in NPQ phenotype is influenced not only by genetic factor but also environmental effects. The GWAS and RIX results for the NPQ trait revealed a total of 27 QTL, of which ***RIX-QTL5-3***, ***QTL5-2***, and ***QTL5-3*** overlapped between the two different mapping approaches. One of the most significant findings from this study is the identification of ***QTL1-4***, which was found predominantly in the coastal condition. This QTL was directly over the PSII protein subunit ***PsbS*** gene, of which the loss of function mutant, non-photochemical quenching 4 (*npq4*), has been shown to lack Energy-dependent quenching (qE). The identification of this a priori gene is significant as although it a known NPQ gene it has not been identified in previous NPQ mapping studies. This suggests that the novel use of climate chambers and GWAS in this study allowed the genetic basis of variation in NPQ specific to certain environments and certain plant developmental stages to be identified.

Taken together, the findings presented here have provided meaningful insight into the naturally occurring genetic variation in *Arabidopsis* accessions during stressful condition, providing the opportunity to identify more genes that are involved in the regulation of photoprotection in response to the natural environment.

Abbreviations

ATP	Adenosine triphosphate
Arabidopsis	*Arabidopsis thaliana*
AsA	Ascorbate
AsA-GSH	Ascorbate glutathione
APX	Ascorbate peroxidase
CAT	Catalase
Chl	Chlorophyll
DHAR	Dehydroascorbate reductase
DNA	Deoxyribonucleic acid
qE	Energy-dependent quenching
GWAS	Genome-Wide Association Studies
GSH	Glutathione
GR	Glutathione reductase
GPX	Glutathione peroxidase
H_2O_2	Hydrogen peroxide
MDHAR	Monodehydroascorbate reductase
MAGIC	Multiparent Advanced Generation Inter-Cross
NPQ	Non-photochemical quenching
QTL	Quantitative trait loci

ROS	Reactive Oxygen Species
RILs	Recombinant inbred lines
RIXs	Recombinant Inbred Intercrosses
$^{1}\mathbf{O}_{2}$	Singlet oxygen
SNPs	Single-nucleotide polymorphism
SPC	SpectralPhenoClimatron
SOD	Superoxide dismutase
$\mathbf{O}_{2}^{\cdot -}$	Superoxide radical
^{3}**Car**	triplet state of the carotenoid
Vio	Violaxanthin
VDE	Violaxanthin de-epoxidase
ZE	Zeaxanthin-epoxidase
Zea	Zeaxanthin

Contents

List of Figures

List of Tables

Chapter 1

Introduction

1.1 THESIS OVERVIEW

Plants are highly sensitive and show plasticity in response to environmental changes. Light is one of the major environmental factors that modulate plant growth and development. Plants have developed a number of different light response mechanisms in order to acclimate and survive under stressful light environments where excess light can cause damage such as photodamage and photoinhibition. Photoprotection, therefore, is potentially one of the most important mechanisms that can reflect phototypic plasticity of plants under dynamic growth environments.

Natural variation in species with a wide distribution range such as *Arabidopsis thaliana* (*Arabidopsis*) is expected to reflect adaptation to their growth environments. The phenotypic difference between naturally occurring accessions is a result of allelic differences at multiple loci, resulting in a quantitative effects, and the interaction of these loci with environmental factors. Understanding both the physiological and biochemical basis of photoprotection, as well as the natural variation in photoprotection, is important for unraveling the genetic architecture underlying this mechanism. The successful use of QTL mapping to study genetic variation in bi-parental crosses (F2 and RILs) has been reported in many traits such as growth rate, yield and stress tolerance (Pérez-Pérez *et al.*, 2002; Zhang *et al.*, 2012), acclimation of photosynthetic light use efficiency (El-Lithy *et al.*, 2005; Rooijen *et al.*, 2015), for NPQ responses to high light (Jung and Niyogi, 2009) and for photosynthetic capacity in response to excess light (Athanasiou *et al.*, 2010). For studying genetic variation in natural populations, the Genome-Wide Association Study (GWAS) approach has been successful in understanding the genetic basis of many complex traits in *Arabidopsis* (Atwell *et al.*, 2010) such as flowering time and climate-sensitivity (Li *et al.*, 2010, 2014), root development (Meijón *et al.*, 2014) and shade avoidance (Filiault and Maloof, 2012). Furthermore, GWAS has been shown to have significant power in detecting candidate genes of many traits in other plant species as well, such as maize (Kump *et al.*, 2011) and rice (Huang *et al.*, 2010; Zhao *et al.*, 2011) under diverse environments.

Currently, little is known about the genetic control of photoprotection in plants, let alone the natural variation in this genetic control. Therefore, this study aims to determine the genetic basis of natural variation in photoprotection, mainly non-photochemical quenching (NPQ), using both bi-parental crosses and the GWAS

approach. To assess the genetic variation of photoprotection, high-throughput phenotyping and large genetically balanced population were used. With the aim to improve knowledge and to find candidate genes responsible for variation in this phenotype, over 280 natural accessions of *Arabidopsis* were used.

Moreover, to gain a better understanding of the effect of dynamic environment on the genetic basis of this trait, simulated natural climates were used as a powerful approach to explore the ability of plants to respond to variable environments. Several specific dynamic growth conditions were designed in order to simulate similar growing condition to a real environment. Simulated climate conditions allowed me to observe and understand plant performance under environmental stresses, especially the ability to dissipate excess energy as heat at different phases of NPQ development including induction, steady state, and relaxation phases.

In this introduction the current knowledge of light responses and photosynthesis is reviewed including the impact of photoinhibition and the importance of photoprotective mechanisms in relation to plant growth and development. The nature of photosynthetic pigments is discussed as well as chlorophyll fluorescence imaging as a tool to study photoprotection. The application of natural variation in *Arabidopsis* to GWAS studies is then outlined. Finally, the aims for this study are provided.

1.2 LIGHT RESPONSES AND PHOTOSYNTHESIS

The sunlight that reaches the Earth provides various wavelengths which release different amount of energy to the earth's surface (Figure 1.1). The visible spectrum that human eyes can detect has a wavelength range between 400 - 700 nm. However, higher plants contains several types of photosynthetic pigments which absorb light energy at different wavelength. Chlorophyll is a green pigment, which in plants has two types named chlorophyll *a* and chlorophyll *b*. Chlorophyll appears green because it absorbs mainly the blue (500 nm) and the red (600 nm) portion of the electromagnetic spectrum (Figure 1.2). Carotenoids appears orange because they absorbs in the 400 to 500 nm.

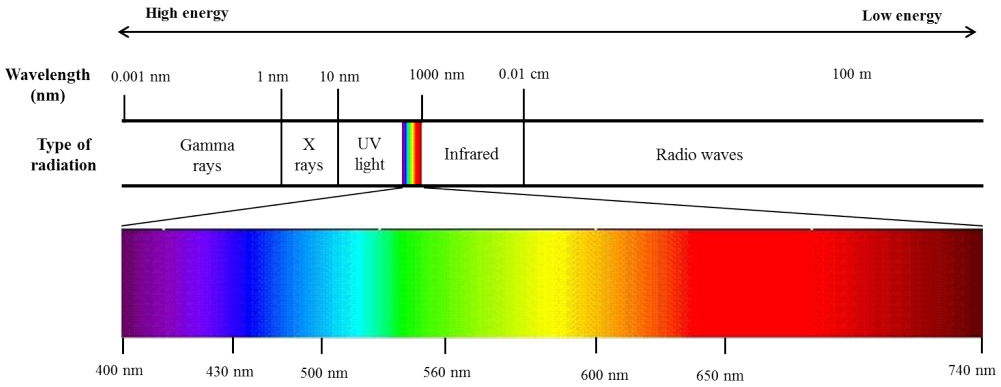

Figure 1.1 – *The electromagnetic spectrum. Human eyes are sensitive to a narrow wavelength, the visible region, which extends from about 400 nm (violet) to about 700 nm (red). (Adapted from (Karp, 2009)).*

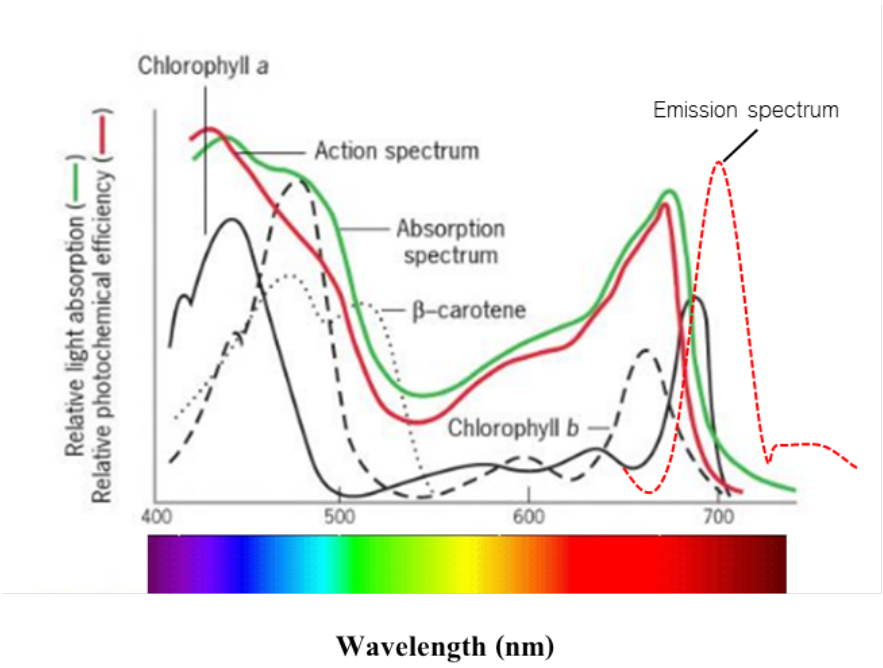

Figure 1.2 – *Absorption spectra of some photosynthetic pigments. The action spectra represented by the red-colour line. The green line indicates the absorption spectrum ranges of major photosynthetic pigments. The absorption peaks of chlorophyll a and b are between 400 nm and 600 nm indicated by the black line and black dashed line. The absorption peak of βcarotene are at 400-500 nm ranges. The chlorophyll fluorescence emission peak of PSII is between 650-700 nm (Adapted from (Karp, 2009)).*

The chlorophyll molecules are located in two pigment-protein complexes of the photosynthetic machinery, photosystem I and II (PSI and PSII), in the chloroplasts' thylakoid membranes (Figure 1.3) (Blankenship, 2002). Light energy is captured by chlorophylls and carotenoids in the Light Harvesting Complexes (LHCs) (Müller *et al.*, 2001). LHC can be divided into two groups, LHCI which are known to primarily associate with PSI, and LHCII which are known to associate with PSII (Green and Durnford, 1996; Sener *et al.*, 2005). This light energy is used to remove electrons from water releasing proton and oxygen in the thylakoid lumen. The resulting electrons then are used to reduce the small molecule plastoquinone (PQ) to plastoquinol (PQH). The excited electrons then flow to the PSI reaction center. The energized electron from PSI are used to reduce Nicotinamide adenine dinucleotide phosphate (NADP) to NADPH (a reduced form of NADP) in the chloroplast stroma. The NADPH synthesis leads to the lowering of the protons concentration in the stroma. The oxidation of water in the lumen, PQH/PQ conversions in the thylakoid, and NADPH synthesis in the stroma, causes build-up of a proton concentration gradient across the thylakoid membrane. Therefore, the movement of protons from lumen to stroma occurs to balance the pH gradient. The movement of protons across the membranes occurs via Adenosine triphosphate (ATP) synthesis channels which generate ATP from Adenosine diphosphate (ADP). The NADPH and ATP are then used as source of chemical energy in the plant (Blankenship, 2002). The amount of light harvested is affected by the size and functionality of the antenna and photosystems; and this can be adjusted to suit the environmental conditions. For example, it has been shown that low light growth condition results in an increase in PSI content and LHCII, while an increase in PSII are found in high light grown plants (Bailey *et al.*, 2001; Walters, 2005).

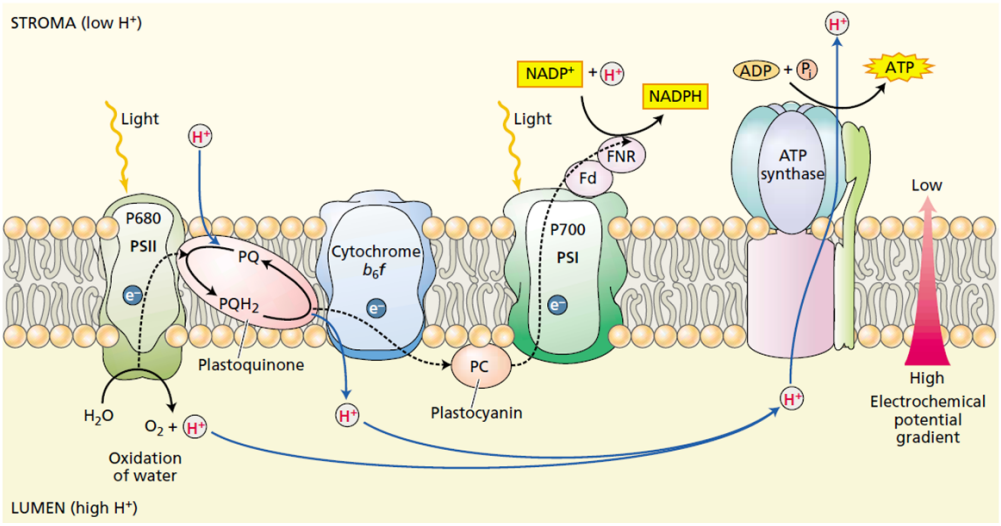

Figure 1.3 – *Schematic model of electron transportation of photosynthetic mechanism at the thylakoid membrane (Allen and Forsberg, 2001).*

1.3 PLANT FITNESSES UNDER VARIABLE ENVIRONMENTAL CONDITIONS

Responses to environmental stress such as light and temperature in plants are physiologically complex phenomena that affect almost all stages of plant growth and development. The response depends on the duration and the intensity of the stress stimulus. Short high light stress responses involve rapid change to optimize light absorption and reduce photo-damage, including enhanced thermal dissipation of light energy through non-photochemical quenching, NPQ (Niyogi, 1998; Johnson and Ruban, 2011) and detachment of the outer antenna system from the photosystem II (PSII) reaction center (Betterle *et al.*, 2009). Long term stress can result in acclimation to maximize photosynthetic capacities such as an increase in the PSI/PSII ratio and the production of RuBisCO (Alboresi *et al.*, 2011). It has also been reported that Electron Transport Rate (ETR) plays a role in photoprotection by affecting the generation of acidification of the thylakoid lumen which is important in modulating the non-photochemical quenching (NPQ) mechanism of PSII (Foyer *et al.*, 2012). The success of these responses can be indicated by the degree of photoinhibition caused by excessive light, this is directly related to the reduction of photochemical quantum yield of PSII (Fv/Fm) in dark adapted plants (Baker, 2008). In addition, other stress response parameters including pigment content such as chlorophylls, zeaxanthin and ROS accumulation which also reflect the extent of photoprotection and associated chlorophyll

fluorescence parameters.

1.4 PHOTOINHIBITION

The rate of photosynthesis is responsive to increasing light intensity. However, the photosynthetic rate has a saturated point where further increases in light intensity have no affect on the photosynthetic rate (Figure 1.4A). Under excess light, the rate of light energy harvesting is more than the rate of light energy utilized by photosynthesis. The excess excitation energy results in dramatic increase in the level of reactive oxygen species (ROS), such as $^1O_2$, superoxide radical ($O_2^{\cdot -}$) and hydrogen peroxide (H_2O_2) (Havaux and Niyogi, 1999). The production of excessive ROS can damage lipids, nucleic acids and proteins including damage to the photosystems known as photoinhibition or photooxidative stress (Turan, 2012; Graßes *et al.*, 2002). In an extreme case it can cause photobleaching of leaf tissue leading to cell death.

Photoinhibition is a term to describe a decrease in photochemical capacity or an increase in PSII damage, which occurs when excess light energy is absorbed by the PSII reaction center. The D1 protein, a core component of the PSII reaction center, is the main target of this damage (Lu, 2016). Thus, there are elegant mechanisms to replace damaged D1 (Murchie and Niyogi, 2011). Hence, the levels of photoinhibition can vary (Figure 1.4B) depending on the levels of light intensity, the rate of repair of damaged PSII and the induction of photoprotective process (Murchie and Niyogi, 2011; Lu, 2016).

1.4.1 Reactive oxygen species and plant stress

Reactive oxygen species (ROS) are produced as by-products of many metabolic pathways and can have deleterious effects on many biomolecules within the cell. ROS also act as signalling molecules and secondary messengers which affect the expression of multiple genes in many abiotic and biotic stress pathways (Ramel *et al.*, 2009; Maruta *et al.*, 2012) and function in a variety of cellular process (Sharma *et al.*, 2012). Chloroplasts, mitochondria and peroxisomes are major sources of ROS production in plant cells (Figure 1.5), because they are sites of highly oxidizing metabolic activity or an intense rate of electron flow (Mittler and Blumwald,

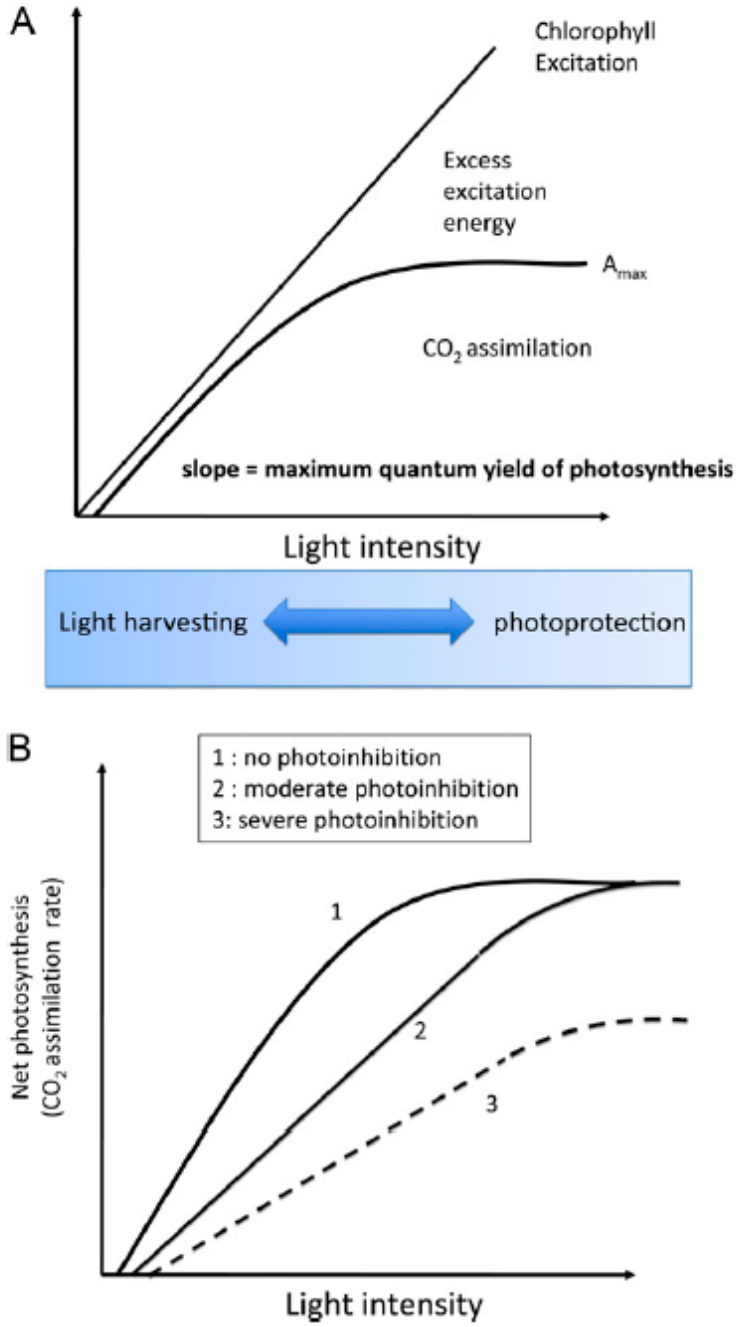

Figure 1.4 – *The principles of photoprotection. A, photosynthetic saturation. When further increases light intensity resulting in no increase in photosynthesis, excess excitation energy is produced from excess absorbed light. B, photoinhibition on the quantum yield. (Murchie and Niyogi, 2011).*

2015).

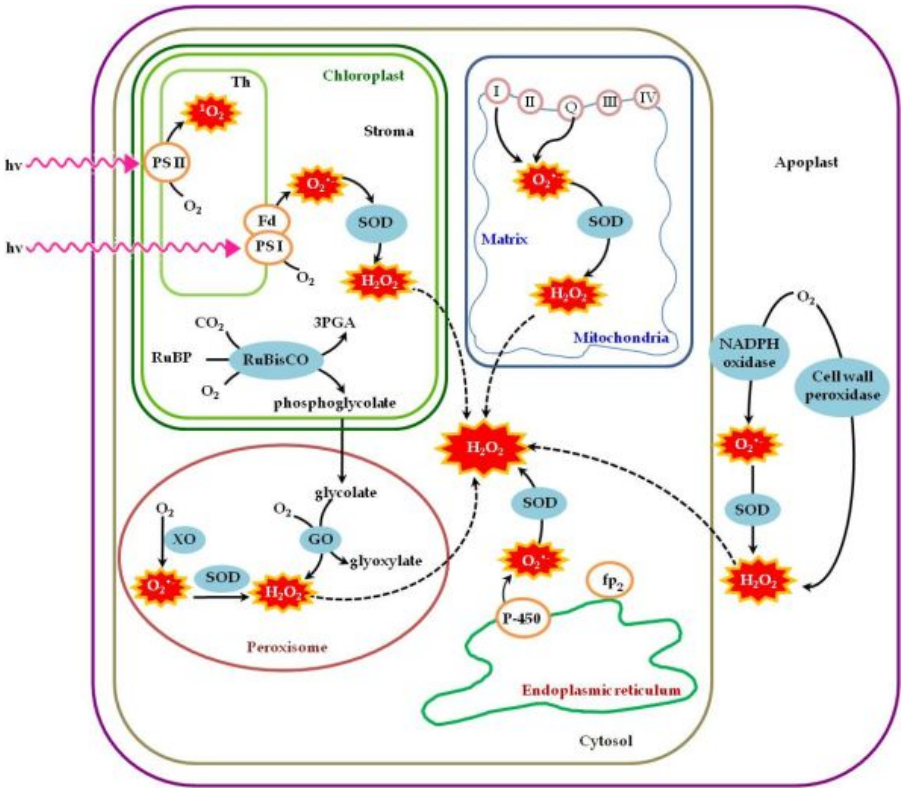

Figure 1.5 – ***Main sources of ROS production during photosynthesis (Hossain* et al., *2011).***

In the chloroplast, during photosynthesis, energy from sunlight is captured and transferred to two light harvesting complexes, PSI and PSII. Superoxide (O_2^-), which is produced mainly by electron leakage from Fe-S centers of PSI or reduced ferredoxin (Fd) to O_2 (Mehler reaction), is then converted to H_2O_2 by superoxide dismutase (SOD) (Gechev *et al.*, 2006). O_2^- can also be produced by the leaking of electrons to molecular oxygen from electron transport chains in PSI and PSII (Sgherri *et al.*, 1996). Singlet oxygen ($^1O_2$), another form of ROS, can be formed by energy transfer. Under excess light conditions PSII is able to generate $^1O_2$ by energy transfer from the triplet state chlorophyll ^{3}Chl (Asada, 2006).

In peroxisomes, ROS is produced mainly during photorespiration and also during β-oxidation of fatty acids. Under abiotic stress conditions that impair CO_2 fixation in the chloroplast, the oxygenase activity of RuBisCO increases and the glycolate that is produced moves from the chloroplast to peroxisomes, where it is oxidized by glycolate oxidase (GO) forming H_2O_2 (Takahashi and Murata, 2008). In peroxisomes, H_2O_2 can also be formed directly from O_2 by enzyme systems

such as xanthine oxidase (XO) coupled to SOD (Mhamdi *et al.*, 2010). The increasing of ROS production by numerous environmental stress can cause severe damaging to plant cells and is known as oxidative stress. Photooxidative stress associated with photosynthesis occurs when plants absorbs light energy beyond the saturating point. It can also occur under low/moderate light intensities with the limitation of CO_2 supplies (Heyneke *et al.*, 2013) or under drought stress by affecting stomatal closure and altering gas exchange (Tripathy and Oelmüller, 2012).

1.4.2 ROS scavenging and detoxification systems in plant

Scavenging or detoxification of excess ROS is undertaken by an efficient antioxidative system including non-enzymic and enzymic antioxidants (Sharma *et al.*, 2012). The enzymic antioxidants include superoxide dismutase (SOD), catalase (CAT), glutathione peroxidase (GPX), enzymes of the ascorbate glutathione (AsA-GSH) cycle such as ascorbate peroxidase (APX), monodehydroascorbate reductase (MDHAR), dehydroascorbate reductase (DHAR), and glutathione reductase (GR). Non-enzymic antioxidants include ascorbate (AsA), glutathione (GSH), carotenoids, tocopherols, and phenolics (Sharma *et al.*, 2012; Heyneke *et al.*, 2013). It has been shown that zeaxanthin and lutein play key roles in inducing ROS scavenging processes. The *npq1lut2 Arabidopsis* mutant, which lacks ROS scavenging and prevention of ROS synthesis components as zeaxanthin and lutein, shows a higher level of singlet oxygen than the wild-type (Alboresi *et al.*, 2011).

1.5 PHOTOPROTECTION

Generally, light radiation in natural environments is not constant. Photosynthetic rate can vary rapidly due to passing clouds, sun-fleck or shading as well as seasonal and diurnal changes. Plants, therefore, can easily be damaged from the variability of light radiation levels in their environment. To survive under these stress condition, they have to develop defense mechanisms to protect themselves from damage under unstable light conditions.

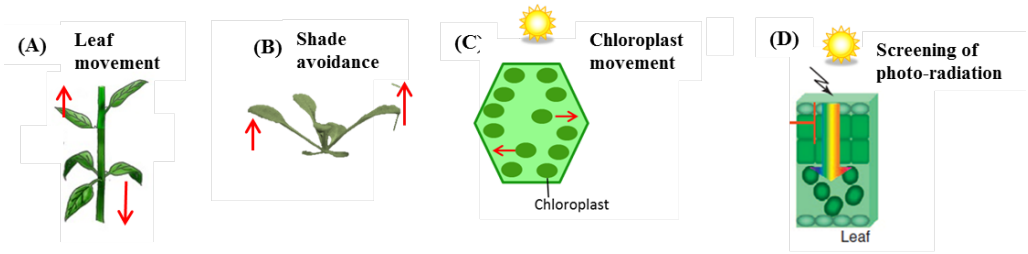

Figure 1.6 – *Examples of short-term avoidance mechanism response to high light absorption. (A) and (B) Leaf movement and shade avoidance to optimize the light energy absorbed. (C) Chloroplast movement, plants adjust their chloroplast position to minimize the light absorption. And (D) Screening of photoradiation. (Adapted from (Takahashi and Badger, 2011)).*

1.5.1 Avoidance mechanisms to light

Some plants have developed several pathways such as avoidance mechanism to avoid photo-damage (Figure 1.6) (Graßes *et al.*, 2002; Takahashi and Badger, 2011). First, some plants are able to adjust leaf angle to optimize light absorption and to avoid direct exposure to high light intensities. Second, plants can also move their chloroplast position and orientation to optimize the light intensity for photosynthesis. Under high light, chloroplasts line up close to cell wall to avoid excessive light absorption. On the other hand, for low light plants, chloroplasts seem to orientate themselves to the center of the cell in order to increase the absorption rate. Under high light environments, plants also reduce the amount of thylakoids per chloroplast section when compared to low light plants (Takahashi and Badger, 2011). Lastly, filtering of damaging radiation minimizes the photo-damage to PSII from UV and visible light. For example, the accumulation of phenolic compounds, such as anthocyanins, in the leaf epidermis can help prevent photo-damage to PSII (Takahashi and Badger, 2011).

1.5.2 The role of carotenoids in photoprotection

Carotenoids are classified into two groups, carotenes and xanthophylls. Carotenes are purely hydrocarbons, while xanthophylls contain hydroxyl groups (oxygenated carotenoids). Thylakoid membranes of higher plants contain β-carotene, xanthophylls (lutein and neoxanthin) and those participating in the xanthophyll cycle (violaxanthin, antheraxanthin, and zeaxanthin) (Young, 1993; Demmig-Adams and Adams, 1996). They absorb light in different wavelengths to that of chloro-

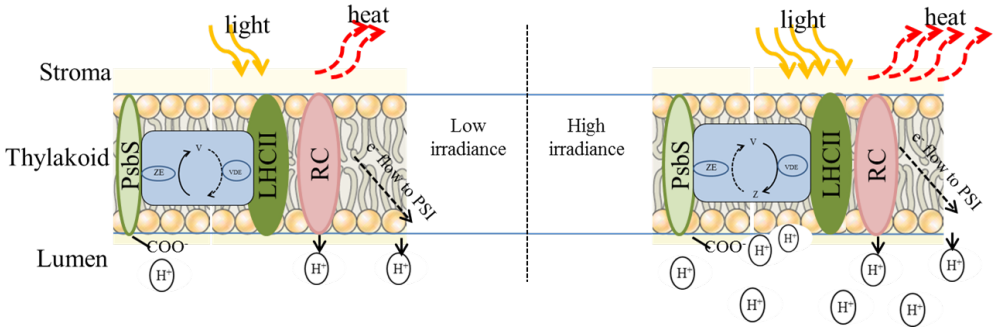

Figure 1.7 – ***Simplified model showing the mechanisms involved in NPQ under low and high irradiance. Under low irradiance, low ΔpH across thylakoid membranes, conversion of zeaxanthin to violaxanthin lead to low NPQ production. Under high irradiance, there is high ΔpH and build up of zeaxanthin which cause high NPQ. (Adapted from (García-Plazaola* et al.*, 2012).***

phylls (Figure 1.2). Carotenoids absorb in the range between 400 - 500 nm of wavelength. Carotenoids are also involved in numerous important functions in higher plants. There are at least four major roles of carotenoids in photoprotection: acting as accessory pigments in the light harvesting complex, absorbing light in the region of the electromagnetic spectrum where the chlorophyll absorption is low; triplet chlorophyll and singlet oxygen scavenging; excess energy dissipation; and structure stabilisation/assembly (Ma *et al.*, 2003). As mentioned above, photo-oxidative damage of the thylakoid membrane and its components is caused by the formation of highly reactive triplet state of the chlorophyll (^{3}Chl) and singlet oxygen ($^1O_2$) species. Carotenoids can remove $^1O_2$ through chemical reactions. It is also quench ^{3}Chl and $^1O_2$ by energy transfer to form the triplet state of the carotenoid, (^{3}Car), (Krinsky, 1971), followed by the nondestructive thermal dissipation (Mathis *et al.*, 1979).

1.5.3 Non-photochemical quenching: NPQ

Non-photochemical quenching (NPQ) is one of the most efficient photoprotective mechanisms in plants. The process of NPQ can eliminate over 75% of absorbed light energy (Niyogi, 1999; Müller *et al.*, 2001). NPQ is the mechanism by which plants dissipate excess absorbed excitation energy as heat in the light-harvesting complexes of PSII and is known as thermal energy dissipation (Figure 1.7); resulting in excitation electrons returning to the ground state. This can reduce ROS production leading to less damage to PSII.

The NPQ mechanism is composed of three components: energy-dependent quenching, qE, state-transition quenching, qT and photoinhibition quenching, qI (Figure 1.8) (Maxwell and Johnson, 2000; Jung and Niyogi, 2009; Eberhard *et al.*, 2008; García-Plazaola *et al.*, 2012). The qE, energy-dependent quenching, is rapidly increased within seconds to minutes (Jung and Niyogi, 2009). The qT is the balancing excitation energy mechanism of PSI and PSII. The last component, qI is caused by photoinhibition.

The contributions of these three components can be very challenging to quantify because the characteristic of their induction and relaxation kinetic can vary as a result of change in environmental conditions. Typically, under non-stressed and most light conditions, the main contributing component is qE (Baker, 2008), (Maxwell and Johnson, 2000; Ihnken *et al.*, 2011), however it also rapidly responds to fluctuations in light intensities (Zaks *et al.*, 2012). A state transition (qT), on the contrary, contributes only small part in NPQ and it is more likely to function under low light (Maxwell and Johnson, 2000), because it can only quench PSII fluorescence. The qI component generally responds over a longer time scale of relaxation. It is more affected by excess light when PSII is damaged or photoinhibition has occurred.

The combinations of stresses such as temperature and high light can be critical for photoprotective mechanisms. Under excess light, low temperature can increase the level of photo-damage by inactivating the enzyme zeaxanthin epoxidase (ZE) in the xanthophyll cycle resulting in retention of zeaxanthin and sustained energy dissipation (García-Plazaola *et al.*, 2012). At the same time, violaxanthin deepoxidas (VDC) is activated by low lumen pH under stress conditions leading to high level of zeaxanthin resulting in enhancing the rate of energy dissipation (García-Plazaola *et al.*, 2012; Johnson and Ruban, 2011). At low temperatures, the levels of excess energy are accelerated, thus photoprotection is required by inactivating the enzymatic carbon reactions including photorespiration, a process that is to complement NPQ for excess energy dissipation (Hendrickson *et al.*, 2004). As the xanthophyll cycle is involved in NPQ and impairing ROS scavenging system, this results in the unsustainability of NPQ in low temperature environments (García-Plazaola *et al.*, 2012).

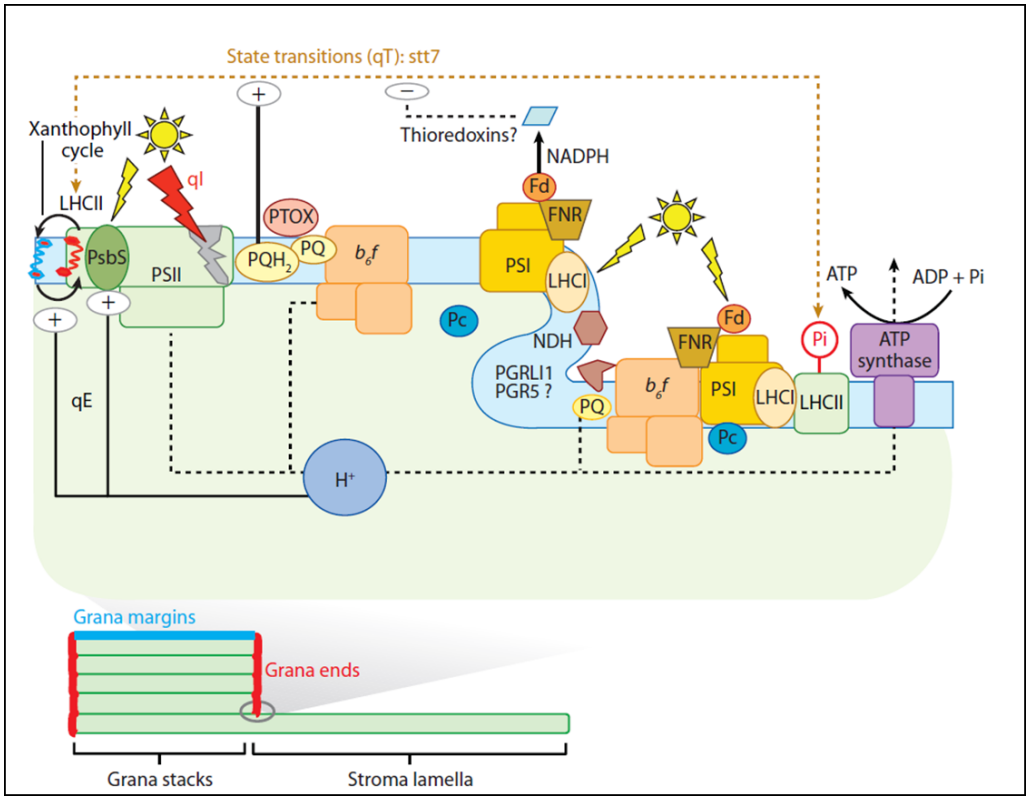

Figure 1.8 – *The formation of NPQ component in outer antenna of PSII within LHCII (qE) is modulated by the xanthophyll cycle and the PSII minor subunit PsbS (PSII-S). Both processes are triggered by acidification of lumenal pH, which activates violaxanthin de-epoxydase, and triggers protonation of two conserved glutamic residues on PsbS. A regulatory kinase (STT7), activated by reduction of intersystem electron carriers, produces reversible protein phosphorylation that induces changes in association of a fraction of antenna proteins between PSII and PSI in a process known as State Transitions (qT). The kinase may be downregulated by reduced thioredoxins. This double control system provides an efficient feedback signaling, which matches light absorption capacity of each photosystem to the redox state of the electron transfer chain. Photoinhibition (qI) is observed upon overexcitation of the photosystems with respect to the capacity for photo-induced electron transfer. Fd, ferredoxin; FNR, Fd: $NADP^+$ oxido-reductase; Pc, plastocyanin; PQ, plastoquinone; PTOX, plastoquinone terminal oxidase; NDH, NADPH plastoquinone reductase (Eberhard* **et al.**, *2008).*

Energy-dependent quenching: qE

NPQ is defined to be the fastest mechanism to dissipate excess light energy as heat and harmless to the plant itself. Energy-dependent quenching, qE, it is considered to be the most important component of NPQ. The recent literature shows that there are three components that regulate qE: the pH gradient, xanthophyll cycle, and the PsbS protein of PSII (Niyogi, 1998; Li *et al.*, 2000; Jung and Niyogi, 2009; Lambrev *et al.*, 2010).

ΔpH is necessary for qE. Plants convert light energy to chemical energy by the photosynthesis in the chloroplast. ΔpH can be produced during the process of linear electron flow (LEF) which involves the oxidation of hydroxyl (HO) by PSII, processing of transferred electrons to NADP through the cytochrome bf and PSI complexes, and the occurrence of cyclic electron flow (CEF). These generate ΔpH across the thylakoid lumen membrane. ΔpH act as a feedback signaling indicating the degree of saturation of photosynthetic electron transport, and the accumulation of ΔpH impacts the rapidly reversibility of qE in the dark (Johnson and Ruban, 2011). It can turn on and off within seconds depending on variabilities of light conditions (García-Plazaola *et al.*, 2012).

The acidification of the thylakoid lumen also contributes to a zeaxanthin-dependent conformational change in the thylakoid membrane (Müller *et al.*, 2001). Furthermore, research which investigated the *Arabidopsis npq2* mutant lacking xanthophyll cycle indicates that NPQ onset in *npq2* essentially reflects the formation of the ΔpH during the first illumination and that the reduced lag seen during the second illumination is due to zeaxanthin retention between the two illumination events (Joliot and Finazzi, 2010).

In addition, an *Arabidopsis CEF* mutant named *pgr5* (proton gradient regulation 5) shows lower NPQ levels compared to the wild-type. The *PGR5* gene encodes a novel thylakoid membrane protein involved in CEF around PSI which affects the formation of ΔpH (Munekage *et al.*, 2002). Therefore, the *pgr5* mutant, which is unable to control the CEF and to produce ΔpH, has low NPQ levels. It has also been reported that *PGR5* plays a crucial rule for protection of PSI against photodamage, especially under fluctuating light (Suorsa et al., 2012). Another mutant

called *pgr1* (proton gradient regulation 1) shows lower NPQ than the wild type, and it is very sensitive to excess light. The *pgr1* mutation is in the *PetC* gene encoding the cytochrome b6f complex (Munekage *et al.*, 2001). The *pgr1* does not have any effect under low light, but it results in the reduction of electron transport rate leading to the decreasing of ΔpH under high light condition.

The evidence above shows the direct impact of the ΔpH on qE and NPQ. However, the ΔpH does not only activate qE directly, but also indirectly from the rise in ΔpH within the thylakoid lumen activating the VDE enzyme (Niyogi, 1998). This causes the accumulation of zeaxanthin leading to the build up of NPQ.

The xanthophyll cycle involved in qE. Xanthophylls are oxygenated derivatives of carotenes which play roles in light harvesting, photoprotection, and the structure of the photosynthetic antenna (Pogson *et al.*, 1998; Golan *et al.*, 2006). The xanthophyll cycle is involved in energy dissipation within light harvesting antenna proteins via NPQ. That is, the interconversion of these pigments is essential for qE component of NPQ. The cycle consists of ΔpH dependent transformation of Violaxanthin (Vio) into Zeaxanthin (Zea), through Antheraxanthin (Miyaji *et al.*, 2015). This cycle is catalyzed by two enzymes: the VDE and ZE (Figure 1.9). High zeaxanthin levels correlate with higher levels of NPQ. Under low light, the enzyme ZE converts Zea to Vio to complete the Vio cycle.

The *Arabidopsis npq1* mutant is a mutation in the gene encoding VDE (Havaux and Niyogi, 1999). The *npq1*, thus, is VDE defective and hence unable to convert violaxanthin to zeaxanthin under excess light (Niyogi, 1999). Observation of NPQ level of *npq1* shows the same increasing rate at induction stage (first 10 seconds) in both *npq1* and wild type, but after that NPQ in wild type keeps rising as opposed to *npq1* for which no further increase is observed. These results suggest that the induction of NPQ at the induction stage is independent of the xanthophyll cycle (Niyogi, 1998). However, the xanthophyll cycle is still needed for maximal NPQ production.

PsbS protein is essential for qE. *PsbS* is a member of LHC protein family, and it is recognised as critical component in NPQ (Li *et al.*, 2002; Roach and Krieger-Liszkay, 2012). DNA analysis of *npq4-1* mutant show the complete deletion of *PsbS* gene (Li *et al.*, 2000). The *npq4-1* retains the function of photosynthesis and the xanthophyll cycle; however, it lacks most of the qE component due to the absence of ***PsbS*** resulting in low NPQ levels. In addition, overexpression of ***PsbS***

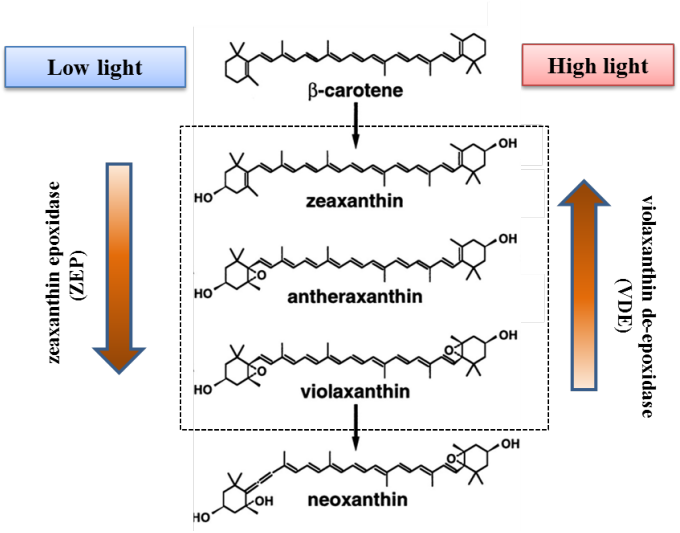

Figure 1.9 – *The xanthophyll cycle in the branch of carotenoid biosynthetic pathway in plants (Adapted from (Miyaji* **et al.***, 2015)). Under high-light conditions, violaxanthin de-epoxidase (VDE) convert violaxanthin to antheraxanthin and then zeaxanthin with release of excessive light energy by heat dissipation (NPQ). In contrast, zeaxanthin epoxidase (ZE) converts zeaxanthin to violaxanthin via antheraxanthin.*

resulted in an increase of the qE capacity compared to wild type (Li *et al.*, 2002).

The role of the *PsbS*, confirmed by the evidence above, indicates that it acts as a sensor of lumen pH that is necessary for the rapid induction and relaxation of qE (Li *et al.*, 2004). It is the site of qE which contributes to ΔpH and xanthophyll-dependent excitation quenching (Li *et al.*, 2000; Müller *et al.*, 2001; Niyogi *et al.*, 2005). Also ***PsbS*** acts as a trigger of the conformational change leading to up-regulation of NPQ (Crouchman *et al.*, 2006). Therefore, it can be proposed that ***PsbS*** is essential for NPQ mechanism instead of being purely involved in light capturing.

State-transition quenching: qT

State transition related quenching (qT) is a mechanism which balances the absorption capacity or excitation pressure of the two photosystems, PSI and PSII (Essemine *et al.*, 2012). The qT is a slow process compared to the qE component and it relaxes with a half time of around 5-10 minutes, representing around 15-20 % of the maximum quenching (Horton and Hague, 1988). The state transitions are directly triggered by changes in the redox state of the electron transfer chain.

The kinase responsible for LHCII phosphorylation is activated upon reduction of intersystem electron carriers (Figure 1.8) (Eberhard *et al.*, 2008). It has been widely noted that under a high light environment, there is dephosphorylation of the LHCII, and down-regulation the function of PSII via thermal dissipation (Tikkanen *et al.*, 2010).

It has been reported that state-transition is involved in NPQ. *Arabidopsis* STN protein kinase mutants (*stn7*) lack ***STN7*** gene; therefore it is deficient in state-transition (Tikkanen *et al.*, 2010; Bellafiore *et al.*, 2005). STN protein kinase is required for phosphorylation of the LHC of PSII (Tikkanen *et al.*, 2006; Willig *et al.*, 2011). The research results show that the state-transition quenching which is involved in phosphorylation has a small impact on the regulation of NPQ but affects plant growth under fluctuating light environment (Tikkanen *et al.*, 2010).

Photoinhibitory quenching: qI

This photoinhibitory quenching is mainly associated with the damaging of D1 protein leading to photoinhibition and a decrease in photosynthesis (Eberhard *et al.*, 2008). It is also a slower process than qE. The induction of qI is accumulated in tens of minutes after exposure to high-light condition and the relaxation of qI is relatively slow. Unfortunately, the process of qI is still unclear, but it has been confirmed to involve the long-term down-regulation of PSII (Müller *et al.*, 2001).

1.6 CHLOROPHYLL FLUORESCENCE IMAGING FOR PHOTOPROTECTIVE PARAMETERS IN PLANTS

In the photosynthetic apparatus, light energy is absorbed by chlorophyll molecules in plant leaves and transfer to PSI and PSII. Absorbed light energy can go through one of three process (Maxwell and Johnson, 2000; Baker, 2008): (1) the absorbed energy will excite electrons via PSII then it will be converted to chemical energy to drive photosynthesis known as photochemistry, which depends on the presence of QA (2) if there are more energy that can be utilized by photochemistry,

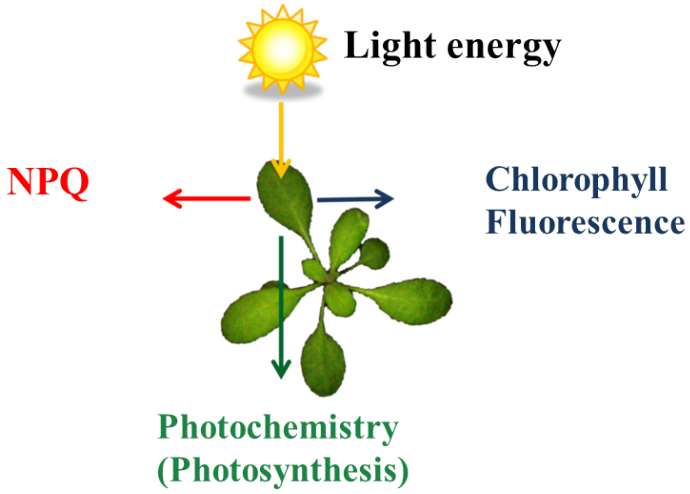

Figure 1.10 – *The simple model of light energy absorbed by PSII and used for either photochemistry, non-photochemical quenching and/or chlorophyll fluorescence.*

or photochemistry is inefficient, excess energy can be dissipated in the form of heat known as non-photochemical quenching (NPQ) (Niyogi, 1999; Takahashi and Badger, 2011) or (3) the excess energy can be re-emitted as chlorophyll fluorescence most of which is emitted by antenna chlorophyll *a* of PSII (Butler, 1978) (Figure 1.10). The process of photochemistry, NPQ and chlorophyll fluorescence occur in competition. If the rates of one process increase, it will result in a decrease in the rates of the other two. As PSII is the first target of excessive light, and it where NPQ and the emission of chlorophyll *a* fluorescence occurs (Krause, 1991; Baker, 2008). Hence, the measurement of chlorophyll fluorescence at room temperature is primary represent the photosynthetic activity of PSII.

Since the Kautsky effect was described in 1931 (reviewed in (Govindjee, 1995)), chlorophyll fluorescence measurement has become a very powerful method for monitoring the photosynthetic capacity, photodamage and the level of stress (Maxwell and Johnson, 2000). The spectrum of light absorbed and re-emitted (fluorescence) are different, therefore, the chlorophyll fluorescence yield can be quantified by illuminated a leaf of defined wavelength and then measured as the amount of light re-emitted at longer wavelength (as shown in Figure 1.2).

The traditional method for chlorophyll fluorescence measurement is usually done by Pulse-Amplitude Modulated (PAM) fluorometers (Maxwell and Johnson, 2000). In the PAM chlorophyll fluorescence technique, a dark-adapted leaf is exposed to various light treatments. The fluorescence quenching analysis was presented in

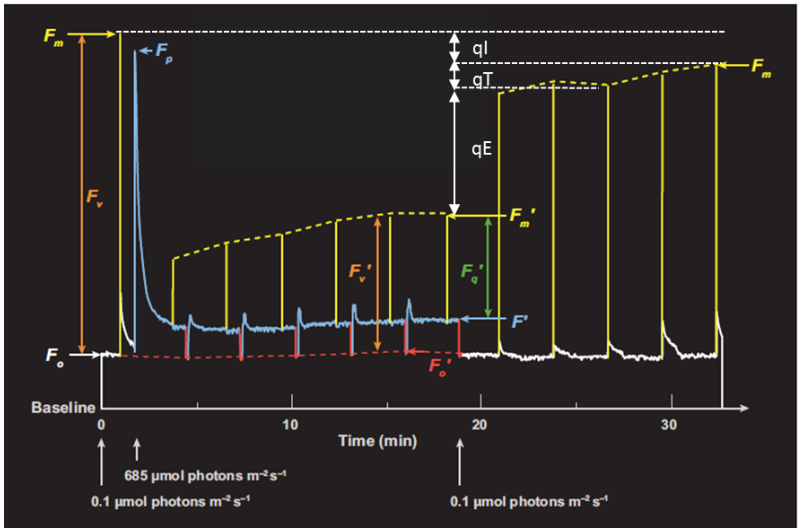

Figure 1.11 – *Chlorophyll fluorescence measurement. The parameters denoted with a prime (') are from the leaf exposed to actinic light. The parameters without a prime are obtained from the leaf in the dark-adapted state. The different colors of the trace indicated different light treatments; blue represents actinic light (∼700 μmol photons $m^{-1}s^{-2}$), yellow represent saturating pulse (≤1 s duration, >6000 μmol photons $m^{-1}s^{-2}$) and white represents weak measuring light alone. (Adapted from (Baker, 2008))*

Figure 1.11. The fluorescence parameters is presented in Table 1.1. The analysis of each parameter will be described below.

Table 1.1 – ***Chlorophyll fluorescence of PSII parameter used in this study.***

Parameter	Definition	Physiological relevance	Calulation
F, F′	Fluorescence emission from dark- or light adapted leaf, respectively	Provides information on photosynthetic performance	
Fo, Fo′	Minimal fluorescence from dark- and light-adapted leaf, respectively	Level of fluorescence when QA is maximally oxidized (PSII center is opened)	
Fm, Fm′	Maximal fluorescence from dark- and light-adapted leaf, respectively	Level of fluorescence when QA is maximally reduced (PSII center is closed)	
Fv, Fv′	Variable fluorescence from dark- and light-adapted	Demonstrates the ability of PSII to perform photochemistry (QA reduction)	
Fq′	Difference in fluorescence between Fm′and F′	Photochemical quenching of fluorescence by open PSII centers	(Fm′ - F′)
Fv/Fm or QY	Maximum quantum efficiency of PSII photochemistry	Maximum efficiency at which light absorbed by PSII is used for reduction of QA	(Fm-Fo)/Fm
Fv′/Fm′	PSII maximum efficiency	Gives an estimate of maximum efficiency of PSII photochemistry at given illumination, which is the PSII operating efficiency if all the PSII centers were open	(Fm′ - Fo′) / Fm′
qP or qL	Photochemical quenching of PSII	Provides the fraction of open PSII reaction center	qP=(Fm′-F)/(Fm/Fo) or qL= qP x (Fo′- F)
qE	Energy-dependent quenching	Associated with light-induced proton transport into the thylakoid lumen	
qI	Photoinhibition quenching	Results from photoinhibition of PSII photochemistry	
qT	Quenching associated with a state transition	Results from phosphorylation of light-harvesting complexes associated with PSII	
ETR	Electron transport rate	Provides information on the rate of linear electron transport in PSII	Fq′/Fm′ x light intensity (PAR) x 0.5 x 0.84
NPQ	Non-photochemecal quenching	Estimates the non-photochemical quenching from Fm to Fm′. Monitors the apparent rate constant of heat dissipation from PSII.	(Fm/Fm′) - 1
ΦPSII	PSII operating efficiency	Provides an estimate of the quantum yield of linear electron flux through PSII	F′q/Fm′

1.6.1 Chlorophyll fluorescence to measure photochemical process

Chlorophyll fluorescence, as measured by PAM fluorometry, can be used as a non-invasive method to gain a lot of useful information about photochemical and photo-protective mechanisms in response to different environments. First of all, the PSII operating efficiency, or quantum yield (ΦPSII) refers to the photochemical quenching parameter. This parameter measures the efficiency of PSII photochemistry, and is calculated as follows: ΦPSII = Fq′/Fm′ (Baker, 2008). It is the proportion of light absorbed by chlorophyll used to drive PSII photochemistry

(Maxwell and Johnson, 2000). Another photochemical quenching parameter is qP calculated as qP = (Fm' - F)/(Fm' - Fo'). Superficially, qP and ΦPSII are similar (both measured the efficiency of PSII photochemistry). The difference is that qP provide an indication of the proportion of the PSII reaction center that are open, while ΦPSII only gives the proportion of the energy being used in photochemistry. Therefore, from this equation, the proportion of the reaction center that are closed can be calculated as followed: 1 - qP. Moreover, the maximum efficiency of PSII in the dark-adapted can be estimated by Fv/Fm = (Fm - Fo)/Fm and the maximum efficiency of PSII in the light-adapted can be calculated from Fv'/Fm' = (Fm' - Fo)/Fm' (Maxwell and Johnson, 2000). The Fv/Fm parameter is frequently used as a sensitive indicator of plant stresses from both biotic and abiotic stresses (Baker, 2008). When plants are exposing to light stresses, the decrease in Fv/Fm can be used as a measure of inactivation of PSII. This phenomenon provides a simple and rapid way to monitor plant stresses and provide insight into the ability of a plant to tolerate such stress condition.

1.6.2 Chlorophyll fluorescence with non-photochemical process

To measure non-photochemical quenching (NPQ), plants or leaves need to be dark-adapted. The purpose of this is to measure the maximum total fluorescence, Fm, when there is no photochemistry and while the thermal dissipation is at a minimum (Maxwell and Johnson, 2000). However, it is important to note that the comparison of NPQ can be done only on similarly dark-adapted leaves subsequently exposed to actinic excess light (Baker, 2008). It can be calculated from the relative change in the maximal fluorescence (from Fm and Fm′) during the illumination as equation NPQ = (Fm - Fm')/Fm'. Normally, the values might be expected in between 0.5 - 3.5 for an actinic light >500 μmol $^{-2}$s^{-1}, however it can vary depending on plant species and growth conditions (Maxwell and Johnson, 2000).

The NPQ mechanism is the sum of three components: energy-dependent quenching, qE, state-transition quenching, qT and photoinhibition quenching, qI as mentioned in Section 1.5.3. Quantifying the contributions of these three components can be very challenging because the characteristic of their induction and relaxation kinetic can vary as a result of environmental conditions. Typically, under non-stressed and most light conditions, the main component is qE (Baker, 2008;

Maxwell and Johnson, 2000; Ihnken *et al.*, 2011), however, it also rapidly responds to fluctuations in light intensities (Zaks *et al.*, 2012). A state transition (qT), on the contrary, contributes only small part in NPQ and it is more likely to be involved by low light (Maxwell and Johnson, 2000) because it can only quench PSII fluorescence. The qI component generally responds in longer time scale during relaxation. It is more important in excess light when PSII is damaged or photoinhibition has occurred.

It has been reported that photoinhibition and photoprotection vary depending on leaf age and plant species. Photosynthetic activities vary markedly during the life span of leaves because of the differences in chloroplast development which is reflected in chlorophyll fluorescence kinetics (Sestak, 1999). The maximum quantum efficiency of PSII (Fv/Fm) is rapidly decreased in senescent leaf. The degree of thermal dissipation of excess light energy (NPQ) tends to decrease in senescent leaves (Havaux and Niyogi, 1999; Wingler *et al.*, 2004). In this study, we developed a method for measuring whole plants prior to senescence response in order to better understand as a whole plant of chlorophyll fluorescence of PSII.

1.7 NATURAL VARIATION IN *ARABIDOPSIS*

Natural variation is defined as genome-encoded differences that can cause phenotypic variation. Natural variation play a major role in plant acclimation under different environments. Many traits that are important for fitness, and are of agricultural value, are quantitative traits, controlled by the expression of many genes as well as the effects of environmental factors and even the interactions between the two. Allelic variation may cause a range of changes that result in different phenotypes. The complexity of identifying the genetic basis of natural variation and the application of quantitative trait analysis in the natural population of *Arabidopsis* will be discussed.

1.7.1 A powerful source of genetic variation in *Arabidopsis*

Arabidopsis thaliana (The Arabidopsis Genome Initiative, 2000) has been used as a model organism for plant research for several decades (Somerville and Koorn-

neef, 2002). There are many reasons that *Arabidopsis* became a powerful tool for many disciplines of plant science. First, it has a small diploid genome which has already been fully sequenced (Weigel and Mott, 2009; 1001 Genome Consortium, 2016). Second, it has a short life cycle (2-3 months in a greenhouse). Third, it is a self-fertilizing plant which gives a large amount of offspring. This model plant has been used to investigate the genetic factors involved in different traits in several growing conditions including germination, flowering time, and stress tolerance (Li *et al.*, 2010; Zhang *et al.*, 2012; Li *et al.*, 2014).

Geographic distribution reflects natural variation in many ways. *Arabidopsis* originated at the vicinity of Europe and Central Asia (Koornneef *et al.*, 2004), however it is now widespread to many areas around the world (Horton *et al.*, 2012) (Figure 1.12). In recent years, more than 2,000 genotypically distinct accessions have been identified (Weigel, 2012). The greatest diversity was found at the western end of the native range, in the Iberian Peninsula and North Africa, whereas the most uniform regions are in Central Asia (Koornneef *et al.*, 2004). Therefore the oldest population is considered to be located in the west and the later distribution is in the east. In addition, it has been reported that climate conditions play an important role in limiting the distribution of this plant species. Under such limitation, however, it still can be found in a wide latitudinal range from 68 N (North Scandinavia) to 0 (mountains of Tanzania and Kenya) and from the sea level up to 4,250 m above sea level (Koornneef *et al.*, 2004; Al-Shehbaz and O'Kane, 2002).

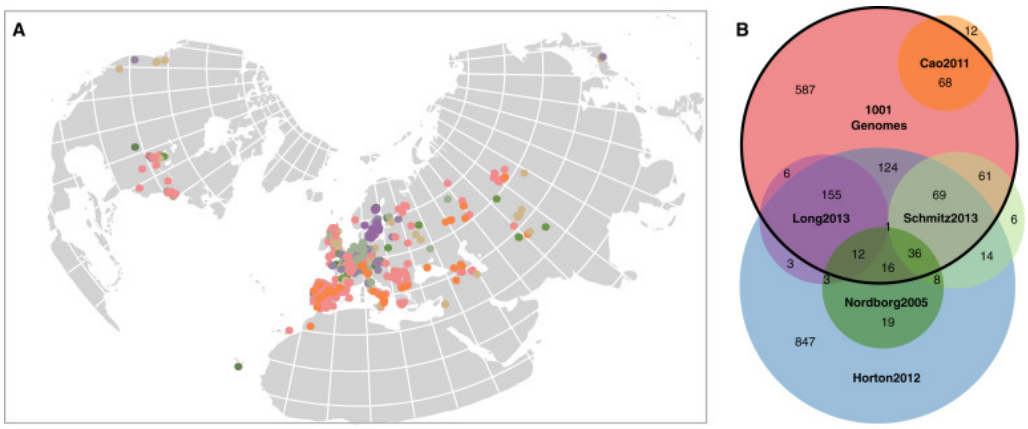

Figure 1.12 – ***Geographic distributions of Arabidopsis of the 1001 genomes accessions. A, represents the location of origin of the 1001 genomes accessions (colours correspond to Van diagram in B). B, represent the relationships between 1001 genomes accessions and other Arabidopsis diversity sets (1001 Genome Consortium, 2016).***

Arabidopsis accessions have adapted and responded to changes in their habitats, such as variable of light intensities and temperatures. This adaptation commonly reflects their ability to engage photoprotection mechanisms in order to survive and reproduce throughout the growing season. There has been research showing the relationships between the latitude of origin on NPQ capacity in several accessions compared to wild-type (Col-0), but there is little correlation between latitude and NPQ among European accessions analysed (Jung and Niyogi, 2009).

1.7.2 Strategies of natural genetic variation analysis in *Arabidopsis*

One of the aims of studying natural variation is to identify the function of individual genes and how the allelic variation in a particular loci are adaptive under specific environmental conditions.

To use natural variation to discover the genetic basis of a complex trait there must be significant variation in that trait in natural populations. Significant variation in NPQ capacity has been described in many plant species. For instance, in 22 British plant species, the maximum NPQ values ranges from 2.5 to 4.5 (Johnson *et al.*, 1993). While, the maximum NPQ values ranges from 2.4 to 3.2 in a subset of 62 *Arabidopsis* accessions (Jung and Niyogi, 2009). Moreover, sun-acclimated plants show four times higher NPQ capacity than in low-light acclimated plants compared within the same species (Jung and Niyogi, 2009).

Quantitative trait locus (QTL) mapping

The genetic variation in a given trait is often presented as a continuous distribution of trait values, and therefore it is called quantitative variation. Quantitative trait loci (QTL) are defined as genomic locations associated with a specific trait, and in which allelic variation could explain a significant variation observed in this trait. Using QTL mapping as a tool to study natural variation, the purpose of quantitative trait mapping is to uncover the genetic basis of quantitative phenotypic variation. QTL mapping is not only important for understanding the genetic basis of quantitative phenotypic variation, it is also useful for plant

breeders to apply the QTL for crop genetic improvement using genetic markers for the favourable QTL. The power and resolution of QTL mapping depend on how many recombination events can be observed, how many molecular marker can be used, and also the genotypic diversity of the parents.

There are several advantages in using QTL mapping to study natural variation. The QTLs mapping can detect the result of multiple genes which may have small effects, and it can detect the interaction between genes and environments, as well as the interaction between genes (epistasis) (Keurentjes *et al.*, 2007; Borevitz *et al.*, 2002). To locate genes associated with particular phenotypic traits, quantitative trait locus (QTL) analysis is still the most popular method.

QTL using a bi-parental cross requires three steps (Weigel, 2012; Trontin *et al.*, 2011; Koornneef *et al.*, 2004). First, creation of a segregating population by crossing between two distinct parent accessions. The segregation of phenotypic variation in F2 or later generation reflects the segregation of genetic alleles which are contributed by both parents. Generally, any segregating population can be used for QTL mapping. However, there are advantages in using particular populations, especially Recombinant Inbred Lines (RILs), where recombinant chromosomes have been fixed through inbreeding. RILs need to be genotyped only once but can be phenotyped repeatedly under different environments for numerous traits (Weigel, 2012). Moreover, RILs population can be reproduced by selfing. Another alternative resource used for genetic mapping is Recombinant Inbred Intercrosses (RIXs). The RIXs population can extend the power of RILs to provide sensitive detection of QTL responsible for complex traits (Zou *et al.*, 2005). RIXs are generated by producing F1 hybrids from crossing between all or a subset of RILs. By dramatically extending the number of unique, reproducible genomes, RIXs share some of the best properties of both the parental RILs and F2 mapping panels. Compared to RILs, the advantages of RIXs include twice the number of recombination sites in a single individual since each is derived from two parental RILs (Zou *et al.*, 2005), and almost fourfold more recombination sites than a single F2 (Williams *et al.*, 2001). The second step in bi-parental mapping is to genotype the population with markers throughout the whole genome and phenotype the phenotypic traits of interest. And finally, the association analysis between phenotypic values of the traits and genotypic classes of the polymorphic markers is conducted to estimate the number and genome position of the segregating QTL.

Bi-parental crossing has been widely used for studying the genetic variation of light responses in *Arabidopsis*. Jung and colleagues measured the amount of NPQ in 62 *Arabidopsis* natural accessions and found that the variation of NPQ is an effect of multiple nuclear factors. The quantitative genetic analysis were performed to identify candidate genes for thermal dissipation using an F2 population (crossed between Sf-2 and Col-0). In addition, two genes (*HQE1* and *HQE2*) have been discovered for NPQ using QTL mapping (Jung and Niyogi, 2009). 105 RILs from crosses between L*er* and Cvi-0 were used to investigate the regulation of light sensitivity on hypocotyl growth; three QTL were identified including *VLE6* QTL which is responsible for enhanced cotyledon unfolding under Far Red light (Botto *et al.*, 2003). Moreover, Wolyn and colleagues used RILs derived from Col-o and Kashmir to measure seedling response to different light conditions. Five from eight QTL identified were localized near photoreceptor loci, two QTL were associated with *CRY1* and *CRY2*, another two QTL were near *PHYB* and *PHYC* and one QTL was localized near *PHYA* (Wolyn *et al.*, 2004). The discovery of the phytochrome genes in the studies of light response has been reported using bi-parental crosses between Cvi and L*er* (Borevitz *et al.*, 2002).

QTL mapping using multiple crosses. One disadvantage of bi-parental population is that they give a very limited sample of genetic variation. Multi-parental crosses design have increased the probability of QTL being polymorphic across the multiple parents (Cavanagh *et al.*, 2008). Thus, this could be an alternative method for studying genetic variation. There are two main types of multi-parent populations. (1) single multi-parent populations created from intercrossing many parents, followed by a few rounds of intercrossing of offspring and then inbred to generate a stable panel of inbred lines; (2) populations consisting of a connected set of crosses or families (Huang *et al.*, 2010). The advantage of using this multi-parent population is easy to test for epistasis in the form of QTL by background interaction which refers to the differences between the crosses that represent a subpopulation (Huang *et al.*, 2010). The wheat Multiparent Advanced Generation Inter-Cross (MAGIC) (Cavanagh *et al.*, 2008; Kover *et al.*, 2009) and *Arabidopsis* multiparent RIL (AMRIL) (Rlasen *et al.*, 2012) population are examples of single multi-parent population. These populations combine high resolution with an increase in allelic and phenotypic diversity over the traditional RILs, potentially increasing the number of the detected QTL that segregates in the cross compared to an F2 and RILs (Kover *et al.*, 2009; Weigel, 2012).

1.8 Genome-Wide Association Studies: GWAS

Although bi-parental and multi parental populations mapping are one of the successful tools used to study natural variation, there are however limitations. For instance, there are still restrictions in allelic diversity (the variation driven by parental accessions) and limited genomic resolution. The use of GWAS has overcome those limitations and become an alternative method to study naturally occurring genetic variation (Brachi *et al.*, 2011; 1001 Genome Consortium, 2016). This alternative approach aims to exploit natural accession collected from a wide geographic distribution. *Arabidopsis* has been found in many different geographic locations and this large distribution then provides a range of natural accessions that can be used to observe the response of different genetic backgrounds to their relevant dynamic growth environments.

There are a number of studies using GWAS in *Arabidopsis*. One of the most well known GWAS study is flowering time. Li and colleagues identified a total of 19 QTL from GWAS analysis, five QTL were found to control flowering time and 5 QTL associated with climate-sensitivity (Li *et al.*, 2010, 2014). Meijón and colleagues conducted research on root development in 201 different accessions of *Arabidopsis* from different geographic origins. They found a candidate gene named KUK, which regulates meristem and cell length (Meijón *et al.*, 2014). Several new candidate genes controlling photosynthetic light use efficiency traits were identified by Rooijen and colleagues (Rooijen *et al.*, 2015). Out of the 63 candidate genes which were identified in the GWAS, they found 13 genes that encoded proteins localized to the chloroplast and are involved in abiotic stress responses (Rooijen *et al.*, 2015).

The recent advances in next-generation sequencing technology and the success of "1001 Genome project" in *Arabidopsis* (1001 Genome Consortium, 2016) provides a very useful resource for characterizing gene function in plants. Studying photoprotective mechanism using GWAS, therefore, will expand the range of genetic diversity by examining naturally occurring genetic variation from natural accessions, which is limited by applying QTL mapping alone. Moreover, the use of high-density genome-wide mapping of single-nucleotide polymorphism (SNPs) used in GWAS can increase the intensive profile of the genetic architecture of the traits of interest (Filiault and Maloof, 2012; Brachi *et al.*, 2011).

1.9 AIMS OF THIS THESIS

The overall aims of this project are to understand the genetic basis of natural variation in photoprotective mechanisms focusing on non-photochemical quenching (NPQ). This was investigated using the following aims:

Aim I: Develop growth conditions and phenotyping protocols for chlorophyll fluorescence measurements to maximise heritability, allowing natural variation screens for NPQ (Chapter 3).

Aim II: Develop tools for high throughput measurement and detailed analysis of NPQ kinetics; including the induction, maximum, and relaxation phases (Chapter 3).

Aim III: Explore quantitative trait locus responsible for NPQ in multiple environments using a Recombinant Inbred Intercrosses (RIXs) population (Chapter 4).

Aim IV: Identify loci responsible for NPQ in multiple different environments using a Genome Wide Association Studies (GWAS) approach and investigate candidate alleles using knockout lines (Chapters 5).

1.10 CHAPTER'S OVERVIEW

This Thesis is structured as five chapters. Below is a summary of the goals and the approaches of each chapter:

Chapter 1: Introduction - This chapter reviews the basis of plant photosynthesis, chlorophyll fluorescence and Genome-Wide Association Studies (GWAS). The photoprotection and photoinhibition components are summarised and consequently discussed more depth in the relevant results chapters.

Chapter 2: Materials and methods - This chapter describes materials and methods used in this study. In particular this chapter describes the novel chlorophyll fluorescence techniques and statistical analysis used for determining photosynthetic performance in *Arabidopsis*. This chapter also describes the details of simulated natural environment systems.

Chapter 3: Establishing high-throughput phenotyping to investigate photoprotection in *Arabidopsis* - This chapter demonstrates the optimisation of different chlorophyll fluorescence protocol, and several simulated natural climates. The preliminary experiments were conducted to observed heritability of photoprotective traits.

Chapter 4: Exploration of photoprotective mechanisms in *Arabidopsis* RIXs population - This chapter presents natural variation under different conditions in the Cvi-0 x L*er* RIXs population, the identification of QTL as well as the identification of candidate genes responsible for NPQ and flowering time. This chapter also demonstrates the effects of seasonal changes on NPQ.

Chapter 5: Natural variation and Genome-Wide Association Studies in photoprotection in *Arabidopsis* - This chapter presents the genetic variation of traits in natural population using GWAS, and describes the mechanisms behind the differences in NPQ kinetics between coastal and inland simulated conditions. This Chapter also presents the results of candidate genes confirmation.

Chapter 6: Final discussion and future prospects - This section provides the final

discussion of the novel findings and techniques developed.

Chapter 2

Materials and Methods

2.1 PLANT MATERIAL AND SEED TREATMENT

The HapMap set of *Arabidopsis* which was selected as a genetically diverse subset of the natural accession (Li *et al.*, 2010) and photoprotective mutants (*npq1*, *npq4*, *aba1*, *lut2* and *pgr5*) as shown in Table 2.1 were used in this work. The recombinant inbred intercross lines (RIXs) between Cvi-0 and L*er* were provided by Joost Keurentjes, Wageningen University. All seeds that were used in this study were planted under controlled conditions, after 4-5 days of stratification at 4°C in the dark in sterilised water to synchronize seed germination.

In 2012 (Experiment I), Each natural accession (Table 2.2) and mutant lines (*npq1*, *npq4*, *lut2* and *aba1-1*) had five replicated per growth condition. This experiment was conducted for optimising the chlorophyll fluorescence measuring protocols.

In 2013 (Experiment II), three replications of 92 Cvi-0 x L*er* RIXs lines (see supplemental data Table A.1) and inbred lines of Cvi-0 and L*er* were grown under five different growing conditions. The purpose of this experiment was to investigate the natural variation of NPQ in the bi-parental cross population.

In 2014 (Experiment III-a), the seedlings of 150 accessions (two plants per accession) of the HapMap set and five mutants were planted under coastal and inland simulated spring condition. Because of the very low percentage of survival plants in this experiment (result presents in the Chapter 3), the Experiment III-b was created with a simulated autumn season. In the Experiment III-b, at the start of the experiment two growth chambers were run the same environment (coastal). When plants were at 32 days of age, one chamber was switched to inland condition. These two experiments were conducted for evaluating the best growth condition for studying photoprotective mechanism and developing an analysis pipeline for natural variation studies.

In 2014 (Experiment IV), 284 accessions (see supplemental data Table A.2) from the global set of *Arabidopsis* (HapMap) and photoprotective mutants seeds were used. The geographic distribution of the 284 accessions is shown in Figure 2.1.

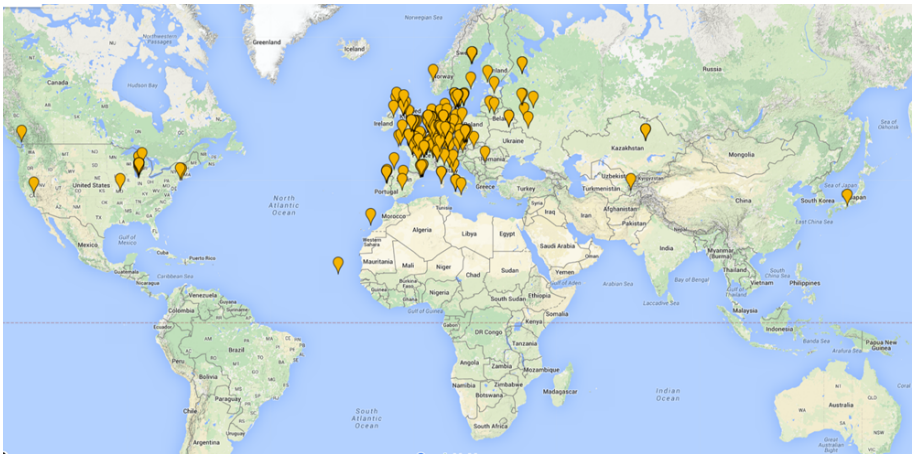

Figure 2.1 – ***The geographic distribution of 284 Arabidopsis natural accessions (subset from HapMap set) were used in this study (image provided by www.google.com).***

In 2015 (Experiment V), fresh *Arabidopsis* seeds from the 2014 experiment, 223 natural accessions (see supplemental data Table A.3), photoprotective mutants (Table 2.1) and knockout lines (Table 5.3) were treated with 10 μM GA_4 (Gibberellins) to promote germination. GA_4 was added into 1.5 ml tube containing *Arabidopsis* seeds, then the seeds were vernalised for four days.

Table 2.1 – ***The mutant lines that were used in this study (data from www.arabidopsis.org)***

Mutants name	AGI ID	Function/Description
lut2	AT5G57030	Light harvesting and xanthophyll biosynthetic."Lutein-deficient 2: involved in carotene biosynthetic process, photosynthesis,
npq1	AT1G08550	NON-PHOTOCHEMICAL QUENCHING 1:Violaxanthin de-epoxidase involved in xanthophyll cycle, the absence of zeaxanthin formation in strong light and the partial inhibition of the quenching of singlet excited chlorophylls in the photosystem II light-harvesting complex.
npq4	AT1G44575	NON-PHOTOCHEMICAL QUENCHING 4: a ubiquitous pigment-binding protein associated with photosystem II (PSII) of higher plants. Involved in non-photochemical quenching, mutant has a normal violaxanthin cycle but has a limited capacity of quenching singlet excited chlorophylls and is tolerant to lipid peroxidation.
aba1-1	AT5G67030	ABA DEFICIENT 1: mutant has a normal violaxanthin cycle but has a limited capacity of quenching singlet excited chlorophylls and is tolerant to lipid peroxidation.
pgr5	AT2G05620	PROTON GRADIENT REGULATION 5: Involved in electron flow in Photosystem I. Essential for photoprotection.

Table 2.2 – ***The 20 Arabidopsis natural accessions that were used in the 2012 experiment and the respective geographical location.***

Accession	Latitudes	Longitudes	Country
Ll-1	41.59	2.49	ESP
Ts-1	41.72	2.93	ESP
Van-0	49.3	-123	CAN
Br-0	49.2	16.61	CZE
Sf-2	41.78	3.03	ESP
Kas-1	35	77	IND
Ag-0	45	1.3	FRA
Kondara	38.48	68.49	TJK
Ws-2	52.3	30	RUS
Ms-0	55.75	37.63	RUS
Tsu-0	34.43	136.31	JPN
Ler-1	47.98	10.87	GER
C24	40.20	-8.42	POR
Col-0	38.3	-92.3	USA
Cvi-0	15.11	-23.61	CPV
Jm-1	49	15	CZE

2.2 SOIL-BASED GROWTH METHODS

In 2011 to 2012, steam pasteurised commercial seed raising mix (Debco, Tyabb, Vic., Australia) supplemented with Osmocote Mini slow releasing fertilizer (Scotts Australia, New South Wales) at a concentration of 3 g/L was used. From 2014 to 2015, pasteurised soil was used without Osmocote. After seed stratification, a few *Arabidopsis* seeds were sown in pots (4 cm x 4 cm x 7 cm). Then pots were moved into conviron controlled environments. After sowing, pots were covered with 4 cm petri dish lids to maintain high humidity until seedling were established. Seedlings were later thinned out to one per pot.

2.3 CONTROLLED GROWTH CONDITIONS

To be able to both control for and mimic natural environments, the SpectralPhenoClimatron (SPC) (Brown *et al.*, 2014) were used in this work. The SPC is a high throughput system that enables to monitor growth phenotyping up to 320 plants per chamber. The SPC is combination of three systems (Figure 2.2). Firstly, the conviron controlled environment (Conviron® model No. PGC20) which is be able to control temperature and humidity. Secondly, multiple wavebands of light emitting diodes (LEDs) (Heliospectra). Lastly, real-time imaging instruments (using Canon) which were developed by Brown (2014) with images taken every 5 min. The first two systems are controlled by the SolarCalc control software (SolarCalcII-Growth Chamber Control Version E-2014) (developed by Kurt Spokas, University of Minnesota, USA) which is used for simulating diurnal and circannual (seasonal) rhythms based on a particular climatic region. SolarCalc can program one minute changes in temperature, relative humidity, light spectrum, and light intensity. After the SolarCal output files were custom made, they were upload to the SPC system using a script written by Kevin Murray (unpublished) in order to created the condition mentioned above. In this study, diurnal and seasonal temperature fluctuations were set to simulate coastal (Wollongong: -34.425, 150.893) and inland (Goulburn: -34.426, 150.892) regions of South East Australia. Light intensities in the inland were increased to provide sufficient stress conditions. However, the maximum light intensity available was 500 μmol $m^{-2}s^{-1}$. These simulated conditions were calculated automatically using SolarCal software which changed in light spectrum diurnally. The amount of far-red

light exceeds the amount of red light during sunrise and sunset periods in both Inland and Coastal conditions. The parameters such as latitude, longitude and other LED intensity parameters are presented in Table 2.3. The summary of mimicking natural environments used in this thesis are presented in Table 2.4.

Table 2.3 – ***The setting parameters for SolarCalc software were used in this study to generate simulated coastal and inland climates.***

Growth conditions	Latitude	Longtitude	Elevation (m)	Light setting						
				LED1 (400NM)	LED2 (420NM)	LED3 (450NM)	LED4 (530NM)	LED5 (630NM)	LED6 (660NM)	LED7 (735NM)
Coastal (Wollongong area)	-34.425	150.893	0	0.95	0.76	0.73	0.69	0.9	0.13	0.67
Inland (Goulburn area)	-34.426	150.892	702	1.47	1.14	1.095	1.035	1.35	0.195	1

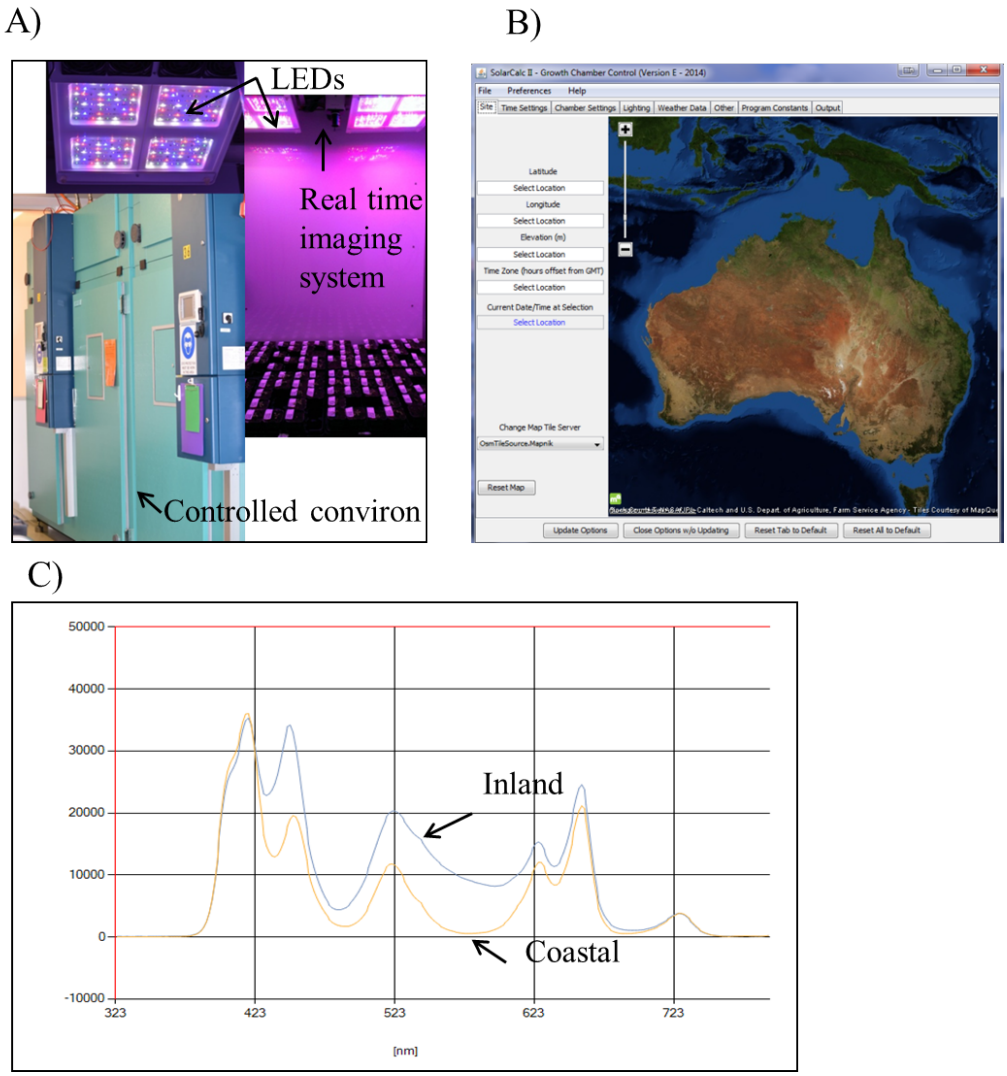

Figure 2.2 – *The SPC system simulated climate of coastal and inland in autumn season. A) images of controlled convirons which included real time imaging and LEDs light. B) SolarCalc software were used to simulate diurnal and seasonal change of coastal and inland climates. C) representation of the differences in wavelengths of coastal and inland conditions measured at 2.00 pm using SpectralPen (PSI).*

Table 2.4 – ***The summary of the simulated natural environment used in this study as generated by SolarCalc software.***

Experiment	Population	Growth conditions	Typical season	Maximum light intensity (µmol $m^{-2}s^{-1}$) [C]	Temperature range (°C) (day/night)
Exp I	Natural accessions and mutants	High light[A]	*	500	21/18
		Low light[A]	*	150	21/18
Exp II	Cvi-0 x L*er* RIXs	Excess light[B]	*	500	25/15
		Sufficient light[B]	*	150	25/15
		Fluctuating light[B]	*	150-500	25/15
		Coastal[B]	**	160	25/10
		Inland[B]	**	350	20/5
Exp III-a	150 Natural accessions and mutants	Coastal[B]	Spring**	160	Dynamic temperature
		Inland[B]	Spring**	350	
Exp III-b	150 Natural accessions and mutants	Coastal[B]	Autumn**	160	Dynamic temperature
		Inland[B]	Autumn**	400	
Exp IV	284 Natural accessions and mutants	Coastal[B]	Late Autumn**	160	Dynamic temperature
		Inland[B]	Late Autumn**	400	
Exp V	223 Natural accessions and mutants	Coastal[B]	Early Autumn**	160	Dynamic temperature
		Inland[B]	Early Autumn**	400	

[A] Plants were grown under constant white light

[B] Plants were grown under LEDs light

[C] Note, maximum light intensity available was 500 µmol $m^{-2}s^{-1}$

* Plant were grown under 12 h light/12 h dark at 75%RH

** Day length and air humidity were diurnal and seasonal changes according to the geographic regions simulated.

In 2012, Experiment I was conducted with 16 *Arabidopsis* natural accessions and four mutants. Plants were grown under excess light and sufficient light conditions. This experiment were designed in order to test chlorophyll fluorescence measuring protocols.

In 2013 (Experiment II), seedling of the Cvi-0 x L*er* RIXs were grown in five differents growth conditions; 1) sufficient light ($\simeq$150 μE), 2) excess light ($\simeq$500 μE), 3) fluctuating light ($\simeq$150 μE and $\simeq$450 μE), 4) Coastal simulated condition ($\simeq$150 μE), and 5) Inland simulated condition ($\simeq$350 μE). The first three conditions were coastal simulated, with temperature and humidity the same across the three chambers.

In 2014 (Experiment III-a), seedling of 150 accessions (two plants per accession) from the HapMap set and the five mutants were grown in the conditions mimicking coastal and inland based on a typical spring season. These two conditions

were controlled by SolarCalc software with five minute interval in SPC. Then Experiment III-b was setup due to very poor survival of plants from Experiment III-a. The same plant material was used in this experiment. The difference in the Experiments III-b was the climatic conditions; simulated coastal and inland setting for typical autumn season was chosen instead of spring season. Both chambers experienced coastal conditions for the first 32 days of age, then one chamber was switched to inland condition.

Experiment IV was conducted in 2014. Seedlings of 284 accessions of the global HapMap set and mutants were grown in coastal and inland conditions mimicking an autumn season. All plants were germinated under simulated conditions starting from April 1st, 2014. These two conditions were controlled by SolarCalc software with five minutes interval in SPC.

In 2015, Experiment V was conducted using fresh seeds from Experiment IV. The 223 accessions, and mutants were grown in coastal and inland conditions mimicking an autumn season. The mimicking conditions were started from March 15th, 2015 and controlled by SolarCalc software with five minutes interval in SPC.

2.4 HIGH THROUGHPUT CHLOROPHYLL FLUORESCENCE MEASUREMENTS

Chlorophyll fluorescence parameters were measured using the PlantScreen system (Photon Systems Instruments, Czech Republic) (Figure 2.3). This system consists of two set of super-bright white and red light emitting diodes (LED's) that provide excitation flashes or a continuous actinic irradiance. Chlorophyll fluorescence kinetics were monitored during illumination of actinic light (700 μmol $m^{-1}s^{-1}$) and saturation flashes (800ms, 2800 μmol $m^{-1}s^{-1}$. A charge-coupled device (CCD) camera was used that detects fluorescence emitted within the area of plant leaves. A computer was used for imaging detection, storage, and analyses. The chlorophyll fluorescence analysis was performed automatically by the FluorCam7 software. A variety of chlorophyll fluorescence measuring protocols were used in this thesis in order to test the power of chlorophyll fluorescence parame-

Figure 2.3 – *The PlantScreen system (Photon Systems Instruments, Czech Republic) used for measuring chlorophyll fluorescence. The left panel is the loading chamber for preparing plants before performing the measurement. The right panel is the chlorophyll fluorescence measuring chamber with a CCD camera attached above.*

ters for quantifying photoprotection which will be described in Chapter 3. There are a large numbers of parameters correlated to the photoprotective mechanism. Prior to measurement plants were dark-adapted for at least 30 minutes. This dark-adapted state results in the reaction center of PSII being open. A minimum fluorescence, Fo is measured using a weak measuring light. It is very important that this measuring light intensity must be low enough to measure it, yet does not activate photochemistry of PSII. It is followed by a short actinic light (less than 1s) with a saturating pulse (at thousands μmol $m^{-1}s^{-1}$) resulting in the reaction center of PSII being closed (fully saturated) and giving the maximum fluorescence, Fm. Leaves are then exposed to continuous illumination with moderately excess light giving the maximal fluorescence level, Fm'. After switching off the light, the reaction center becomes relaxed; this results in relaxation stage which is observed from the increase of fluorescence as shown in the Figure 1.11.

2.5 BIOCHEMICAL MEASUREMENTS

2.5.1 Quantification of Reactive Oxygen species using Amplex® Red

To detect leaf hydrogen peroxide (H_2O_2) the Amplex® Red Hydrogen Peroxide/Peroxidase Assay Kit (Molecular Probes, Invitrogen) which contains Amplex® Red reagent (10-acetyl-3,7-dihydroxyphenoxazine) was used in this work. Leaf H_2O_2 was quantified in soil grown plants at the transition to flowering stage. Approximately 50 mg of fresh leaf tissue was flash frozen in liquid nitrogen. The samples were ground to a fine powder using TissueLyser (Qiagen Inc, Australia) at 25 Hz for one minute and extracted with 250 μL of 20 mM K_2HPO_4/KH_2PO_4 buffer (pH 6.5). The samples were incubated at 4 °C in TissueLyser (Qiagen Inc, Australia) at 10 Hz for 30 minutes to increasing the extraction efficiency. The plant extract was then centrifuged at 3,000 rpm for 10 minutes at 4 °C. The supernatant (50 μL) was transferred into a black 96-well flat bottom polystyrene plate (Nunc®) and incubated with 50 μL of working solution (50 μL of 100 mM Amplex® Red reagent, 100 μL of 10 Uml^{-1} horseradish peroxidase (HRP) and 4.85 mL of 1X reaction buffer) at room temperature for 30 minutes in the dark. As Amplex® Red is photodegradable, the extractions were protected from light during the assays. The fluorescence of the formed substrate resorufin was measured using a monochromator-based reader (Infinite® M1000 PRO, Tecan) with excitation filter 410 and emission filter 590. The concentration of H_2O_2 was calculated using a standard curve (H_2O_2 standards range from 0.5, 1, 2, 5 and 10 μM were used).

2.5.2 Determination of chlorophyll using a microplate reader

Chlorophyll *a* and *b* extraction

The chlorophyll concentration of the *Arabidopsis* leaf samples was measured using the method of Porra et al. (1989), Ritchie (2006), Warren (2008), and Hu et al. (2013). Fresh leaf tissue was harvested (approximately 50 mg) into FluidX 1.4 mL 2D Barcode Screw Top Tubes. Samples were ground to a fine powder using TissueLyser (Qiagen Inc, Australia) at 25 Hz for one minute. Pigments were extracted by adding 1.00 mL of chilled methanol to the tube containing

the frozen ground samples and homogenised by shaking the sample at 4 °C for two minutes to prevent chlorophyllide formation. The samples then were centrifuged at 3,000 rpm for three minutes at 4 °C to remove debris. The chlorophylls content were measured by pipetting 200 μL of supernatant into a 96-well flat bottom polystyrene plate (Nunc®). Sample absorption was measured with a monochromator-based reader (Infinite® M1000 PRO, Tecan) at 652 nm (A_{652}) and 665 nm (A_{665}).

Calculation of chlorophylls concentration

The absorbance of 200 μL of sample in microplate at 652 nm (A_{652}, microplate) and 665 nm (A_{665}, microplate) was converted into a 1- cm pathlength corrected absorbance. For this work, the microplate pathlength determined by Warren's method (pathlength = 0.51) was used (Warren, 2008):

$$A_{652,1cm} = (A_{652,microplate} - \text{blank})/0.51$$

$$A_{665,1cm} = (A_{665,microplate} - \text{blank})/0.51$$

Chlorophyll *a* and *b* concentration and chlorophyll *a/b* ratio were estimated using the following equations using 1-cm corrected pathlength (Warren, 2008; Ritchie, 2006):

$$\text{Chl } a\ (\mu g/ml) = -8.0962(A_{652,1cm}) + 16.5169(A_{665,1cm})$$

$$\text{Chl } b\ (\mu g/ml) = 27.4405(A_{652,1cm}) - 12.1688(A_{665,1cm})$$

$$\text{Chl } a/b = \frac{Chla}{Chlb}$$

2.6 GENOTYPING BY PCR

2.6.1 CTAB genomic DNA extraction

Plant DNA was isolated from leaf tissue using CTAB DNA extraction protocol adapted from Clark, 2009. Approximately 50 mg of fresh leaf tissue was harvested in a 1.5 mL Eppendorf tube and flash frozen in liquid nitrogen. The tissue

was then ground to a fine powder with a 1/8 inch steel ball bearing using a TissueLyser registered trademark II (Qiagen, Hilden, Germany) for two minutes at a shaking frequency of 25 s^{-1}. Cetyl-trimethyl-ammonium bromide (CTAB) buffer (2% (w/v) CTAB, 1.4 M NaCl, 100 mM Tris-HCL (pH 8.0) and 20 mM EDTA) pre-heated at 65 °C were added into the tube (300 μL per 100 mg of tissue). The sample was mixed in the TissueLyser as before followed by incubation at 65 °C for 30 minutes. The sample was centrifuged at 16,000 g for one minute at room temperature and the upper aqueous layer was transferred to a new tube. Isopropanol (300 μL) was added to precipitate DNA and gently mixed by inversion. The sample was again centrifuged at 16,000 g for five minutes and the supernatant was discarded. The DNA pellet was washed with 70% ethanol and centrifuged as before. After centrifugation, the ethanol was removed and the sample was air-dried for 10 minutes. Finally, the DNA was resuspended in 50 μL of sterile MilliQ water and stored at -20 °C.

2.6.2 Quantification of nucleic acids

The concentration of nucleic acids was determined using a ND-1000 spectrophotometer (NanoDrop Technologies, Wilmington, Delaware, USA) with NanoDrop software (version 3.1.0). The measurements of DNA or RNA were taken at 260 nm (A_{260}) and can be converted to concentration using the Beer-Lambert equation, in which A represents the absorbance of the DNA sample, ε is the extinction coefficient of the sample (50 for DNA, 40 for RNA). and l is the pathlength:

$$[\text{Nucleic Acid}] = \frac{Ax\varepsilon}{1}$$

The quality of DNA or RNA samples can be assessed using the A_{260}/A_{280} ratio, in which the ratio of 1.8 indicates pure DNA.

2.6.3 Polymerase chain reaction (PCR) amplification

Primer design

Gene-specific oligonucleotides were designed using published sequences obtained from TAIR website (www.arabidopsis.org). Primers were designed using the following conditions: 50 mM salt condition, GC content approximately 50%, Tm of 50-60°C with around 300bp of product size. All primers used throughout this study were obtained from Sigma-Aldrich (http://www.sigmaaldrich.com). A list

of Knockout genotyping primers used in this study was summarised as in supplementary Table A.4. Generally, primers were designed using Primer-BLAST tool from NCBI and T-DNA Primer Design Tool from SIGnAL.

Standard PCR conditions

Standard PCR condition was used for genotyping mutant plants. All PCR reactions were carried out on a T100TM Thermal Cycler (BioRad, USA). Polymerase used for standard PCR reactions was FastStart Taq DNA Polymerase (Roche, Germany). PCR reactions generally contains of the following: 0.2 mM dNTPs, 1X Buffer (20 mM Tris-HCl, 10 mM $(NH_4)2SO_4$, 10 mM KCl, 2 mM $MgSO_4$, 0.1% Triton® X-100, pH 8.8), 1 μM forward primer, 1 μM reverse primer, template DNA (200-500 ng.μl^{-1}) and 1 unit of FastStart Taq DNA Polymerase. Typical PCR conditions were: 30 s at 95 °C, 40 cycles of 30 s at 95 °C, 30 s at primers' annealing temperature and 72 °C for 1 min per kb PCR product, before a final heating at 72 °C for 5 mins. The resulting PCR products were assessed by agarose gel electrophoresis as described in section 2.6.4.

2.6.4 Agarose gel electrophoresis

A 1% w/v agarose gel was prepared prior to gel loading. A 3 mL aliquot of PCR amplification products was mixed with 0.5 mL of loading buffer (50% Glycerol, 0.1 mM EDTA pH 8.0, Bromophenol Blue) and resolved on a 1% w/v agarose gel, prepared and run in 1 TBE [89 mM Tris base, 89 mM Boric acid, 2 mM EDTA pH 8.0], with 1 mM ethidium bromide added to the gel for visualisation of DNA under UV light. Samples were run on the gel for 30 mins at 200 V in Super120 Screener (6MGel) trays together with 100 bp and/or 1000 bp DNA ladder (NEB, USA). Band patterns were visualised using the GelDoc System UV transilluminator (Fisher Biotech, USA).

2.7 GENOTYPING-BY-SEQUENCING (GBS)

To confirm the genotype of each line used in this study GBS was undertaken. Approximately 50 mg of fresh leaf tissue was harvested for DNA sequencing. A basic schematic of the protocol used for performing GBS as shown in Figure 2.4. The GBS library protocol was adapted by Niccy Aitken (Research officer, Borevitz's Lab, Plant genomics for climate adaption, ANU). The protocol was modified from published method of Elshire and colleges (2011), and the detail shows in supplementary Table A.5. After DNA library extraction was performed, sample was sent to The Biomolecular Facility (BRF) for the sequencing and The Genome Discovery Unit (GDU) for analysis at The John Curtin School of Medical Research, ANU College of Medicine, Biology and Environment. Genotyping-by-sequencing was carried out by the GDU. The sequencing results were compared to the public sequence data from 1001 genomes project to confirm the plant's ID of the HapMap lines which was performed with Riyan Cheng. For the 15 lines that were found to be incorrectly labeled after the confirmation, new plant IDs was used for GWAS analysis.

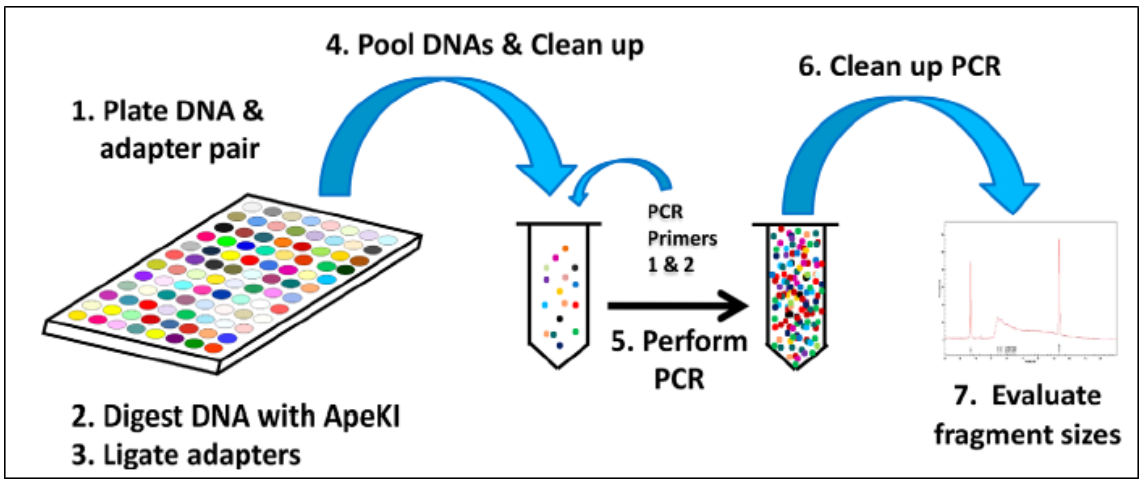

Figure 2.4 – *Steps in GBS library construction using 96 well format. (1) DNA samples, barcode, and common adapter pairs are plated and dried; (2-3) samples are then digested with ApeKI and adapters are ligated to the ends of genomic DNA fragments; (4) T4 ligase is inactivated by heating and an aliquot of each sample is pooled and applied to a size exclusion column to remove unreacted adapters; (5) appropriate primers with binding sites on the ligated adapters are added and PCR is performed to increase the fragment pool; (6-7) PCR products are cleaned up and fragment sizes of the resulting library are checked on a DNA analyzer (BioRad ExperionH or similar instrument). Libraries without adapter dimers are retained for DNA sequencing (Elshire* **et al.***, 2011).*

2.8 GWAS AND STATISTICAL ANALYSIS

To identify genetic variants underlying phenotypes with good statistical power, a large panel of 280 natural accessions of *Arabidopsis* were selected from the HapMap collection. The average trait value of the biological replicates for some accessions was taken for GWAS analysis. The GWAS analyses were performed with assistance of Riyan Cheng for each time point using the R package QTLRel (Cheng *et al.*, 2011) based on model (2), which has been shown to correct population structure confounding, and SNP data from the 250K SNP chip (Atwell *et al.*, 2010; Horton *et al.*, 2012) with a minor allele frequency <5% being filtered out. In the analysis of the chlorophyll fluorescence data, we also used 6M SNPs data set. The 0.05 genome-wide significance threshold was determined by the Bonferroni procedure, i.e., χ^2(1-0.05/m,1), where mis the number of SNPs. This threshold turned out to be very close to empirical thresholds estimated by the permutation test.

The following model can be considered for identifying QTL and QTL x environment interaction (Cheng *et al.*, 2013; Li *et al.*, 2014)

$$Y_{ij} = \beta_0 + e_0\beta + x_i a + e_j x_i b + u_{ij} + \epsilon_{ij}\ ,\ i\epsilon\{1,2\}\ ,\ j\ \epsilon\ \{1,2,...,n\}.....(1)$$

where y_{ij} is the phenotypic value of j-th accession in the i-th environment e_i (i.e., one of the two climate conditions, "coastal" and "inland", coded as 0 and 1 respectively), β_0 is the intercept, β is the effect of the environment, x_j is a coding variable (with a value 0 or 1) of two genotypes at the scanning locus and a is the effect of the putative QTL, b is the interactive effect between the environment and the putative QTL, u_{ij} represent polygenic variation, and ϵ_{ij} denotes the residual effect. u_{ij} and ϵ_{ij} are random, and the rest are fixed effects. As in Li et al. (2014),ϵ_{ij} $\sim$iid $N(0,\sigma^2)$, $u_{ij} \sim N(0,2K_{ij}\ \sigma^2_{i,a})$ and $cov(u_{i1j1}, u_{i2j2}) = \mathbf{2}\boldsymbol{K}_{i1j2}\ \sigma_{i1a}\ \sigma_{i2a}$ with $\boldsymbol{K}$ = (K_{ij}) being the kinship matrix, and $cov(u_{i1j1}, u_{i2j2}) = 0$. Equation (1) leads to

$$Y_{i2j} - Y_{i1j} = \beta + x_j b + (u_{i2j} - u_{i1j}) + (\epsilon_{i2j} - \epsilon_{i1j})$$

or simply

$$Y_j = \beta + x_j b + u_j + \epsilon_j\ .....(2)$$

where ϵ_{ij} $\sim$iid $N(0,\sigma^2)$ and $u_j \sim N(0,2K\ \sigma^2_a)$. Either (1) or (2) can be used to test QTL x environment interaction. Model (2) is simpler, and can be directly used

for QTL detection in each environmental conditions as well. Therefore, it is the model used in all data analyses.

Kinship coefficients are estimated by using SNP data as in Cheng et al. (2013). Specifically, when a chromosome is scanned for QTL, SNPs on other chromosome are used to estimate the coefficients. SNPs on the chromosome under scan are excluded because inclusion of linked SNPs can result in a loss of statistical power for QTL detection.

Phenotypic data at each time point was used for GWAS analysis. In addition, three phases of NPQ kinetics were examined (induction, steady state, and relaxation phases). The induction phase was determined by NPQ formation at the time of 0s to 120s of actinic light illumination. The steady phase was determined from 120s to 450s of actinic light illumination. Lastly, the relaxation phase was indicated by NPQ kinetics at time of 450s to 720s during dark relaxation period.

Heritability estimation

Heritability is a term which is used to estimate how heritable a phenotype of traits (P) is, or if a particular trait is due to environmental effects (E) or genetic effects (G).

$$\textit{Phenotype (P) = Genotype (G) + Environment (E)}$$

Estimation of heritability is defined as a proportion of total variance in a population for a specific traits and specific time (Visscher *et al.*, 2008) which the total variance of observed phenotype in a population (${\sigma^2}_P$) is a sum of genetic variance (${\sigma^2}_G$) and environmental variance (${\sigma^2}_E$).

$${\sigma^2}_P = {\sigma^2}_G + {\sigma^2}_E$$

Heritability can be divided into two terms. Firstly, broad-sense heritability (H^2) is defined as a proportion of phenotypic variances that can be attributed due to total variances of genetic values including additive, dominant, epistatic, and paternal effects:

$$H^2 = {\sigma^2}_G \;/\; {\sigma^2}_P \;\; \textit{where } {\sigma^2}_G = {\sigma^2}_A + {\sigma^2}_D + {\sigma^2}_I$$

Secondly, narrow-sense heritability (h^2) is phenotypic variance due to additive effects only.

$$h^2 = \sigma^2{}_A \; / \; \sigma^2{}_P$$

In this thesis, to determine heritability of growth and chlorophyll fluorescence traits, variance components were estimated from model (2) without any QTL. Narrow-sense heritability was then estimated by $(2(k_{11}+k_{22}+...+k_{nn})\sigma^2)$ / $(n\sigma^2)$, where k11 is the i-th diagonal element in $\boldsymbol{K}$.

2.9 CANDIDATE GENES IDENTIFICATION

From GWAS analyses result, SNPs with LOD score above 5.13 (the significant threshold for 250K SNPs), and SNPs with LOD score above 6.67 (the significant threshold for 6M SNPs) were classified as quantitative loci (QTLs). The candidate genes listed were selected on the basis of annotation from within a 20-kb window surrounding each of the most strongly associated SNPs using publicly available database (www.arabidopsis.org).

Candidate genes prioritisation criteria
From the candidate genes listed, it was ranked based on four selection criteria as followed (www.arabidopsis.org).:

1. Gene function related to photosynthesis and photoprotection.
2. Gene expression in the leaf tissue.
3. Gene function related to abiotic stress.
4 .Unknown function genes that located on top of the identified QTL.

If any of candidate genes scored well for any or all of these four criteria, they were to be considered as a potential candidate gene for further analysis.

Chapter 3

Establishing high-throughput phenotyping to investigate photoprotection in *Arabidopsis*

3.1 OVERVIEW

In the photosynthetic apparatus, light energy is absorbed by the antenna pigments (chlorophyll *a* and *b*), and then the excitation energy is transferred to the reaction centers of the two photosystems (PSI and PSII). Under optimal conditions, more than 90% of absorbed light energy is utilised by photosynthesis (Björkman, 1987). A competing process of relaxation of excited chlorophylls can split the energy three ways as explained in detail in Chapter 1. NPQ is considered to be one of the most important photoprotective mechanisms in plants, which can reflect the levels of adaptability and acclimation in plants. The fact that chlorophyll fluorescence yield is a direct measure of excited chlorophyll molecules indicates that the change in dark adapted fluorescence yield is due to change in photosynthetic capacity. Therefore, it can be expected that chlorophyll fluorescence is a good measure of photosynthetic performance in plant.

Photoprotection in plants is considered a physiologically complex phenomenon. The levels of stress depends on the duration, intensity and quality of light stress stimulus. Absorption of excess light can cause photodamage and photoinhibition to the plant itself (Niyogi *et al.*, 2001; Golan *et al.*, 2006). Photoprotection in plants can act as a short-term response or long-term acclimation in order to survive a stressful conditions (Takahashi and Badger, 2011). Chlorophyll fluorescence imaging can be used as an indicator of photoinhibition and photosynthetic performance in plants (Maxwell and Johnson, 2000; Baker, 2008), and allows investigation of the natural variation in photoprotection. In this chapter a variety of chlorophyll fluorescence measuring protocols are tested in order to increase our understanding of NPQ responses of the plants. Furthermore, different natural environments mimicked in controlled conditions have been used to elucidate photoprotective response in response to different environments in *Arabidopsis*.

Conventional research on chlorophyll fluorescence tended to focus on one plant at a time due to technological limitations; and was time consuming, labour intensive and relatively expensive (Zhang *et al.*, 2012). To conduct the large-scale experiment attempted in this study, a better technology with high resolution phenotyping procedures was required. The newly developed PlantScreen high-throughput phenotyping system (as described in Chapter 2) can automatically measure up to 300 plants per day. This new system uses a conveyor belt to take

plants past a thermal camera used to monitor leaf transpiration; a fluorescence camera used to automate chlorophyll fluorescence measurements; RGB cameras used for real time phenotyping of leaf development; and a watering and weighing system which can be used to monitor drought responses.

In addition to the high-throughput chlorophyll fluorescence phenotyping system, the newly developed climate controlled chamber called SpectralPhenoClimatron (SPC) (Li *et al.*, 2010, 2014; Brown *et al.*, 2014) which are available in the NCRIS facility at ANU used in this study. Instead of fixed on/off white light and high/low temperature growth conditions, the SPC system was able to simulate natural environments, which change throughout days and throughout seasons. The SPC is a combination of new technology including LEDs; which provide seven different wavelengths, real time imaging for real time phenotyping, and diurnal and seasonal control of light colour and temperature. Using these two systems allowed me to conduct a large-scale experiment to reveal the photoprotective responses employed by plants to acclimate to the field environments.

This chapter describes the optimisation of the chlorophyll fluorescence measuring protocols and the simulated growing conditions. This allowed investigation into the photoprotective response in plants and the generation of uniform data for accurate data analysis. In this chapter I focus mainly on non-photochemical quenching analyses and also examined variations in response to different environments.

3.2 RESULTS

3.2.1 High-throughput chlorophyll fluorescence phenotyping

Traditional protocols for measuring NPQ are very time consuming and hence were not compatible with high-throughput phenotyping. For example a traditional protocol would take approximately 30 minutes to complete one single leaf. Thus, it would take up to 150 hours for measuring 300 plants in a single chamber. Hence a number of shorter protocols were tested to see if a steady state of NPQ could be measured within a shorter time frame. The summary of three main protocols which were tested in this study is presented in Figure 3.1.

Experiment I was designed for testing chlorophyll fluorescence measuring protocols. Plant lists can be found in Table 2.1 and 2.2. Experiment I was undertaken in three sets, which were used for testing P1, P2 and P3 protocols. Whole plant chlorophyll fluorescence imaging was performed using the PlantScreen system as described in the Chapter 2. Plants were measured at the age of 25, 35 and 45 days old. Plants were dark adapted for 30 min before measurements.

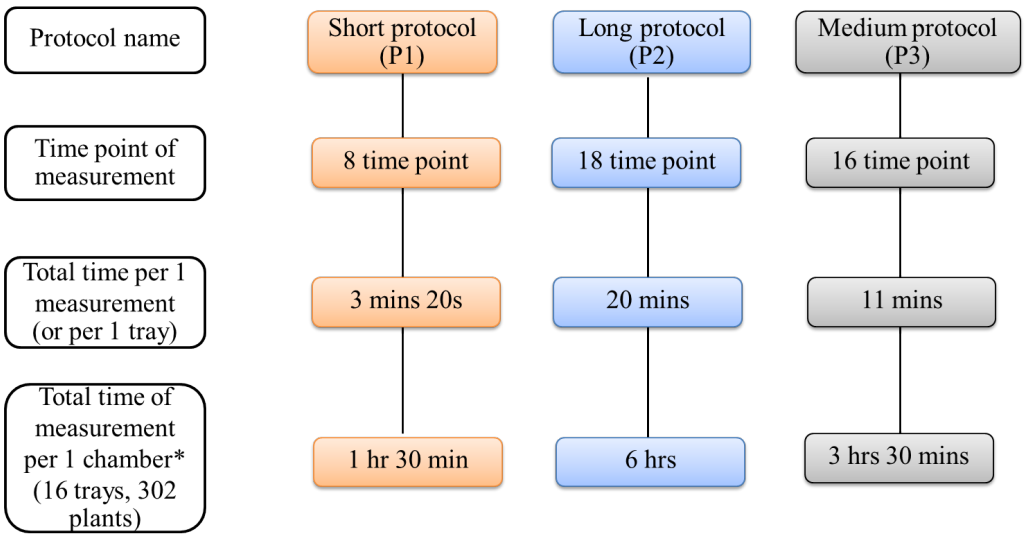

Figure 3.1 – ***The summary of the three main chlorophyll fluorescence measuring protocols that were tested in this thesis.***

Protocol 1: Short measuring protocol (P1) does not reveal NPQ kinetics

The short NPQ protocol (P1), totalling 3 minutes 20 seconds, was tested on 11 *Arabidopsis* natural accessions and four mutants. The P1 protocol composed of one minute 10 seconds of actinic light illumination followed by 1 minute 30 seconds dark relaxation period (see supplementary data Section B.1 for P1 protocol). A saturation pulse of white and red light (800ms, 2800 μmol m^{-2} s^{-1}) and actinic light (500 μmol m^{-2} s^{-1}) was applied to determine chlorophyll fluorescence parameters. The NPQ kinetics of *Arabidopsis* grown under low light (light intensity around 100 μmol m^{-2} s^{-1}) and under high light (light intensity around 300 μmol m^{-2} s^{-1}) showed a similar NPQ kinetics results (Figure 3.2(A)). As expected the photoprotective mutants, *npq1*, *npq4* and *lut2* (as negative controls), showed the lowest NPQ induction. The steady stage of NPQ in these mutants was also significantly lower compared to other accessions. However, this protocol could not distinguish the differences in NPQ between the two growth conditions. It would be expected that those plants grown in high light would show a higher NPQ steady state than those grown in low light. The protocol also failed to resolve the differences between genotypes during the induction phase and relaxation phase. As the protocol could only reveal the maximum NPQ of each accessions within 1 minute and 30 seconds of actinic light illumination, the majority of genotypes did not reach a steady state. These results indicated that using the short measuring protocol would not provide sufficient power to study natural variation in the NPQ mechanism.

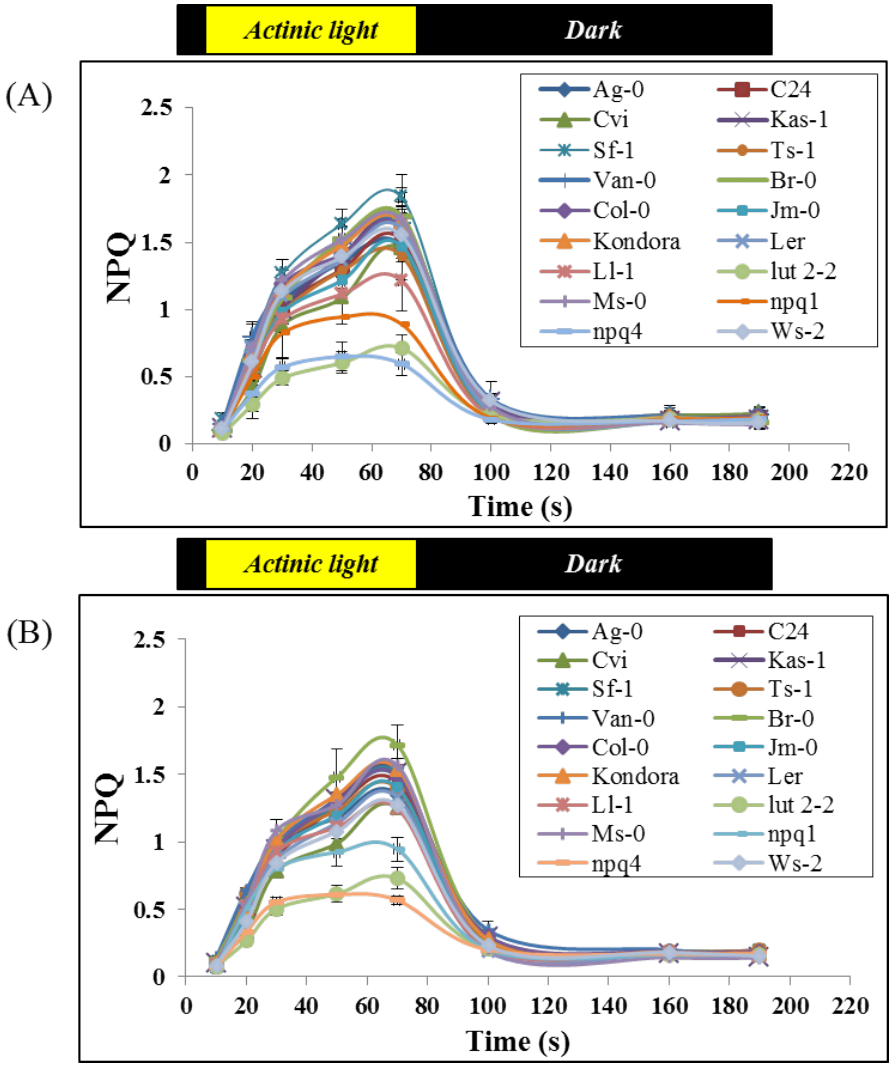

Figure 3.2 – *NPQ measurement of Arabidopsis natural accessions and mutants at 35 days old under low light (A) and high light (B) using chlorophyll fluorescence measurement protocol called P1 protocol (1 minute 10 seconds of actinic light and 1 minute 30 seconds dark relaxation).*

Protocol 2: Extending actinic light illumination period does not provide more information

Based on results from P1 protocol, I decided to increase the actinic light illumination period and increase the number of time points measured. The purpose of this was to determine the maximum NPQ upon the illumination of actinic light and to determine the slope at the induction stage. This modified protocol, called "Long protocol (P2)", composed of 15 minutes of actinic light illumination followed by 5 minutes dark relaxation period (see supplementary data Section B.2 for protocol). A saturation pulse of white and red light (800ms, 2800 μmol m^{-2} s^{-1}) and actinic light (700 μmol m^{-2} s^{-1}) were applied to determine chlorophyll fluorescence parameters. The P2 protocol gave a total measurement time of 20 minutes. The results of the P2 protocol are shown in Figure 3.3. From this protocol, the differences in NPQ responses were observed between the two growth conditions. Under low light, NPQ increased slightly as long as the actinic light illumination continued. However, under excess light, the maximum NPQ was observed during the first minute of illumination, then it slightly declined. In addition, the maximum NPQ from P2 protocol was higher than using P1 protocol (3.2) in both conditions and in all accessions. This may be caused by increasing the actinic light intensity (higher than their growth conditions) in P2 protocol and giving enough time in P2 protocol to observe the NPQ capacities.

There are two negative attributes of this protocol. First, it does not reflect the early induction of NPQ, which is important to understand how quickly the plant responds to high light stress, thus reflecting the type of photoprotective mechanism employed (Niyogi *et al.*, 2001). Second, the extension of actinic light illumination did not seem to provide more information about the NPQ steady state. Finally, this protocol was time consuming, taking 20 min per tray. Hence, a third protocol was developed to address these concerns.

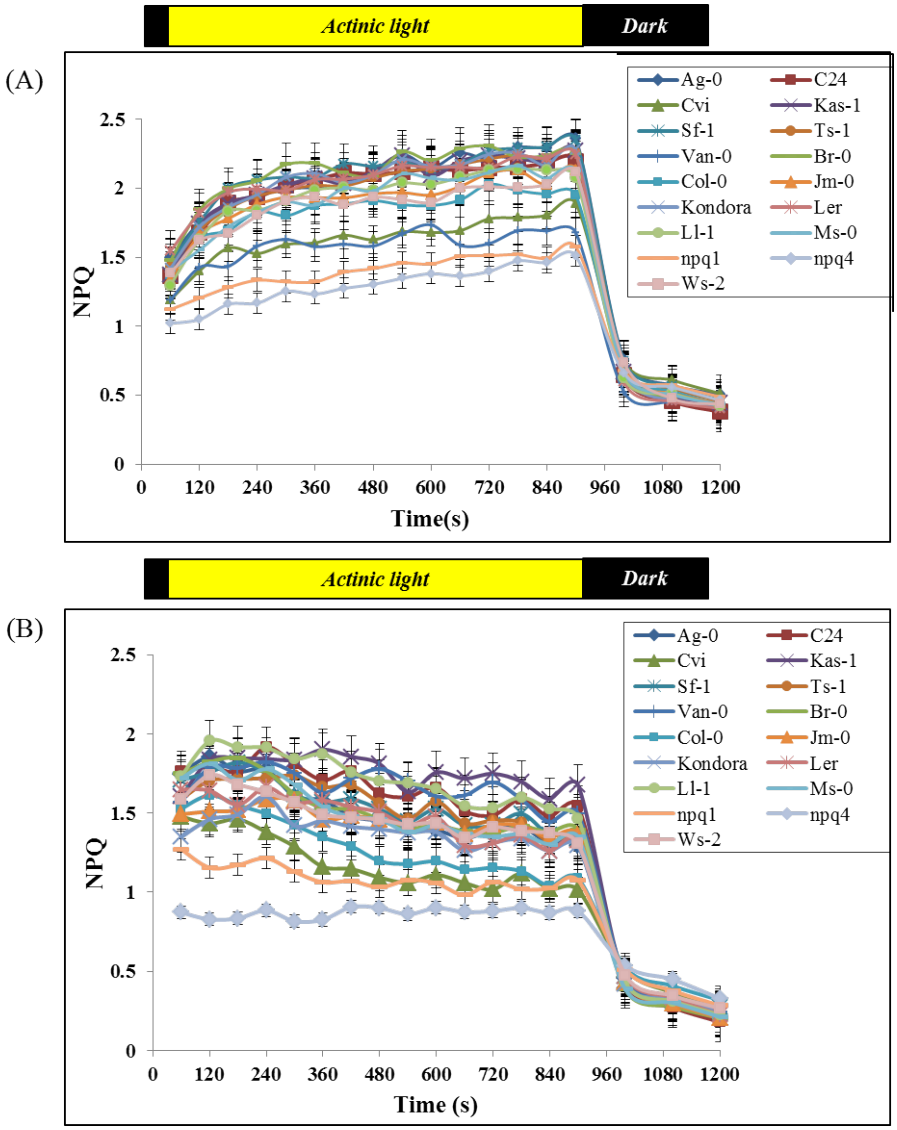

Figure 3.3 – *NPQ capacity of low light plants (A) and high light plants (B) at the age of 35 days old using chlorophyll fluorescence measurement protocol called P2 (15 minutes of actinic light and 5 minutes dark relaxation) protocol.*

Protocol P3: Shorter period of actinic light and more frequency measuring time points revealing NPQ kinetics

The third protocol, called "Medium protocol (P3)", comprised of eight minutes of actinic light illumination followed by a three minutes dark relaxation period (see supplementary data Section B.3 for protocol). A saturation pulse of white and red light (800ms, 2800 μmol m^{-2} s^{-1}) and actinic light (700 μmol m^{-2} s^{-1}) were applied to determine chlorophyll fluorescence parameters. The total time of the measurement of the P3 protocol was 11 minutes. The NPQ results from the P3 protocol are shown in Figure 3.4. A higher resolution of measurements at the beginning of the protocol provided some insight into how quickly plants responded to high light stress (Figure 3.4 (C and D)). This key information explains the qE component of NPQ which is important for plant fitness in variable light conditions rather than for the induction of tolerance to high-intensity (Kulheim *et al.*, 2002). In addition, the qE component is quickly reversible, thus it is easily measured by adding more time points at the start and the end of the measurement.

The different NPQ responses between high and low light growth conditions were observed as in Figure 3.4 (A and B) using the P3 protocol. The maximum NPQ was lower in high light-grown plants than low light. Moreover, high light-grown plants showed a rapid decrease in NPQ after 60s of actinic light illumination. The rate of NPQ induction appeared to be slightly faster in plants grown under high light than low light which was not observed in P2 protocol. The tendency of NPQ decline in inland plants after two minutes and increase in coastal plants as the illumination progresses was similar to that observed in P2 protocol. The NPQ production also was significantly different in the individual accessions, such as Col-0, *npq4* and *npq1* using the P3 protocol, similar to the results reported by Li and colleges using 6 minutes actinic light followed by four minutes dark relaxation (Li *et al.*, 2000). The results suggested that using eight min of actinic light followed by three minutes dark relaxation period is sufficient to observe maximum NPQ and NPQ induction, as wellas steady state and relaxation phases in both growing conditions. Another benefit of this protocol is the measurement of 20 plants that can be done within 11 minutes,this is manageable when performing large-scale phenotyping.

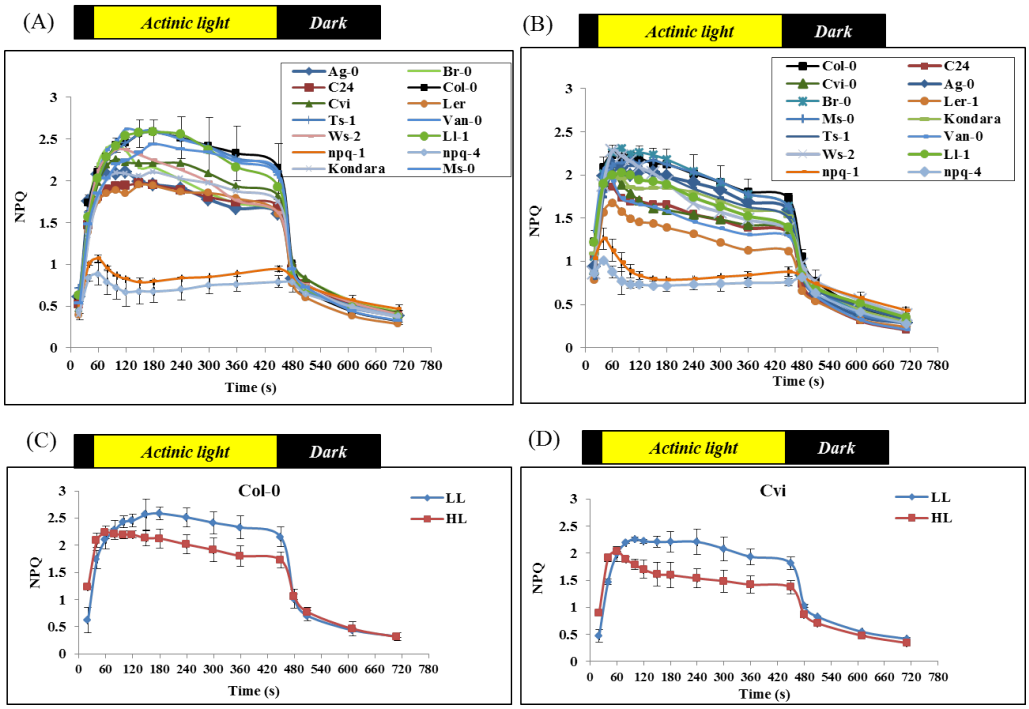

Figure 3.4 – *NPQ measurement under low light (A) and high light (B) using chlorophyll fluorescence measurement protocol called eight minutes of actinic light and three minutes dark relaxation protocol, Protocol 3. (C) and D represent NPQ formation of Col-0 and Cvi respectively (mean ± sd, n=5).*

3.2.2 Heritability of traits

One of the main questions to consider when studying natural variation is to understand how the genetic variation between accessions controls phenotypic variability of the traits in the population. To assess what part of the variability is due to genetic variation, we have calculated trait heritabilities, which are a measure of the extent of trait variation that is due to genetic variation. The 20 accessions from Experiment I were used to calculate narrow-sense heritability (h^2). The narrow-sense heritability is a measure of additive genetic variants contributed to the phenotypic variants which can predict how strongly the phenotype is affected by the genotype. The narrow-sense heritability results are presented in the Table 3.1.

Plants at younger stage (25 and 35 days old) present higher values for narrow-sense heritability in most of the photoprotective traits, than plants at an older stage (45 days old). This result was the same in two conditions. The estimated heritability range was between 40.8% - 68.8% under low light condition in 25 days old plants. At the age of 35 days, the estimated heritability was in the range of

42.2% - 76.9%. The estimated heritability dramatically decreased at 45 days of age with the range of 13.4% - 34.0%. There was also a similarity in heritabilities estimated between the two environments with the range between 54.5% - 75.1% at 25 days of age and 18.4% - 62.2% at the age of 35 days. The decreased heritabilities estimated at the age of 45 days was also observed with the range between 24.9% - 24.3% which is the same as under low light condition. The heritability also varied between traits, which NPQ and *Fv/Fm* showed higher heritability.

Table 3.1 – ***Narrow-sense heritability in photosynthetic parameters. Narrow-sense heritability was calculate from 20 accessions with five replicates per condition.***

Traits	Low light			High light		
	25 days	35 days	45 days	25 days	35 days	45 days
Size	52.0	61.9	17.6	54.5	44.5	37.2
F0	40.8	42.2	13.4	63.8	18.4	24.9
Fm	55.6	50.5	15.3	73.0	20.7	35.9
Fv	56.4	50.5	15.6	72.8	20.9	36.7
QY	45.5	43.3	29.6	61.4	39.2	37.5
Fv/Fm	55.0	63.6	34.0	68.0	48.8	44.3
NPQ	68.8	76.9	22.0	75.1	62.2	41.4

Relatively high heritability estimated for photosynthetic parameters of 20 *Arabidopsis* natural populations showed that much of the variation, in the given conditions, is genetically determined with heritability estimated greater than 50% (Table 3.1). In the mature plants (35 days old), the variation for maximum photochemical quantum yield of PSII (*Fv/Fm*) was mainly genetically controlled with the average of 63.6% and 48.8% under low light and high light conditions respectively. For the NPQ capacity, much of the variation is genetically controlled in both conditions with the average greater than 60%, and the heritability is much lower at the age of 45 days with the average of 22% and 41.4 % under low light and high light conditions respectively.

3.2.3 Establishing growth conditions to investigate photoprotective mechanisms

To understand the natural variation in how growing conditions affect NPQ, a variety of simulated environments were conducted using SolarCalc software and the SpectralPhenoClimatron (SPC) system (as described in the Chapter 2). The different climatic conditions in Coastal and Inland areas may allow resolution of subtle differences in NPQ that are normally masked under standard laboratory conditions. Additionally, within a particular geographic location, seasonal variation in climatic conditions provide a secondary screen for subtle NPQ phenotypes which can be a gradual change dependent on environmental change, and may lead to the acclimation. To determine the most powerful climatic conditions for investigating NPQ variation a pilot experiment was run with 150 natural accessions of *Arabidopsis* grown in four conditions: Coastal-Spring, Inland-Spring, Coastal-Autumn, and Inland-Autumn conditions (Table 2.4). Under the Inland-Spring condition (Experiment III-a), plants experienced extreme temperatures (around 4 °C) and higher light intensity (around 300 μmol $m^{-2}s^{-1}$) in the early morning while at the seedling stage. The growing season was early to mid spring with day length and temperature increasing during the growing season with the converse occurring for autumn. This environment caused excessive damage to plant development, resulting in a reduction in the survival rate to 29% (Table 3.2). In contrast, the simulated autumn condition (Experiment III-b), allowed more than 90% of plants grown under Coastal-Autumn and Inland-Autumn conditions to survive until completion of their life cycle.

Table 3.2 – *The percentage of plants surviving under different typical climate conditions. Under simulated natural climates, light intensity and temperature changed accordingly to seasons.*

Typical season	Growth condition	Percentage (%)	
		Survival	Die
Early to mid Spring	Coastal	69.00	31.00
	Inland	28.76	71.24
Mid to late Autumn	Coastal	93.43	6.57
	Inland	90.79	9.4

Natural variation in NPQ in *Arabidopsis* under shifted environment

Results from Experiment III-b demonstrated a higher percentage of surviving plants in the Coastal and Inland condition with a mid to late autumn season. Therefore, further analyses on NPQ production were performed with these conditions. In the subsequence experiment, duplicated plants grown in two identical chambers side-by-side experienced the same environment (Coastal) for the first 32 days of their life, then one chamber was shifted to Inland conditions in order to study the stress response and acclimation of NPQ in different accessions. NPQ was measured at 32 days old (before shifting) and 40 days old (after shifting). A relatively high heritability around these ages was observed, and the results were presented in Figure 3.5. At the age of 32 days under the Coastal-Autumn climate, NPQ reached maximum after 180 seconds of actinic light, with the average range of NPQ value at 1.6 - 2.7 in both chambers. In some genotypes the maximal NPQ continued to increase after 60s of actinic light, while for some genotypes the NPQ slightly decreased after 60s of actinic light. After 40 days of coastal climate and eight days of inland climate, the rate of NPQ induction was rapidly increased, reaching the maximum value within 40 seconds, with a range of 1.5 - 2.5. After 40 seconds, NPQ levels of Inland plants was decreased significantly compared to Coastal plants which maintained relatively high NPQ levels (Figure 3.5 (B and D). In spite of that, the photoprotective mutants, *npq1* and *npq4*, were unable to promote NPQ under both growing conditions as shown at the bottom the each graph in Figure 3.5.

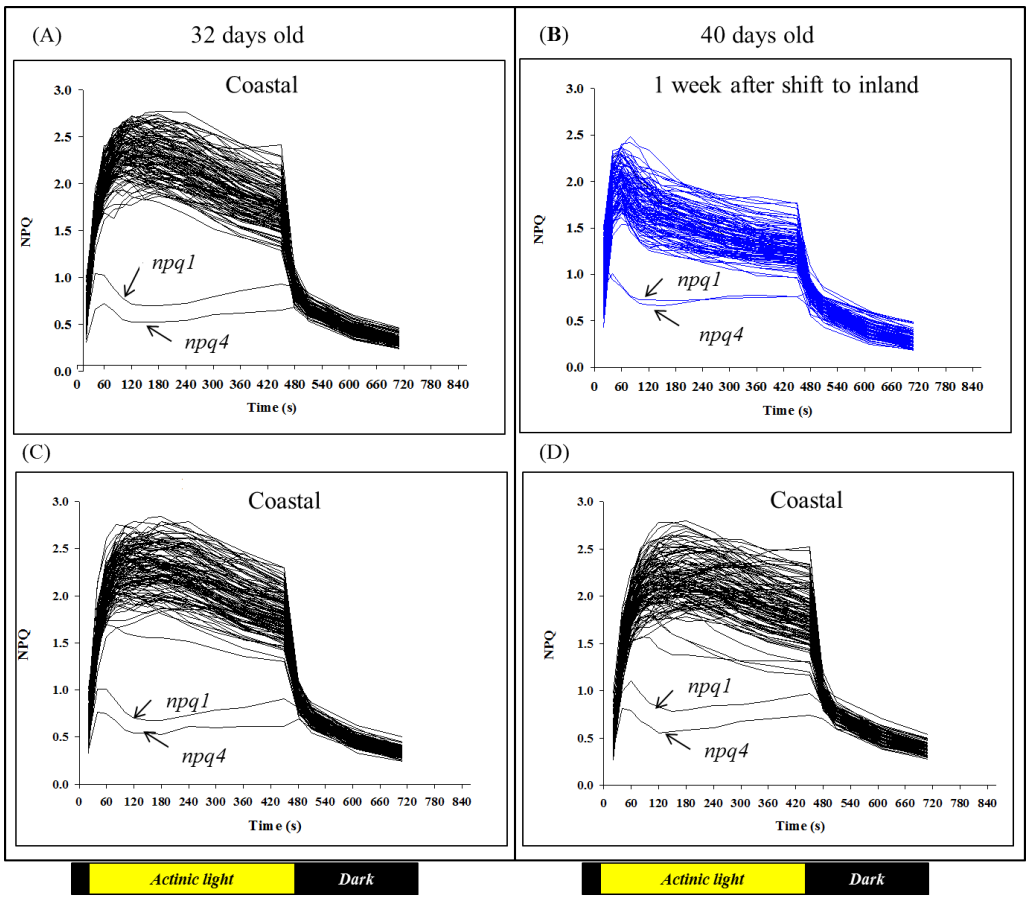

Figure 3.5 – ***Non-photochemical quenching (NPQ) production of Arabidopsis wild population and photoprotective mutants grown under different environments. (A) and (C) show NPQ capacity at 32 days old plants under Coastal condition. (B) represents NPQ production after the shift to Inland condition for eight days. (D) NPQ capacity of plants that remain in the Coastal condition. (B) and (D) were measured at 40 days old.***

The results shown in Figure 3.5 indicate that *Arabidopsis* shows Population variation in NPQ both when constitutively grown under Coastal conditions and when subsequently shifted to harsher Inland conditions. To investigate the genetic architecture of this variation, genome-wide association (GWAS) was performed using genotype data from the 250K SNP chip. NPQ trait at each time points as well as NPQ at three different phases (NPQ induction phase, NPQ steady phase and NPQ relaxation phase) was analyses using GWAS. Unfortunately, the GWAS results for NPQ revealed no significantly associated SNPs from before (Figure 3.6) and after the shifted (Figure 3.7) environments with LOD score > 5.13. There was also no significantly associated SNPs for the genotype and environment interaction (*GxE*).

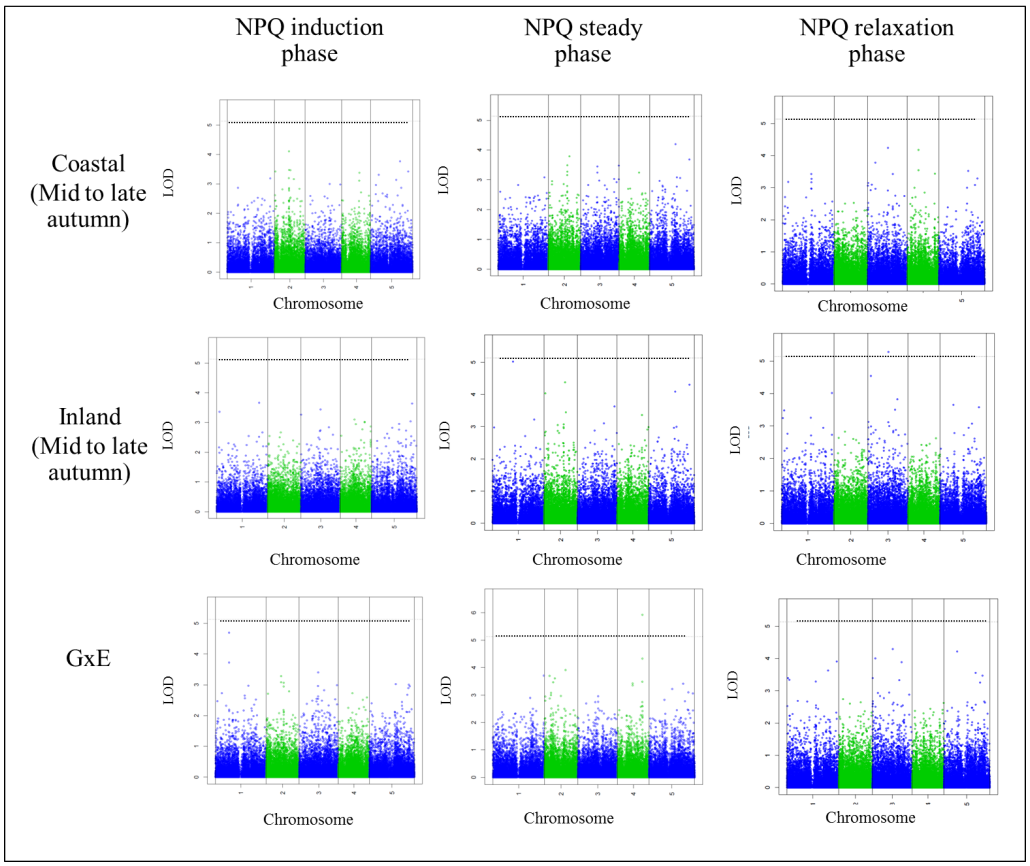

Figure 3.6 – *Manhattan plots of GWAS results using 250K SNP database for NPQ traits at 32 days old plants under Coastal condition. The five chromosomes are depicted in different colors on x axis. The horizontal dash-dot line corresponds to a nominal P < 0.05 significance threshold.*

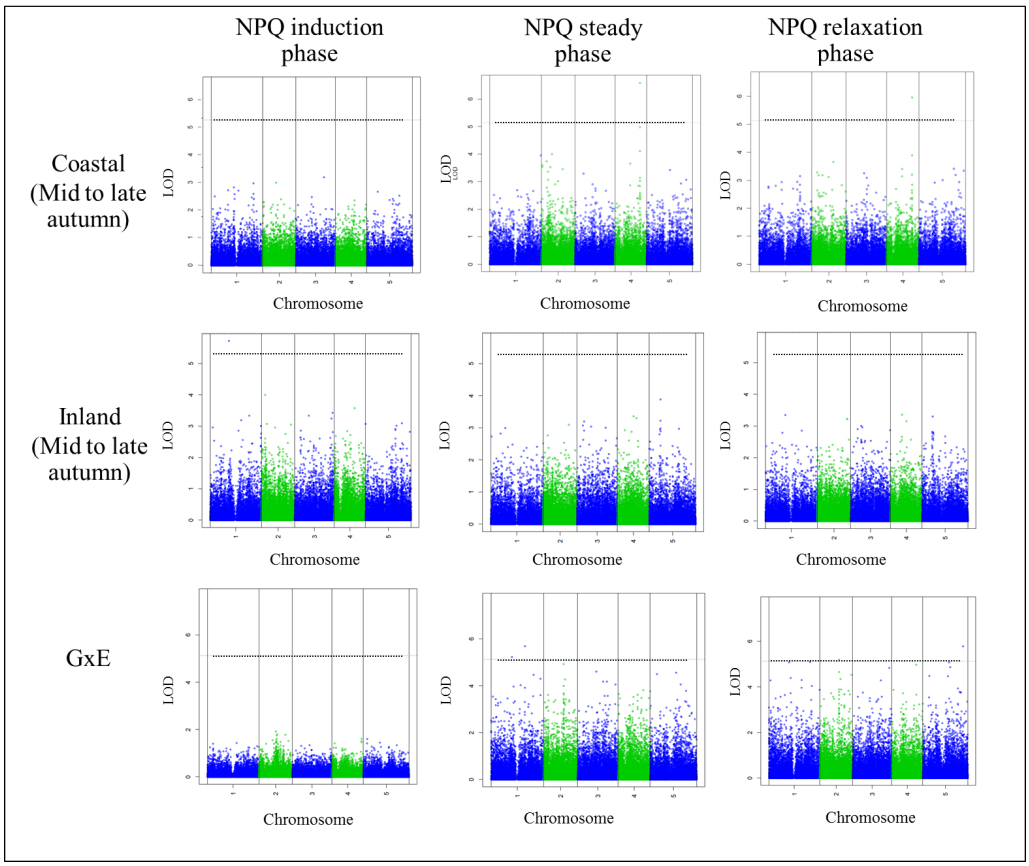

Figure 3.7 – ***Manhattan plots of GWAS results using 250K SNP database for NPQ trait at 40 days old plants. Coastal plants were grown under the Coastal for 40 days; and Inland plants were grown under the Coastal condition for 32 days, then shifted to Inland for 8 days. The chromosomes are depicted in different colors on x axis. The horizontal dash-dot line corresponds to a nominal P < 0.05 significance threshold***

3.3 DISCUSSION

3.3.1 Chlorophyll fluorescence imaging reveals non-photochemical quenching (NPQ) kinetics in *Arabidopsis* natural accessions.

The improvements in chlorophyll fluorescence measuring techniques have made fluorescence imaging an important approach to study photosynthetic function, especially of PSII (Maxwell and Johnson, 2000). A number of reviews on chlorophyll fluorescence have presented a wide range of options to study different aspects of stress under various growth conditions using different measuring methods (Ruban and Horton, 1995; Woo *et al.*, 2008; Baker, 2008; Ruban and Murchie, 2012). Non-photochemical quenching (NPQ), one of the photoprotection mechanisms, is often used as an indicator of excess light energy dissipation as heat, which occurs in the PSII antenna. Thus, NPQ responses can be observed using chlorophyll fluorescence techniques. Although it is easy to measure, if the experiments and measuring protocols are not designed correctly, it can also be difficult to interpret the results.

Several different NPQ measuring protocols have been presented in a number of different studies (Niyogi, 1998; Li *et al.*, 2004; Jung and Niyogi, 2009). Jung and Niyogi (2009) have developed a NPQ protocol of 10 minutes under actinic light followed by five minutes of dark relaxation (one minute interval of measuring pulse) to determine the qE component of NPQ. Based on this research, I tried to develop several protocols to suit a large-scale experiment, provide biologically accurate results, as well as to get uniform data from the same measuring time of the day. As a result of these experiments I was able to show that there is natural variation in NPQ among *Arabidopsis* natural accessions, and that we can distinguish between high and low NPQ capacity accessions.

First, the short protocol (P1) shown in Figure 3.2, was able to distinguish the differences in NPQ kinetics between photoprotective mutants (*npq1*, *npq4* and *lut2*) and the wild-type. However, it did not provide enough separation of the NPQ phenotype to be able to distinguish between different growth conditions and at different stages of the NPQ process (i.e. induction, steady state and relaxation). The maximum NPQ was not obtained within the one minute and 30 seconds of

actinic light in the measurement. Moreover, the measuring pulse intervals were not sufficient to measure the induction component, due to its relatively fast induction and relaxation kinetics on the time scale of seconds to minutes (Niyogi *et al.*, 2001; Li *et al.*, 2002). Thus, as the P1 protocol was not suitable for high-throughput screening of differences between natural accessions, the P2 protocol was developed.

The P2 protocol was designed to increase the length of actinic light exposure such as to ensure all plants reached maximum NPQ. This protocol had 15 minutes of actinic light followed by five minutes dark relaxation with one minute intervals of the measuring pulse, compared to the 10 minutes of actinic light in the Jung and Niyogi protocol. As shown in Figure 3.3, the P2 protocol reveals the difference of NPQ kinetics between low light and high light grown plants. High light plants showed acclimatised to excess light, as observed by the fast induction of NPQ compared to low light plants. However, when comparing the results from the P2 protocol to Jung and Niyogi's protocol (Jung and Niyogi, 2009) where growth conditions were different, NPQ capacity in most accessions was lower and induction of NPQ formation was slower. A possible explanation for this phenomenon is that Jung and Niyogi's measurement was performed on individual attached rosette leaves, while the P2 protocol was measured on the whole plant. Hence my measurements were the average results of the whole rosette, incorporating leaves of a range of ages. In addition, the differences at the earlier stage of NPQ induction were observed using the P2 protocol. NPQ in the first minute was two-fold higher in high light plants than in low light plants.

To improve resolution of the differences in induction of NPQ between the environments, the P2 protocol was modified by adding more measuring time points at the start of the actinic light period and at the start of dark relaxation period. This provided more insight into qE, because the qE component is quickly inducible and reversible within seconds or minutes (Jung and Niyogi, 2009), as seen in Figure 3.4. Moreover, a part from the differences in NPQ kinetics observed between two growth conditions, differences between genotypes were also observed.

In such a manner, it is possible that using the P3 protocol can help to use natural variation to understand the biological basis of the fast increase in the NPQ

capabilities of plants grown under excess light as compared to low light plant. Moreover, the P3 protocol allows up to 300 plants to be measured with out presenting diurnal variation effects. There are several studies on diurnal variation in NPQ levels in rice, maize, freshwater algae and moss (Roach et al., 2015; Ishida et al., 2013; Ding et al., 2006; Hamerlynck et al., 2000). These studies suggest that NPQ is lower in the morning and evening. NPQ will increase at noon correlation to the increasing of irradiation resulting from diurnal effect. Therefore, the chlorophyll fluorescence measurements in this thesis were performed during highest irradiation of the day (between 12.00 - 16.00) to obtain the highest NPQ levels. Also, the experiments were designed to have a control plant (Col-0) in every tray. The variation of the control plant (Col-0) shows non-significant different in NPQ levels that were measured from 12.00 to 16.00.

3.3.2 Simulated natural climates can provide insight into for natural variation in NPQ and genetic basis

Environmental conditions have a large effect on plant growth and development. Plants exhibit high phenotypic plasticity in many traits as they respond to their natural habitat in order to survive (Pigliucci, 2002; Alonso-blanco *et al.*, 2009). The main rationale for performing experiments in controlled climate chambers simulating natural environments is to minimise variations in the measured traits apart from those due to applied treatments and to obtain knowledge on natural variation in photoprotection. Johansson Jänkänpää (2011) and Mishra *et al.* (2012) found that NPQ was higher in field grown plants compared to plants grown in traditional growth chambers, and variation between accessions was much larger in the field. This could be the result of unpredictable changes in the environment including light intensity, temperature, and higher light intensity in the field. Increasingly, there is evidence supporting the idea that growing plants under control condition with simulated natural climates can provide valuable complementary information on how plants respond (adapted/acclimated) to natural conditions in the field (Zhang *et al.*, 2012). In this Chapter, I have described optimisation of growth conditions that can distinguish NPQ kinetics between accessions and also differences between accessions, responses to contrasting climatic conditions.

Accessions with a 2-fold increase in qE capacity within one minute of actinic light exposure were observed in high light adapted plants (Inland condition). This demonstrated that excess light intensity activates the qE capacity in wild-type *Arabidopsis*, as well as in mutants, supporting that qE depends upon duration of light exposure (Niyogi *et al.*, 2001). These results are consistent with the idea that variations in NPQ capacity are responsible for specific environment induced differences in qE formation observed in nature (Müller *et al.*, 2001; Alter *et al.*, 2012). In-depth discussion on how coastal and inland conditions revel different NPQ patterns is presented in Chapter 5. In addition, using simulated natural climate conditions allowed the wider rang of NPQ capacity to be observed (Johansson Jänkänpää, 2011) as well as the variation at the induction and relaxation phase, which could not be seen under standard growth conditions (Jung and Niyogi, 2009; Li *et al.*, 2009).

Together, these results, show distinct acclimation responses of all natural accessions to Coastal and Inland climates. This strongly suggests the involvement of light intensity, duration and temperature in adjusting photoprotective mechanism to different levels, especially in NPQ as shown in Figure 3.5. The combination of low temperature (5 °C) and continuous increases in light intensity (up to 350 μmol m$^{-2}s^{-1}$) in the morning in the Inland-Spring conditions may affect plant development after germination of *Arabidopsis* natural accessions, which can be observed in the very poor percentage of surviving plants. This might be because the seedling are very sensitive to the extreme stress at the earlier stages of plant development (Suorsa *et al.*, 2012). This is also due to the high levels of photo-damage and a lack of photoprotective mechanisms in young stressed plants (Havaux *et al.*, 2000). In contrast, the warmer Coastal condition seedling were able to grow and develop much better as observed in the higher percentage of surviving plants. Survival was much greater in the Autumn conditions where the conditions were mild during earlier development but there was an increase in stress conditions as time went on.

Relatively high heritability observed at the middle of vegetative growth stage (35 days) for most of photoprotective parameters. This is similar to a study conducted by Rooijen et al (2015) which found heritability greater than 50% for photosynthetic light use efficiency in 12 accessions. A similar result was reported by Li *et al.*, (2010) using 473 accessions (HapMap set) which showed a

very high heritability for flowering time within the same condition with an average of 98%, while there was slightly lower heritability observed for yield with the average greater than 50%. The dramatic decrease in heritability in 45-day-old-plants was observed in both conditions in comparison to younger plants. This could cause by plant transition to senescence stage and more sensitive to environmental change. Therefore, when performing QTL and GWAS analysis, the decline of heritability in the older plant could be considered, as it might reduce the power to detect QTL.

3.4 SUMMARY

The first aim of this chapter was to optimise the chlorophyll fluorescence measuring protocols. Testing of a variety of the chlorophyll fluorescence measuring protocols showed that eight minutes of actinic light followed by three minutes of dark relaxation, the (P3) protocol, was the most promising protocol for investigating NPQ kinetics, which can then be used to further understand the NPQ mechanism in *Arabidopsis*. This protocol is also suitable for chlorophyll fluorescence screening of 300 plants in a day, when starting the measurement at mid-day and finishing before sunset.

The second aim of this chapter was to establish growth conditions for studying natural variation in photoprotection, with a particular focus on the effect of environment on NPQ. Natural variation in NPQ was observed under the Coastal condition, and also after switching to the Inland condition. The NPQ kinetics changed in response to the different growth conditions. Candidate genes, however, were not identified using this shifted environment. There are two possible reasons that causative SNPs could not be identified, despite the diversity of NPQ values measured. This might be due to damage to the plants from the environmental shifting, for instance if they didn't have sufficient time to recover from the shock of the sudden stress. Alternatively, using only 150 natural accessions might not provide enough genetic resources to reveal the genetic architecture of NPQ under these conditions, even though there are a lot of variation for this trait under simulated conditions. These results suggest that the success of finding the new candidate gene can depend on the growth conditions and developmental stage, as it can affect the expression of genes.

Two alternative approaches to study naturally occurring genetic variation will be further explored in Chapter 5.

Chapter 4

Exploration of photoprotective mechanisms in *Arabidopsis* RIXs population

4.1 OVERVIEW

A mapping population can be used to identify sequence variants causal for natural variation in photoprotection by identifying quantitative trait loci (QTL) responsive to NPQ. In many systems, including *Arabidopsis*, an effective way to identify QTL uses recombinant inbred lines (RILs) (Balasubramanian *et al.*, 2009). RILs can be generated by first crossing between two inbred accessions to get F1. Then the F1 seeds are grown and self-fertilized to produce F2. The F2 seeds are then grown individually and self-fertilized to produce F3. Single seed descent (SSD) is then performed across multiple generations to produce F7 seeds (Loudet *et al.*, 2002; Balasubramanian *et al.*, 2009). After this, individual progeny of the F7 RILs represents a new inbred line with > 98% homozygosity, albeit a combination of the two parents. A special advantage of RILs is that they need to be genotyped only once for multiple propagating and phenotyping (Broman, 2005). QTL discovery with RILs has been successfully employed in many traits such as flowering time (Loudet *et al.*, 2002; Balasubramanian *et al.*, 2009), the phytochrome-mediated response (Magliano et al., 2005), seed dormancy (Bentsink *et al.*, 2010) and root development (Svistoonoff *et al.*, 2007). More than 60 Arabidopsis RIL populations have already been developed and are available from the stock center (http://arabidopsis.org) (Bergelson and Roux, 2010).

One of most well-characterized RIL populations derives from the Cape Verde Islands (Cvi-0) and Landsberg erecta (L*er*) accessions. Published studies have exploited the Cvi-0 x L*er* RILs for identification of novel allelic variation for more than 40 traits (Koornneef *et al.*, 2004). One of the most outstanding characterizations from the Cvi-0 x L*er* RILs is the isolation of the *EDI* allele of the *CRY2* photoreceptor which account for the difference in flowering time (El-Assal *et al.*). The Cvi-0 accession is genetically distinct from most accessions because of its isolated origin (Nordborg *et al.*, 2005), thus, it is a good resource to scan for natural genetic variation in many traits. Although RIL populations present a unique combination of parental genotypes, the large QTL size resulting from RIL populations results in challenges in identifying and confirming candidate genes. RIL populations typically define QTL regions of a few megabases covering thousands of genes due to a low number of recombination events in the original cross (Price *et al.*, 2006).

Another approach to studying natural variation is using recombinant inbred intercross lines (RIXs) which have been reported to provide more sensitive detection of QTL responsible for complex traits than RILs (Zou *et al.*, 2005; Rockman and Kruglyak, 2008). To create a RIX population a set of RILs is intercrossed to produce multiple F1 progeny per RIL (Figure 4.1). As a result, although RIXs are also derived from two parental lines, the same as RILs, RIXs have an increase in the number of recombination site in comparison to RILs (Zou *et al.*, 2005). This is beneficial because it increases the resolution of QTL and thus reducing the number of non-causative genes in the region. In contrast to RILs, the replicates within a line of RIXs have identical genotypes but share only half their genetic composition with other lines. Given the advantages above, Cvi-0 x L*er* RIXs were generated by collaborator Joost Keurentjes at Wageningen University to provide sensitive detection of QTL in such complex traits as NPQ. In *Arabidopsis*, this approach represents a powerful alternative method to classical genetics studies because the small size of the *Arabidopsis* genome, combined with its complete sequencing, makes it possible to follow-up QTL mapping and allowing the identification of the causative allele more easily.

This chapter reports the natural genetic variation in non-photochemical quenching (NPQ) using Recombinant Inbred Intercross lines (RIXs) between Cape Verde Islands (Cvi-0) and Landsberg (L*er*), Cvi-0 x L*er* RIXs, under a variety of growth conditions. This was achieved through the observation of NPQ by chlorophyll fluorescence imaging. QTL mapping was then undertaken to identify loci that determine natural variation for the NPQ phenotype.

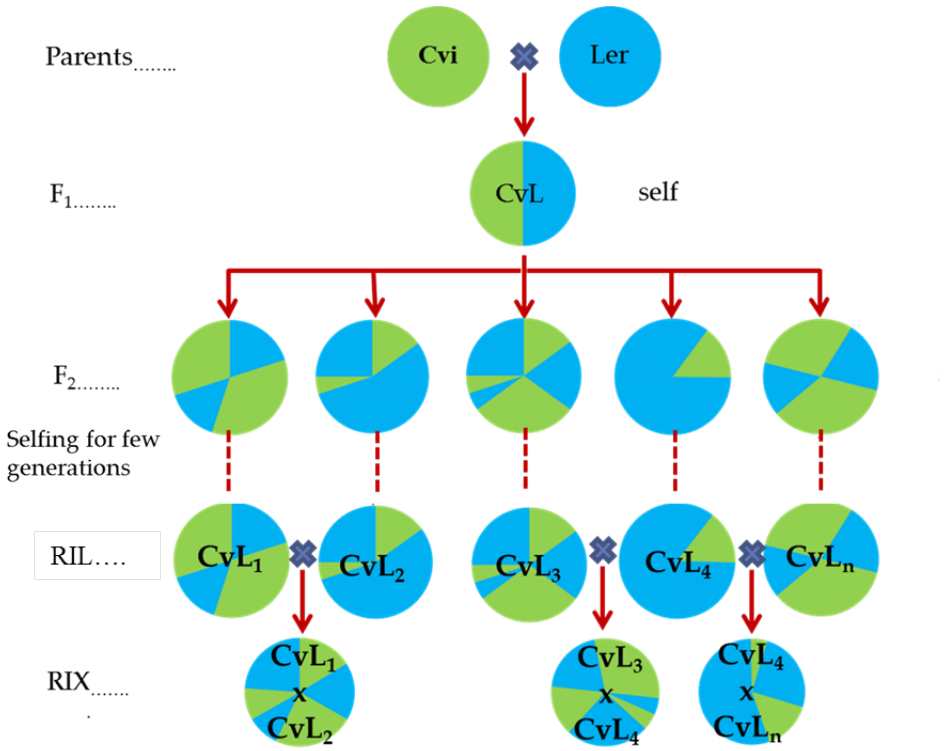

Figure 4.1 – *Diagram shows production of Cvi-0 x Ler RIXs population. Cvi-0 x Ler RIXs are generated by producing F1 hybrids between recombinant inbred lines between Cvi-0 and Ler.*

4.2 RESULTS

4.2.1 Natural variation in NPQ in the Cvi-0 x L*er* RIXs population

Significant variation in the NPQ response between accessions under various growth conditions was observed in Chapter 3. This suggested that there is natural variation in the NPQ phenotype among different accessions and that this variation is affected by environment. To further investigate natural variation for NPQ, 92 recombinant inbred intercross lines between Cvi-0 and L*er* (Cvi-0 x L*er* RIXs) were grown under five different conditions as presented in Figure 4.2. The simulated natural conditions used in this chapter were different from the conditions used in Chapter 3, as it was designed to extend the investigation of NPQ under several excess light and environmental stresses. In this chapter, five simulated natural conditions were designed: three coastal simulated conditions with diurnal and seasonal changes, low light (max. 150 μmol $m^{-2}s^{-1}$), excess light (max. 500 μmol $m^{-2}s^{-1}$), and fluctuating light (5 minute interval between a maximum 150 and 500 μmol $m^{-2}s^{-1}$), the other two simulated coastal and inland, of which inland represented more extreme temperature range (between 5 °C - 20 °C) compared to coastal (between 10 °C - 25 °C). The summary of these five conditions was presented in Table 4.1.

Table 4.1 – *Simulated growth condition of the Cvi-0 x Ler RIXs experiments.*

Experiment	Population	Growth conditions	Maximum light intensity (µmol $m^{-2}s^{-1}$) [C]	Max. dynamic Temp. range (°C) (day/night)
Exp II	Cvi-0 x L*er* RIXs	Excess light	500	25/15
		Sufficient light	150	25/15
		Fluctuating light	150-500	25/15
		Coastal	160	25/10
		Inland	350	20/5

* Plants were grown under LEDs light

** Note, maximum light intensity available was 500 µmol $m^{-2}s^{-1}$

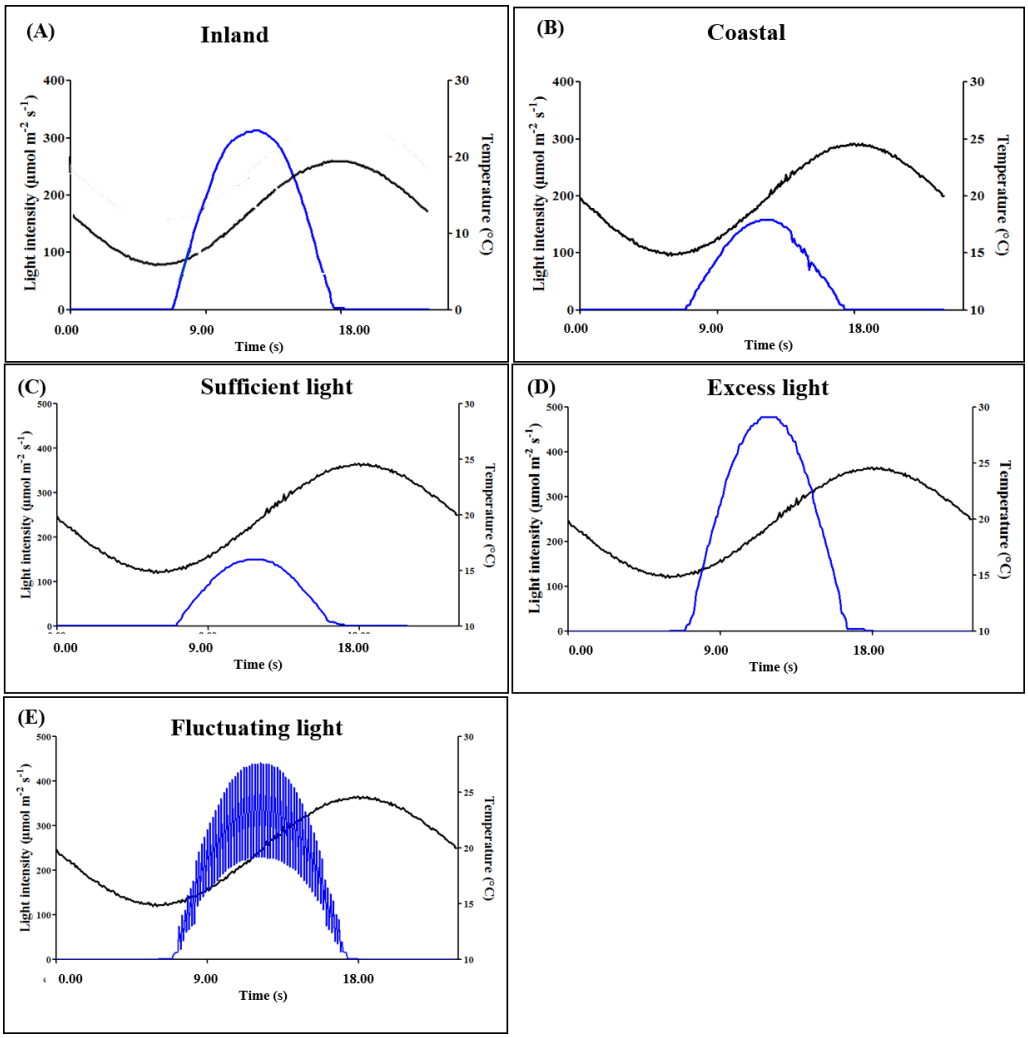

Figure 4.2 – *Diagram shows five different growth conditions used in the Cvi-0 x Ler RIXs experiments. Inland (A), coastal (B), sufficient light (C) , excess light (D), and fluctuating light (E) were simulated SolarCalc software as described in Chapter 2. Each plot represents the first day of simulated conditions.*

The variation in NPQ responses of the RIX population after 35 days in the growth conditions is shown in Figure 4.3. Two different protocols were used in this experiment (protocol P3 and the extension of ExP3). The P3 protocol which was descripted in Chapter 3 was used to measured chlorophyll fluorescence of plants under sufficient, excess, and fluctuating light conditions. The ExP3 was developed from P3 by adding more timepoints during the actinic light measurement; and it was used in coastal and inland conditions. Different trends of NPQ production were observed in plants grown under coastal simulated condition and sufficient light environment as shown in Figure 4.3. The NPQ formation patterns at steady phase were also different among conditions. Under low light intensities (sufficient light and coastal conditions), NPQ slightly increased at the steady state phase, while under excess light (fluctuating light and inland conditions), NPQ levels declined slowly.

The variation in maximum NPQ of the Cvi-0 x L*er* RIXs population was measured in five growth conditions, as shown in Figure 4.4. The maximum NPQ levels of plants grown in the inland conditions show the highest range (between 2.4 - 3.2) compared to the other four conditions, whereas the coastal condition resulted in the lowest range (between 1.8 and 2.5). Similar trends in NPQ levels were observed under excess, sufficient, and fluctuating light conditions ranging between 2 - 2.9, 2.3 - 3.2, and 2.1 -3 respectively. For the parental accessions, Cvi-0 and L*er*, maximum NPQ accumulation fell in the middle of NPQ range in all five growing conditions. The results presented considerable variation in response to five growth conditions along with transgression, suggesting that multiple loci contribute to NPQ variation in Cvi-0 x L*er* RIXs population.

The different distribution of NPQ production at induction, steady state and relaxation phase were observed between growth conditions as shown in Figure 4.5. The induction phase can be described as the period from the start of measurement to the 120s time point. Plants grown under excess light, fluctuating light and the inland environment had rapid NPQ production at the induction phase (where maximum NPQ levels were observed in stressed plants) with the average of NPQ at 2.34, 2.38 and 2.47 respectively (Figure 4.5). Those three conditions showed much higher NPQ levels (average from all RIX lines) compared to plants grown under sufficient light and coastal at induction phase, which ranged between 2.26 and 2.02 respectively. After 120 seconds NPQ enters a steady phase

where the maximum NPQ level are normally observed in non-stress plants. The highest level of NPQ were observed in the plants grown under sufficient light with levels much higher than at the end of the induction phase. However, under the stress conditions of excess light and inland condition, NPQ levels were decreased in the steady state as compared to the end of the induction phase. There was no difference in NPQ kinetics at the relaxation stage between the different treatments.

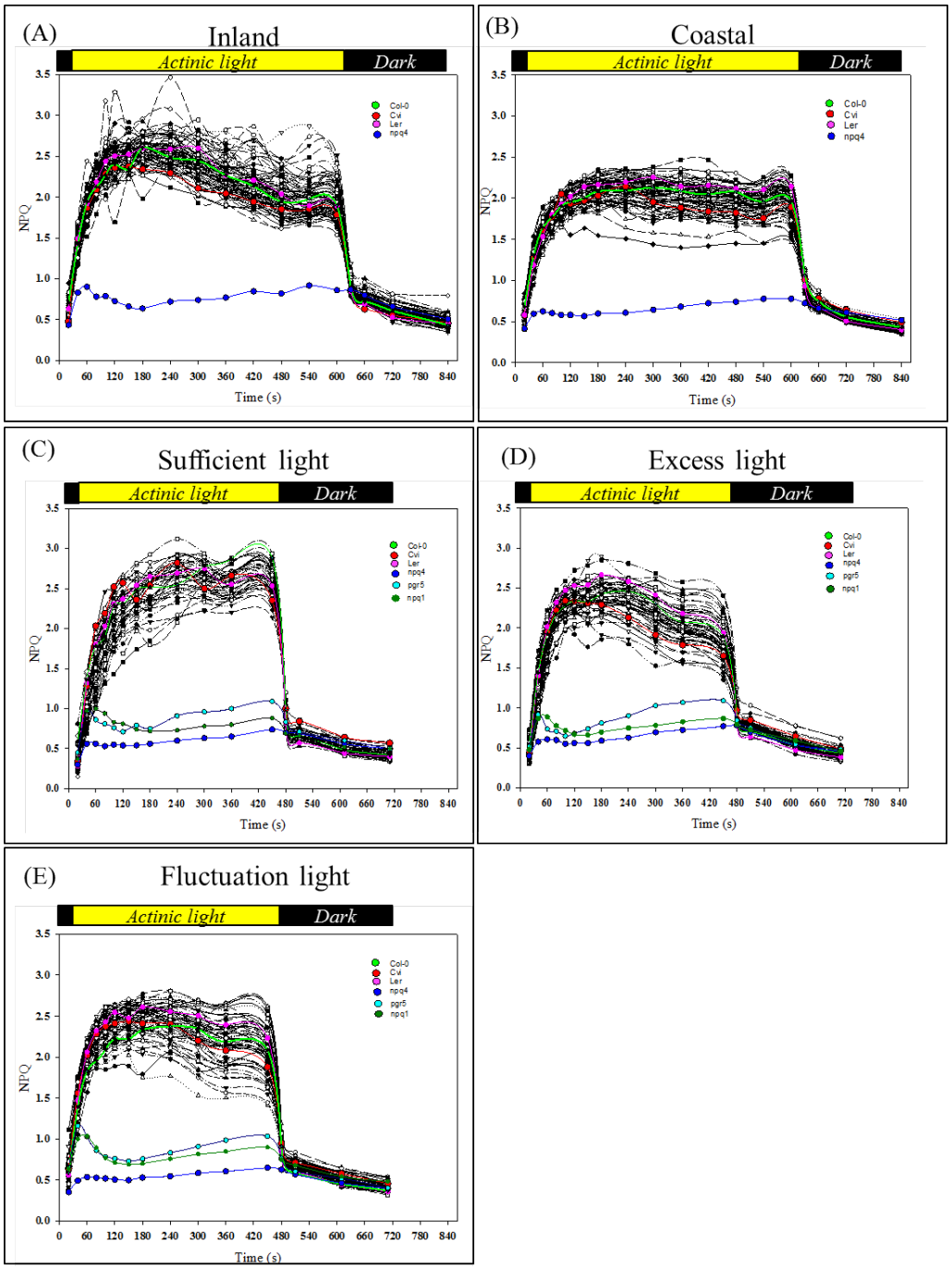

Figure 4.3 – *Natural variation in NPQ capacity of CvL RIXs population and mutants (npq1, npq4 and pgr5) grown under five different light regimes. Graphs represent NPQ kinetic of plants grown under (A) inland condition (max. 350 μmol $m^{-2}s^{-1}$), (B) coastal condition (max. 150 μmol $m^{-2}s^{-1}$), (C) sufficient light (max. 150 μmol $m^{-2}s^{-1}$), (D) excess light (max. 500 μmol $m^{-2}s^{-1}$), and (E) fluctuating light (light fluctuate between a maximum of 150 and 500 μmol $m^{-2}s^{-1}$).*

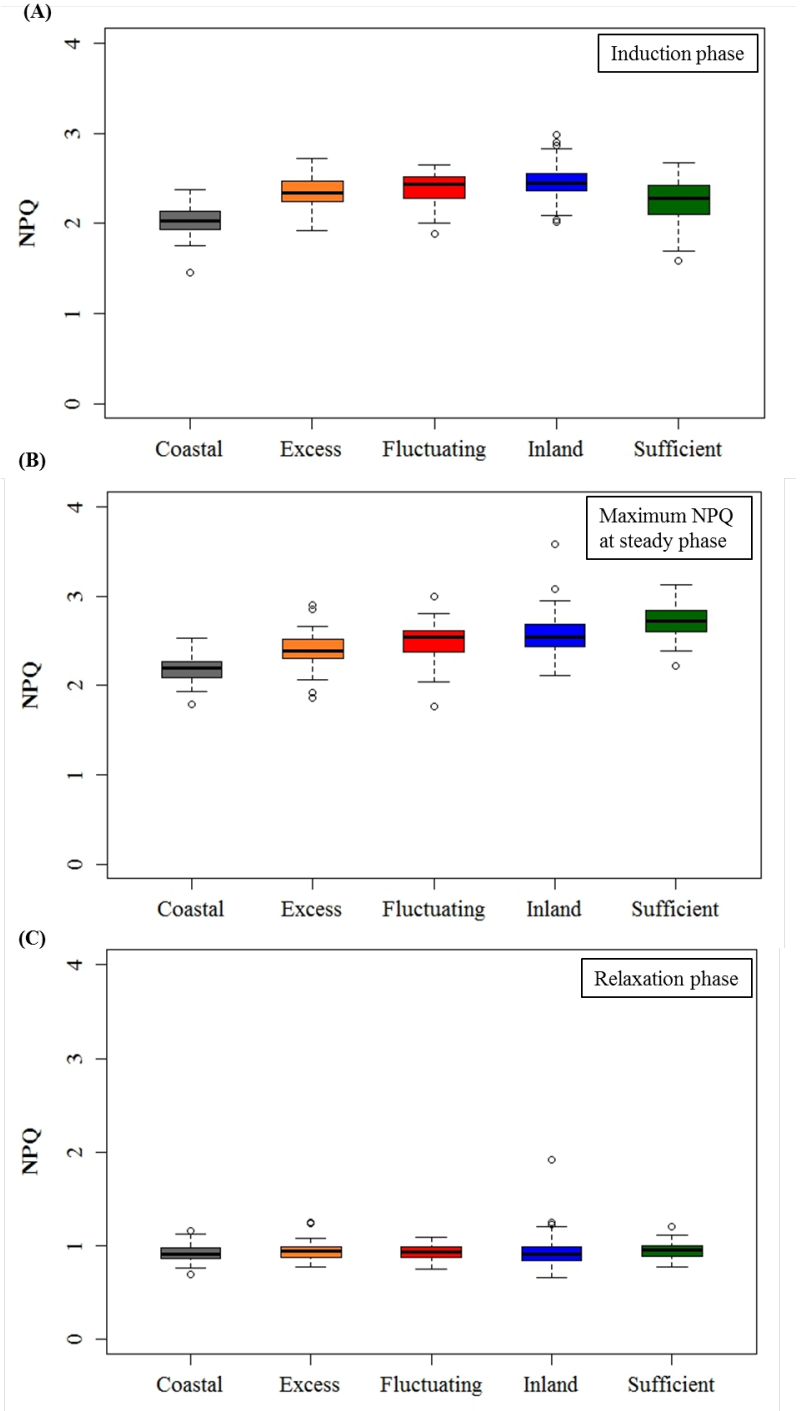

Figure 4.4 – *Variation in maximum NPQ of the Cvi-0 x Ler RIXs population in response to five different growth conditions, sufficient light (A) (dark green colour), excess light (B) (orange colour), fluctuating light (C) (red), coastal (D) (gray colour), and inland (E) (blue colour). Histogram showing the distribution of mean maximum NPQ (n = 3) among Cvi-0 x Ler RIXs, Cvi-0 and Ler for each condition examined. Coloured arrows indicated the NPQ value of parental lines (Cvi-0 and Ler).*

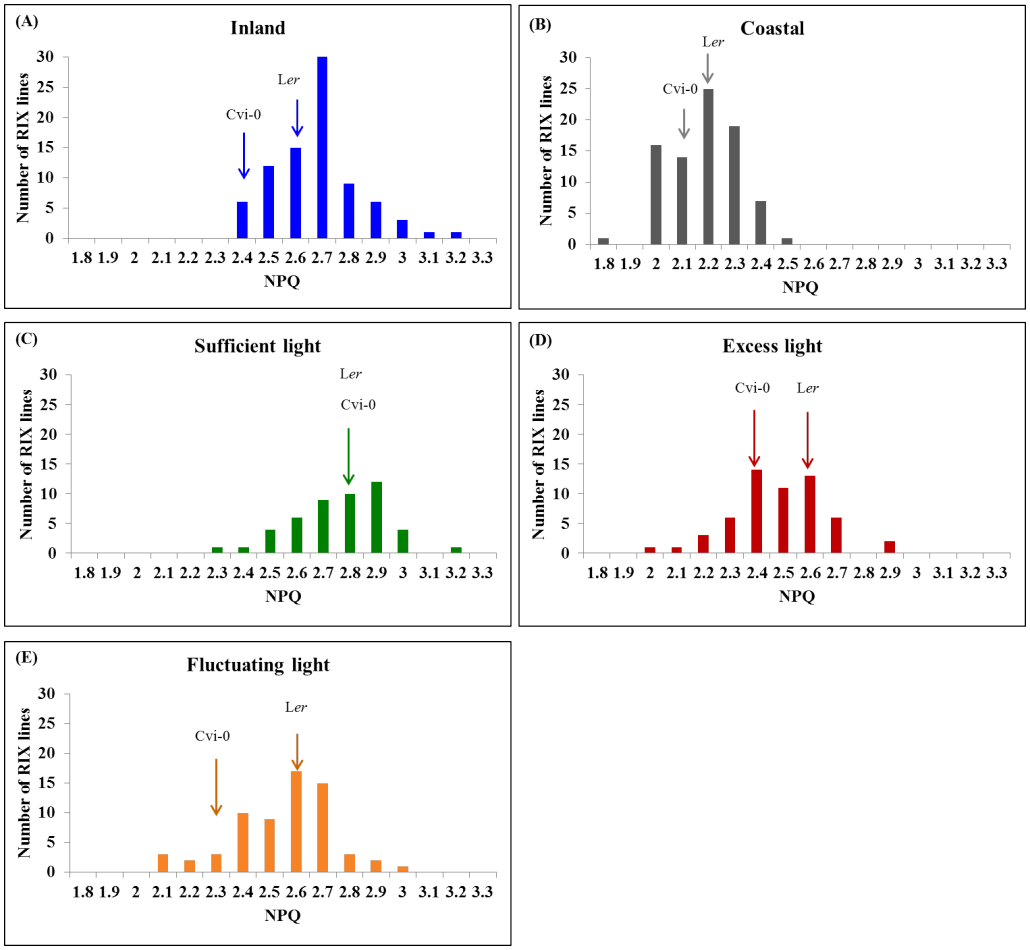

Figure 4.5 – *Distribution in NPQ of the Cvi-0 x Ler RIXs population in response to five different growth conditions, coastal (gray colour), excess light (orange colour), fluctuating light (red), inland (blue colour) and sufficient light (dark green colour).*

4.2.2 Quantitative trait loci (QTL) for NPQ

To investigate how variation in non-photochemical quenching (NPQ) is controlled, quantitative trait loci (QTL) analyses were performed in *Arabidopsis* recombinant inbred intercross lines (RIXs) by analysing using a mixed model QTL approach. The analysis was done by Riyan Cheng (Postdoctoral Scientist, Borevitz Lab, ANU). From the evidence above (Figure 4.5), NPQ variation is a multigenic trait and QTL analysis is required to identify and map the corresponding QTL. The QTL were calculated at each time point from 20 - 600 seconds under the five environments, and a summary of significant markers is presented in Table 4.2. The candidate genes are presented in Table C1.

Under excess light, three significant QTL for NPQ were identified during the ac-

tinic light illumination, as shown in Figure 4.6. ***RIX QTL1-1***, were detected at the top of chromosome 1 at 150s with CRY2 and ARX-1 markers located at this QTL. At the bottom of chromosome 2, ***RIX QTL2-2*** was identified at 60s with the marker MSAT2.22. At the middle of chromosome 5, ***RIX QTL5-3*** was detected at 180s which is the location of the DF.77C marker. However, no significant QTL for NPQ at dark relaxation period were detected.

Under the fluctuating light, QTL for NPQ were detected and located on chromosome 1, 2, 3 and 5 during actinic light illumination and dark relaxation period as shown in Figure 4.7. Two QTL (***RIX QTL2-1*** and **RIX QTL3-1**) were found to be significant at the early time point of the NPQ kinetics (40s, 60s, and 100s). Two QTL were identified at steady state of NPQ (***RIX QTL1-1*** and ***RIX QTL5-3***). The ***RIX QTL5-3*** was also detected at the dark relaxation phase as well as ***RIX QTL3-4***.

For plants grown in sufficient light, Figure 4.8 presents one strong QTL for NPQ at the top of chromosome 3, ***RIX QTL3-2***, which was detected at the early state of NPQ induction (20s, 40s, 60s, and 80s). The same markers, EC.83C, AD92L, and GD.318C, were presented to overlap among these four time points.

Under coastal environment, ***RIX QTL3-1*** appeared at the induction phase at 4 time points (20s, 40s, 60s, and 80s), as shown in Figure 4.9. ***RIX QTL 5-1*** presented as highly significance at the steady state of NPQ kinetics. It was presented at 150s, 180s, 240s, 300s, 360s, and 450s of actinic light illumination. This QTL was located at the middle of chromosome 5 which has two strong markers, GH.473C and BH.180C, and was present at all time points. In addition, one QTL, ***RIX QTL1-2***, was detected at the first time point of relaxation phase.

Under inland condition, at the induction state (20s, 40s, 60s, and 100s) ***RIX QTL3-1*** was detected with the DF.77C marker appearing at several time points. ***RIX QTL3-3*** was also identified at the induction phase at 20s and 40s as shown in Figure 4.10.

Two significant QTL, ***RIX QTL1-2*** and***RIX QTL3-3***, for the genotype and envi-

ronment interaction (*GxE*) for NPQ under coastal and inland were detected at the induction phase (20s and 40s) of NPQ development, which are located on chromosome 1 and 3 respectively as shown in Figure 4.11.

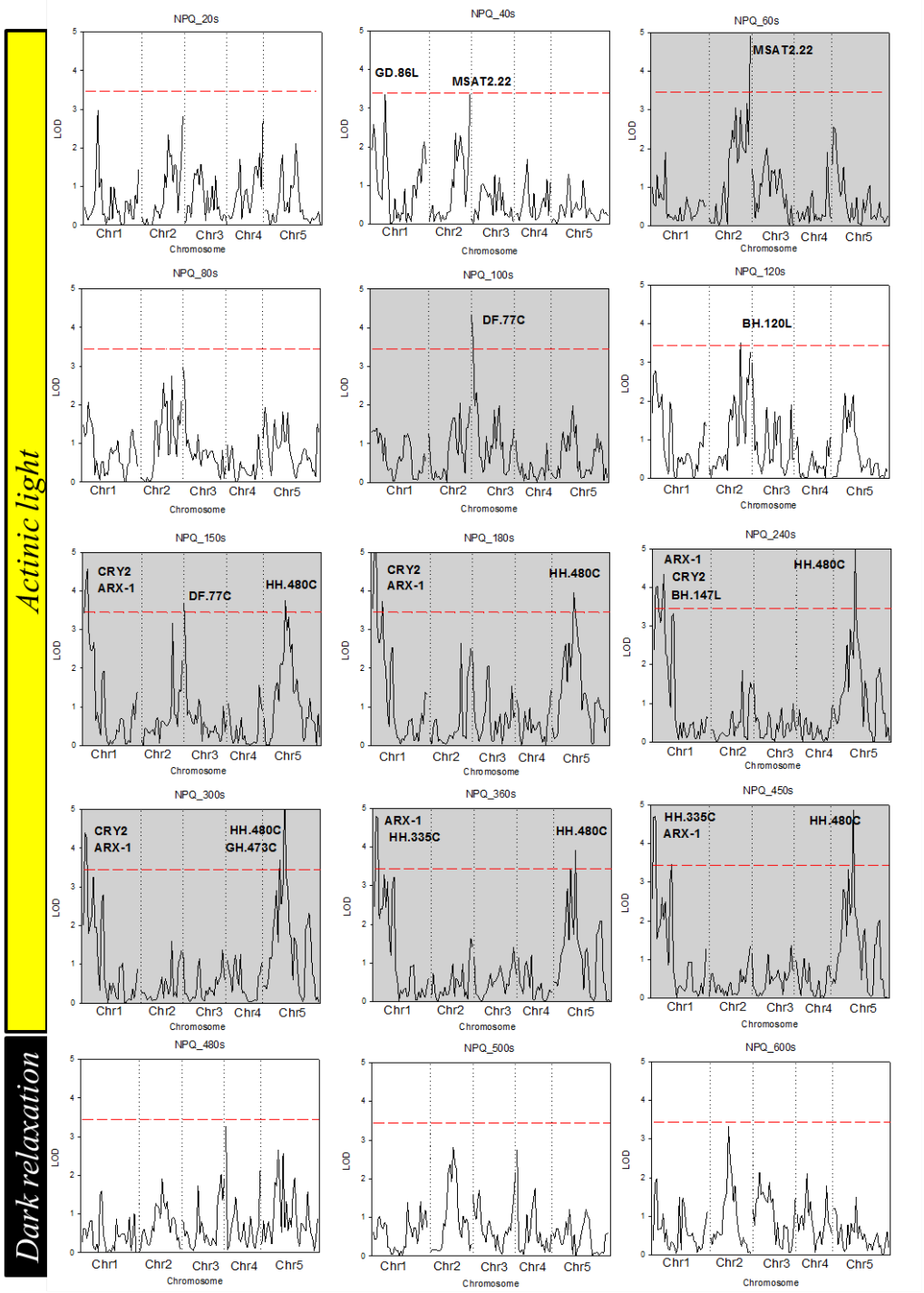

Figure 4.6 – *NPQ QTL mapping for plants grown under excess light were measured during actinic light at 20s, 40s, 60s, 80s, 100s, 120s, 150s, 180s, 240s, 300s, 360s, 450s, and during dark relaxation period at, 480s, 500s, and 600s. The horizontal line represents significance threshold (P < 0.05).*

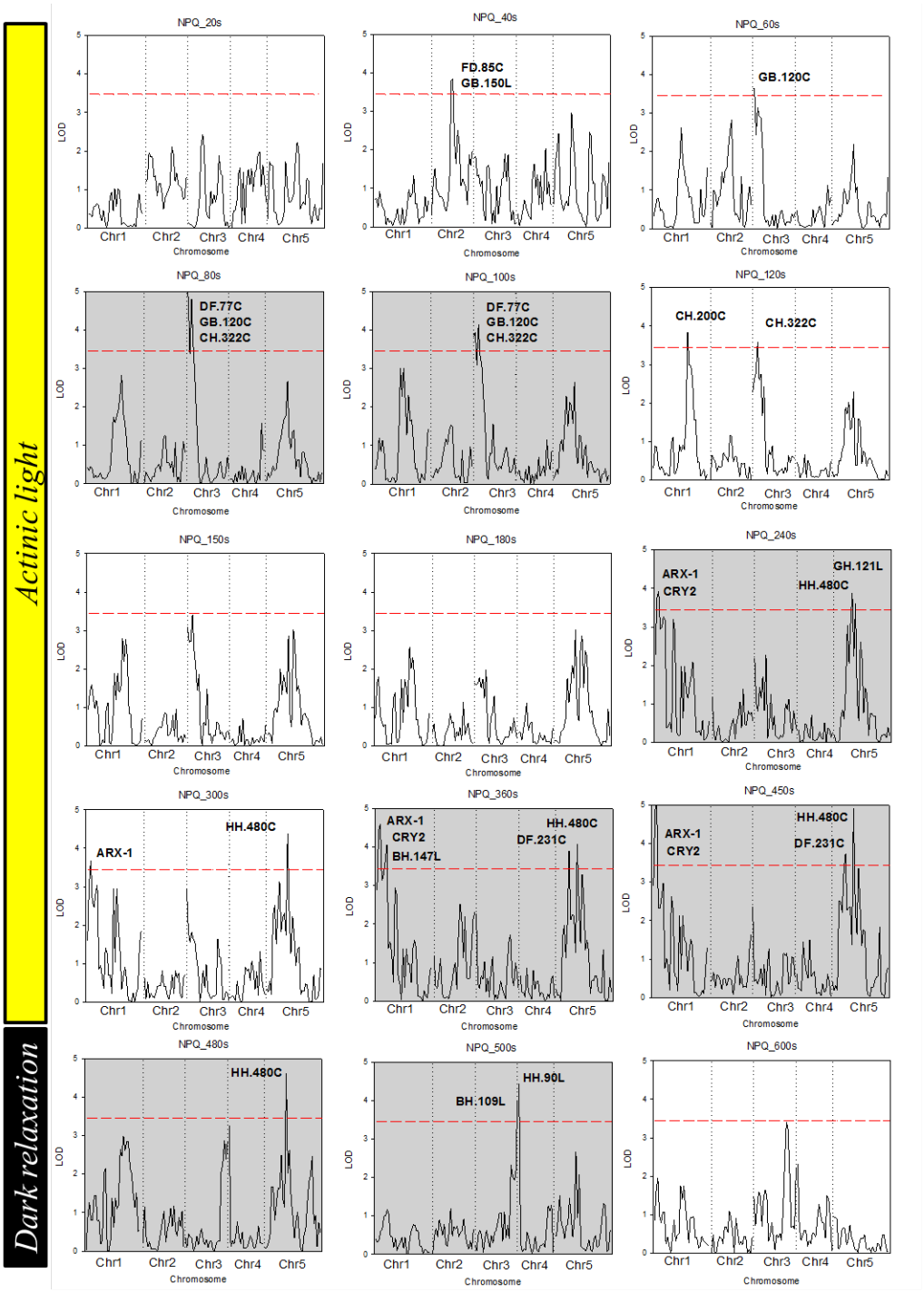

Figure 4.7 – *NPQ QTL mapping for plants grown under fluctuating light were measured during actinic light at 20s, 40s, 60s, 80s, 100s, 120s, 150s, 180s, 240s, 300s, 360s, 450s, and during dark relaxation period at, 480s, 500s, and 600s. The horizontal line represents significance threshold ($P < 0.05$).*

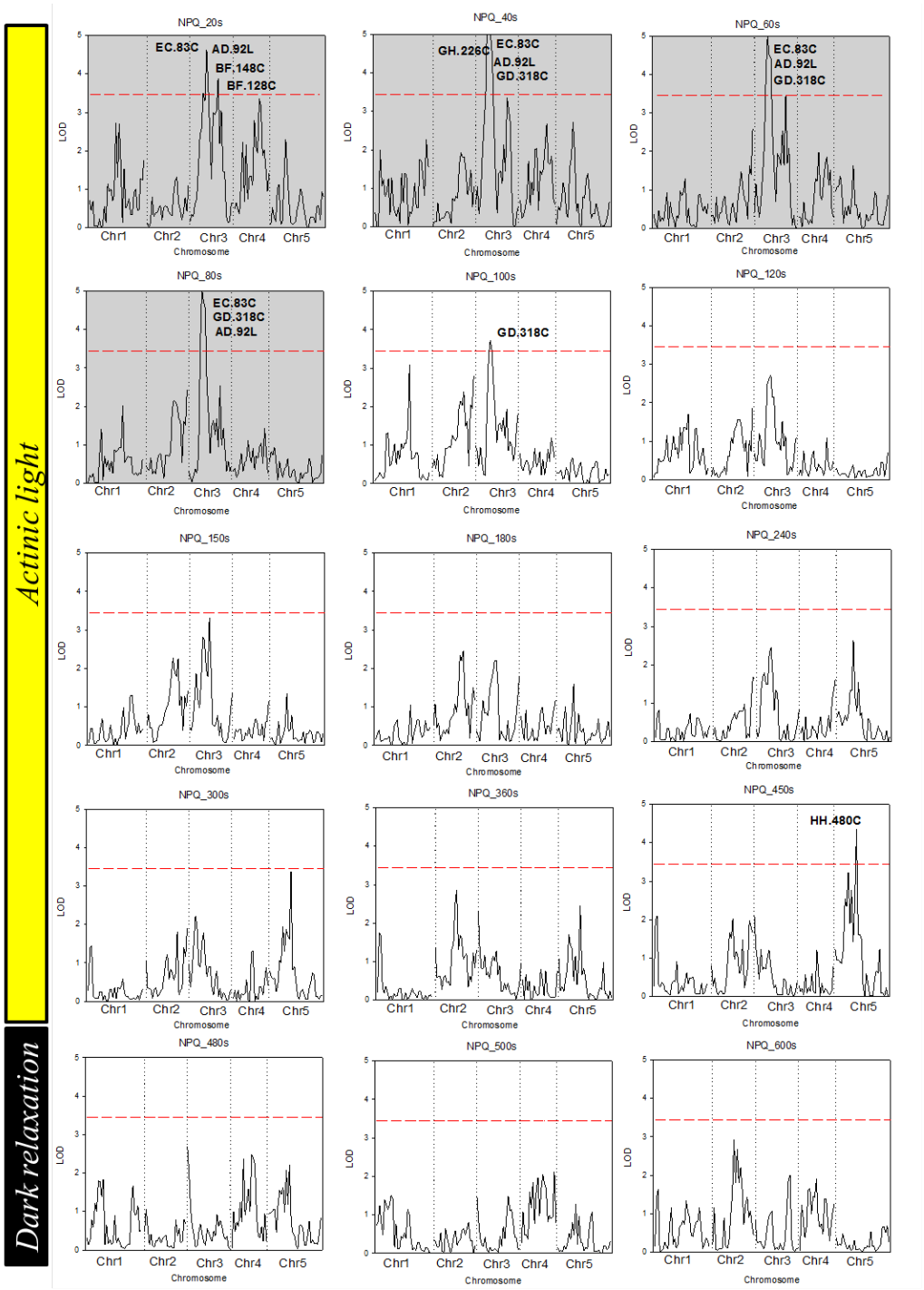

Figure 4.8 – ***NPQ QTL mapping for plants grown under sufficient light were measured during actinic light at 20s, 40s, 60s, 80s, 100s, 120s, 150s, 180s, 240s, 300s, 360s, 450s, and during dark relaxation period at, 480s, 500s, and 600s. The horizontal line represents significance threshold (P<0.05).***

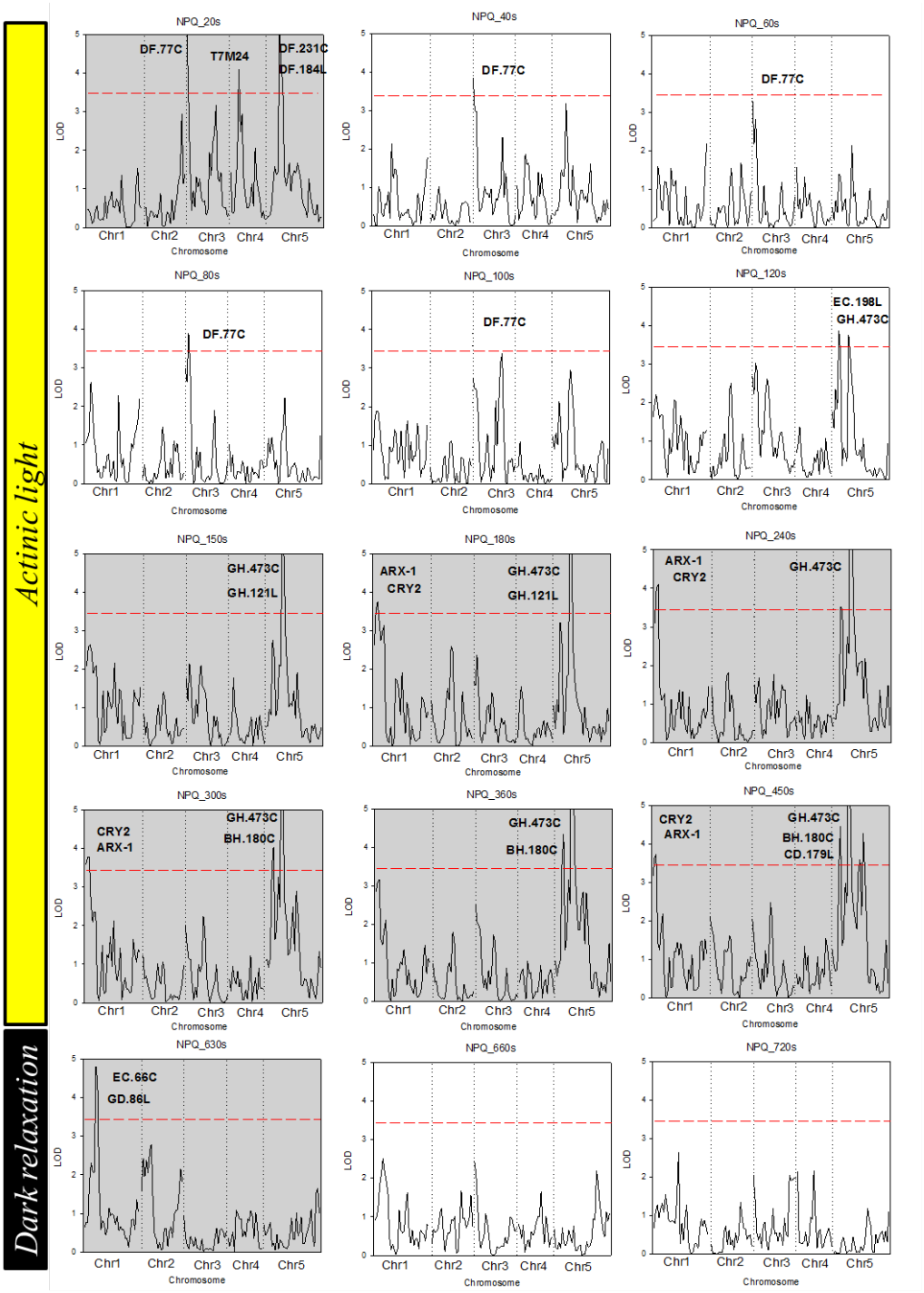

Figure 4.9 – *NPQ QTL mapping for plants grown under coastal condition were measured during actinic light at 20s, 40s, 60s, 80s, 100s, 120s, 150s, 180s, 240s, 300s, 360s, 450s, and during dark relaxation period at, 480s, 500s, and 600s. The horizontal line represents significance threshold (P<0.05).*

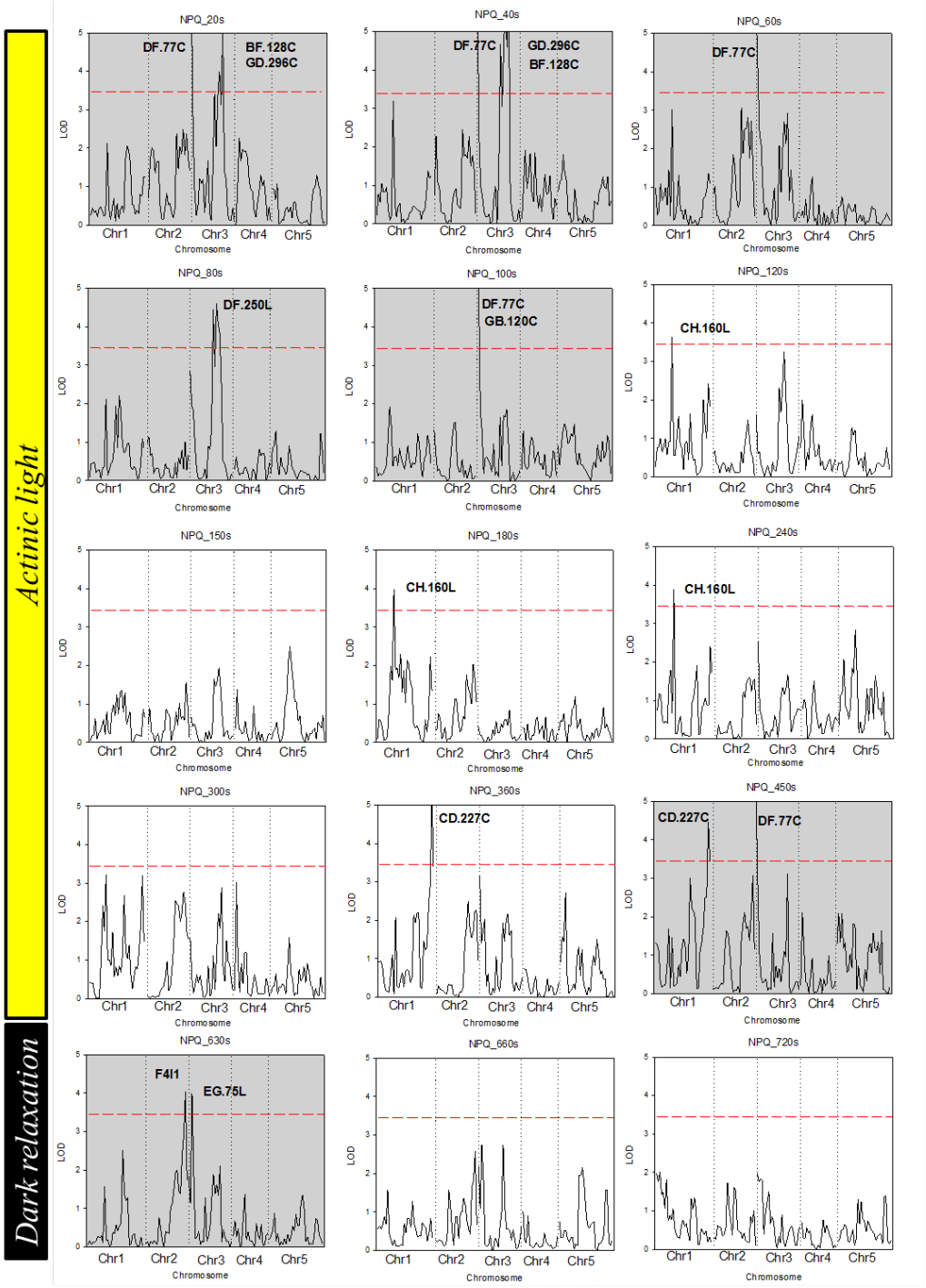

Figure 4.10 – *NPQ QTL mapping for plants grown under inland condition were measured during actinic light at 20s, 40s, 60s, 80s, 100s, 120s, 150s, 180s, 240s, 300s, 360s, 450s, and during dark relaxation period at, 480s, 500s, and 600s. The horizontal line represents significance threshold (P < 0.05).*

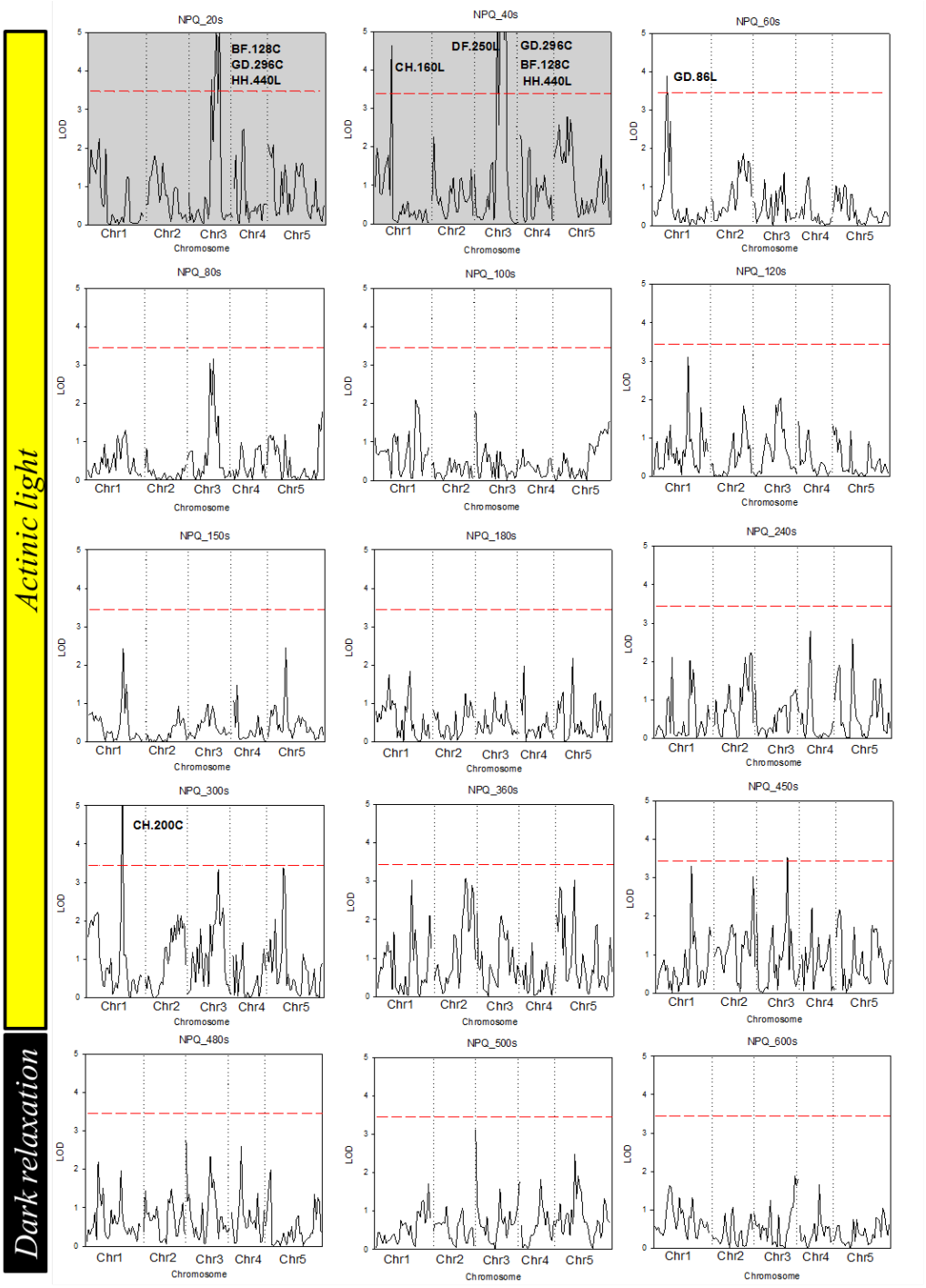

Figure 4.11 – *NPQ QTL mapping for genotype x environment (GxE) interaction. QTL analysis was undertaken for NPQ measured during actinic light at 20s, 40s, 60s, 80s, 100s, 120s, 150s, 180s, 240s, 300s, 360s, 450s, and during dark relaxation period at, 480s, 500s, and 600s. The horizontal line represents significance threshold ($P < 0.05$).*

There are a number of significant markers that appeared more than once across five growth conditions (DF.77C, CRY2, ARX-1, HH.480C, CH.473 and GH.121L) as shown in Table 4.2. Also, some of the markers, DF.77C and GB.120C, repeatedly appeared at induction and steady phase of NPQ. A total of 12 QTL for NPQ were identified in Cvi-0 x L*er* RIXs under the five growing conditions. Comparing the position of QTL and known markers has enabled the identification of candidate genes for most of the QTL. From 12 identified QTL, 76 potential candidate genes were identified. The potential genes listed in the supplementary data Table C1 are classified by two criteria, 1) located within 10 kb surrounding of the significant marker region, and 2) gene expression is in leaf tissue. From 76 candidate gene, only 6 candidate genes were found to have a known association with the photosynthesis. These 6 candidate genes are not known to have a directed effect on the NPQ mechanism, however, they may be involved in other mechanisms that are related to NPQ.

4.2.3 Quantitative trait loci (QTL) for flowering time

As many *a priori* candidate genes have been identified for the control of flowering pathways, flowering time was measured on all lines in the inland and coastal conditions as a positive control for the methods used. There was a highly significant difference between the average flowering time between the coastal and inland conditions as shown in Figure 4.12(A). Plants grown under the simulated coastal environment show an average of 4 days faster flowering time compared to plants grown under the inland environment. The majority of the RIXs population flowered at 21 days under the coastal condition, while it takes around 27 days for inland plants to flowering as observed in Figure 4.12(B). There was also greater variation in flowering time within the RIX in the coastal condition, 33 days, as compared to the inland condition, 24 days. This indicate that the cold climate and high light intensity altered the flowering time of plants grown under inland condition. The population showed transgressive segregation in both environment types with the flowering time of the parents falling within the six days of each other in both environment.

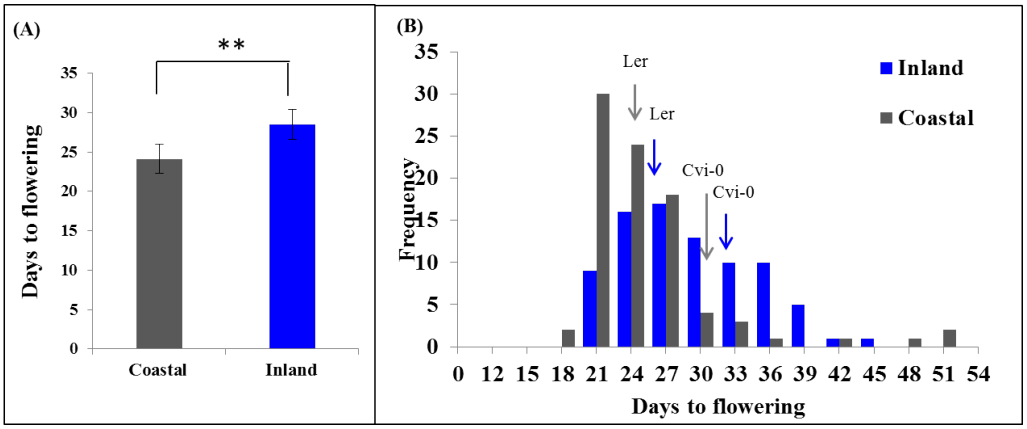

Figure 4.12 – *Variation in flowering time of the Cvi-0 x Ler RIXs population in response to two different growth conditions, coastal (gray colour) and inland (blue colour). (A) represent mean of days to flowering under inland and coastal (92 lines, n=3, ±sd). Asterisks denote statistically-significant different (∗:P<0.01). (B) represent histogram showing the distribution of mean days to flowering among the Cvi-0 x Ler RIXs lines, Cvi-0 and Ler for each condition examined (n = 3).*

To determine the genetic architecture of flowering time in the Cvi-0 x L*er* RIXs population, the flowering time data from inland and coastal were analysed by QTL mapping. Using these 92 Cvi-0 x L*er* RIXs, the flowering time QTL of plants in the simulated coastal environment were identified. There are a number of sig-

nificant markers identified as QTL located on top of chromosome 5. These flowering time QTL were found locating near FLOWERING LOCUS C (*FLC*; **At5g10140**) in the coastal condition, but it was not found in the inland condition As a known flowering time QTL was identified in this study, it validates the analytical method that have been developed by Riyan Cheng for identifying QTL for NPQ in the Cvi-0 x L*er* RIXs population.

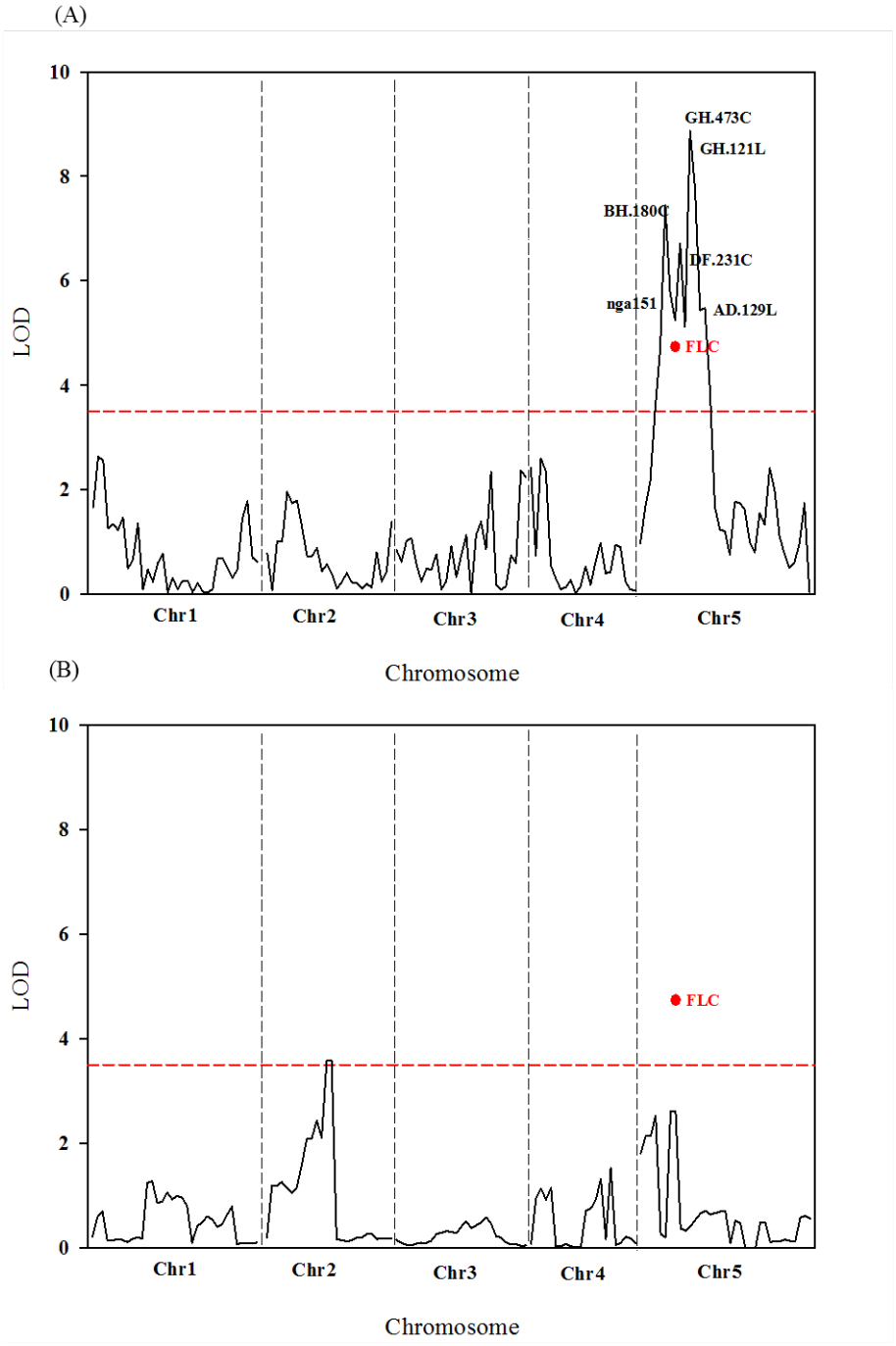

Figure 4.13 – *Results of QTL mapping for flowering time. Significant markers were found on chromosome 5 which were identified as flowering time QTL of plants grown in coastal simulated environment (A). (B) represent QTL mapping result of plants grown in inland simulated environment which no significant markers were identified. The identified flowering time QTLs were located near the FLC gene (flowering time responsive gene).*

Table 4.2 – ***Summary of QTL mapping of the Cvi-0 x Ler RIXs population. Significant markers were detected across five growth conditions and the interaction between genotype and environment (GxE). Potential loci of known photoprotective genes are shown in red colour.***

NPQ phase	Chr	Repetition	Growth conditions					GxE
			Excess light	Sufficient light	Fluctuation light	Coastal	Inland	
Induction	1		GD.86L					GD.86L
	1							CH.160L
	2		MSAT2.22					
	2				FD.85C			
	2				GB.150L			
	3	**				DF.77C	DF.77C	
	3				GB.120C			
	3			EC.83C				
	3			AD.92L				
	3			BF.148C				
	3							HH.440L
	3			BF.128C			BF.128C	BF.128C
	3						GD.296C	GD.296C
	4					T7M24		
Subtotal			2	4	3	2	3	5
Steady	1*	*	CRY2		CRY2	CRY2		
	1*	*	ARX-1		ARX-1	ARX-1		
	1		HH.335C					
	1				CH.200C			CH.200C
	1						CH.160L	
	1						CD.227C	
	2		BH.120L					
	3	**	DF.77C		DF.77C	DF.77C	DF.77C	
	3				GB.120C			
	3				CH.322C			
	5					EC.198L		
	5					BH.180C		
	5				DF.231C			
	5	*	HH.480C	HH.480C	HH.480C			
	5	*	CH.473C			CH.473C		
	5	*			GH.121L	GH.121L		
Subtotal			7	1	9	7	3	1
Relaxation	1					EC.66C		
	1					GD.86L		
	2						F4I1	
	3				BH.109L			
	3				HH.90L			
	5				HH.480C			
Subtotal			0	0	3	2	1	0
Total			**9**	**5**	**15**	**12**	**7**	**6**

* significant markers that appeared more than one growing condition

** significant markers that appeared in both induction and steady phases of NPQ

4.3 DISCUSSION

4.3.1 Natural variation in NPQ in the Cvi-0 x L*er* RIXs population under five growing conditions

In this study, the novel Cvi-0 x L*er* RIXs QTL mapping set was first studied for genetic variation in NPQ. The Cvi-0 x L*er* RIXs population presented a wider range of NPQ variation compared to their parents. This confirmed that NPQ phenotype is a quantitative trait which is controlled by multiple genes (Jung and Niyogi, 2009). As the NPQ mechanism is triggered in response to high light exposure (Osmond *et al.*, 1993; Ruban and Horton, 1995; Jung and Niyogi, 2009; Alter *et al.*, 2012), different light regimes were used in order to pull out the specific light response pattern and the candidate genes involved. The results have confirmed that NPQ is variable in response to light condition, as the Cvi-0 x L*er* RIXs responded differently under five different light regimes (Figure 4.2).

Under the sufficient light and coastal conditions, plants had limited photosynthetic capacity (Bailey *et al.*, 2004), as a result, they showed continuously increasing NPQ during the high actinic light exposure. In contrast, a different pattern was observed for plants grown under excess light, fluctuating light, and inland; which presented the rapid increases in NPQ at the induction phase as previously seen in other studies with high light exposure (Müller *et al.*, 2001; Schöttler and Tóth, 2014). After the rapid induction there was a slight decrease at the steady phase, likely resulting from a higher photosynthetic rate of high light grown plants (Schöttler and Tóth, 2014). Since Cvi-0 x L*er* RIXs displayed faster and greater induction of NPQ when grown under higher light stress conditions, this suggests improved ability of the plants to dissipate the excess light energy in the short term. This protects the plants from suffering from photoinhibition and photo-oxidative stress (Niyogi, 1999; Essemine *et al.*, 2012). This confirms that NPQ is one of the most rapid responses which can improve photoprotective mechanism against photoinhibition (Essemine *et al.*, 2012). While, under non-stress conditions (coastal and sufficient light), plants show no sign of acclimation to high light stress as observed in the continuing increase in NPQ during actinic light illumination at the steady phase.

4.3.2 QTL mapping on NPQ and flowering time

The second aims described in this chapter was to find the genetic basis for variation in the NPQ phenotype using two accessions of *Arabidopsis*, Cvi-0 and L*er*, and the Cvi-0 x L*er* RIXs mapping population. In the QTL analysis for NPQ of 92 Cvi-0 x L*er* RIXs lines grown under five different environments, significant QTL were detected across five chromosomes. Three outstanding QTL found in this study were ***RIX-QTL3-1***, ***RIX-QTL3-2***, ***RIX-QTL5-1***, and ***RIX-QTL5-3*** which localised on the chromosome 3,and 5 respectively (Figure 4.14). These three significant QTL are reproducible as they were observed in several different environments. More importantly, the most interesting QTL was ***RIX-QTL3-1***; because it has two candidate genes that involved in the photosynthetic mechanism (*ZDS*; **At3g04870**, and *DRT102*; **At3g04880**). *ZDS* is known to be a biosynthetic enzyme involved in the xanthophyll pathway, which is a key component of NPQ formation. Even though *DRT102* is not yet known to have a direct effect on NPQ, it is known to have a role in response to environmental stress.

Despite several promising QTL being identified, these studies highlighted a number of problems with mapping potential NPQ QTL in this RIXs population. Firstly, Cvi-0 and L*er* presented very similar NPQ capacity in all conditions, even though the Cvi-0 x L*er* RIXs presented high transgressive segregation within the population. This may suggest that the Cvi-0 x L*er* RIXs may be of limited usefulness for studying of natural genetic variation for the NPQ phenotype due to the limitation of phenotypic diversity between the two parents.

Secondly, the effects of putative QTL could not always be detected across different environments, even under conditions that were assumed to be consistent with the natural environments. This could be because of the environmental factors that were not harsh enough compared to the field conditions, or becauses the effects of QTL depending on epistatic interactions with other loci. This also suggests that different genetic loci control the trait in different environments. Finally, although significant QTL were identified in several genomic regions that influence differences in NPQ, no candidate genes were identified with a known role in NPQ. This could be a novel finding of new genes that could potentially involve in this mechanism. To fully understand the role of natural variation in NPQ, a large number of natural accessions must be investigated for NPQ under a variety of ecologically relevant conditions. If QTL can be identified multiple

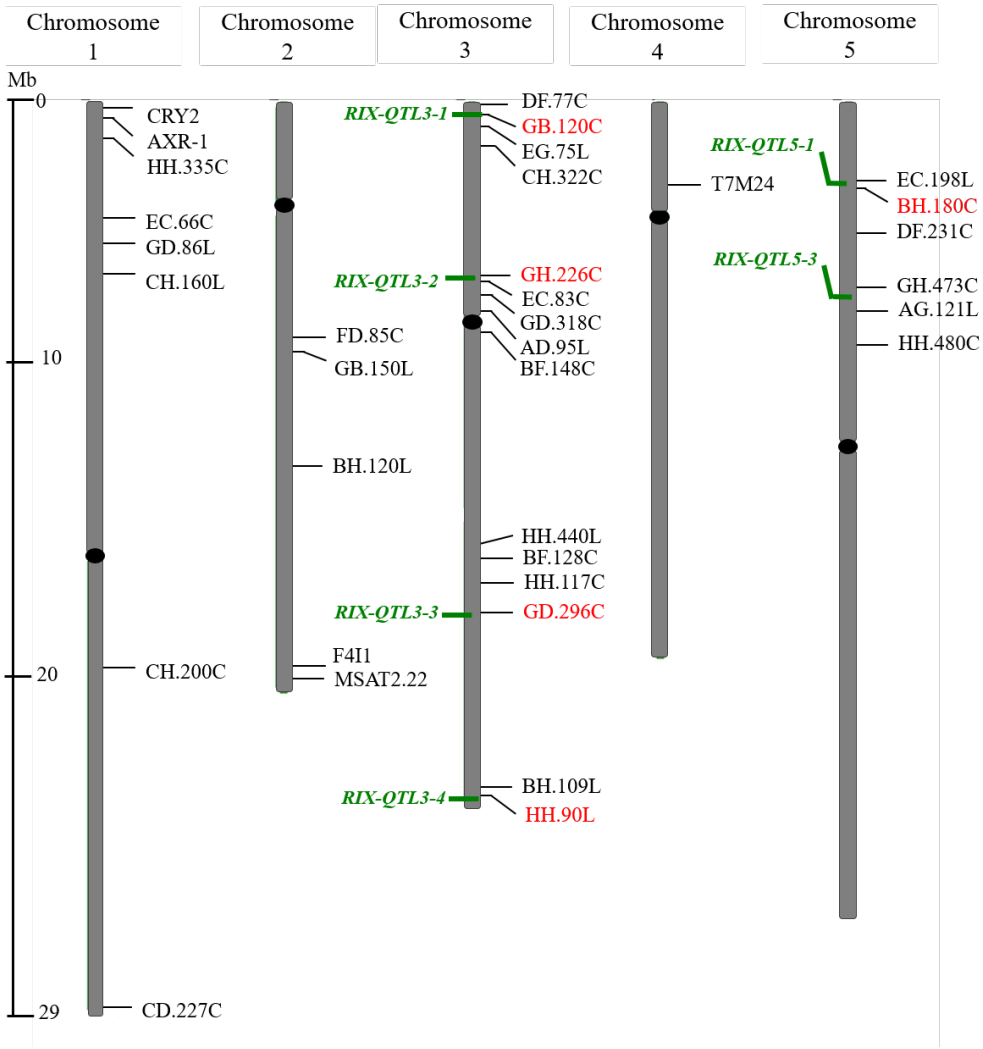

Figure 4.14 – *Genetic linkage map of Arabidopsis showed subset of markers that have been discovered in Cvi-0 x Ler RIXs QTLs analysis. Position of microsatellite markers used in genotyping the Cvi-0 x Ler RIXs and map distance are shown in Mb. Significant QTL associate to photoprotective mechanism are shown in green colour. Potential loci linked to photoprotective mechanism are shown in red colour.*

times then they would warrant confirmation by testing the effects the genetic variants on NPQ under natural and controlled conditions.

In addition to QTL mapping for NPQ, flowering time QTL were also identified to validate the QTL protocol. The flowering time of plants grown under inland and coastal conditions was analysed by measuring the days to flowering. The flowering time analysis revealed extensive variation in the ability of the RIXs to discriminate between the two dynamic growth conditions (coastal and inland), which also simulated season. As presented in the results Section 4.3.2, there is considerable variation in response to the dynamic growth conditions along with transgressive segregation, suggesting that multiple loci contribute to flowering time variation in the Cvi-0 x L*er* RIXs population. A strong QTL for flowering time was detected on the top of chromosome 5 in coastal condition which promoted rapid flowering in the RIXs population. This QTL encompasses a region that contains FLOWERING LOCUS C (*FLC*), a floral repressor that has been shown to be responsible for natural variation in *Arabidopsis* for flowering (Shindo *et al.*, 2007; Horton *et al.*, 2012; Li *et al.*, 2014). The markers with the strongest association for the QTL are less than 1 Mb from the *FLC* locus. Flowering time QTL were not detected under the inland condition, possibly because the colder condition had satisfied the vernalisation requirement of those lines with an *FLC* allele requiring vernalisation.

4.4 SUMMARY

Significant variation in NPQ was found in the Cvi-0 x L*er* RIXs population. This was due to a combination of the differences in light intensities and other stress factors between the different environments, and also due to new recombinations of the gene pool (between Cvi-0 and L*er*). Interestingly, the effect of environment on flowering time was much larger than the effect on maximum NPQ capacity.

The genetic architecture that is identified by QTL mapping using a bi-parental approached is specific to the parental lines in the segregating populations and may not reveal the genetic variation on which natural selection is involved. Therefore, using Genome-wide association studies (GWAS) approach can overcome

this limitation. The GWAS approach uses worldwide populations; thus, it can reveal the genetic basis of complex traits, such as NPQ, where the effect of natural habitat plays an important role on plant performance. Therefore, using the GWAS approach in *Arabidopsis* natural accessions to identify candidate genes underlying this phenotype seems to be the most appropriate method, which will be investigated in the Chapter 5.

Chapter 5

Natural variation and Genome-Wide Association Studies in photoprotection and photoinhibition in *Arabidopsis*

5.1 OVERVIEW

In the previous experiments, Experiment II (as in the Chapter 4) and Experiment III-b (as in the Chapter 3), I mainly focused on measuring NPQ variation by artificially simulating natural growth environments under which I grew natural accessions and a recombinant inbred intercross (RIX) population. The results showed that there is abundant natural variation in the NPQ phenotype, and that it is environmentally sensitive. In this chapter, to further investigate natural variation in the response to sustained light stress, the induction of photoprotective mechanisms and the amount of photodamage was quantified using high throughput imaging and biochemical techniques. To quantify photodamage, photochemical quantum yield and the levels of the ROS, Hydrogen Peroxide (H_2O_2), were measured. To understand the induction of photoprotective mechanisms non-photochemical quenching (NPQ) was monitored. To get an indication of acclimation to the stress electron transport rate (ETR) and chlorophyll content was measured. The genetic architecture of these traits was then investigated using Genome Wide Association Studies (GWAS).

Plants deal with excess light stress in a number of ways. Avoidance strategies include long term acclimation to different light intensities, including a decrease in the number of photosynthetic reaction centers, and increasing in the leaf thickness due to the expanded of palisade cells (Björkman, 1987). Leaf chlorophyll content is an important parameter that is frequently used as an indicator of chloroplast development and photosynthetic capacity Porra (2002); Ling *et al.* (2011). The chlorophyll *a/b* ratio is also used as an indicator of sun acclimated plants as they often presented a higher chlorophyll *a/b* ratio (Anderson, 1986). Therefore, chlorophyll content (μg/gFW) were measured using the method of Porra *et al*. (1989), Ritchie (2006), Warren (2008), and Hu *et al*. (2013).

Accumulation of ROS is one of the indicators of cell damage, but ROS also acts as signalling molecules into stress response pathways. ROS are toxic by-products of aerobic metabolism resulting in the photo-damaging of plant cells (Alboresi *et al.*, 2011). Plant organelles such as chloroplast, mitochondria and/or peroxisomes are the main sources of ROS production since they have an intense rate of electron flow (Wituszynska and Karpinski, 2013). The extremely short lifespans of some ROS molecules can make the investigation of their production in plants

very difficult (Fryer *et al.*, 2002). In this study, hence, one of the longer lived ROS molecules, hydrogen peroxide (H_2O_2), was measured using the Amplex® Red Hydrogen Peroxide/Peroxidase Assay Kit (Molecular Probes, Invitrogen) (as explained in Section 2.5.1).

As mentioned in the Chapter 4, using the Cvi-0 L*er* RIXs population may not reveal the full genetic variation on which natural selection occurs because of the limitation of bi-parental genetic distribution, although rare variants in Cvi can be identified as shown in many previous studies (El-Assal *et al.*; Teng *et al.*, 2008). Genome-Wide Association Studies (GWAS) is considered to be one of the best approaches to investigate the natural variation and genetic architecture of plants subjected to environmental stress. Several studies in *Arabidopsis* have looked at genetic variation of photosynthetic efficiency parameters under various environments using mutants or smaller collections of accessions under standard laboratory conditions (Eberhard *et al.*, 2008; Jung and Niyogi, 2009; Takahashi and Badger, 2011; Alter *et al.*, 2012; Rooijen *et al.*, 2015). However, none have used a GWAS approach to identify the genetic basis of natural variation in photoprotection. In this study, I have simulated diurnal and seasonal climates in growth chambers, varying light and temperature as would be experienced in a typical field location. I then measured photosynthetic performance, chlorophyll content, and H_2O_2 in *Arabidopsis* natural accessions and photoprotective mutants. These natural accessions are a genetically balanced subset of the global *Arabidopsis* accessions. Then a genome-wide association studies (GWAS) was performed in order to identify SNPs and candidate genes response to these traits including non photochemical quenching (NPQ).

This chapter covers the investigation of possible mechanisms contributing to the photoprotective responses in *Arabidopsis* natural population and mutants. Different physiological and biological analyses were performed to evaluate natural variation in photoprotective mechanism under two contrasting environments. Results of an investigation into the effects of NPQ, H_2O_2 and chlorophyll content on photoprotective responses are presented.

5.2 RESULTS

The first part of the results will describe the average responses for traits examined using high throughput phenotyping methods established in Chapter 3. This will be followed by the results from the GWAS looking into the genetic variation of traits of interest., This was analysed with Riyan Cheng, a postdoc in the Borevitz Lab at ANU, using his package QTLRel (Cheng *et al.*, 2011). The last part of this results section will represent the candidate gene confirmation using knockout analysis.

Two experiments were conducted in this part of the study. In the first experiment, Experiment IV, 284 *Arabidopsis* natural accessions from the HapMap set (see supplemental data Table A.2) and two photoprotective mutants (*npq1* and *npq4*) were selected based on genetic distribution and the study of Jung and Niyogi (2009). Plants were grown under a simulated coastal (Wollongong, Australia) and inland (Goulburn, Australia) in a typical autumn season. The simulated date started from April 1st, 2014, so from this point I will call the conditions Coastal-Late Autumn and Inland-Late Autumn. The maximum light intensity at noon was around 150 μmol $m^{-2}s^{-1}$ and 300 μmol $m^{-2}s^{-1}$ for Coastal-Late Autumn and Inland-Late Autumn respectively. The temperature range between 14 °C - 23 °C and 10 °C - 23 °C for Coastal-Late Autumn and Inland-Late Autumn respectively, and these temperatures decreased to 10 °C - 18 °C and 5 °C - 15 °C by the end of the experiment due to the season changing to winter.

To confirm the accuracy of our accession labels, all the genotypes from Experiment IV were resequenced by GBS (as described in the Chapter 2); and the genotype data were compared to the genotype data from 1,001 genome project (1001genomes.org). For the second experiment, 223 *Arabidopsis* natural accessions (Table A.3) from Experiment IV, Knockout lines (as described in Table 5.3) and photoprotective mutants (as described Table 2.1) were included. Initially, the purpose of conducting Experiment V was to repeat Experiment IV. Thus, plants were germinated and grown under simulated coastal and inland autumn seasons. Unfortunately, there were issue with low germination and survival in Experiment V, so Experiment V was started again with the start date shifting two weeks earlier (started on March 15th). Hence, this second experiment was called Coastal-Early Autumn and Inland-Early Autumn. The maximum light intensity at noon for

Coastal-Early Autumn and Inland-Early Autumn was around 150 μmol $m^{-2}s^{-1}$ and 300 μmol $m^{-2}s^{-1}$ for respectively. The temperature range between 10 °C - 25 °C and 5 °C - 25 °C for Coastal-Early Autumn and Inland-Early Autumn respectively, and these temperatures decreased to 10 °C - 18 °C and 5 °C - 18 °C for Coastal-Early Autumn and Inland-Early Autumn respectively by the end of the experiment. As the capacity for elevated light was constrained temperature variation provided a variable for increasing photo-oxidative stress.

Acclimation of PSII activity to coastal (mild condition) and inland (stress condition) was studied in the vegetative stage of *Arabidopsis* plants. The two contrasting dynamic growth conditions were conducted in the SpectralPhenoClimatron (SPC). The conditions were controlled by SolarCalc software with 5 minute intervals simulating autumn season of coastal and inland conditions as discussed above. Model of the simulated climates was presented in Figure 5.1. As there is significant natural variation in plant development, which is further affected by the growth conditions, chlorophyll fluorescence parameters were recorded at several time points. To compare plants at the same developmental stages across growing conditions, plants were compared at the same number of leaves based on the average leaf number of the highly replicated reference genotype, Col-0.

5.2.1 Plant growth and development

Phenotyping for growth and rosette area under dynamic growth conditions

The growth characteristics of 284 *Arabidopsis* natural accessions from Experiment IV were analysed by the Phenomics group in the Borevitz Lab (including Tim Brown, Joel Grandos and Sarah Namin) and are presented in Figure 5.2. The Figure 5.2 shows the variation in leaf morphology between accessions and differences in plant development between the two growth conditions at an average 16 leaves stage. The reference genotype plants, Col-0, were spread across the growth chamber to account for any position effects. The distribution plots of the Col-0 replicates for flowering time, chlorophyll content, H_2O_2, ETR, and NPQ are presented in supplementary FigureD.27. Rosette area was calculated daily from real time imaging. Data were recorded daily from day one (the day that true leaves emerged) to day 36 for Coastal-Late Autumn plants, and from day one to day

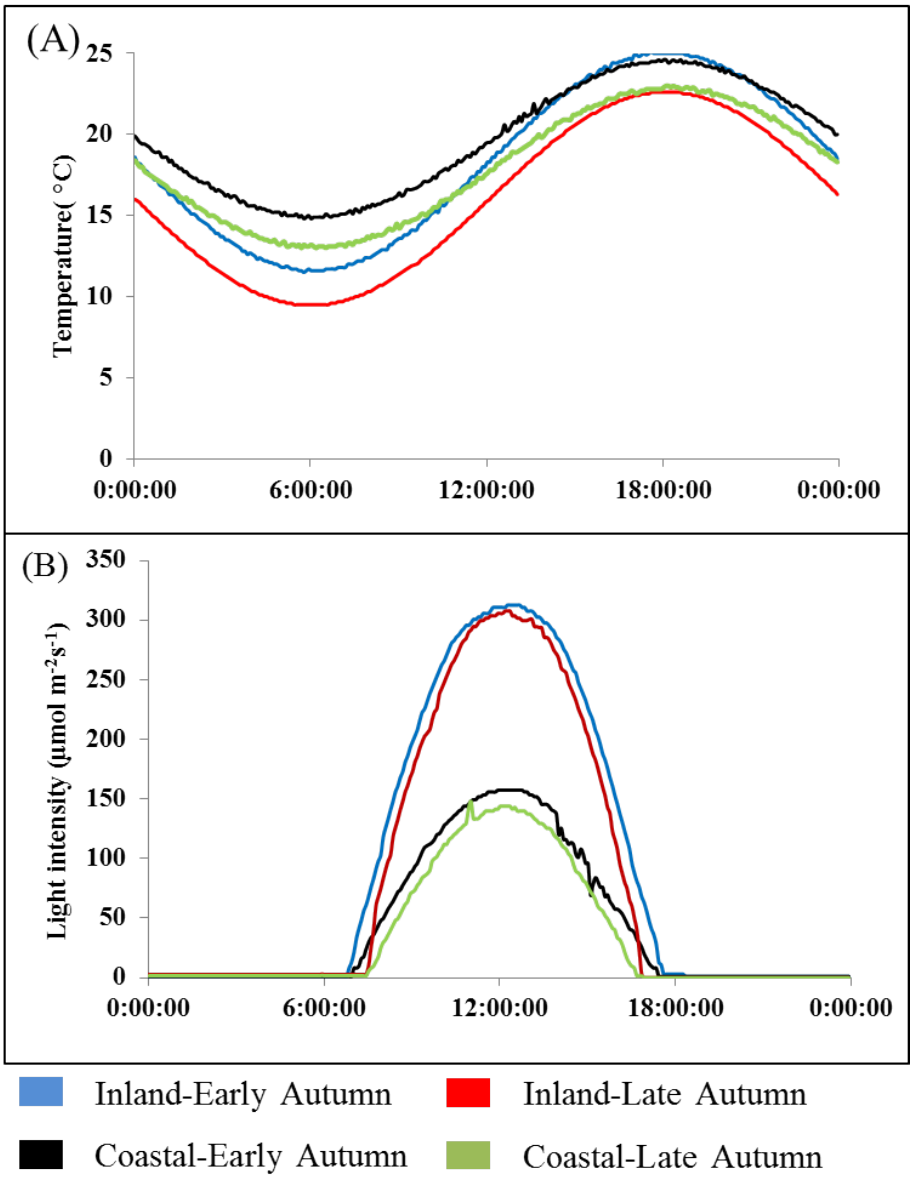

Figure 5.1 – *Model of simulated Coastal and Inland conditions in early and late autumn showing dynamic changes in temperature (A) and light intensity (B).*

43 for Inland-Late Autumn plants. The data that used for analysis are till day 36 and 43. Data beyond day 36 and 43 are not suitable, as plant leaves/rosette are overlapping. Then data were normalized by removing the day with missing data >25% and plants with missing data > 50%.

The real-time imaging captured rosette area every 15 minutes, thus, the raw data gave a non-smooth curve (Figure 5.3A). This may be caused by plant movement or variation in imaging processing. Therefore, data were normalized by taking the median predicted values of rosette area from each day, then plot them again using LOESS method (Jacoby, 2000) to remove variation which might occur from imaging processing and leaf movement. Then LOESS method was applied again for fitting smooth curves across multiple days by removing unwanted variation (Figure 5.3B). Figure 5.3 showed that the development in rosette area of all plants under the Inland-Late Autumn condition was considerably slower than the plants under the Coastal-Late Autumn conditions, for example it took the Inland-Late Autumn plants 10 more days to reach the 16 leaves stage than the Coastal-Late Autumn plants. At the same age, the average rosettes area of the Inland-Late Autumn plants was three times smaller than that of the Coastal-Late Autumn plants. Despite the general effects of environment there were differences in leaf morphology and growth rate between accession in each growth conditions (Figure 5.2). This suggests that there are differences between accessions in their ability to undergo acclimation under the given conditions. This phenomenon can be due to genetic variation.

GWAS analysis for rosette area

To evaluate the influence of genetic and environmental condition on plant development, single traits GWAS analysis was performed for all timepoints in the experiment. The GWAS profile is presented as a heatmap in Figure 5.4, with the size and colour of the dots changing with increasing LOD score. Two QTL were associated with leaf area in the coastal condition with LOD score > 5.1 ($p<0.05$). The first QTL, ***LA-QTL4***, is localized on chromosome 4 (snp4_13,091,298) and was detected at the later developmental stage (35 days old coastal plants). The second QTL, ***LA-QTL5***, is localized on chromosome 5 (snp5_24,474,120 and snp5_24,478,009) and presented at the earlier vegetative growth stage (6 - 16 days old coastal

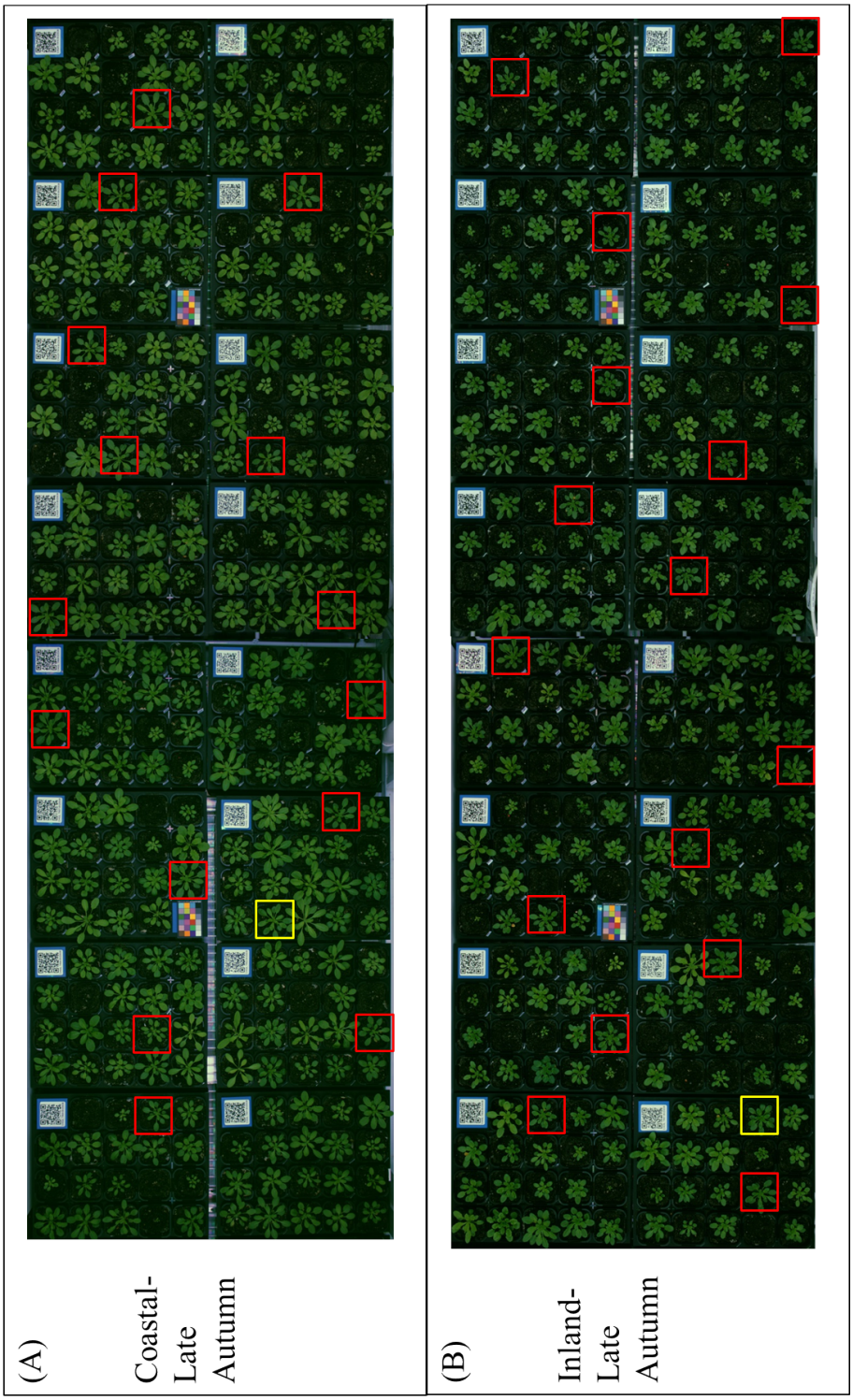

Figure 5.2 – *The natural variation in rosette development of coastal and inland plants in the experiment IV at the same developmental stage (16 leaves). (A) Coastal-Late Autumn plants at 35 days old and (B) Inland-Late Autumn plants at 45 days old. The plant in red square is Col-0 and in yellow square are npq4 mutant.*

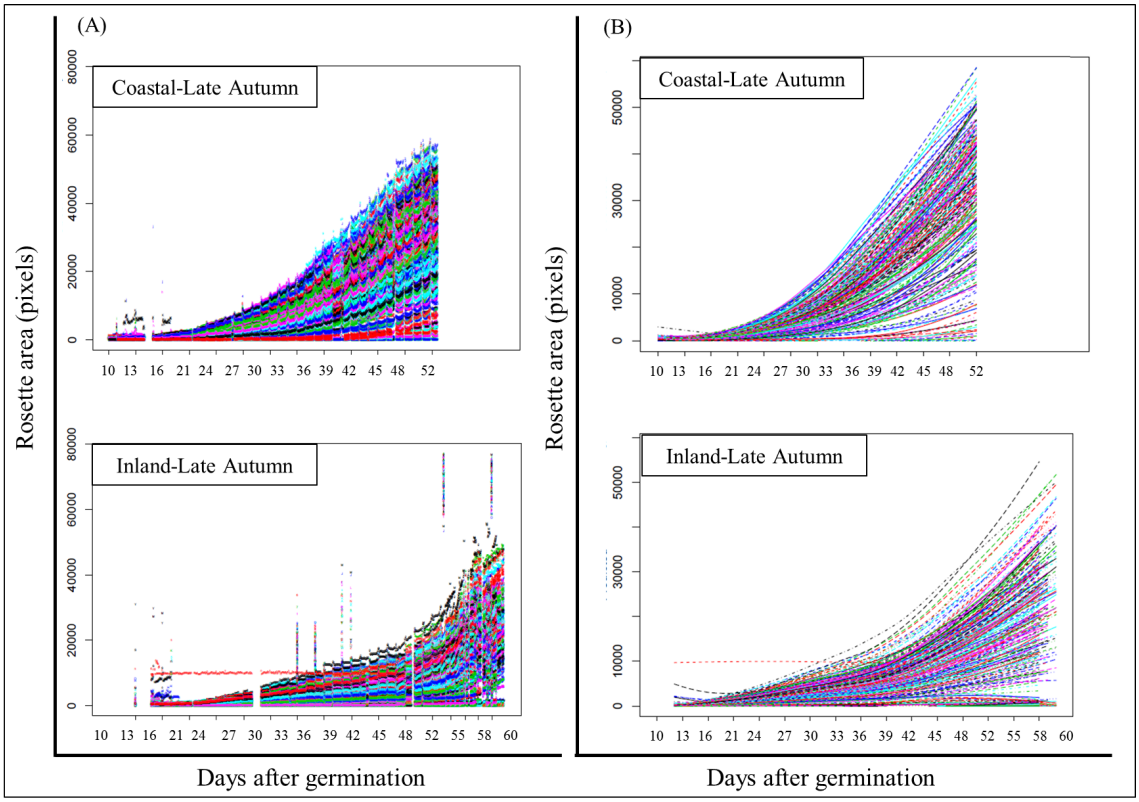

Figure 5.3 – *The leaf area of Coastal-Late Autumn and Inland-Late Autumn plants in experiment IV. Each different line color represents each accession. A non-smooth curve from raw data (A) and fitting smooth curve using LOESS method (B). At 58 days old of inland plants show the same developmental stage as coastal plants at 48 days old. Plant growth analysis were done with Riyan Cheng and Tim Brown.*

plants). There are 10 candidate genes located within 20kb a window of those two potential QTL (see supplementary Table D.1). However, none of the candidate genes have previously been shown to have a direct function in leaf development, suggesting novel alleles at novel loci are controlling growth at specific stages under specific conditions.

Because the variation in plant development over time is different under the two conditions, a time shifting model was created by shifting the starting day of the inland plants growth slopes forward so that both sets started with the same rosette area. The single trait GWAS analysis after time shifting is presented in Figure 5.5. The GWAS results showed a new discovery of one strong QTL associated (LOD > 5.13) with leaf area in the inland condition. This new QTL, ***LA-QTL1***, was detected at the earlier developmental stage (from day 1 to day 12) located on chromosome 2 (snp2_16,744,849 and snp2_16,745,468). There were no significant QTL associated with leaf area after time shifting in the coastal condition. The 20kb window of this new, ***LA-QTL1***, was searched for potential candidate genes (see supplementary Table D1). The results showed six potential candidate genes; one gene (*LHCB4.3*; **At2g40100**) is associated to light harvesting complex of PSII, two genes (**At2g40081** and **At2g40113**) have unknown function, and three genes (**At2g40110**, **At2g40116** and **At2g40120**) have no known association to leaf development.

5.2.2 Days to Flowering

Variation in flowering time

A delay in flowering time was observed under the inland environment as shown in Figure 5.6. The average of the days to flowering of the Inland-Early Autumn plants was around 25 days slower than the Coastal-Early Autumn plants. The day to flowering is not only influenced by the developmental status, leaf number (Salomé *et al.*, 2011), it is also sensitive to photoperiod and day/night temperature (Halliday *et al.*, 2003). The results showed faster flowering time under the coastal condition which supports the concept that warm temperature promotes flowering in *Arabidopsis* (Thines *et al.*, 2014).

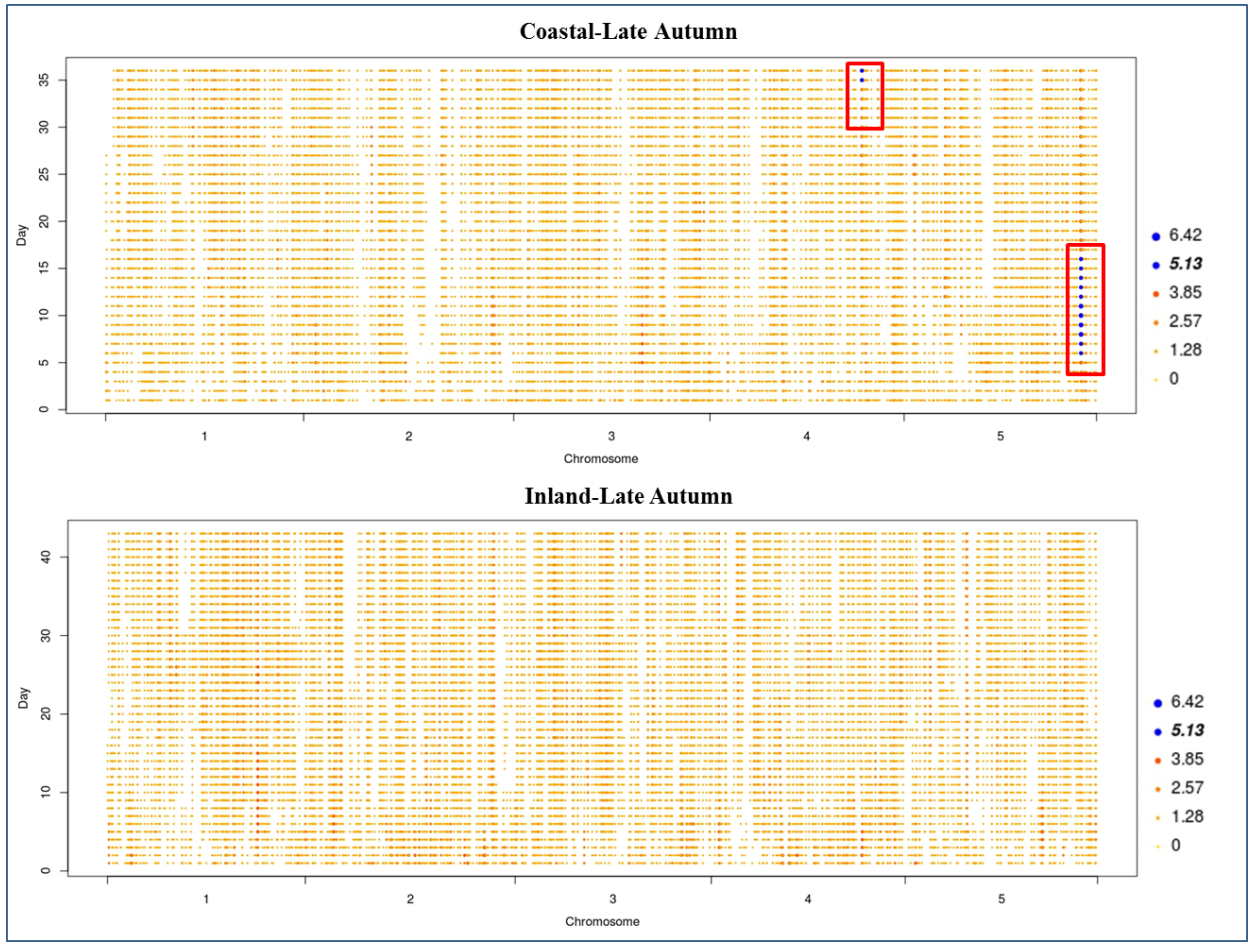

Figure 5.4 – *Single trait GWAS analysis for leaf area over time. Significant association were presented by blue colour dot (LOD > 5.13, P < 0.05 significance threshold). The chromosomes are presented on x axis. Red circle represent a potential QTL region.*

Figure 5.5 – *GWAS analysis for rosette area after time shifting. Significant association were presented by blue colour dot (LOD > 5.13, P < 0.05 significance threshold). The chromosomes are presented on x axis. Red circle represent a potential QTL region.*

Variation in flowering time

One QTL were identified for flowering time under Coastal-Early Autumn condition which is located on the top of chromosome 4 as presented in Figure 5.7. The highest SNP peak was at snp4_1,357,747. There was no QTL detected under Inland-Early Autumn and for *GxE*. Based on the TAIR database, there are 14 genes located within 20 kb upstream and downstream of this QTL. However, none of those 14 genes has known functions that are involved or associated with flowering time mechanisms. Hence this QTL could indicate natural variation in a novel flowering time gene that is environment sensitive.

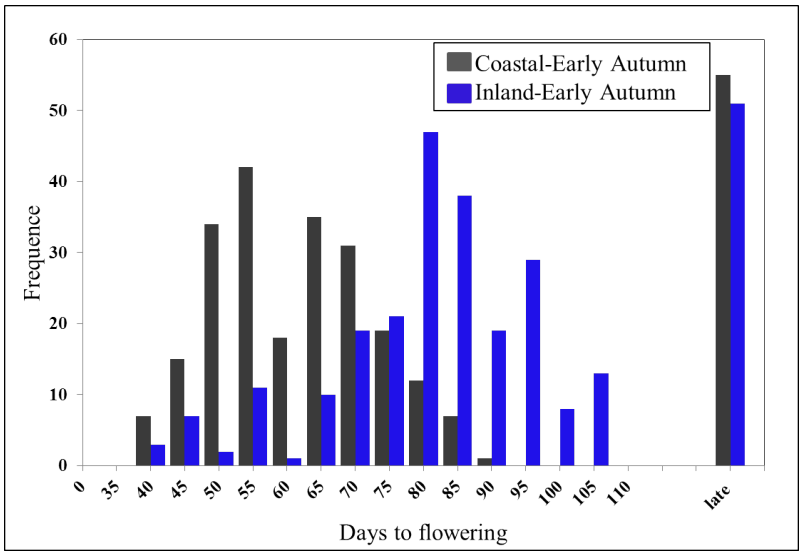

Figure 5.6 – ***The bar plot of days to flowering of the Coastal-Late Autumn plants (black color) and the Inland-Late Autumn plants (blue color) of Experiment IV. The accessions that were classified as late are flowering later than 120 days after germinating or not flowering at the time of harvesting. The Inland-Late Autumn plants show later flowering time in comparison to the Coastal-Late Autumn plants.***

5.2.3 Chlorophyll content

Variation in chlorophyll *a* and *b*

Chlorophyll content was measured in mature leaves at the transition to flowering stage, to investigate the variation in acclimation being experienced by the plants under the different growth conditions.

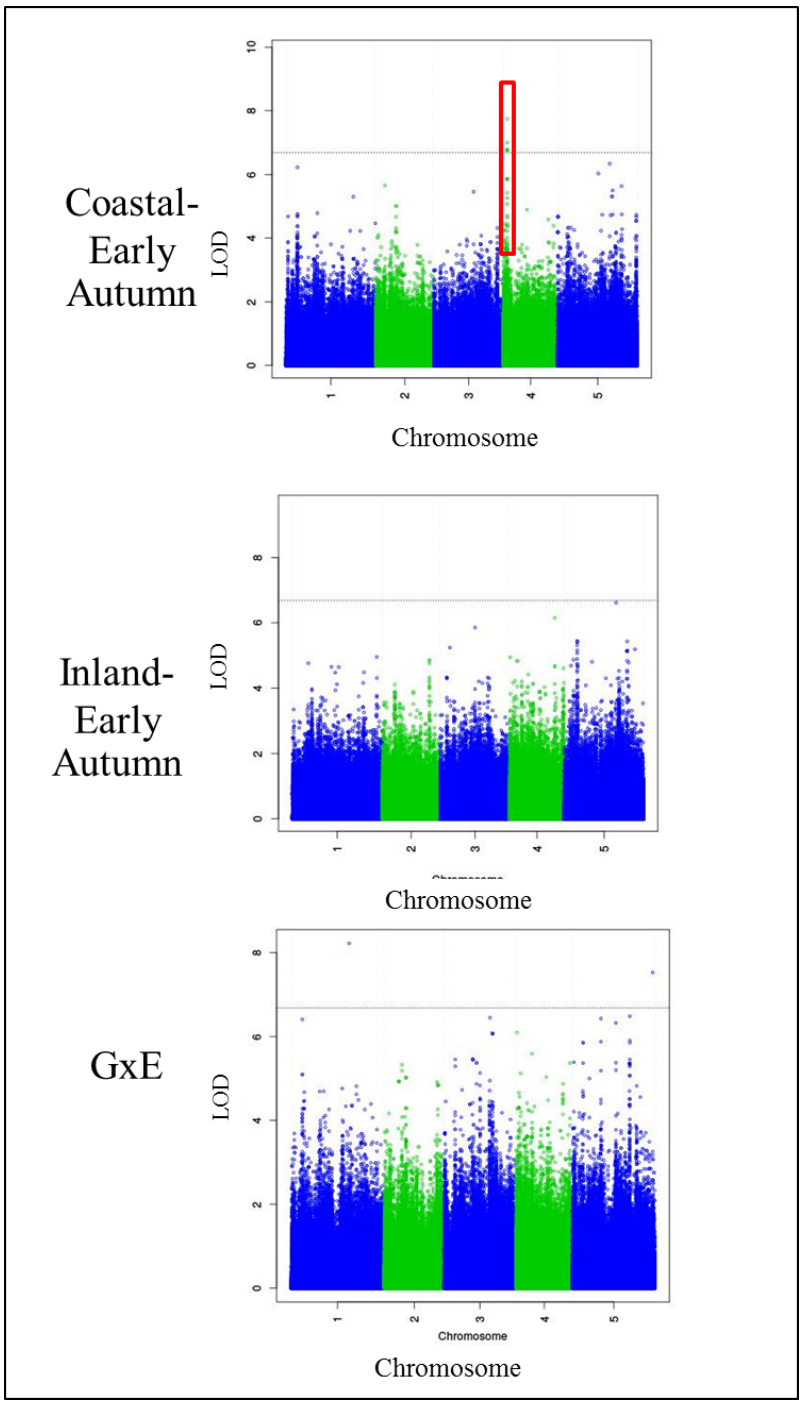

Figure 5.7 – *GWAS analysis for flowering time. Significant association were presented by blue colour dot (LOD > 5.13, P < 0.05 significance threshold). The chromosomes are presented on x axis. Red circle represent a potential QTL region.*

The concentrations of chlorophyll a and b of the 284 natural accessions in Experiment V showed significant differences between the two growth conditions. Chl *a* and Chl *b* levels were observed to be higher in the Coastal-Early Autumn plants (low light) with the average concentration at 0.83 and 0.19 μg/gFW respectively

in comparison to the Inland-Early Autumn plants (excess light) where the average was 0.41 and 0.08 as shown in Figure 5.8. This is equivalent to on average 50.60% and 57.89% lower levels of chl *a* and chl *b* in Inland-Early Autumn plants compared to plants exposed to low light conditions (Coastal-Early Autumn). Chl *a/b* ratio was not significantly different between the two conditions when considering the entire population. However, when looking at the individual accessions some, such as Col-0 and Ba4-1, presented much lower Chl *a/b* ratios under the stress condition.

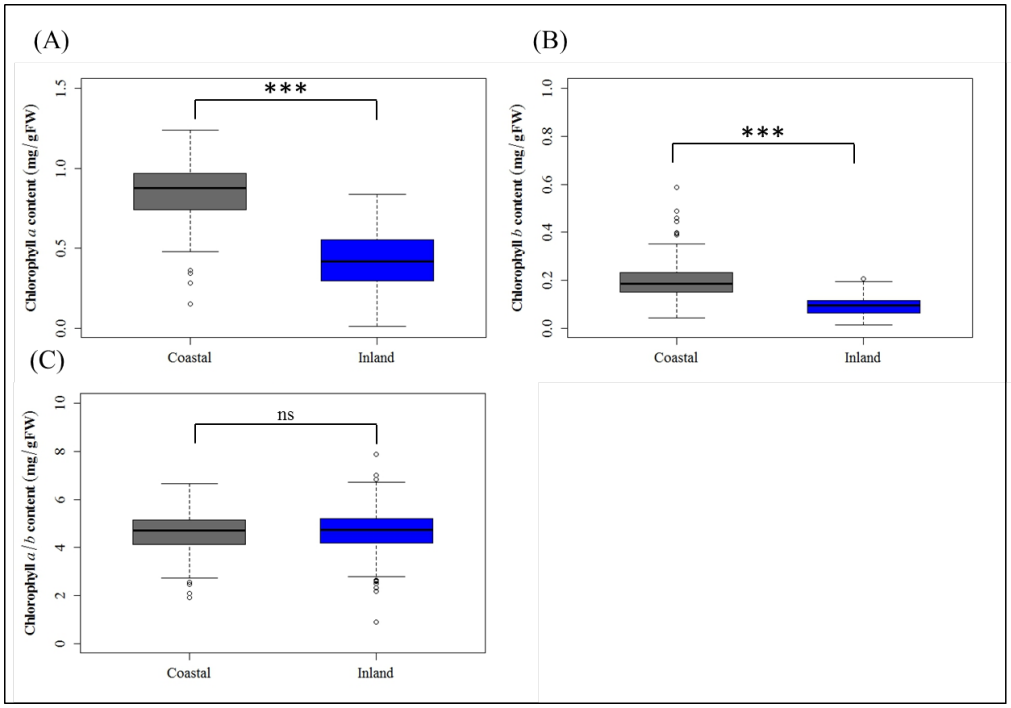

Figure 5.8 – ***Chlorophylls accumulation from Experiment V. (A), (B) and (C) are chlorophyll a, b and a/b content respectively of plants grown under coastal and inland late autumn conditions. Chlorophylls content were extracted from fully expanded leaf at the transition to flowering stage. Statistically-significant differences are indicated by asterisk (∗∗∗:P<0.001).***

GWAS for chlorophyll *a* and *b*

Quantification of chlorophyll *a* and *b* in mature leaf showed quantitative variation, with a 2-fold and 3-fold variation in total chlorophyll content seen within the Coastal-Early Autumn and Inland-Early Autumn conditions, respectively, in Experiment V. GWAS mapping was conducted to identify genetic factors underlying the variation in chlorophyll content in response to the different environments.

The GWAS profiles as presented in Figure 5.9 showed that no significant associations were detected with a LOD score above 6.7 in either the inland and coastal conditions. However, there is one potential QTL localised on chromosome 3 between 10.93 and 10.94 Mb (LOD score = 6.29) which appeared under the inland simulated condition for chlorophyll *a* and under the coastal simulated condition for chlorophyll *a/b*. The expansion of this potential QTL region and candidate gene list nearby was presented in Figure D.1. The Figure D.1 shows that there are two candidate genes, **At3g28918** and **At3g28920** which are located within 20 Kb window from the highest peak. The functions of those two genes were found to have no known association to chlorophyll biosynthesis or photosynthesis.

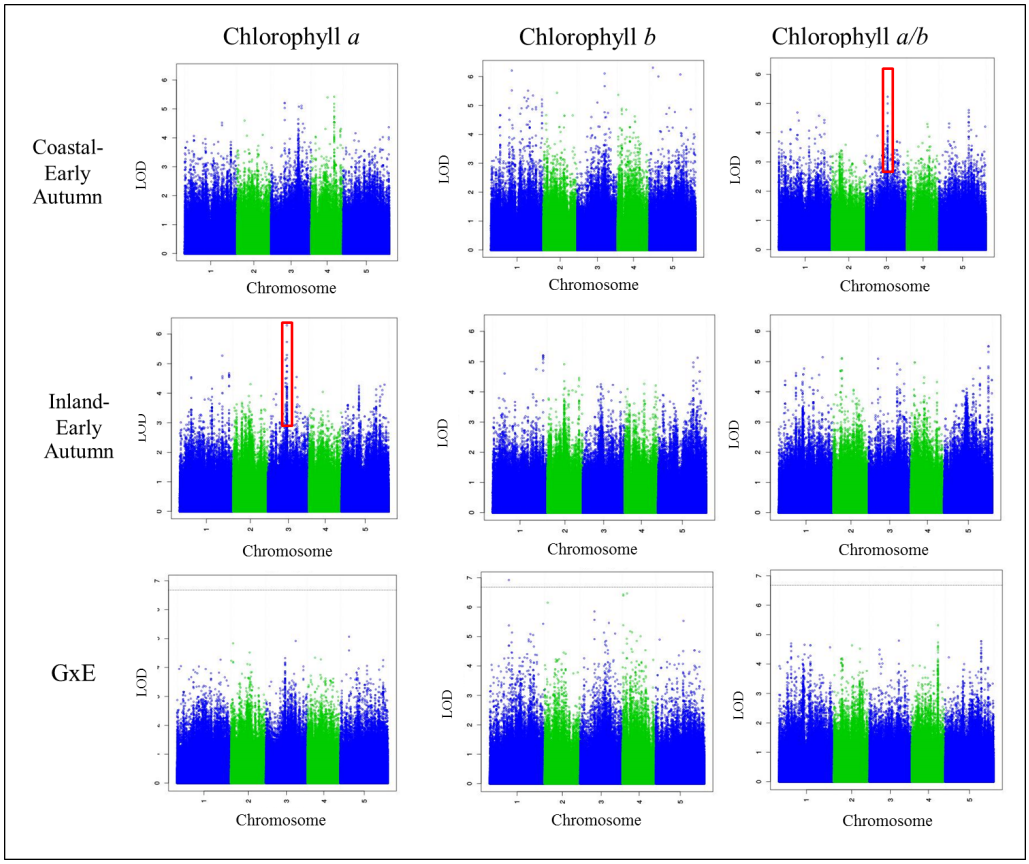

Figure 5.9 – *Manhattan plots of GWAS results using 6M SNP database for Chlorophylls content from Experiment V. The chromosomes are depicted in different colors on x axis. The significant threshold is LOD > 6.7. Red boxes represent a potential QTL region.*

5.2.4 H_2O_2 accumulation

High levels of H_2O_2 in response to stress condition

Hydrogen peroxide (H_2O_2) was measured at the transition to flowering, in Experiments IV and V, to get an idea of the amount of photodamage being experienced by the plants. In Experiment IV, frozen tissues from the whole plants were used, while in Experiment V, a fully expanded leaf was used for H_2O_2 detection using Amplex Red (as explained in Section 2.5.1). The results of Experiment IV are shown in Figure 5.10 (A, C and E), high levels of H_2O_2 were found in Inland-Late Autumn plants in comparison to Coastal-Late Autumn plants. H_2O_2 accumulation was slightly higher in the Inland-Late Autumn plants with the average concentration at 0.44 μg/gFW, while Coastal-Late Autumn plants accumulated lower H_2O_2 with the average concentration at 0.38 μg/gFW. In addition, the result was significantly different at $P<0.01$ between the two conditions. Interestingly, for Col-0, there were a greater difference in mean H_2O_2 accumulation between inland and coastal conditions, than between the populations means as shown in Figure 5.10B.

Similar patterns of H_2O_2 accumulation were observed in Experiment V as shown in Figure 5.10 (B, D and F). The results show a higher H_2O_2 concentration in Inland-Early Autumn plants with the average concentration at 0.17 μg/gFW, while under lower irradiance (Coastal-Early Autumn), plants accumulated much lower H_2O_2 with the average concentration at 0.09 μg/gFW as shown in Figure 5.10 (B and D). The difference between the two condition means was highly significant at $P<0.001$. From these two experiments, the results confirmed that exposure to excess light stress conditions cause the accumulation of reactive oxygen species (H_2O_2).

GWAS for H_2O_2

It was shown that there was natural variation in H_2O_2 concentrations under the inland condition with the variation 2-fold greater than the coastal condition. There was a significant difference in H_2O_2 concentrations in some accessions between the two conditions, as well as within the same condition. This variation is

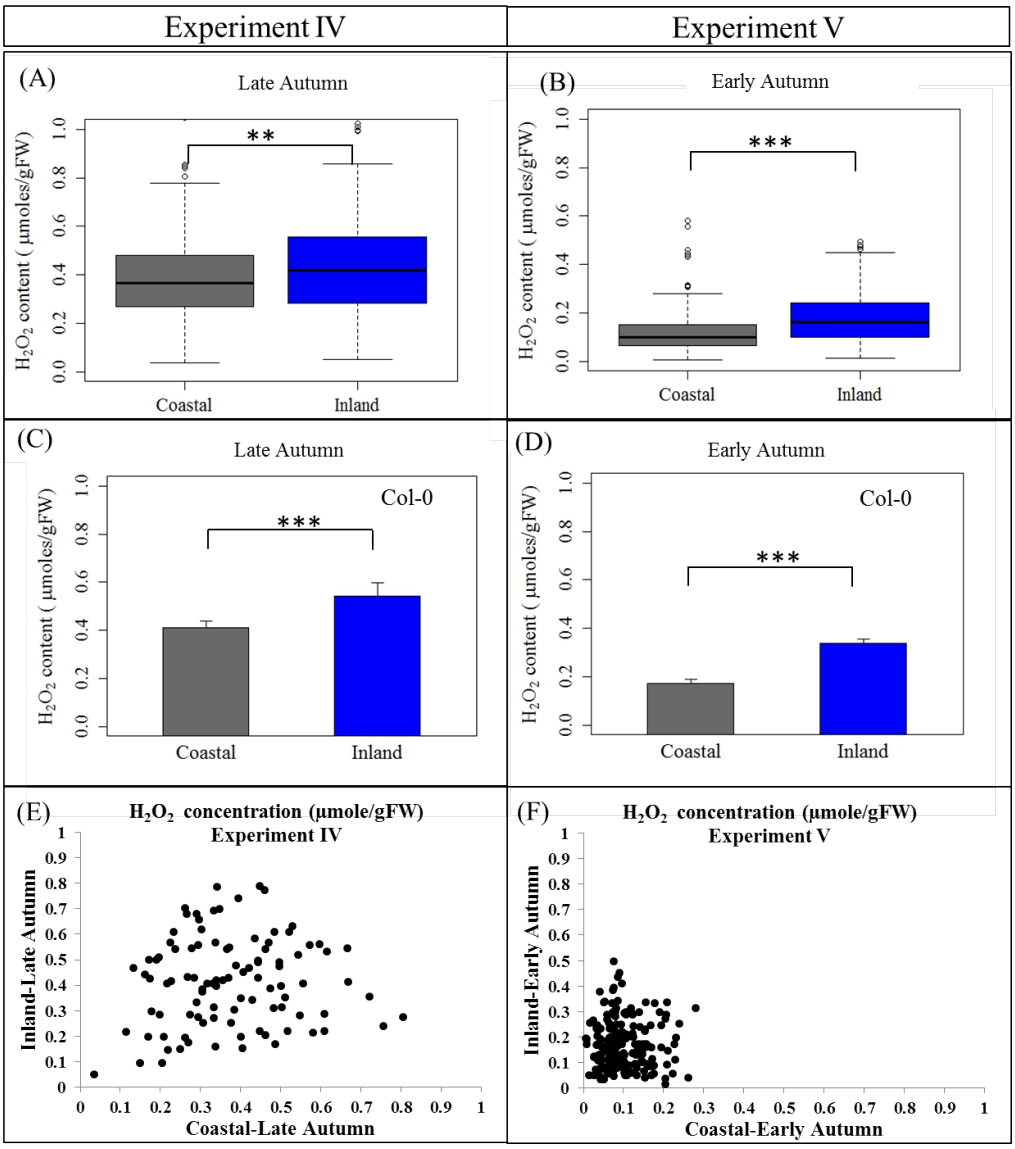

Figure 5.10 – *H_2O_2 accumulation in coastal and inland plants in Experiment IV and V. (A) is a box plot of H_2O_2 content of plants grown under inland and coastal conditions in Experiment IV; (B) is a boxplot of H_2O_2 content of plants grown under inland and coastal conditions in Experiment V; (C) is H_2O_2 content of Col-0 of Experiment IV. (D) is H_2O_2 content of Col-0 of Experiment V. The data (C) and (D) are mean ±SD, for ten biological replicates. Statistically-significant differences are indicated by asterisk (∗∗:P<0.01 and ∗∗∗:P<0.001). (E) and (F) represented distribution of H_2O_2 concentration in Experiment IV and V respectively under coastal and inland conditions.*

not likely to be due to experimental error in measurement or in biological noise as the replicates of Col-0 had low standard deviations (Figure 5.10). Therefore GWAS analysis was conducted to identify genetic factors underlying the accumulation of H_2O_2 in response to the growth conditions. The GWAS profiles, as

shown in Figure 5.11, did not show any significant association in both inland and coastal conditions, as well as the interaction between genotype and environment (*GxE*).

5.2.5 Photochemistry and photoinhibition

Photosynthetic electron transport rate (ETR) was calculated from the chlorophyll fluorescence parameters in the different growth conditions for all *Arabidopsis* natural accessions as shown in Figure 5.12. ETR was calculated using ETR = Fq'/Fm' x light intensity (PAR) x 0.5 x 0.84 where PAR is the photosynthetically active radiation, the factor 0.5 accounts for partitioning of energy between PSII and PSI and the factor 0.84 accounts for the reduced light intensity that is absorbed by the leaf (Stemke and Santiago, 2011). In both experiments, the ETR through PSII was different between coastal and inland conditions. Inland-Late Autumn plants showed a much higher ETR than Coastal-Late Autumn plants with the ETR ranging between 82 - 140 μmol $m^{-2}s^{-1}$ and 50 - 110 μmol $m^{-2}s^{-1}$ respectively. Inland-Early Autumn plants showed a higher ETR than Coastal-Early Autumn plants with the ETR ranging between 100 - 150 μmol $m^{-2}s^{-1}$ and 40 - 100 μmol $m^{-2}s^{-1}$ respectively. The maximum quantum yield, as observed in Figure 5.12C, indicates the amount of photoinhibition that has occurred. Plants grown under excess light condition (Inland-Late Autumn and Inland-Early Autumn) shown a slight, but significant, reduction of photochemical quantum yield of PSII (Fv/Fm) in comparison to low-light plants (Coastal-Late Autumn and Coastal-Early Autumn).

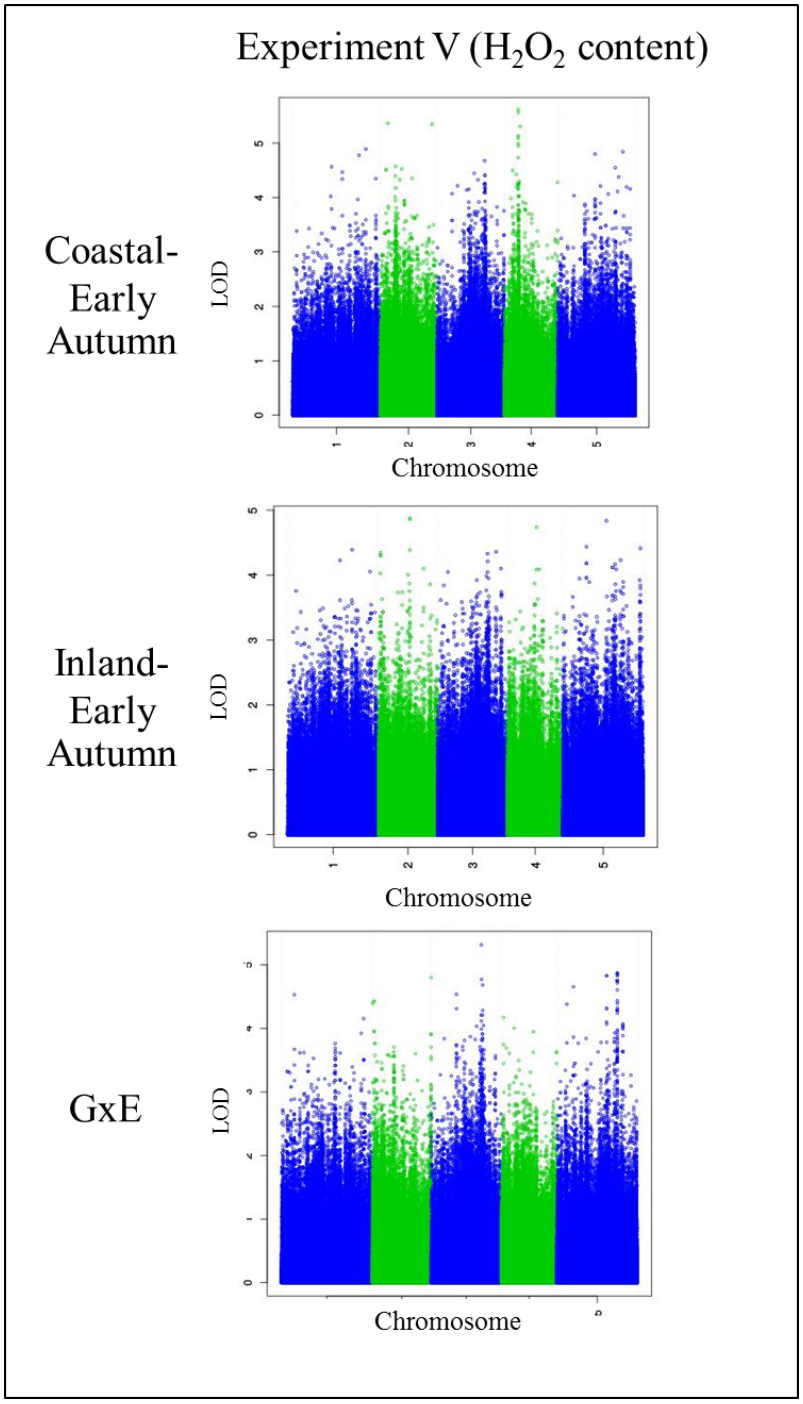

Figure 5.11 – *Manhattan plots of GWAS results using 6M SNP database for the H_2O_2 content trait from Experiment V. The chromosomes are depicted in different colors on x axis. The significant threshold is LOD > 6.7.*

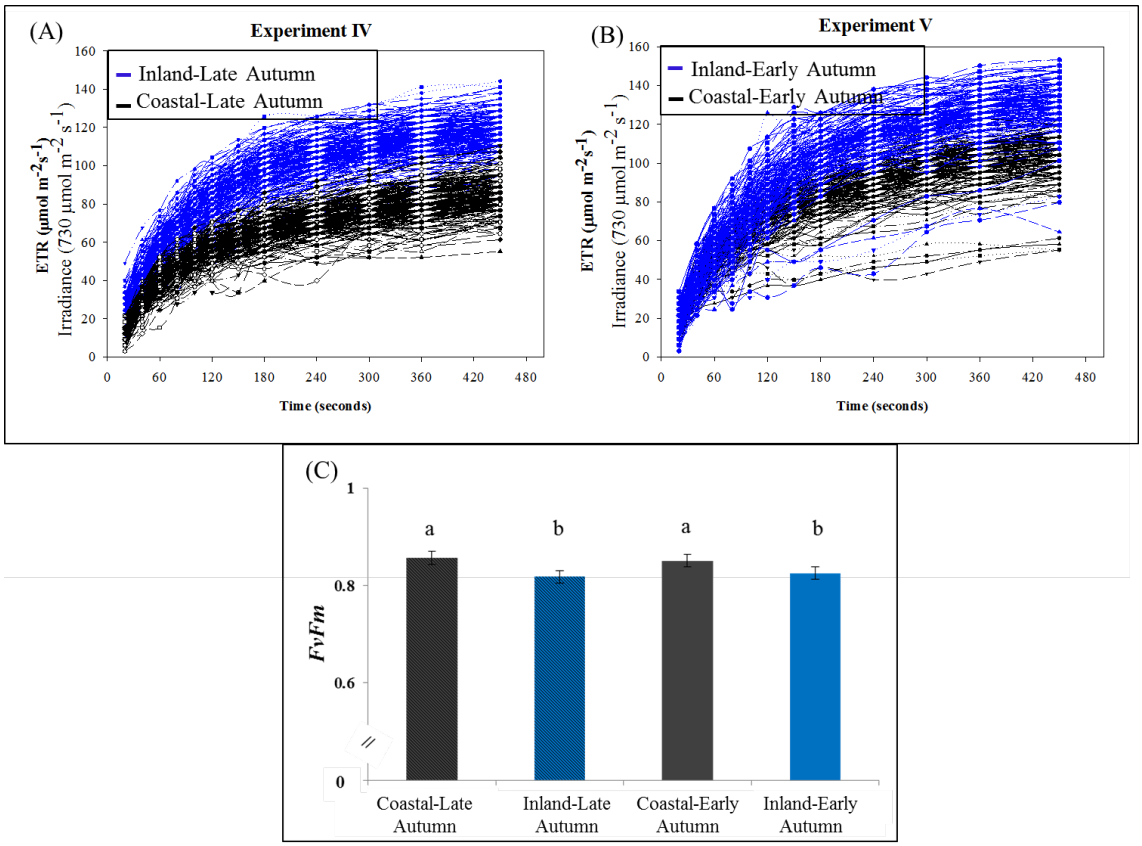

Figure 5.12 – *Electron transport rate (ETR) during light induction of Experiment IV (A), Coastal-Late Autumn (black colour) and Inland-Late Autumn (blue colour), and Experiment V (B),Coastal-Early Autumn (black colour) and Inland-Early Autumn (blue colour). The values were calculated from the effective PSII efficiency measured under 730 $\mu mol\ m^{-2}s^{-1}$ using the PlantScreen system. Plants were dark-adapted for 30 mins before the measurement, and were measured at the 16 leaves stage (the average of Col-0 plants). Statistically-significant differences are indicated by a and b ($p<0.05$).*

5.2.6 Non-photochemical quenching

Natural variation in NPQ

Non-photochemical quenching, as measured by chlorophyll fluorescence, was quantified for both Experiment IV and Experiment V to determine how the different growth environments affected natural variation in this photoprotective mechanism. To maximise the genetically-determined proportion of the variation measured and reduce biological variance, NPQ measurement was started at midday and finished by 5 pm. The P3 protocol (as presented in Chapter 3) was used. Data were compared at the same number of days since sowing (Figure 5.13) as well as the same developmental stage which was determined by the leaf number of Col-0 plants (Figure 5.14).

In this study, three phases of NPQ kinetics were examined (induction, steady state, and relaxation phases). The induction phase was determined by NPQ formation at the time of 0s to 120s of actinic light illumination. The steady phase was determined from 120s to 450s of actinic light illumination. Lastly, the relaxation phase was indicated by NPQ kinetics at time of 450s to 720s.

In Experiment IV, NPQ was quantified during rosette development in two simulated seasonal conditions (Coastal-Late Autumn and Inland-Late Autumn) with 284 natural accessions per condition. In Experiment V, NPQ was also quantified during rosette development for plants grown in two simulated seasonal conditions (Coastal-Early Autumn and Inland-Early Autumn) with 223 accessions per condition. In both experiments, all of *Arabidopsis* natural accessions showed high variation between the two different growing conditions and also at different developmental stages (Figure 5.13). In Experiment IV, when plants in both growth conditions were 25 days old, the Inland-Late Autumn plants had lower NPQ capacity than Coastal-Late Autumn plants. After 40 days growth NPQ capacity of Inland-Late Autumn plants was found to increase to the same levels of Coastal-Late Autumn plants. A slightly different pattern of NPQ was found in Experiment V (Figure 5.13 (C and D). At 25 days old, faster NPQ induction was observed in Inland-Early Autumn plants, while the average NPQ capacity was lower than Experiment IV in both Coastal-Early Autumn and Inland-Early Autumn with the range 2.4 - 3.4 and 1.2 - 3.5 respectively. At the age of 40 days,

NPQ capacity of Coastal-Early Autumn plants was increased with the range 2.5 - 3.8 which is nearly the same levels as Coastal-Late Autumn plants, while NPQ capacity of Inland-Early Autumn plants had not changed, with the same levels as the age of 25 with the fast induction pattern.

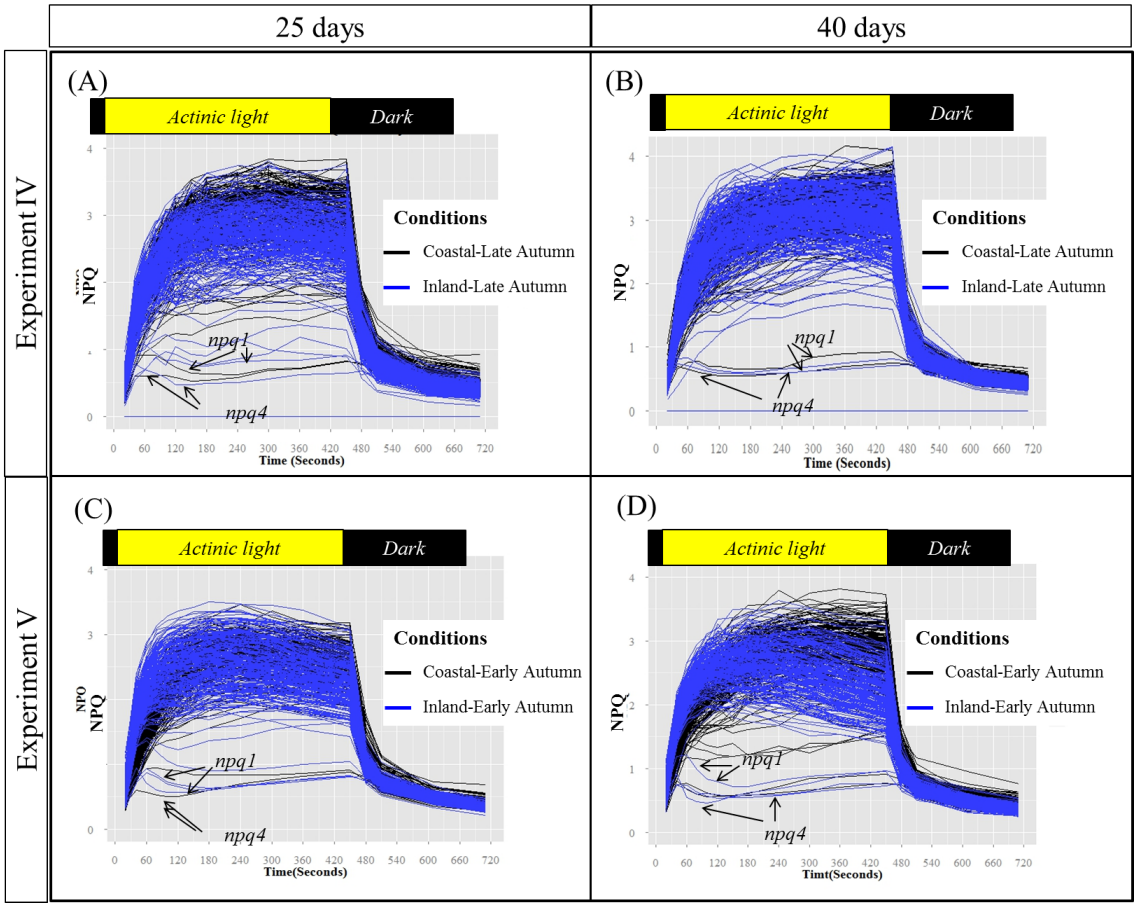

Figure 5.13 – *NPQ kinetics in different Arabidopsis genotypes showing the genetic variation of NPQ of Experiment IV (A and B), and Experiment V (C and D). The 284 Arabidopsis natural accessions, 3 photoprotective mutants were grown under inland (blue) and coastal (black) conditions. The NPQ measurement was performed at 25 days old plants (A) and at 40 days old plants (B). The 223 Arabidopsis natural accessions, 3 photoprotective mutants and 11 Knockout lines were grown under inland (blue) and coastal (black) conditions. The NPQ measurement was performed at 25 days old plants (C) and at 40 days old plants (D).*

Due to the differences in plant developmental rates between growth conditions, the NPQ kinetics was also compared between plants of the same leaf number. Figure 5.14A shows the time course of NPQ formation at the 14 leaves stage of Coastal-Late Autumn and Inland-Late Autumn plants. NPQ reached a maximum levels after 6 minutes of actinic light in both conditions and in all genotypes ex-

cepted photoprotective mutants (*npq1* and *npq4*). At the 16 leaves stage, illumination of whole plants grown under Inland-Late Autumn condition resulted in a fast upregulation of NPQ at the induction phase (within 120 seconds of illumination), with most of accessions presenting the same trend of induction (Figure 5.14B). In contrast, plants grown under the Coastal-Late Autumn condition, showed a slower increases in NPQ at the induction phase and maximum NPQ was reached after 450 seconds of illumination. Under the Inland-Late Autumn condition, the variation in NPQ capacity ranges between 1.6 - 3.5, while Coastal-Late Autumn plants showed a variation in NPQ capacity between 2.3 - 4.2 at steady phase. Two photoprotective mutants, *npq1* and *npq4*, are completely devoid of the fast quenching phase (Müller *et al.*, 2001; Lambrev *et al.*, 2010). The fluorescence quenching of these lines reached a maximum value four times lower than all natural accessions in both dynamic conditions. Dark relaxation of fluorescence quenching was clearly different between accessions; *npq1* and *npq4* mutants showed almost no relaxation, while both inland and coastal plants recovered the most fluorescence quenching with approximately 75% of fluorescence within one minute.

When comparing plants of the same leaf number, similar NPQ kinetics were presented in Experiment V as in Experiment IV, as shown in Figure 5.15 (C and D). The variation of NPQ capacity of Inland-Early Autumn plants at the end of the induction stage (120 seconds of illumination) ranged between 1.8 - 3.2 was not different to the NPQ levels of Inland-Late Autumn plants in Experiment IV. However, the Coastal-Early Autumn plants show much lower maximum NPQ capacity than the Coastal-Late Autumn plants with a range of 2.5 -3.7.

GWAS for NPQ

GWAS was undertaken to find the genetic basis of the natural variation in NPQ found in response to the different environments. First, GWAS was performed using data from all time points of Experiment IV using 250K SNP chip as a preliminary test. To increase the resolution of detected QTL, the 6M SNP data set was then used in both Experiments (IV and V) for a genome-wide scan. For the *GxE* analysis, results from the different growth conditions were compared at the same number of leaves to eliminate any effects of developmental delay. From this

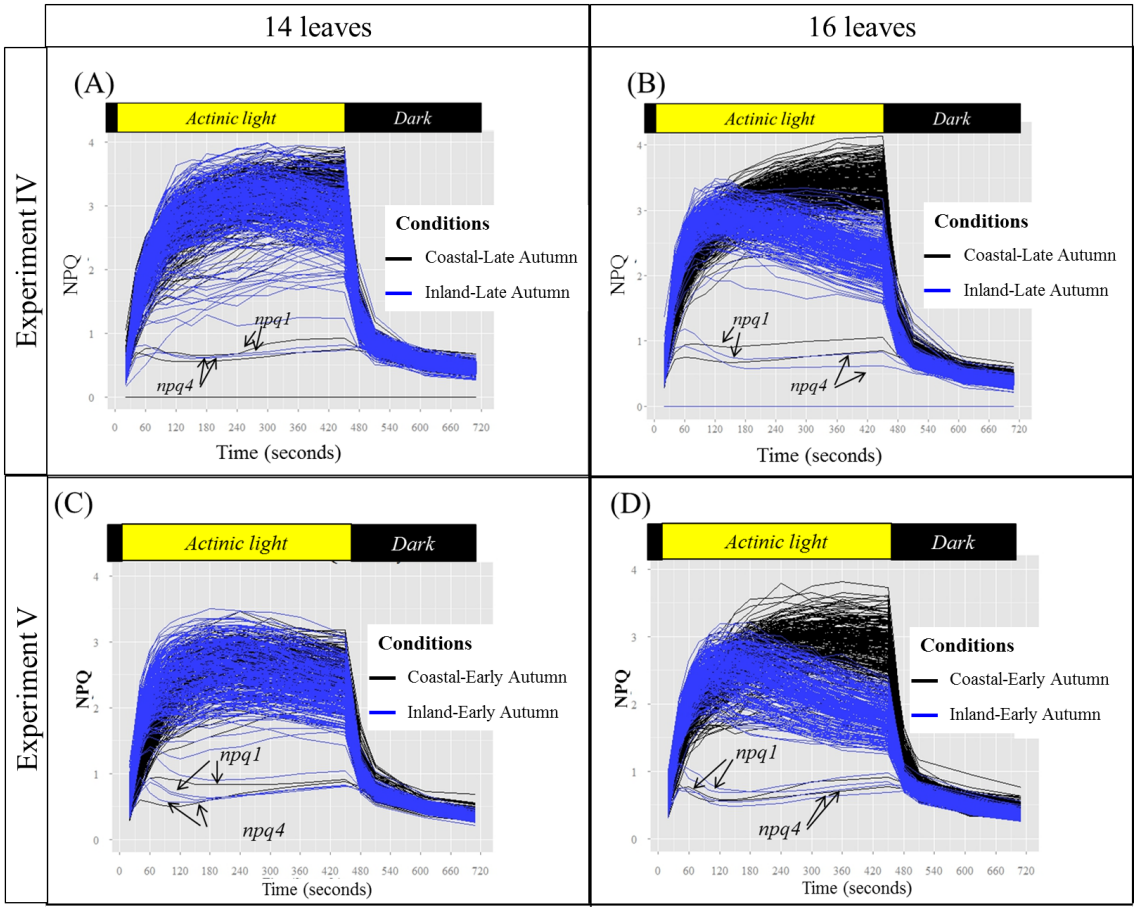

Figure 5.14 – *NPQ kinetics in different Arabidopsis genotypes showing the genetic variation of NPQ of Experiment IV (A and B), and Experiment V (C and D). The 284 Arabidopsis natural accessions, 3 photoprotective mutants were grown under inland (blue) and coastal (black) conditions. The NPQ measurement was performed at 25 days old plants (A) and at 40 days old plants (B). The 223 Arabidopsis natural accessions, 3 photoprotective mutants and 11 Knockout lines were grown under inland (blue) and coastal (black) conditions. The NPQ measurement was performed at 25 days old plants (C) and at 40 days old plants (D).*

analysis 15 QTL were identified (Table D.4). The summary of identified QTL and their estimated effects across two experiments was shown in Table 5.1.

In Experiment IV, six QTL were identified, ***QTL1-1***, ***QTL1-3***, ***QTL1-4***, ***QTL2-1***, ***QTL2-2*** and ***QTL5-1*** which are located on chromosome 1, 2 and 5 respectively. Different QTL were identified across three kinetic parameters of NPQ production as shown in Figure 5.15 and 5.16 and summarised in Table 5.1. Four additional QTL were identified from Experiment V using 6M SNP data: one QTL was specific for the coastal growth condition (***QTL5-6***), two QTL were presented under inland growth condition (***QTL1-6*** and ***QTL5-3***), and one QTL was for *GxE* in-

teraction (***QTL2-6***) as shown in Figure 5.17. These additional QTL are located in a different region (more than 250Kb) from the QTL identified from Experiment IV. However, the most interesting QTL is ***QTL1-4*** as shown on the manhattan plots (Figure 5.15 and 5.16). ***QTL1-4*** was shown with high SNP density at the QTL locus, and also this QTL appeared at many time points across the three NPQ kinetics phases (the SNP location was found between snp1_16,814,879 and snp1_16,868,681).

Multiple traits GWAS analysis for NPQ

The power to determine the genetic architecture of the NPQ response in Arabidopsis can be increased by considering the NPQ values at multiple timepoints during the NPQ measuring protocol. For such an approach, multiple traits analysis were performed under a GWAS model. Multi traits analysis for the NPQ response over time was performed with different frequencies of NPQ time points. The Manhattan plot showed a discovery of a significant SNPs associated with the NPQ phenotype located on chromosome 2 (***mQTL2***), as shown in F5.18 (A and B), when including multiple NPQ values over time. Another QTL on Chromosome 1 identified using Multi-trait analysis, was at a similar locus to ***QTL1-4*** identified in single trait analysis. In comparison, when combining a smaller numbers of NPQ time points, the multi QTL analysis showed the same association as the single QTL analysis, as in Figure 5.18 (C and D) and Figure 5.19.

There is one new significant QTL, ***mQTL2***, with LOD score greater than 6 located on chromosome 2 at snp2_5,294,186. To find candidate genes under the mQTL2, the 10 kb upstream and 10 kb downstream from the significant SNPs region were searched. The summary of multiple QTL candidate genes was presented in Table 5.2. This SNP was located in a range of candidate genes: (1) **At2g12875**, a gene with no described function, (2) **At2g12880**, a Zinc knuckle (CCHC-type) family protein, and (3) **At2g12900** a Basic-leucine zipper (bZIP). All three candidate genes had no previously known effect on photosynthetic or photoprotective mechanisms.

Table 5.1 – *The comparison of NPQ QTL and their estimated effects across two experiments using 6M SNP data. Grey, blue and green colours represent the QTL as a result of genetic variation grown under coastal, inland and the interaction between coastal and inland (GxE) respectively.*

QTL[a]	Chr	Position[b]	LOD[c] score	Freq[d] (%)	%variation	Trait apperence					
						Exp IV			Exp V		
						Coastal	Inland	GxE	Coastal	Inland	GxE
QTL1-1	1	347,233	8.66	0.24	3.4	NPQ Steady [e]					
QTL1-2	1	9,729,376	7.04	0.36	9.2				FvFm [f]		
QTL1-3	1	16,351,441	7.04	0.52	5.6		NPQ Slope Induction [f]				
QTL1-4	1	16,869,695	8.15	0.79	9.5	FvFm [f]	QY-max [f]				
						NPQ Steady [f]	NPQ Induction [f,ns]				
						NPQ Max [f]					
						NPQ Slope Relaxation [f]					
QTL1-5	1	20,680,932	7.93	0.05	13.7					NPQ Steady [f]	
QTL2-1	2	10,934,450	8.07	0.07	10.1		FvFm [f]				
QTL2-2	2	10,984,417	7.95	0.06	12.2		NPQ Steady [e]				
							QY-max [f]				
QTL2-3	2	11,680,235	7	0.21	6.7						NPQ Slope Induction [f]
QTL4-1	4	1,509,645	7.95	0.19	0.91					FvFm [f]	FvFm [f]
QTL4-2	4	5,270,810	7.14	0.22	7.5					NPQ Induction [f]	
QTL4-3		13,911,309	9.13	0.06	0.1				NPQ Steady [e]		
QTL5-1	5	15,037,793	6.93	0.09	1.37	NPQ Relaxation [f]					
QTL5-2	5	15,930,795	7.27	0.22	11.67					NPQ Relaxation [f]	
QTL5-3	5	18,511,604	7.23	0.26	2.3			NPQ Slope Induction [f]			
QTL5-4	5	25,477,423	7.71	0.11	14.0				NPQ Steady [f]		

[a] QTL identified from the Exp IV and V

[b] Physical position (in base pair) according to TAIR

[c] LOD of the 5% empirical genome-wide significance threshold (> 6.17)

[d] Reference Col-0 allele frequency

[e] Analysis results at 14 leaves stage

[f] Analysis results at 16 leaves stage

[ns] Indicate QTLs that did not have a statistically significant effect on traits values by GWAS

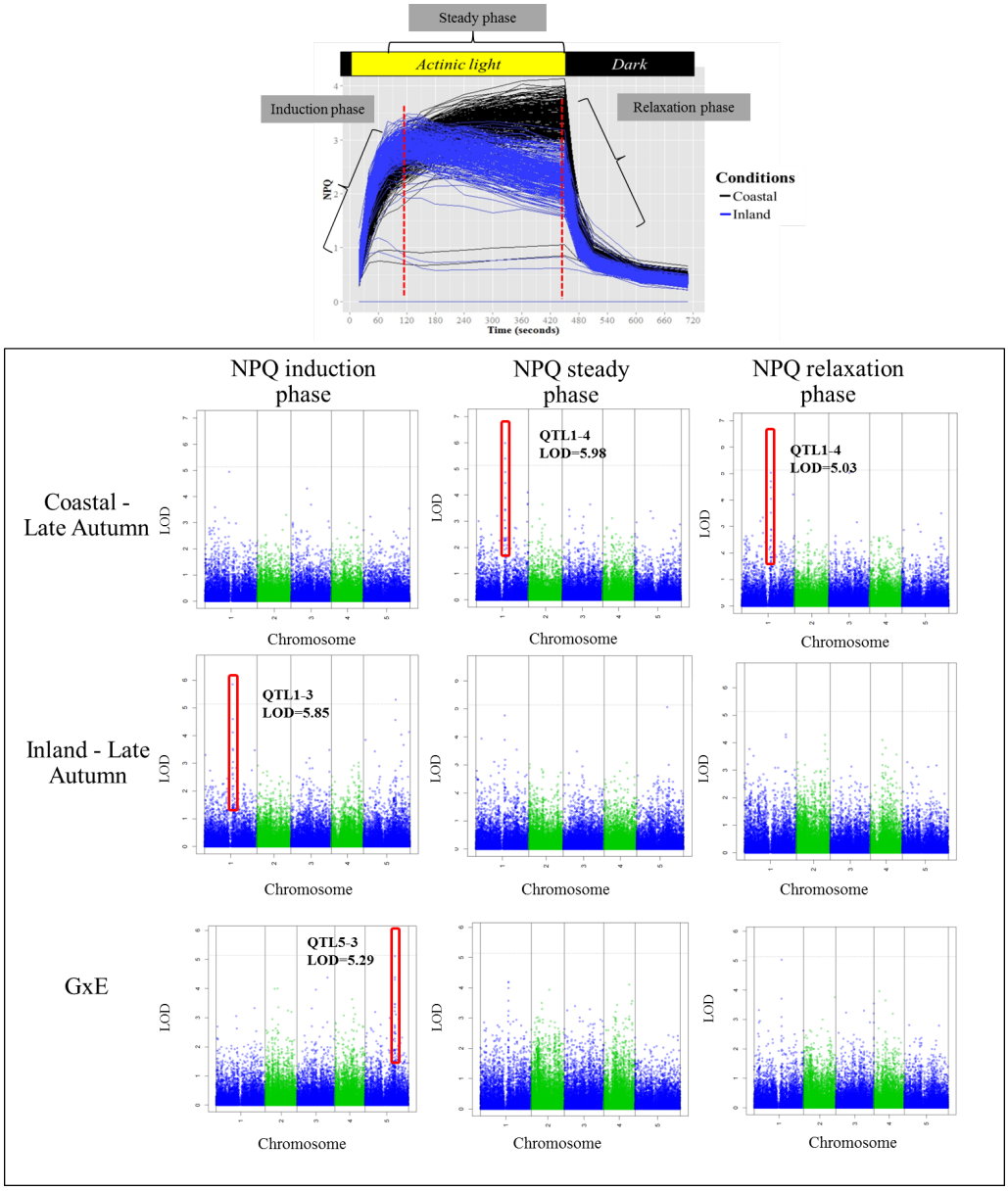

Figure 5.15 – *Manhattan plots of GWAS results using 250K SNP database for NPQ trait of experiment IV. The chromosomes are depicted in different colors on x axis. The horizontal dash-dot line corresponds to a nominal P < 0.05 significance threshold.*

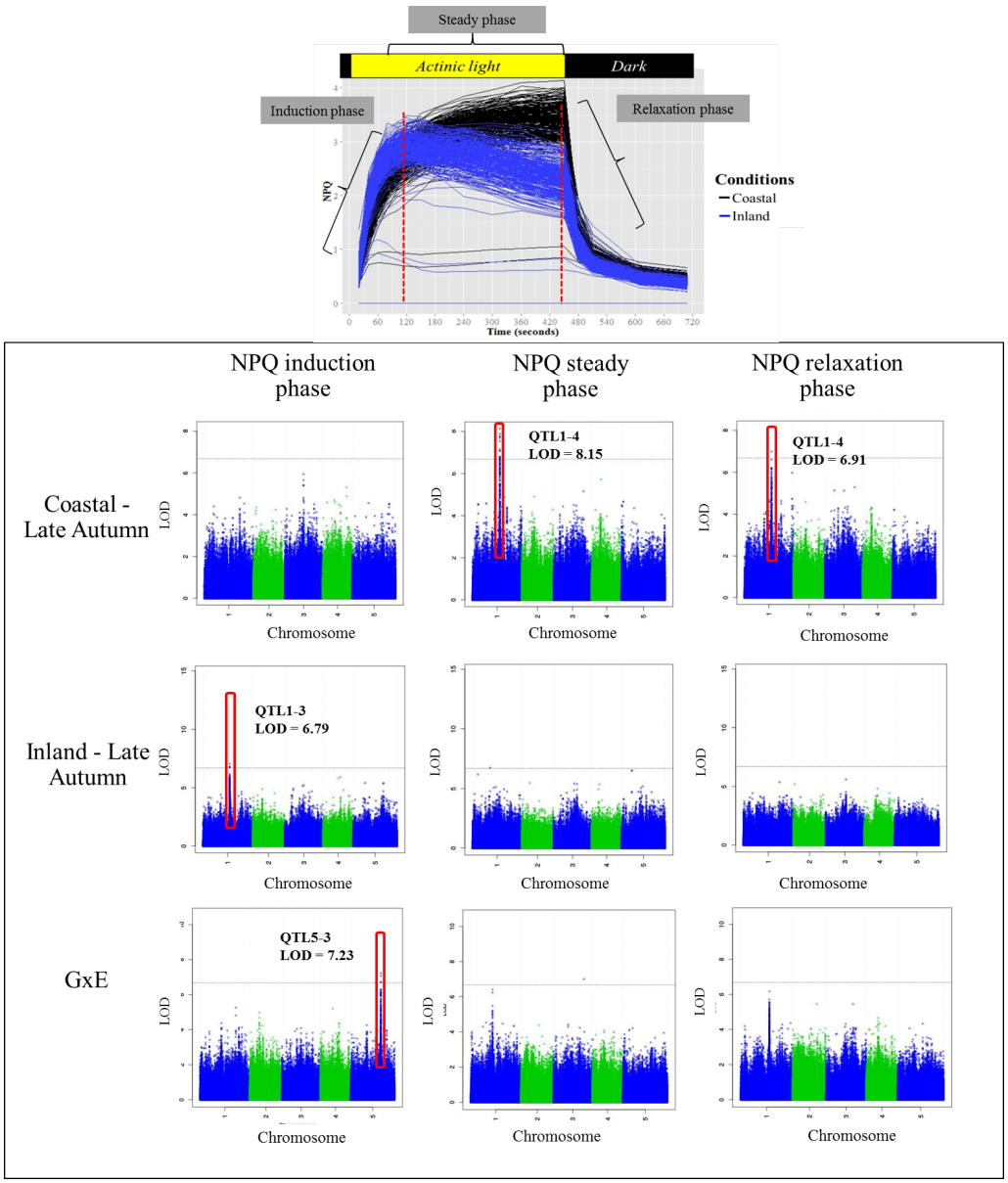

Figure 5.16 – *Manhattan plots of GWAS results using 6M SNP database for NPQ trait of Experiment IV. The chromosomes are depicted in different colors on x axis. The horizontal dash-dot line corresponds to a nominal P < 0.05 significance threshold*

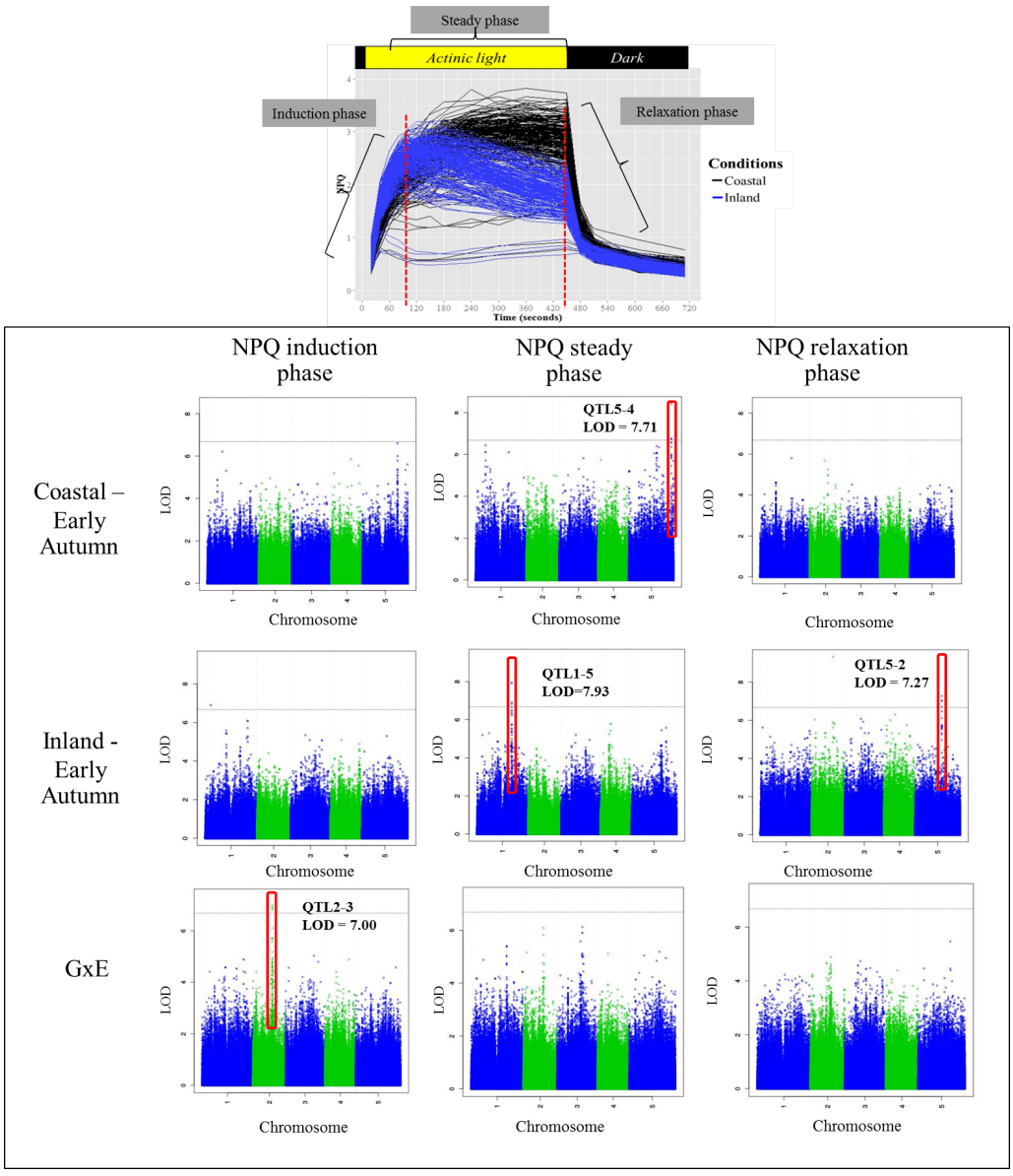

Figure 5.17 – *Manhattan plots of GWAS results using 6M SNP database for NPQ trait of Experiment V. The chromosomes are depicted in different colors on x axis. The horizontal dash-dot line corresponds to a nominal P < 0.05 significance threshold.*

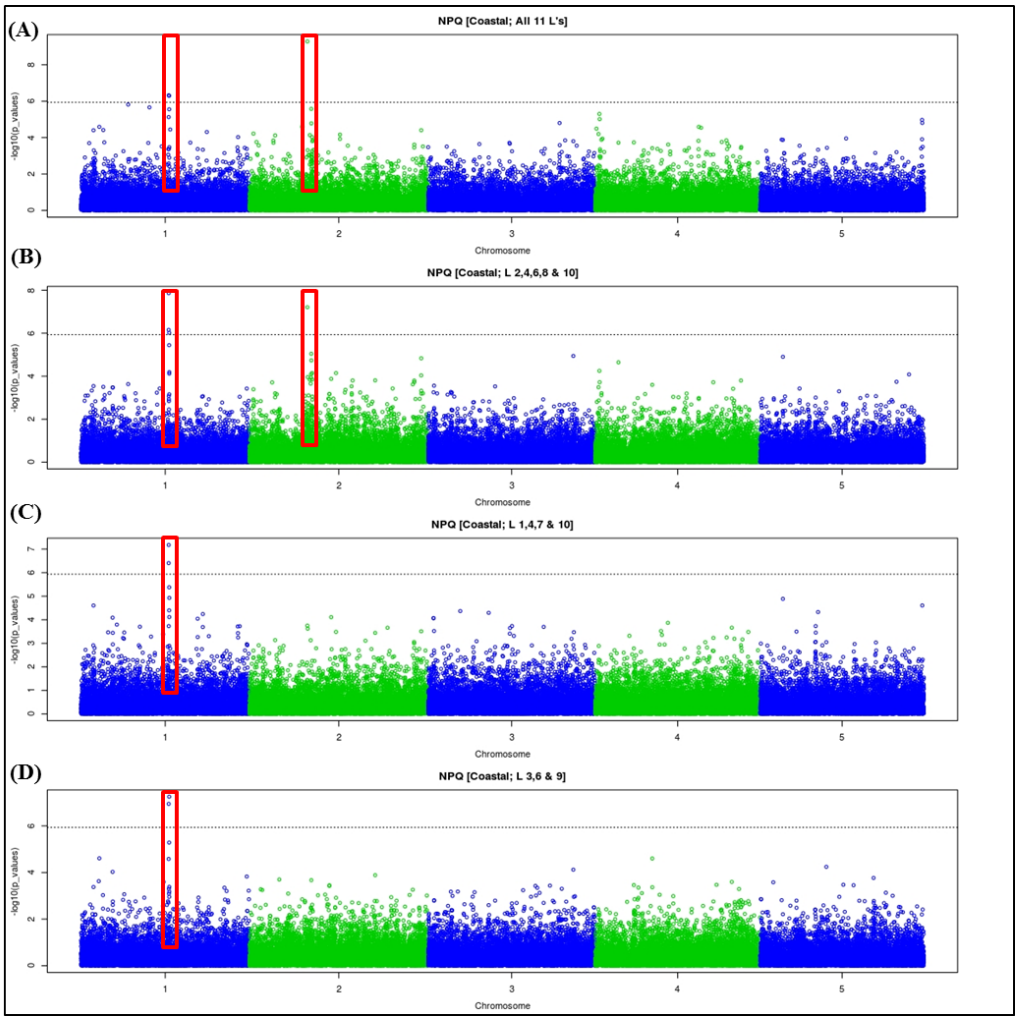

Figure 5.18 – *The Manhattan plot showing the results of multi traits NPQ QTL analysis of Experiment IV under Coastal-Late Autumn. The results showed a discovery of QTL on chromosome 2. The Manhattan plots represent multi traits GWAS analysis for NPQ over time at 20s to 360s (A), from 40s, 80s, 120s, 180s and 300s (B), from 20s, 80s, 150s and 360s (C), and from 60s, 120s and 240s (D). The chromosomes are depicted in different colors on x axis. The horizontal dash-dot line corresponds to a nominal $P < 0.05$ significance threshold.*

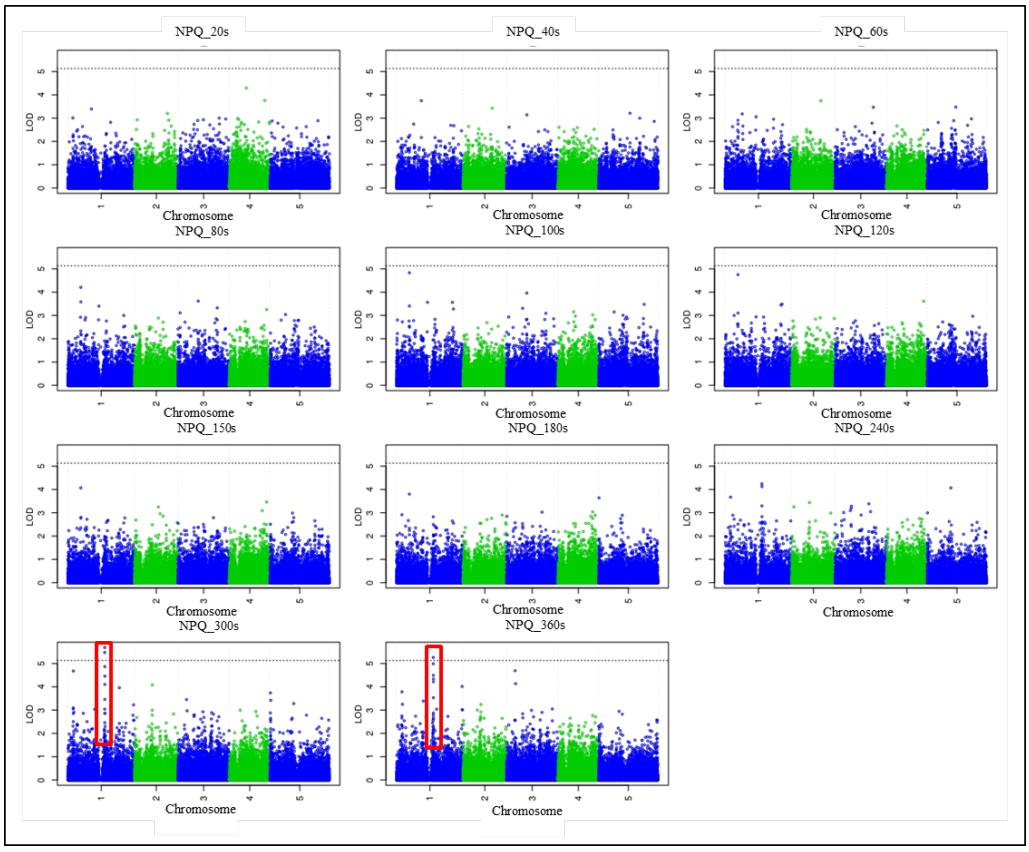

Figure 5.19 – *The Manhattan plot showing the results of single traits GWAS analysis of Experiment IV for NPQ from 20s âĂŞ 360s after illumination. The chromosomes are depicted in different colors on x axis. The horizontal dash-dot line corresponds to a nominal P < 0.05 significance threshold.*

Table 5.2 – *Summary of the Multi trait QTL analysis and candidate gene listed for NPQ under Coastal-Late Autumn condition.*

QTL	Chr	QTLs region	LOD[A] score	Freq[B] (%)	% variation	Candidate genes		Description
						Gene name	Location	
mQTL2	2	5294186	9.28	0.12	0.05	AT2G12875	5289411-5291470	unknown protein
						AT2G12880	5291523-5291882	Zinc knuckle (CCHC-type) family protein
						BZIP33: AT2G12900	5293897-5295480	Basic-leucine zipper (bZIP). INVOLVED IN: regulation of transcription

5.2.7 Candidate gene confirmation

As previously demonstrated in Section 5.2.6, the GWAS analysis provided promising results on identifying candidate genes responsible for variation in photoprotective mechanism in the model plant *Arabidopsis* under coastal and inland simulated environments. A total of 15 strong QTL for NPQ led to the identification of 69 potential candidate genes (Table D.4). Then, those potential candidate genes were selected on the basis of the five criteria. The first criteria was location within a certain distance of the QTL (20 kb), and the remaining four selection criteria were as follows; (A) gene function related to photosynthesis and photoprotection, (B) gene expression in the leaf tissue, (C) gene function related to abiotic stress, and (D) unknown functional genes that are located under the identified QTL as shown in Table D.4. Those criteria eliminated a total of 45 candidate genes resulting in only 24 candidate genes remaining, as presented in Table 5.3.

Of the 24 candidate genes, nine genes, including the PsbS gene (*npq4* mutant), were found to be involved in photosynthesis and photoprotection and expressed in leaf tissues. Three genes were related to abiotic stress and express in leaf tissue. Two identified genes were found to be expressed in leaf tissue, involved in photosynthetic mechanisms and abiotic stress. Two genes were abiotic stress related. Five genes had unknown biological function reported. Three were found to only express in leaf tissue.

To confirm whether these genes are related to NPQ process, knockout lines were obtained from the Arabidopsis Biological Resource Centre (ABRC) and the presence and the location of the T-DNA insert was confirmed by PCR (see Section 2.6 for details). Confirmed knockouts were then phenotyped for NPQ capacity and kinetics under the coastal and inland growth conditions. From the potential candidate genes listed in Table 5.3, 24 knockout lines were ordered from ABRC, and two photoprotective mutants, *npq4* and *npq1* (*npq4* was identified as candidate), were harvested from previous experiments. Two out of 24 candidate mutants (*npq4* and *cul4*) seem to be the strongest candidate mutants as they fitted into 3 criteria.

A total of 24 knockout lines were phenotyped for NPQ under Coastal-Late Au-

Table 5.3 – *Summary of 24 candidate genes classified based on four criteria. (A) gene function related to photosynthesis and photoprotection, (B) gene express in the leaf tissue, (C) gene function related to abiotic stress, and (D) unknown function gene that located under identified QTL. Colour indicates group of genes that have the same selection criteria.*

No.	AGI ID	Name	Description	Selection criteria				Seed stock ID
				A	B	C	D	
1	AT1G44191		Encodes a ECA1 gametogenesis related family protein				✓	SALK_119440C
2	AT1G44575	NPQ4	Encoding PSII-S (CP22), Involved in NPQ, Mutant has a normal violaxanthin cycle but has a limited capacity of quenching singlet excited chlorophylls and is tolerant to lipid peroxidation.	✓	✓	✓		npq4
3	AT1G55370	NDF5	NDH-dependent cyclic electron flow 5 (NDF5); functions in: carbohydrate binding, catalytic activity; INVOLVED IN: positive regulation of gene expression, photosynthetic electron transport in photosystem I	✓	✓			SALK_019994c
4	AT1G79650	RAD23B	Encodes a member of the RADIATION SENSITIVE23 (RAD23) family;	✓	✓			SALK_023070C
5	AT1G79680	WAKL10	Encodes a twin-domain, kinase-GC signaling molecule that may function in biotic stress responses		✓	✓		SALK_132887C
6	AT2G18050	HIS1-3	Encodes a structurally divergent linker histone whose gene expression is induced by dehydration and ABA.			✓		SALK_025209C
7	AT2G18790	PHYB	Red/far-red photoreceptor involved in the light-promotion of seed germination and in the shade avoidance response.	✓	✓			CS6217
8	AT2G30440	TPP	Encodes a thylakoidal processing peptidase that removes signal sequences from proteins synthesized in the cytoplasm and transported into the thylakoid lumen.	✓	✓			SALK_104367
9	AT4G00360	CYP86A2:	Encodes a member of the CYP86A subfamily of cytochrome p450 genes. Expressed at moderate levels in flowers, leaves, roots and stems.		✓			SALK_005826C
10	AT4G00370	ANTR2	Encodes an inorganic phosphate transporter (PHT4;4). It has been shown to play a role in the xanthophyll cycle during photosynthesis and may be required for tolerance to strong light stress.	✓	✓			CS26443
11	AT4G03280	pgr1	Mutant has reduced electron transport at saturating light intensities and Q-cycle activity is hypersensitive to acidification of the thylakoid lumen.		✓	✓		SALK_019871C
12	AT4G03430	STA1	STA1 expression is upregulated by cold stress, and the sta1-1 mutant is defective in the splicing of the cold-induced COR15A gene.			✓		SALK_007933
13	AT4G05520	EHD2	Encodes AtEHD2, one of the Arabidopsis Eps15 homology domain proteins involved in endocytosis (AtEHD1, At3g20290).				✓	SALK_046090
14	AT4G08340		Unknown				✓	SALK_014160C
15	AT4G12060	CLPT2	Involved in: protein metabolic process		✓			SALK_132943C
16	AT4G19580		DNAJ heat shock N-terminal domain-containing protein; functions in: heat shock protein binding	✓	✓			SALK_025164C
17	AT4G19640	ARA7	GTP binding				✓	SALK_090266C
18	AT4G39910	UBP3	Encodes a nuclear ubiquitin-specific protease.				✓	SALK_139828C
19	AT5G12130	PDE149	Seedling development, thylakoid membrane organization		✓			SALK_002037C
20	AT5G39790	PTST	Encodes a chloroplast localized protein that is involved in protein translocation and starch metabolism.	✓	✓			SALK_012617C
21	AT5G39830	DEG8	Encodes DEG8, Involved in the cleavage of photodamaged D2 protein of photosystem II (PSII).	✓	✓			SALK_004770C
22	AT5G46210	CUL4	The partial loss of CUL4 function resulted in a constitutive photomorphogenic phenotype with respect to morphogenesis and light-regulated gene expression.	✓	✓	✓		SALK_077684C
23	AT5G63570	GSA1	The expression of this gene was demonstrated to be light-induced; involved in chlorophyll biosynthetic process	✓	✓			SALK_089309
24	AT5G63650	SNRK2.5	Encodes a member of SNF1-related protein kinases (SnRK2) whose activity is activated by ionic (salt) and non-ionic (mannitol) osmotic stress.		✓	✓		SALK_075624

tumn condition. The Coastal-Late Autumn condition was chosen as it was allowed identification of NPQ QTL (as described in Figure 5.1). NPQ capacities were compared with wild-type plant (Col-0), the background genotype of all knockouts. The NPQ kinetics of all knockout lines was presented in supplementary Figure D.2 - D.5. From the total of 24 knockout lines, most of them showed nearly identical NPQ kinetics to Col-0. Four interesting KO mutants are presented in Figure Figure 5.20. The *Arabidopsis* NDH-Dependent Cyclic Electron Flow 5 mutant, ***KO-NDF5***, showed a different pattern compared to others knockout lines. The NPQ kinetics of ***KO-NDF5*** showed significant differences at the 60s and 80s time points of illumination with a lower NPQ induction rate compared to Col-0. The NPQ levels then increased to higher than Col-0 after 180s through the illumination period. The *KO-PHYB* mutant showed slightly lower NPQ formation after 180s of actinic light illumination, however it was not significantly different. For the *npq1* and *npq4* mutants, defective NPQ productions was seen under this condition, which was consistent with all of the experiments in this study.

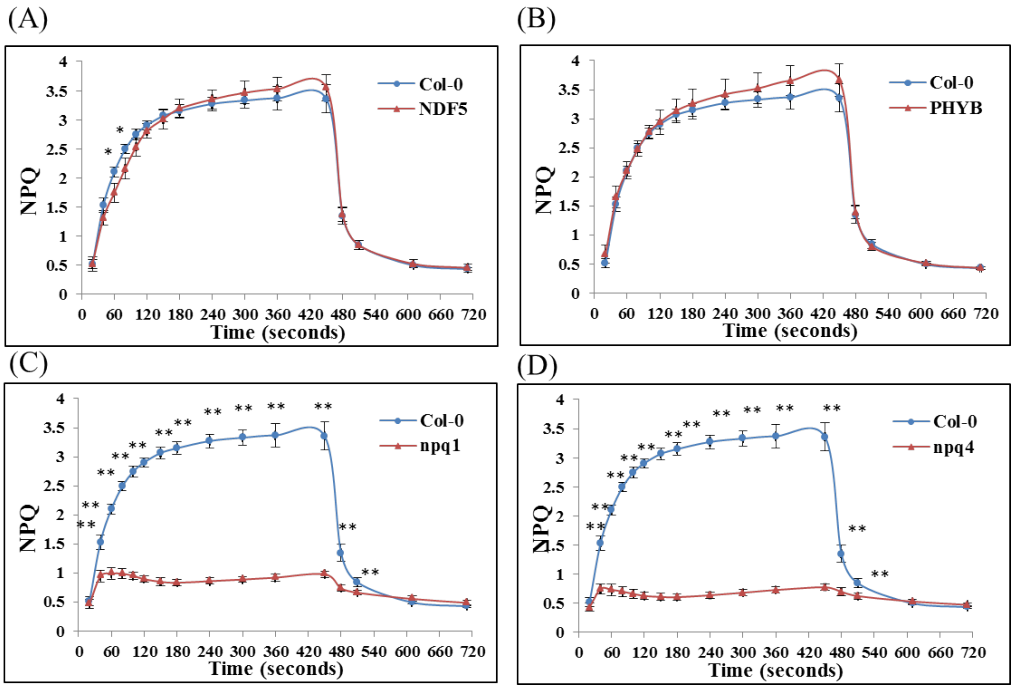

Figure 5.20 – ***NPQ kinetic of 4 knockout lines screening compared to Col-0 plants under coastal condition. Blue lines represent the NPQ kinetics of Col-0 plants (n=5), and red lines represent knockout lines (n=5). A, B, C, and D represented NPQ kinetics of NDF5, PHYB, , npq4, and npq1 respectively. The data are mean ±SD. Asterisks indicated statistically significant differences between Col-0 and each knockout lines (∗:P<0.05, ∗∗:P<0.01, and ∗∗∗:P<0.001).***

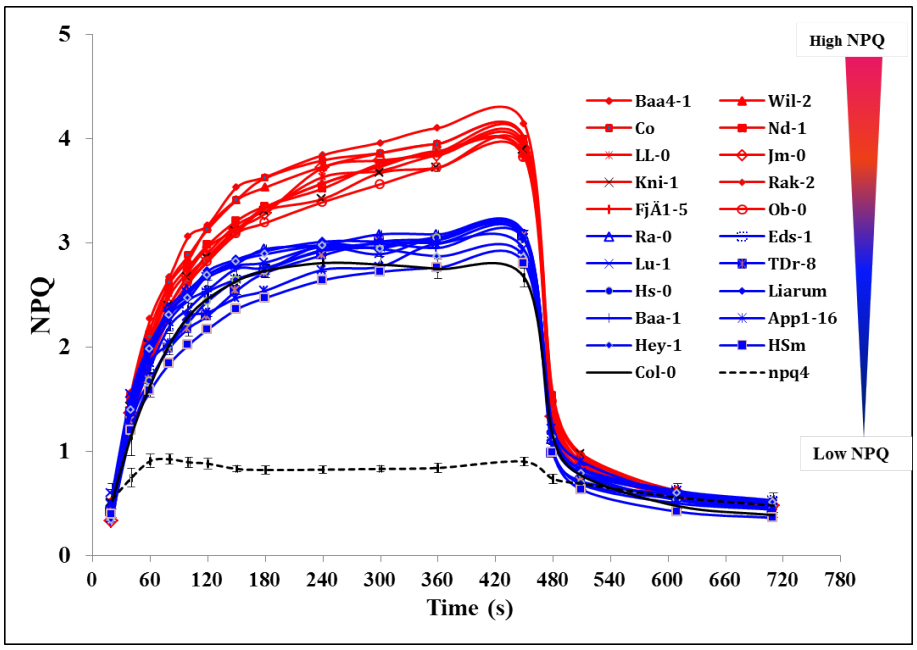

Figure 5.21 – *NPQ kinetics of low and high accessions. NPQ values in low and high NPQ accessions were grown under Coastal-April in Experiment IV at 16 leaves stage which were measured from the whole rosette areas using protocol P3 (as described in Chapter 3). The low NPQ accessions are in blue and the high NPQ accessions are in red. Col-0 plants are presented in a black solid line which represents the mean ± SD (n=16). The npq4 mutant are presented in a black dotted line which represents the mean ± SD (n=4).*

5.2.8 High and Low NPQ Haplotype

High and low NPQ accessions

As seen in Section 5.2.6, natural variation in NPQ formation was observed among accessions and between growing conditions. To study the genetic variation of NPQ capacity, 10 of the low and 10 of the high NPQ accessions were selected based on NPQ profiles under coastal condition as this conditions presented the most significant QTL (as shown in Figure 5.21. Baa4-1, Wil 2, Co, Nd-1, Ll-0, Jm-0, Kni-1, Rak-2, Fja1-5 and Ob-0 are classified as high NPQ *Arabidopsis* accessions with total NPQ capacity higher than 3.8, whereas Ra-0, Eds-1, Lu-1, TDr-8, Hs-0, Liarum, Baa-1, App1-16, Hey-1, HSm, and Col-0 are classified as low NPQ accessions having total NPQ capacity below 3.0. The maximum NPQ capacity of *npq4* mutant is 0.9.

Correlation between geographic distribution and NPQ levels

Previous results showed that some accessions exhibited relatively high NPQ capacity compared to the standard wild-type (Col-0). What caused those high NPQ accessions to have higher NPQ capacity? Is there correlation between natural habitat and NPQ capacity? The geographic distribution of 283 *Arabidopsis* natural accessions as shown in Figure 5.22 indicated that there is no obvious correlation between the capacity of NPQ and place of origin. The high and the low NPQ accessions are randomly spread around European (Figure 5.22B). Among these European accessions, the latitude and altitude of geographical origin has been shown to have no significant relationship with the NPQ capacities of plants growing under coastal condition (as shown in Figure 5.23).

High and low NPQ haplotypes of *PsbS*

From GWAS analysis and the NPQ profile, one of the strongest candidate genes that has a known function in NPQ was non-photochemical quenching 4 gene: *PsbS* (**At1g44575**) identified for ***QTL1-4*** as SNP_16,869,695. ***QTL1-4*** is located on *PsbS*, a ubiquitous pigment-binding protein associated with PSII of higher plants. ***QTL1-4*** was presented at several timepoints during the NPQ measurement protocol, and it also appeared in both coastal and inland in late autumn conditions. The GWAS profiles at ***QTL1-4*** showed high frequency of SNPs change in the PsbS promoter and coding region. To see if any of these SNPs were in transcription factor motifs or caused significant animo acid changes, the different haplotype mapping of SNPs between the low and high NPQ accessions were analysed using TAIR10 (http://signal.salk.edu/atg1001/3.0/gebrowser.php), as shown in Figure 5.24. The haplotype mapping results indicated two different haplotypes, with one for high NPQ accessions and one for low NPQ accessions. There are at least 17 common SNPs within the 2 kb of the PsbS promoter, which are found in high NPQ accessions and are different from those in the low NPQ accessions. In addition, most of the common SNPs found in the low NPQ accessions showed similar haplotype to Col-0. There were only a few SNPs that appeared different. Form haplotype mapping, hence, two new sequence sets (high and low NPQ sequences) were generated based on common SNPs obtained from the web browser (http://signal.salk.edu/atg1001/3.0/gebrowser.php).

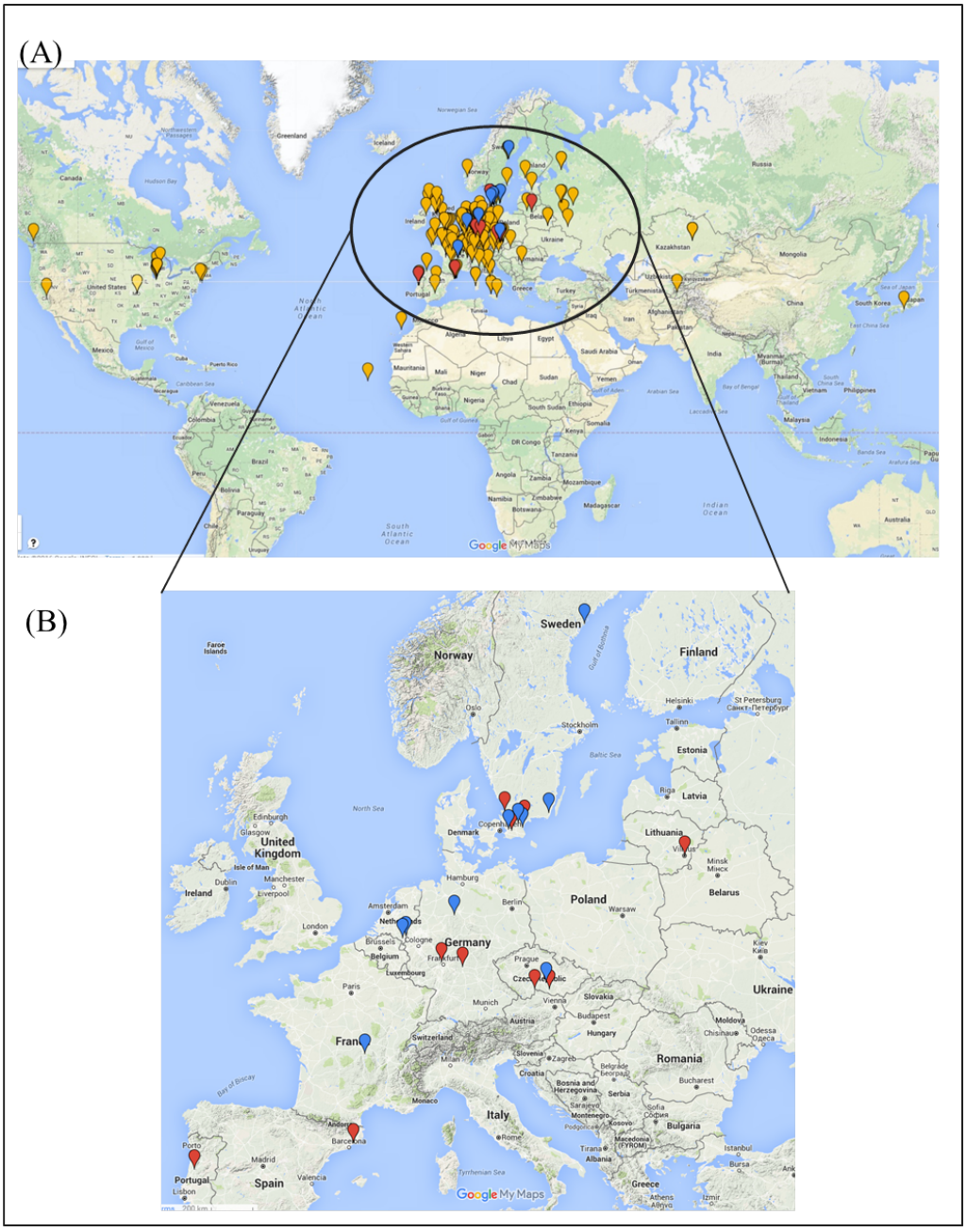

Figure 5.22 – *The geographic distribution of 284 Arabidopsis natural accessions (subset from HapMap set). (A) represents the distribution of 283 accessions used in this study. High NPQ accessions are represented in red, while low NPQ accessions are presented in blue. (B) is the expansion of country of origin of high and low NPQ accessions. The images are generated using www.google.com/map).*

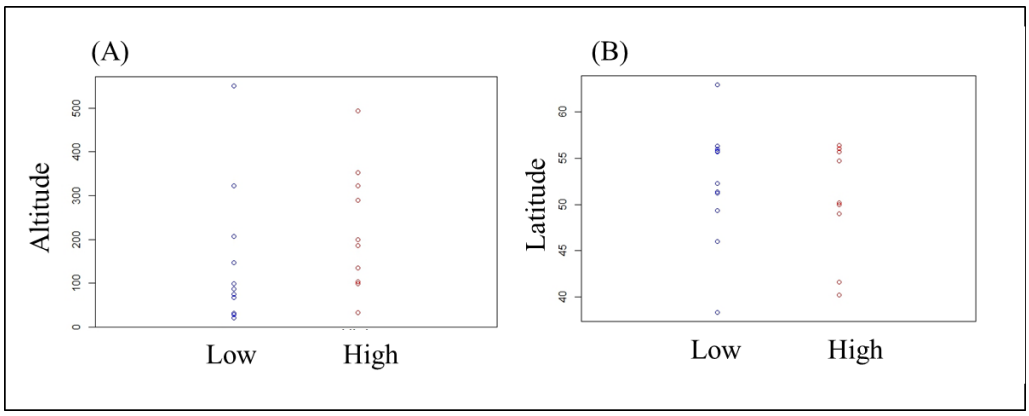

Figure 5.23 – ***The correlation between Arabidopsis natural accessions (subset from HapMap set) and altitude and latitude. (A) represents the correlation of 283 accessions and altitude. High NPQ accessions are represented in red, while low NPQ accessions are presented in blue. (B) is the correlation of 283 accessions and latitude of high (red) and low (blue) NPQ accessions.***

Amino acid change was also investigated between the high and low NPQ accessions as presented in Figure 5.25. To answer whether common SNPs that differ from the referent genotype (Col-0) resulted in changes in amino acid between high and low NPQ accessions, amino acid polymorphisms were mapped in the coding sequence of the *PsbS* gene. According to the results presented in Figure 5.24, high NPQ accessions have four synonymous amino acid changes, one that correlates with a significant SNP (snp_16871887) in the GWAS results. These synonymous amino acid changes between the haplotypes are in both splice variants and are located at A40A, I83I, L119L, and A177A.

The results obtained from haplotype mapping indicated that the high NPQ phenotype is controlled by the non Col-0 haplotype, whereas accessions that have most of Col-0 alleles at this SNPs positions presented as low NPQ phenotype. Although the low NPQ accessions contain most of Col-0 allele, there is allelic variation among these low accessions compared to Col-0.

5.2.9 Motifs change in the *PsbS* promoter

Two haplotypes (high NPQ and low NPQ) were established for the *PsbS* promoter where high NPQ accessions contain non-Col-0 allele, whereas low NPQ accessions contain Col-0 allele (as discussed in Section 5.2.8. The function of

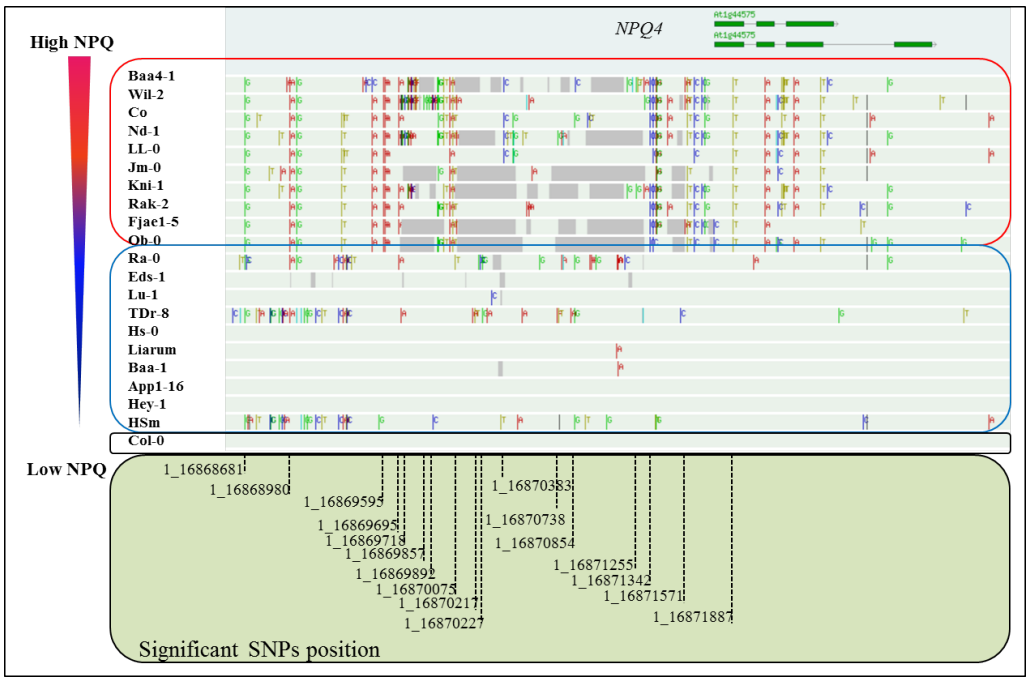

Figure 5.24 – ***Haplotype mapping of high and low NPQ accessions showing common SNPs differences at the SNPs peaks from GWAS analysis. A, C G, and T SNPs are indicated by red, blue, green, and yellow colour respectively. Gray area represented unsequenced regions. Data was generated using free online software: http://signal.salk.edu/atg1001/3.0/gebrowser.php.***

three different motif sequences (Col-0, high NPQ, and low NPQ sequences) was investigate in 2kb of *PsbS* promoter using the web-based PlantCARE database (http://bioinformatics.psb.ugent.be/webtools/plantcare/html/). The sequence at *PsbS* promoter of Col-0, high and low NPQ sequence contains a total number of 30 motifs (Table D.3 including a number of light responsive elements; two auxin and one gibberellin responsive elements; cis-acting element involved in heat and low temperature stress response elements; and gibberellin responsive elements.

The analysis of the two promoter regions showed that high and low NPQ sequences share the similar motif compositions. Although, they share similar motif sets, the position of some of the motifs was different between the three groups. As seen in Figure 5.26, two motifs, CAAT-box motif and TATA-box motif, were found to have different positions compared to predicted motifs in the Col-0 *PsbS* promoter. In the low NPQ promoter, the CAAT-box motif was identified in different positions of the three group promoters and was absent at +1148 position of the low NPQ promoter (motif analysis started from 2kb upstream of *PsbS* gene). The TATA-box motif was also absent in some positions in the high and the low

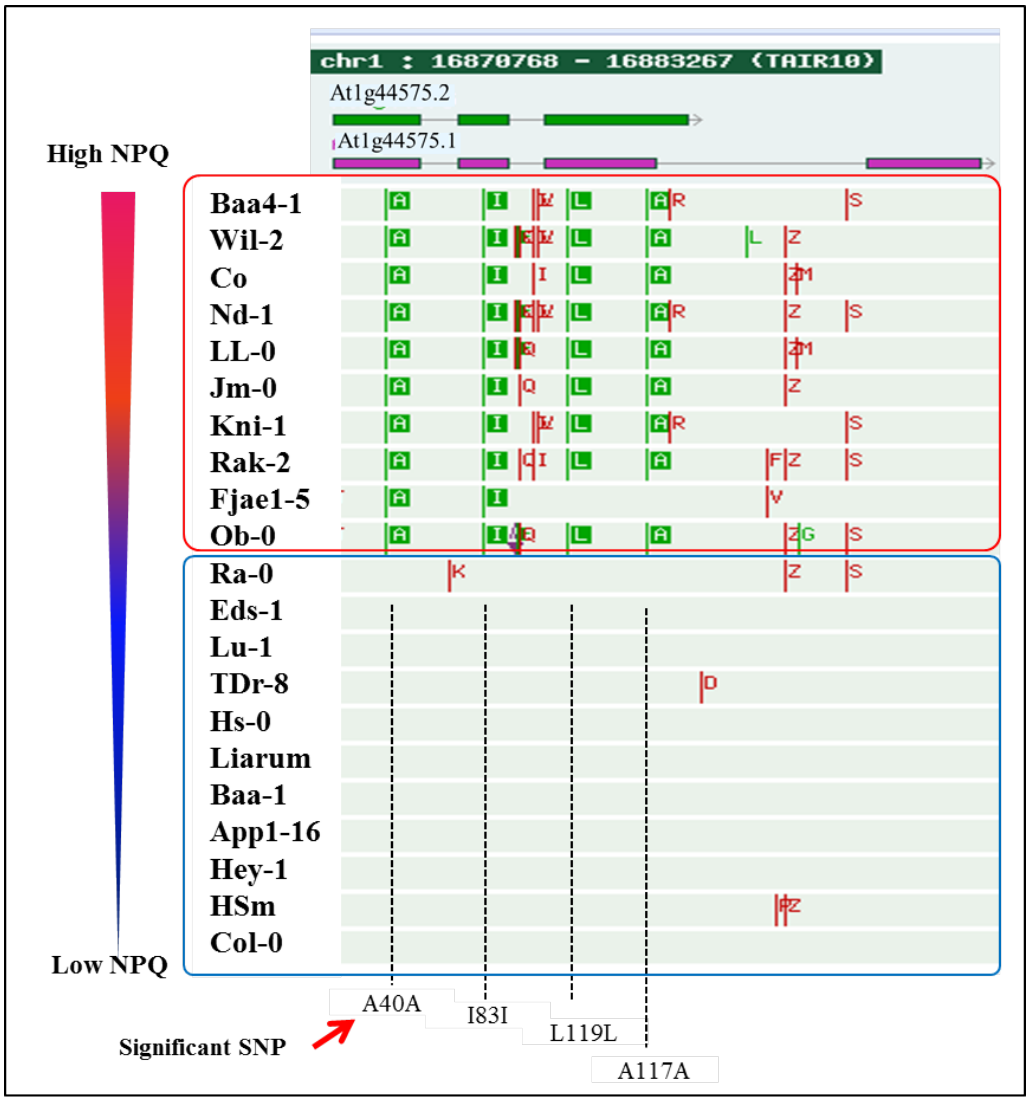

Figure 5.25 – *Haplotype mapping of high and low NPQ accessions showing amino acid change at the SNPs peaks: non-synonymous amino acids (red) and synonymous amino acids (green). Data was generated using from online software: http://signal.salk.edu/atg1001/3.0/gebrowser.php. (also in supplementary Figure D.8.)*

NPQ promoters. In addition to the different position of predicted motifs, there is one interesting motif, GAG motif, which is described as part of a light responsive element, which was absent in the high NPQ promoter.

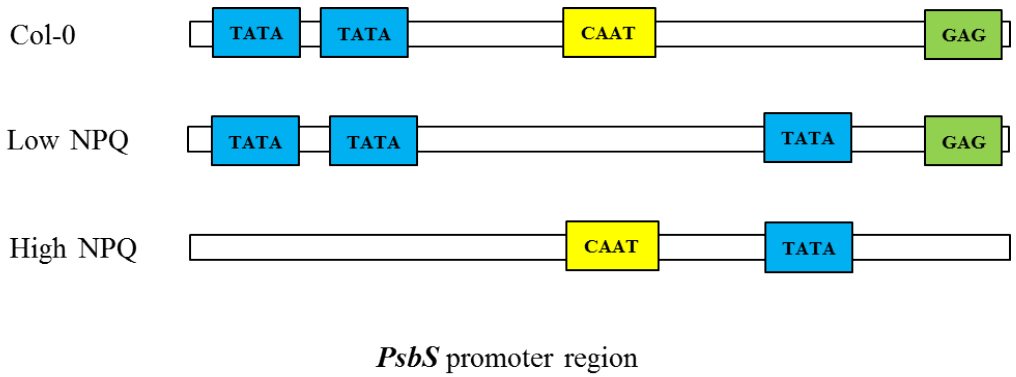

Figure 5.26 – *Diagram of high and low motif sets compared to Col-0 at PsbS promoter.*

5.3 DISCUSSION

Relatively high heritability was observed in the natural accessions for most of the traits investigated in this study; such as plant size, NPQ, and Fv/Fm traits, as presented in Table 3.1. High heritabilities have also been reported in others traits, such as flowering time, that have been studied successfully using GWAS (e.g. (Li *et al.*, 2010). This is evidence that the traits investigated in this study are suitable for future investigation into genetic association using a GWAS approach.

5.3.1 Genetic variation of plant development

Differences in rosette area are reported to be influenced by changes in light conditions (Mishra *et al.*, 2012), and in this study the smaller rosette area was found in the higher light Inland-Late Autumn condition compared to the Coastal-Late Autumn condition at the same chronological age. This is similar to the effect reported by Mishra and colleagues (Mishra *et al.*, 2012) with coastal plants presenting three times faster growth rates than inland plants. The slower development in the inland plants can be explained by the combination of factors such as low temperature and high light intensity during vegetative growth (Tsukaya, 2005; Cookson and Granier, 2006; Mishra *et al.*, 2012). Natural variation in leaf morphology and rosette area, for example leaf shape and longer petioles, was also present in this population. The results demonstrate that *Arabidopsis* accessions can survive and thrive under contrasting dynamics conditions. These results also suggest that differences in plant growth and leaf morphology are controlled by genetic factors as well as how the environment influences the expression of the genotype.

Under the more stressful inland condition, there is not only delayed vegetative growth, but also a delay in the number of days to flowering. This study showed that most of the natural accessions exhibited later flowering times under high light intensity and low temperature conditions (Inland-Late Autumn) compared to low light and warmer condition (Coastal-Late Autumn) (Figure 5.6). The delay in flowering time found in Inland-Late Autumn condition may be due to a decreased photosynthetic rate and slower developmental rate resulting from the combination of environmental stress factors such as light intensity and low tem-

perature.

Three QTL for rosette area were identified in the single traits GWAS analysis. The most interesting finding from this work is that SNPs in the *LHCB4.3* (Light Harvesting Complex Photosystem II) candidate gene were associated with differential growth under the inland condition. The knockout of this gene shows a slight reduction in photosystem II/I ratio (Bianchi *et al.*, 2011); and it has been reported to play a role in photoprotection (Umate, 2010). Light-harvesting chlorophyll binding (LHC) antenna protein is a primary unit for absorbing light energy for photosynthesis in higher plants. As a result this protein may act as an environmental sensor and changes in the expression or function of the LHC protein could change how the plant responds to environmental variation, possibly affecting plant growth and morphology.

5.3.2 Genetic variation in Chlorophyll content

Reduction in leaf chlorophyll content is a typical characteristic of high light acclimation in a wide range of species (Demmig-Adams and Adams, 1996; Matsubara *et al.*, 2009), and was also seen in this study (Figure 5.8). The Inland-Early Autumn, *Arabidopsis* plants accumulated less Chl *a* and *b*. Several previous studies have showed that high light stress resulted in a reduction in Chl *a* and *b*, compared to low light conditions (Bailey *et al.*, 2001; Ballottari *et al.*, 2007). This tendency was also observed in most of the natural accessions when they were compared individually. In general, an increase in Chl *a/b* ratio results from a decrease in PSII antenna size, which can be caused by the photoinhibition from exposure to excess light (Kouřil et al., 2013). This occurs as PSII antenna proteins have both chlorophyll *a* and *b*, while PSII core proteins have only chlorophyll *a* (Kim *et al.*, 2009; Matsubara *et al.*, 2009). However, in this study there was no difference in the mean Chl *a/b* ratio between environments (Figure 5.8) indicating that there is no photodamage or change in antenna size in the inland plants and they may have acclimated to the higher light.

GWAS results showed no significant association of SNPs to chlorophylls content. However, there was one QTL identified for chlorophyll a content, named

Chl-QTL, which showed a relatively high, although non-significant, association in the GWAS analysis (Figure 5.9). Interestingly, the two potential candidate genes, **At3g28918** and **At3g28920**, have no known involvement in photosynthesis or chlorophylls content. Furthermore, **At3g28920** encodes a transcription factor which might indicate that this QTL may be involved in the regulation of chlorophyll production or photosynthetic mechanisms.

5.3.3 Genetic variation in H_2O_2

The results showed that there is natural variation for H_2O_2 both within the same and between different conditions. The presence of relatively high concentrations of H_2O_2 in leaf tissues was found under the inland condition in comparison to the coastal condition, and this was reproducible between experiments. This indicates that the inland simulated condition resulted in excess light stress resulting in H_2O_2 accumulation either as a results of ongoing photo-oxidative stress or as a signalling molecule.

Interestingly, the H_2O_2 concentration results from both experiments were different, with higher concentrations observed in Experiment IV. As presented in Figure 5.10, 3-fold higher H_2O_2 concentrations was found in late autumn compared to early autumn. There are some possible explanations as follows: (1) Experiment IV was started in late autumn, while Experiment V was started in early autumn, thus plants in early autumn did not receive as cold conditions as the plants in late autumn at the younger growth stage; the combination of high light and cold in the early morning in late autumn may have exacerbate the photo-oxidative stress. (2) there were some errors with the climate control network connection during the experiment resulting in fluctuating in temperature and light intensity between the two experiments which may have caused additional stress (see supplementary Figure D.7 and D.6, and (3) the differences in H_2O_2 concentrations between the two experiments might be caused by the differences in the tissue samples as a whole rosette in Experiment IV and a single leaf in Experiment V. This may have an effect due to the younger tissues being more susceptible to the stress than older tissues, which decline in various cellular process including photosynthesis (Khanna-Chopra, 2012). Hence, whole rosettes may accumulated a higher average H_2O_2 than individual mature leaves.

Interestingly, the GWAS analyses found no significant associations for this trait. This suggested that H_2O_2 concentration is an environmentally sensitive trait but that the conditions and methods in this study were not able to reveal the genetic basis for ROS accumulation. This may be because the conditions used in this experiments might not provide enough stress to reveal QTL for H_2O_2, as light intensities were much lower compared to the full sunlight intensity in the field which can exceed up to 2,000 μmol m^{-2} s^{-1} (Mishra *et al.*, 2012). Alternatively, using higher light intensity conditions and combined with other stress such as drought might be able to identify QTL which would identify the genetic basis of H_2O_2 accumulation in response to combined abiotic stresses. In addition, the difficulty in QTL for H_2O_2 identification might be related to the nature of the genetic architecture: for instance if it is many QTL of small effect or multiple rare variants then they would not result in significant QTL in my study.

5.3.4 Genetic variation in NPQ

As presented in the Chapter 3 and 4, NPQ capacity was quickly upregulated in plants grown under excess light conditions in both wild-type and the Cvi-0 x L*er* RIXs population. Similar results were observed in 284 *Arabidopsis* natural accessions in Experiment IV and in 223 natural accessions in Experiment V as presented in this Chapter. Under the given growing conditions (coastal and inland), there is natural variation in NPQ among accessions within the same condition and also among how the accessions responded in the two conditions.

The pattern of NPQ kinetics of plants grown under coastal condition showed a similar pattern to plants grown under other low light conditions (100 - 150 μmol m^{-2} s^{-1}) which has been reported in many studies (Johnson *et al.*, 2009; Jung and Niyogi, 2009; Nilkens *et al.*, 2010). The studies showed that in wild-type, NPQ formation is continuously increased as long as the actinic light continued, and NPQ reversed rapidly (within 1 minute in the dark) to the same low NPQ level. This indicated that it is the qE component of NPQ that is affected in the most accessions. The similar pattern was also observed in the inland plants at younger stage (14 leaves), suggesting overall there is lower photoprotection due to photoinhibition and no acclimation at this age. This is logical, as the conditions are

milder at the start of autumn then get more progressively stressful later on as the conditions move into winter. In contrast, at the 16 leaf stage in inland plants, a rapid induction of NPQ was observed, reflecting the higher capacity for qE formation driven by rapid ΔpH formation from exposed to high light intensity (Li *et al.*, 2000; Johnson *et al.*, 2009). The decline of NPQ at steady phase in the inland plants at the 16 leaves stage may indicate acclimatization to the excess light stress which is accompanied by an increase of photosynthesis (Cardol *et al.*, 2009) as observed by a higher ETR (Figure 5.12).

From the single trait GWAS analysis (Figure 5.15 - 5.17), 15 QTL and a total 69 candidate genes were identified across two growth conditions at the 16 leaf stage. Furthermore, the results also demonstrate the effect of genotype by environment (*GxE*) interactions for NPQ at the induction phase by identifying two QTL (***QTL2-3***, ***QTL5-3***). This suggested that the NPQ trait is not only strongly genetically controlled, but also affected by the interaction of genotype with environmental factors. The results observed in this study shows no single QTL appeared in both Experiment IV and V. There are two possible explanations. First, low reproducibility of the GWAS analysis results for NPQ. This may due to the specific loci involved in NPQ difference across populations. Second, the strong effects of the environmental conditions as seen in the differences between the Early and Late Autumn conditions (shown in 5.1) on NPQ-related QTL at the 16 leaf stage. In addition, the use of multi-traits GWAS analysis allowed discovering of one more QTL ***mQTL2***). Hence, the multi-traits GWAS approach not only allowed the confirmation of ***QTL5-3*** from the single-trait analysis, it also allowed the identification a new QTL which might link to the traits of interest.

The ***QTL1-4*** presented a high association with a LOD score = 8.15. It was located right above the candidate gene, *non-photochemical quenching 4*, (*npq4*; **At1g44575**), which is also called PhotosystemII subunit S (*PsbS*). *PsbS* has been found to be involved in the quenching of singlet excited chlorophylls (Havaux and Niyogi, 1999), and has been hypothesized to function as a sensor of luminal pH (Li *et al.*, 2000). The limited capacity to dissipate excess energy as heat in the *npq4* mutant has been confirmed by all experiments in this study (e.g. Figure 5.13). Another candidate gene (*NDF5*, **At1g55370**) under ***QTL1-5*** could also possibly have a direct association with NPQ. It has been suggested that the chloroplast NAD(P)H dehydrogenase (NDH) complex, which reduces plastoquinones (PQs) in thylakoid

membranes, is involved in PSI cyclic electron flow (Ishida *et al.*, 2009).

5.3.5 Different NPQ kinetics in the knockout lines

A different pattern in NPQ induction and at steady phase was observed in *KO-NDF5* mutant in comparison to wild-type. A novel finding from this study is the decrease of NPQ at induction phase, which was not reported in the previous characterisation of *KO-NDF5* (Ishida *et al.*, 2009). A slightly higher NPQ capacity at steady phase of *KO-NDF5* was observed which is consistent with the finding from Ishida *et al.*, (2009). They found that mutants that lack NDH activity, including *ndf2*, *ndf5*, and *ndf2/ndf5*, had NPQ levels that were nearly identical to wild-type plants, excepted *ndf5* which showed slightly higher NPQ than wild-type (Ishida *et al.*, 2009). It has been reported that the *NDF5* is essential for chloroplast NAD(P)H dehydrogenase (NDH) activity which is involved in PSI cyclic electron transport by reducing plastoquinones (PQs) in thylakoid membranes (Ishida *et al.*, 2009; Peng and Shikanai, 2011). Although, there is no dramatic difference in NPQ capacity between *ndf5* and wild-type, the absence of NDH effects the NPQ kinetics which may be caused by cyclic electron flow through PSI (Ishida *et al.*, 2009).

The *npq4 Arabidopsis* mutant for the *PsbS* gene, which is one of the strongest candidate genes, showed a dramatic reduction of NPQ capacity compared to wild-type plants even under low light condition (coastal) (i.e Figure 5.13). This result is consistent with other studies that showed the *npq4* deletion mutant resulted in defectiveness in most of the short term NPQ mechanism, especially the qE component (Li *et al.*, 2002; Finazzi *et al.*, 2004). A study by Johnson and Ruban (2010) has shown that there is NPQ in the mutant lacking *PsbS*, however, it responds in a slower time scale (after 60 minutes of high light) which suggests the role of *PsbS* is in rapidly responses and upregulated NPQ under excess light (Johnson and Ruban, 2010). Despite this absence of most of the NPQ capacity, other phenotypes in this mutant were found to be normal in this study. For instance, growth and leaf morphology were indistinguishable from the wild-type, which is similar to what was reported by Li *et al.*, (2000). In addition, chlorophyll *a* and *b* contents were similarly unaffected in the *npq4* mutant compared to wild-type, which was similar to the finding from Roach and Krieger-Liszkay (2012). These

results provided very strong evidences of the function of *PsbS* in NPQ and the ability of our system to identify loci important to the NPQ mechanism.

Additionally, there are a number of identified candidate genes that are unknown function and have not been studied. Further characterised of these candidate genes may provide a new evidence on what are other mechanisms may be involved in NPQ. This should be done under simulated natural conditions to reveal the NPQ response under natural pressures.

5.3.6 Changes in Haplotype sequence of high and low NPQ accessions

Further investigation of variation at *PsbS* identified two haplotype groups based on allelic variation at the promoter and coding sequence. As presented in Section 5.2.8, two sequence sets at the promoter and coding region of accessions with high and low NPQ alleles were aligned (supplementary Figure D.9 and D.10).

The differences in NPQ capacity between haplotypes may be a response to different expression levels of the *PsbS* protein. Allelic variation at the promoter region may result in different motifs composition between high and low haplotypes. Missing, or change of location, of the motifs at the *PsbS* promoter region may affect ability of regulatory protein binding, resulting in altering the expression levels. Therefore, to functionally test whether allelic variation at promoter and/or coding region of *PsbS* may alter NPQ capacity, the constructs of those two sequence (high and low NPQ) should be transformed into the PsbS loss of function mutant. The ability of these sequences to complement the mutant could then be tested by phenotyping for NPQ in the standard coastal growth conditions. This validation would provide evidence that genetic variation at this loci changes the ability of thermal dissipation in *Arabidopsis*. In summary, the outcomes of this future research would confirm the role of the *PsbS* locus in the genetic basis of NPQ variation in *Arabidopsis*.

The results here suggest that there are several factors involved in NPQ under dynamic environments. The levels of NPQ, chlorophyll content, and H_2O_2 under

stressful condition is functionally related to each other in order for plants to survive and later acclimate against excess light. The dynamic excess light stress in the inland conditions resulted in accumulation of H_2O_2, a decrease in the chlorophyll content, a small amount of photoinhibition and an increased NPQ capacity. This indicated an increase in damage due to excess light energy but also a partial acclimation to the stress conditions. Although, H_2O_2 levels were changed under inland, the levels are much lower than other studies (Alboresi *et al.*, 2011; Stewart *et al.*, 2015). Furthermore, there is no evidence of the correlation between H_2O_2 and chlorophyll content with NPQ reported in this study. This may be due to the differences in growth conditions, the population used and the levels of stress. Thus, it is necessary to distinguish the role of each component and observe the relationship among them. This could be overcome by increasing the stress levels such as light intensity. Another factor to consider is to measure $^1O_2$, as it has been reported to be a more accurate oxidative stress indicator than H_2O_2 in responses to high light stress (GonZalez-Pérez *et al.*, 2011; Shumbe *et al.*, 2016).

5.4 SUMMARY

The first aim of this study was to investigate the natural variation of growth, NPQ, H_2O_2 and chlorophyll content under variable growth conditions. The results presented in this Chapter showed that the mechanisms involved in photoprotection and photoinhibition are genetically controlled and also sensitive to growth conditions, as can be observed in the natural variation among population and between growth conditions. This leading to the identification of 15 QTL.

Another main focus in this study was to understand the genetic architecture underlying variation in NPQ under simulated coastal and inland environments in a large diverse mapping set of *Arabidopsis*. By simulating diurnal and seasonal environments, using controlled climate chambers, a few candidate genes were identified. The use of the 6M SNPs data set increased SNP density and provided a higher resolution in QTL detection when undertaking GWAS mapping. ***QTL1-4*** provided positive confirmation of the methodology, as it located right on the *PsbS* gene which is known to be directly involved in NPQ. Screening of knockout lines has confirmed the function of PsbS and NDF5 in the NPQ mechanism. The allelic polymorphism between high and low NPQ sequence at PsbS promoter suggests

a cause for the phenotypic differences in NPQ levels.

Chapter 6

FINAL DISCUSSION AND FUTURE PROSPECTS

FINAL DISCUSSION AND FUTURE PROSPECTS

Despite a large amount of research into understanding the mechanism of non-photochemical quenching, the natural genetic variation of this trait remains under-explored. My thesis aims to gain a basic knowledge of what genetic architecture controls plant photoprotective responses under different natural environments. The genetic basis of photoprotection in *Arabidopsis*, focusing on the NPQ mechanism, was investigated with the use of Arabidopsis natural accessions (HapMap set), the Cvi-0 x L*er* RIXs, and several photoprotective mutants. Simulated diurnal and seasonal growth conditions were used to explore photoprotective responses under dynamic conditions typically experienced in the wild. GWAS analysis was used to finely dissect the complex genetic basis of photoprotective response.

To achieve the aims of this project a number of methods needed to be optimised. The study presented in Chapter 3 demonstrated the optimization of different chlorophyll fluorescence measuring protocols in a new high-throughput PlantScreen system in order to provide comparable data for analysis across multiple trays, time points and growth chambers. I developed the P3 protocol (eight minutes of actinic light illumination followed by a three minutes dark relaxation period) which give high genetic signal and low environmental noise across my large experiment. The increased temporal resolution of this protocol also enabled me to distinguish different states of NPQ kinetics was used to determine different factors contributing to the different components of the NPQ mechanism. Chlorophyll fluorescence results from this protocol using plants grown under standard conditions, are comparable with results from other studies (Jung and Niyogi, 2009; Mishra *et al.*, 2012; Dall'Osto *et al.*, 2014).

The different simulated diurnal and seasonal growth environments had a clear impact on the expression of the NPQ phenotype. This indicated that NPQ is a dynamic mechanism governed by both genetic and environmental factors. In nature, variation in climatological (seasonal and diurnal) parameters can affect the levels of induced photoprotection and photoinhibition in plants (Kulheim *et al.*, 2002). The advantage of using the simulated environment systems can be seen in the 4-fold variation in NPQ capacity seen in this study, which is much greater than constant light experiment where less than 2-fold variation in NPQ capacity

have been reported (Jung and Niyogi, 2009; Alter *et al.*, 2012). The combination of climatically controlled growth environments and high-throughput chlorophyll fluorescence phenotyping is something that has not been published before. Its utility has been proven here in the ability to provide insight on how plants may respond under natural environment as observed in different patterns of NPQ.

As presented through this study and others, NPQ is primarily triggered by exposure to higher light intensity (Müller *et al.*, 2001). However, other effects such as low temperature can also increase photo-inhibitory stress levels (Harvaux and Kloppstech, 2001). This combination is further exacerbated in younger plants, as shown by the effect on plant growth, fitness and NPQ resulting from growth in a Winter to Spring season as compared to an Autumn to Winter season. In contrast, experiencing this kind of stress at the later stages of plant development allows for acclimation and the development of the photoprotection process, as shown in different patterns of NPQ formation in the early and late autumn conditions.

The impact of growing under excess light and low temperature, as seen on a typical Autumn morning in our simulated inland conditions, increased the plant's ability to dissipate excess energy. It was observed in the inland plants as a rapid increase in NPQ, in contrast to coastal plants which demonstrated slower NPQ induction. The combination of light and temperature stress increases the amount of excess energy harvested and could play an important role in rapidly activating ΔPH accumulation (Dall'Osto *et al.*, 2014), which then triggers the xanthophyll cycle (Müller *et al.*, 2001; Alter *et al.*, 2012; Ruban and Murchie, 2012) resulting in higher NPQ levels at the induction phase (Johnson *et al.*, 2008). The maximum photochemical quantum yield of PSII (Fv/Fm) of inland plants was also slightly down regulated possibly as a result of photoinhibition. However, the levels of Fv/Fm of inland plants remained above 0.8 which is considered a low level of non-stressed for plants (Björkman, 1987). This suggests that acclimation had occurred in inland conditions . This was seen by the reduction of chlorophyll content and higher ETR when compared to coastal plants. This higher ETR could be one of the factors that influence the decay of NPQ seen in inland plants at steady state phase, consistent with previous report (Foyer *et al.*, 2012). Coastal plants have lower ETR and as a result need to maintain high NPQ to dissipate excess light to prevent photodamage under the higher light conditions in the NPQ protocol. Therefore, it could not be excluded that the differences in ETR rate among

natural accession and between growth conditions may have a large impact on NPQ kinetics.

In nature, plants are unable to avoid continuous exposure to excess light. Natural selection has led to development of photoprotective mechanisms as a response to excess light stress, the intensity of which is dependent on their geographic region. To compare the geography of the site of collection with NPQ capacity, the 10 accessions of highest NPQ capacity (greater than 3.8) and the 10 accessions of lowest NPQ accessions (lower than 3.0) were identified under Coastal-Late Autumn. A previous study had reported a significant relationship between the latitude of the collection location and the variation of NPQ capacity (Jung and Niyogi, 2009). In this study, however, there was no significant correlation between latitude and NPQ as well as no correlation between altitude and NPQ capacity. The results reported here may disagree with the above result as the previous study used a population with a smaller geographic distribution, with only 20 countries represented instead of 32 countries in this study. In addition, this different finding may also be due to the higher capability of the simulated natural climate system in revealing the highest NPQ capacity. The maximum NPQ capacity in the previous study was around 3.2 (Jung and Niyogi, 2009) whereas in this study it was up to 4.2. Therefore, it seems that these differences in latitude and altitude at the origin of an accession may not have direct impact on selecting for NPQ capacity. This is counter to previous findings that suggested that latitude and altitude were factors in selection for other phenotypes such as plant size and relative growth rate (Li *et al.*, 1998; Stewart *et al.*, 2015). This also suggests that light regimes can vary on small spatial and temporal scales and a detailed study of the local environment: genotype relationship would be needed to determine adaptive basis for this trait.

Despit the lack of a clear overall correlation between NPQ and latitude as an indicator of abiotic stress, research has shown a correlation between low NPQ capacity and sensitivity to biotic stress such as herbivory (Johansson Jänkänpää *et al.*, 2013). This correlation may be caused by the trade-off between pathogen defence mechanisms and abiotic stress that has a large effect due to that climates (Demmig-Adams *et al.*, 2014). Therefore, plants have to balance different amounts of photoprotection, depending on the nature of biotic stress that they encounter in their habitats (Johansson Jänkänpää *et al.*, 2013).

Despite the identification of photoprotective mechanisms, the genetic basis of this trait has been under-explored. One of the novel results observed in Chapter 5 showed that the allelic variation among natural accessions resulted in different NPQ phenotypes to be expressed under different environmental conditions. The GWAS methods used in this study were validated by the identification of two a priori genes with known roles in NPQ. A significant association was found within the promoter and coding region of the *PsbS* gene, which encodes a protein known to be very important in one of the NPQ components, qE. The testing of knockouts of 24 candidate genes identified through GWAS analysis also suggested that *NDF5* may play an important role in NPQ in the natural environment. The *NDF5* knockout showed a particularly interesting phenotype with down regulation of NPQ induction and then higher capacity for NPQ after one minute exposure to high light. The *NDF5* protein, a chloroplast NAD(P)H dehydrogenase, is involved in cyclic electron flow in PSI (Ishida *et al.*, 2009), but how this then relates to the changed kinetics of NPQ in the *NDF5* knockout requires further investigation. The finding of the function of the *NDF5* and *PsbS* candidate genes in the NPQ process is not novel, however, they serve as a valuable proof-of-concept that supports further study into the other 13 QTL for which the causative candidate has not been identified. These QTL could contain novel regulators of NPQ. Furthermore, research into the allelic variation in *PsbS* and *NDF5* may also provide novel insight into the regulation and function of these proteins.

Interestingly, the QTL that were identified in this study are different from the results of Jung and Niyogi (2009). They have found two QTL, ***HQE1*** and ***HQE2***, for which ***HQE1*** is more likely to be responsive to the sudden change in light intensity, while both ***HQE1*** and ***HQE2*** respond to extended high light (Jung and Niyogi, 2009). The location of these two QTL is on chromosome 1 (at 8 Mb) and chromosome 2 (at 13 MB), respectively. This study I has identified five QTL on chromosome 1 and three QTL on chromosome 2, however, none of these QTL are located near***HQE1*** and ***HQE2***. Based on my results, ***QTL1-4***, the strongest QTL, showed a similar pattern to ***HQE1*** with the QTL significant at all the timepoints of the 8 minute illumination, as presented in Table 5.1. The reason that different QTL were identified in the two studies may be due to a number of factors. It may be expected that the different mapping populations used in each study could be a factor. However, the Sf-2 and Col-0 RIL parents used in this experiment have

contrasting haplotypes with Sf-2 having the same high NPQ haplotype that was identified in the HapMap population. Another possible explanation would be the difference in growth conditions. The major difference was temperature which was much more variable in my study, between 8 °C - 22 °C, while it was constant at 22 °C in Jung and Niyogi's experiment. This exposure to cooler temperatures at the start of the photoperiod could have played a crucial role in finding different QTL contributing to the NPQ mechanism.

Similarly to the lack of identification of ***QTL1-4*** in the study by Jung and Niyogi (2009) the ***QTL1-4*** was not identified in the Cvi-0 x L*er* RIXs experiment. This is likely due to the same haplotype being present in Cvi-0, L*er*, and the high NPQ accession haplotype at the ***QTL1-4*** locus, with a gene alignment between L*er* and Cvi-0 showing 99.6 % identity 2kb upstream to 2kb downstream of *PsbS* (**At1g44575**) (http://www.ebi.ac.uk/). This indicates that there is no allelic variation or segregation at this location in the Cvi-0 x L*er* RIXs population, hence ***QTL1-4*** could not be detected. Although the use of bi-parental populations may have limitation in regards to allelic variation they can be useful way to confirm QTL across different mapping techniques. As noted in Section 4.2.2 and Section 5.2.6, there is one overlapping QTL between the Cvi-0 x L*er* RIXs and the HapMap population. ***RIX-QTL5-3*** was found to overlapped with ***QTL5-2*** and ***QTL5-3***. These QTL were identified under the same Coastal condition. This suggests that the two population may have a shared varient responsive to NPQ located in that region. This could be a QTL to focus on in future studies.

When looking at the wider HapMap population the results showed that the allelic variation at *PsbS* in natural populations leads to the changes in both promoter motif location and several non-synonymous amino acid changes in the coding region of *PsbS* (**At1g44575**). At this point it is unclear which allelic difference may be causative at this locus. Further confirmation of *PsbS* as the correct candidate gene should be undertaken by functional complementation of those two sequence (high and low NPQ) into the *npq4* mutant. The ability of these sequences to complement the mutant could then be tested by phenotyping for NPQ in the standard coastal growth conditions. This validation would provide evidence that genetic variation at this locus changes thermal dissipation in *Arabidopsis*.

Given the results presented in this thesis, GWAS has been demonstrated to be a new powerful tool than the RIX population to dissect natural genetic variation in photoprotection. However, it has negative features too as it can be hard to distinguish true from false positives and to detect rare alleles (Korte and Farlow, 2013). As the accessions used in GWAS are not the result of random intercrossing. There are background effects where co-inheritance of alleles across the genome due to population structure which when not controlled for can cause false positive results (Brachi *et al.*, 2011). This has been largely controlled for in this study with the incorporation of kinship in the GWAS analysis. The power of GWAS to distinguish a true association between a SNP and phenotype is also subjected to the proportion of phenotypic variation within the population explained by the SNP (Korte and Farlow, 2013). The phenotypic variation is determined by how much the phenotypic effects of the two allelic variants differ; variants with small effect size also present problems for GWAS analysis (Gibson, 2012). In this study we have identified QTL that explain between 0.1 to 14 % of the phenotypic variation. This is in line with other studies where the QTL explained up to 45 % in flowering time (Li *et al.*, 2010) and 28 % in shoot fresh weight (Wintermans *et al.*, 2016).

Unlike traditional QTL analysis, GWAS does not require an artificial cross of parental lines, only an evenly sampled population from the different genetic backgrounds is needed. This provides the benefit of a high level of different genetic combinations resulting in high QTL resolution but it has limited ability to detect rare alleles. In contrast, linkage mapping in a RIL population has limited genetic variation from just 2 parental genomes, low genetic resolution from few recombinant events. RILs have power to detect rare parental alleles. There is a benefit from using a combination of GWAS and traditional linkage mapping (Brachi *et al.*, 2011). Combining the QTL mapping and GWAS approaches can be powerful to validate associations, by increasing the power to detect rare alleles, and reducing the number of candidate genes (Korte and Farlow, 2013). In my thesis, I found the same QTL in both the RIXs population and GWAS in natural accessions.

The use of newly developed climate controlled growth chambers in this study provided a lot of power to dissect phenotypic responses to the environment but also has some limitations. Although, the system can stimulate climate in any regions, the ability of controlled chambers are limited regarding to very high light

intensity. As the maximum light intensity at the time of conducting this study was 500 μmol $m^{-2}s^{-1}$, while light intensity can be up to 2000 μmol $m^{-2}s^{-1}$ in the open field. This could be improved in the future experiments in order to explore how plants respond to variable environments such as excess light stress and sunflecks that normally occur in the field. The combination of various stress factors may also help to unlock the genetic architecture behind natural selection.

Several experiments could be conducted in order to further understand what other factors may be associated with natural variation in NPQ capacity and the response to the dynamic growth conditions. To achieve this goal, the quantification of other parameters is required. Quantifying other carotenoid pigments which have been reported to vary upon light exposure (Matsubara *et al.*, 2012), such as zeaxanthin, lutein, and violaxanthin, by using the High-Performance Liquid Chromatography (HPLC) technique is one approach. This will clarify the relationship between NPQ and the production of carotenoids. It has been reported that the replacement of lutein by zeaxanthin or violaxanthin affected the amplitude of NPQ (Johnson *et al.*, 2009; Matsubara *et al.*, 2012). Although, NPQ capacity has been shown to associate with the conversion of violaxanthin to zeaxanthin in the xanthophyll cycle (Jung and Niyogi, 2009; Xu *et al.*, 2012), the genetic basis of these pigments has not been reported. Hence, the investigation of variation in those pigments could provide insightful knowledge into the relationship between those pigments and the capacity of NPQ in the natural accessions. Furthermore, GWAS mapping can be applied to extend the understanding of the genetic basis of the variation of carotenoids.

One of the most interesting findings in this study is that using different growing conditions, for instance small differences in light quality and intensity, temperature and seasonal changes leads to different finding in the GWAS results. This suggested NPQ is a complex trait which is likely controlled by multiple genes that are responsive to the environment, the acclimation state of the plant and the developmental stage of the plant. In summary, the outcome of this study provides insight and contributes to advance knowledge into the natural genetic variation for photoprotection that is necessary for plants growing under unavoidable stress conditions in the natural environment.

Appendices

Appendix A

Supplementary Data for Chapter 2

Table A.2 – The list of the 284 accessions of *Arabidopsis* used in Experiment IV.

No.	ID_473	ID_250K	ABRC	Native	Latitude	Longitude	Country
1	66	66	CS76108	CAM-61	48.2667	-4.58333	FRA
2	81	81	CS76115	CUR-3	45	1.75	FRA
3	96	96	CS76158	LAC-5	47.7	6.81667	FRA
4	149	149	CS76163	LDV-58	48.5167	-4.06667	FRA
5	173	173	CS76182	MIB-22	47.3833	5.31667	FRA
6	178	178	CS76183	MIB-28	47.3833	5.31667	FRA
7	258	258	CS76205	PAR-3	46.65	-0.25	FRA
8	259	259	CS76206	PAR-4	46.65	-0.25	FRA
9	260	260	CS76207	PAR-5	46.65	-0.25	FRA
10	281	281	CS76252	TOU-A1-115	46.6667	4.11667	FRA
11	328	328	CS76256	TOU-A1-62	46.6667	4.11667	FRA
12	362	362	CS76259	TOU-C-3	46.6667	4.11667	FRA
13	373	373	CS76261	TOU-H-12	46.6667	4.11667	FRA
14	374	374	CS76262	TOU-H-13	46.6667	4.11667	FRA
15	378	378	CS76263	TOU-I-17	46.6667	4.11667	FRA
16	379	379	CS76264	TOU-I-2	46.6667	4.11667	FRA
17	383	383	CS76266	TOU-J-3	46.6667	4.11667	FRA
18	386	386	CS76267	TOU-K-3	46.6667	4.11667	FRA
19	641	641	CS76165	LI-OF-095	40.7777	-72.9069	USA
20	1867	1867	CS76188	MNF-Pot-68	43.595	-86.2657	USA
21	2057	2057	CS76180	Map-42	42.166	-86.412	USA
22	2150	2150	CS76208	Paw-3	42.148	-86.431	USA
23	2274	2274	CS76228	SLSP-30	43.665	-86.496	USA
24	5056	5056	CS76281	UKSE06-192	51.3	0.5	UK
25	5122	5122	CS76283	UKSE06-278	51.3	0.4	UK
26	5158	5158	CS76284	UKSE06-349	51.3	0.4	UK
27	5160	5160	CS76285	UKSE06-351	51.3	0.4	UK
28	5202	5202	CS76286	UKSE06-414	51.3	0.4	UK
29	5245	5245	CS76289	UKSE06-482	51.2	0.6	UK
30	5341	5341	CS76291	UKSE06-628	51.1	0.4	UK
31	5380	5380	CS76275	UKNW06-059	54.4	-3	UK
32	5381	5381	CS76276	UKNW06-060	54.4	-3	UK
33	5606	5606	CS76278	UKNW06-436	54.7	-3.4	UK
34	5742	5742	CS76272	UKID37	51.3	1.1	UK
35	5753	5753	CS76273	UKID48	54.7	-2.7	UK
36	5785	5785	CS76274	UKID80	54.7	-2.9	UK
37	5805	5805	CS76270	UKID101	53.2	-1.4	UK
38	5832	5832	CS76092	App1-16	56.3333	15.9667	SWE
39	5837	5837	CS76099	Bor-1	49.4013	16.2326	CZE
40	5987	5987	CS76122	DraIV 6-16	49.4112	16.2815	CZE

Continued on next page.

Table A.2 – continued from previous page

No.	ID_473	ID_250K	ABRC	Native	Latitude	Longitude	Country
41	6005	6005	CS76123	DraIV 6-35	49.4112	16.2815	CZE
42	6008	6008	CS76124	Duk	49.1	16.2	CZE
43	6016	6016	CS76834	Eds-1	62.9	18.4	SWE
44	6019	6019	CS76131	FjÃĎ1-2	56.06	14.29	SWE
45	6020	6020	CS76132	FjÃĎ1-5	56.06	14.29	SWE
46	6039	6039	CS76143	Hovdala-2	56.1	13.74	SWE
47	6040	6040	CS78019	Kni-1	55.66	13.4	SWE
48	6042	6042	CS76174	Lom1-1	56.09	13.9	SWE
49	6046	6046	CS76175	Lov-5	62.801	18.079	SWE
50	6096	6096	CS76234	T1060	55.6472	13.2225	SWE
51	6169	6169	CS76243	TAD 01	62.8714	18.3447	SWE
52	6190	6190	CS76248	TDr-3	55.7686	14.1381	SWE
53	6194	6194	CS76249	TDr-8	55.7706	14.1342	SWE
54	6243	6243	CS76251	Tottarp-2	55.95	13.85	SWE
55	6318	6318	CS76269	UduI 1-34	49.2771	16.6314	CZE
56	6449	6449	CS76308	ZdrI 2-25	49.3853	16.2544	CZE
57	6727	6727	CS28140	CIBC-2	51.4083	-0.6383	UK
58	6729	6729	CS28141	CIBC-4	51.4083	-0.6383	UK
59	6744	6744	CS28181	CSHL-5	40.8585	-73.4675	USA
60	6810	6810	CS28407	KNO-11	41.2816	-86.621	USA
61	6987	6987	CS28011	Ak-1	48.0683	7.62551	GER
62	6989	6989	CS28013	Alst-1	54.8	-2.4333	UK
63	6990	6990	CS28014	Amel-1	53.448	5.73	NED
64	6992	6992	CS28018	Ang-0	50.3	5.3	BEL
65	6994	6994	CS28049	Ann-1	45.9	6.13028	FRA
66	6996	6996	CS28017	An-2	51.2167	4.4	BEL
67	7000	7000	CS28007	Aa-0	50.9167	9.57073	GER
68	7002	7002	CS28054	Baa-1	51.3333	6.1	NED
69	7004	7004	CS28097	Bs-2	47.5	7.5	SUI
70	7013	7013	CS28061	Bd-0	52.4584	13.287	GER
71	7015	7015	CS28079	Bla-1	41.6833	2.8	ESP
72	7021	7021	CS28081	Bla-3	41.6833	2.8	ESP
73	7024	7024	CS28084	Bla-6	41.6833	2.8	ESP
74	7025	7025	CS28078	Bl-1	44.5041	11.3396	ITA
75	7026	7026	CS28091	Boot-1	54.4	-3.2667	UK
76	7028	7028	CS28058	Bch-1	49.5166	9.3166	GER
77	7029	7029	CS28059	Bch-3	49.5166	9.3166	GER
78	7030	7030	CS28060	Bch-4	49.5166	9.3166	GER
79	7031	7031	CS28099	Bsch-0	40.0167	8.6667	GER
80	7032	7032	CS28100	Bsch-2	40.0167	8.6667	GER

Continued on next page.

Table A.2 – continued from previous page

No.	ID_473	ID_250K	ABRC	Native	Latitude	Longitude	Country
81	7035	7035	CS28090	Blh-2	48	19	CZE
82	7044	7044	CS28102	Bu-2	50.5	9.5	GER
83	7062	7062	CS28128	Ca-0	50.2981	8.26607	GER
84	7073	7073	CS28137	Chi-1	53.7502	34.7361	RUS
85	7078	7078	CS28163	Co-2	40.12	-8.25	POR
86	7079	7079	CS28164	Co-3	40.12	-8.25	POR
87	7098	7098	CS28208	Di-1	47	5	FRA
88	7102	7102	CS28210	Do-0	50.7224	8.2372	GER
89	7106	7106	CS28211	Dr-0	51.051	13.7336	GER
90	7109	7109	CS28229	Ema-1	51.3	0.5	UK
91	7110	7110	CS28217	Ede-1	52.0333	5.66667	NED
92	7113	7113	CS28224	Ei-4	50.3	6.3	GER
93	7116	7116	CS28227	Eil-0	51.4599	12.6327	GER
94	7128	7128	CS28243	Est-0	58.3	25.3	RUS
95	7135	7135	CS28268	Fr-4	50.1102	8.6822	GER
96	7139	7139	CS28252	Fi-1	50.5	8.0167	GER
97	7143	7143	CS28279	Gel-1	51.0167	5.86667	NED
98	7145	7145	CS28277	Ge-1	46.5	6.08	SUI
99	7149	7149	CS28330	Gu-0	50.3	8	GER
100	7151	7151	CS28282	Go-0	51.5338	9.9355	GER
101	7152	7152	CS28283	Go-2	51.5338	9.9355	GER
102	7158	7158	CS28326	Gr-5	47	15.5	AUT
103	7163	7163	CS28336	Ha-0	52.3721	9.73569	GER
104	7165	7165	CS28350	Hn-0	51.3472	8.28844	GER
105	7166	7166	CS28344	Hey-1	51.25	5.9	NED
106	7169	7169	CS28345	Hh-0	54.4175	9.88682	GER
107	7176	7176	CS28362	Is-1	50.5	7.5	GER
108	7178	7178	CS28373	Jm-1	49	15	CZE
109	7186	7186	CS28395	Kn-0	54.8969	23.8924	LTU
110	7192	7192	CS28386	Kil-0	55.6395	-5.66364	UK
111	7195	7195	CS28390	Kl-1	50.95	6.9666	GER
112	7199	7199	CS28394	Kl-5	50.95	6.9666	GER
113	7205	7205	CS28423	Krot-2	49.631	11.5722	GER
114	7206	7206	CS28420	Kro-0	50.0742	8.96617	GER
115	7210	7210	CS28440	La-1	52.7333	15.2333	POL
116	7227	7227	CS28457	Li-5:2	50.3833	8.0666	GER
117	7228	7228	CS28458	Li-5:3	50.3833	8.0666	GER
118	7229	7229	CS28459	Li-6	50.3833	8.0666	GER
119	7238	7238	CS28471	Ll-1	41.59	2.49	ESP
120	7239	7239	CS28472	Li-2	41.59	2.49	ESP

Continued on next page.

Table A.2 – continued from previous page

No.	ID_473	ID_250K	ABRC	Native	Latitude	Longitude	Country
121	7245	7245	CS28488	Ma-0	50.8167	8.7667	GER
122	7246	7246	CS28489	Ma-2	50.8167	8.7667	GER
123	7255	7255	CS28492	Mh-0	50.95	7.5	POL
124	7256	7256	CS28493	Mh-1	50.95	7.5	POL
125	7260	7260	CS28575	Nw-2	50.5	8.5	GER
126	7265	7265	CS28528	Nd-0	50	10	SUI
127	7276	7276	CS28579	Ob-0	50.2	8.5833	GER
128	7277	7277	CS28580	Ob-1	50.2	8.5833	GER
129	7280	7280	CS28583	Old-1	53.1667	8.2	GER
130	7282	7282	CS28587	Or-0	50.3827	8.01161	GER
131	7284	7284	CS28849	Ors-2	44.7203	22.3955	ROU
132	7287	7287	CS28590	Ove-0	53.3422	8.42255	GER
133	7291	7291	CS28595	Pa-2	38.07	13.22	ITA
134	7292	7292	CS28596	Pa-3	38.07	13.22	ITA
135	7297	7297	CS28601	Pf-0	48.5479	9.11033	GER
136	7299	7299	CS28639	Pi-2	47.04	10.51	AUT
137	7300	7300	CS28640	Pla-0	41.5	2.25	ESP
138	7301	7301	CS28641	Pla-1	41.5	2.25	ESP
139	7306	7306	CS28650	Pog-0	49.2655	-123.206	CAN
140	7309	7309	CS28649	Po-1	50.7167	7.1	GER
141	7310	7310	CS28651	Pr-0	50.1448	8.60706	GER
142	7328	7328	CS28731	Sf-2	41.7833	3.03333	ESP
143	7333	7333	CS28729	Sei-0	46.5438	11.5614	ITA
144	7340	7340	CS28725	Sav-0	49.1833	15.8833	CZE
145	7344	7344	CS28732	Sg-1	47.6667	9.5	GER
146	7351	7351	CS28786	Ty-0	56.4278	-5.23439	UK
147	7352	7352	CS28757	Te-0	60.0585	23.2982	FIN
148	7353	7353	CS28758	Tha-1	52.08	4.3	NED
149	7355	7355	CS28760	Tiv-1	41.96	12.8	ITA
150	7373	7373	CS28780	Tsu-0	34.43	136.31	JPN
151	7376	7376	CS28784	Tu-1	45	7.5	ITA
152	7378	7378	CS28787	Uk-1	48.0333	7.7667	GER
153	7381	7381	CS28790	Uk-4	48.0333	7.7667	GER
154	7382	7382	CS28795	Utrecht	52.0918	5.1145	NED
155	7386	7386	CS28802	Vi-0	50.1946	8.74639	GER
156	7391	7391	CS28809	Wag-4	51.9666	5.6666	NED
157	7392	7392	CS28810	Wag-5	51.9666	5.6666	NED
158	7397	7397	CS28823	Ws	52.3	30	RUS
159	7404	7404	CS28813	Wc-1	52.6	10.0667	GER
160	7405	7405	CS28814	Wc-2	52.6	10.0667	GER

Continued on next page.

Table A.2 – continued from previous page

No.	ID_473	ID_250K	ABRC	Native	Latitude	Longitude	Country
161	7408	7408	CS28833	Wt-3	52.3	9.3	GER
162	7411	7411	CS28822	Wl-0	47.9299	10.8134	GER
163	7413	7413	CS28820	Wil-2	54.6833	25.3167	LTU
164	7418	7418	CS28847	Zu-1	47.3667	8.55	SUI
165	7423	7423	CS28368	Jl-2	49.2	16.6166	CZE
166	7430	7430	CS28527	Nc-1	48.6167	6.25	FRA
167	7449	7449	CS28513	N7	61.36	34.15	RUS
168	7457	7457	CS28688	RLD-2	56.25	34.3167	RUS
169	7479	7479	CS28610	PHW-10	51.2878	0.0565	UK
170	7482	7482	CS28613	PHW-13	51.2878	0.0565	UK
171	7483	7483	CS28614	PHW-14	51.2878	0.0565	UK
172	7498	7498	CS28628	PHW-28	50.35	-3.5833	UK
173	7504	7504	CS28633	PHW-33	52.25	4.5667	NED
174	7506	7506	CS28635	PHW-35	48.6103	2.3086	FRA
175	7507	7507	CS28636	PHW-36	48.6103	2.3086	FRA
176	7508	7508	CS28637	PHW-37	48.6103	2.3086	FRA
177	7514	7514	CS28713	RRS-7	41.5609	-86.4251	USA
178	8222	8222	CS76170	Lis-2	56	14.7	SWE
179	8234	8234	CS76138	Gul1-2	56.3	16	SWE
180	8236	8236	CS76146	HSm	49.33	15.76	CZE
181	8241	8241	CS76166	Liarum	55.95	13.85	SWE
182	8242	8242	CS76167	Lillo-1	56.1512	15.7844	SWE
183	8243	8243	CS77173	PHW-2	43.7703	11.2547	ITA
184	8247	8247	CS78396	San-2	56.07	13.74	SWE
185	8248	6962	CS76227	Shahdara	38.35	68.48	TJK
186	8251	6897	CS76087	Ag-0	45	1.3	FRA
187	8252	6988	CS76088	Alc-0	40.31	-3.22	ESP
188	8253	6898	CS76091	An-1	51.2167	4.4	BEL
189	8254	8254	CS78402	Ang-0	50.3	5.3	BEL
190	8256	8256	CS76093	Ba1-2	56.4	12.9	SWE
191	8258	8258	CS78404	Ba4-1	56.4	12.9	SWE
192	8259	8259	CS78405	Ba5-1	56.4	12.9	SWE
193	8260	6899	CS76094	Bay-0	49	11	GER
194	8261	6709	CS76096	Bg-2	47.6479	-122.305	USA
195	8264	8264	CS76097	Bla-1	41.6833	2.8	ESP
196	8268	6903	CS76100	Bor-4	49.4013	16.2326	CZE
197	8269	6904	CS76101	Br-0	49.2	16.6166	CZE
198	8270	8270	CS78414	Bs-1	47.5	7.5	SUI
199	8271	8271	CS76103	Bu-0	50.5	9.5	GER
200	8272	6905	CS76105	Bur-0	54.1	-6.2	IRL

Continued on next page.

Table A.2 – continued from previous page

No.	ID_473	ID_250K	ABRC	Native	Latitude	Longitude	Country
201	8273	6906	CS76106	C24	40.2077	-8.42639	POR
202	8274	8274	CS76109	Can-0	29.2144	-13.4811	ESP
203	8278	7081	CS78422	Co	40.2077	-8.42639	POR
204	8279	6909	CS76113	Col-0	38.3	-92.3	USA
205	8280	6910	CS76114	Ct-1	37.3	15	ITA
206	8281	6911	CS76116	Cvi-0	15.1111	-23.6167	CPV
207	8288	6914	CS76126	Edi-0	56	-3	UK
208	8289	6915	CS76478	Ei-2	50.3	6.3	GER
209	8291	6916	CS76127	Est-1	58.3	25.3	RUS
210	8294	8215	CS76129	Fei-0	40.5	-8.32	POR
211	8295	6919	CS76133	Ga-0	50.3	8	GER
212	8296	8296	CS76134	Gd-1	53.5	10.5	GER
213	8301	6922	CS76498	Gu-0	50.3	8	GER
214	8302	8214	CS76139	Gy-0	49	2	FRA
215	8303	7461	CS76897	H55	49	15	CZE
216	8304	8304	CS76140	Hi-0	52	5	NED
217	8308	6923	CS76940	HR-10	51.4083	-0.6383	UK
218	8309	6924	CS76144	HR-5	51.4083	-0.6383	UK
219	8310	8310	CS76145	Hs-0	52.24	9.44	GER
220	8312	8312	CS28361	Is-0	50.5	7.5	GER
221	8313	8313	CS78454	Jm-0	49	15	CZE
222	8314	8314	CS76149	Ka-0	47	14	AUT
223	8316	6926	CS76153	Kin-0	44.46	-85.37	USA
224	8320	6930	CS78460	Kz-1	49.5	73.1	KAZ
225	8321	6830	CS76994	Kz-13	49.5	73.1	KAZ
226	8322	6931	CS78461	Kz-9	49.5	73.1	KAZ
227	8324	6932	CS76164	Ler-1	47.984	10.8719	GER
228	8326	8326	CS76169	Lis-1	56	14.7	SWE
229	8328	6933	CS76172	LL-0	41.59	2.49	ESP
230	8329	8329	CS76173	Lm-2	48	0.5	FRA
231	8333	7521	CS76177	Lp2-6	49.38	16.81	CZE
232	8334	8334	CS77056	Lu-1	55.71	13.2	SWE
233	8336	6936	CS76179	Lz-0	46	3.3	FRA
234	8337	8337	CS76551	Mir-0	44	12.37	ITA
235	8338	7522	CS76190	Mr-0	44.15	9.65	ITA
236	8339	6937	CS76191	Mrk-0	49	9.3	GER
237	8340	6938	CS76555	Ms-0	55.7522	37.6322	RUS
238	8342	6940	CS76193	Mz-0	50.3	8.3	GER
239	8343	8343	CS76195	Na-1	47.5	1.5	FRA
240	8344	6942	CS76197	Nd-1	50	10	SUI

Continued on next page.

Table A.2 – continued from previous page

No.	ID_473	ID_250K	ABRC	Native	Latitude	Longitude	Country
241	8349	7518	CS76200	Omo2-1	56.14	15.78	SWE
242	8350	7519	CS78486	Omo2-3	56.1481	15.8155	SWE
243	8352	6946	CS76203	Oy-0	60.23	6.13	NOR
244	8357	8357	CS78492	Pla-0	41.5	2.25	ESP
245	8359	7523	CS76213	Pna-17	42.0945	-86.3253	USA
246	8360	8213	CS76214	Pro-0	43.25	-6	ESP
247	8361	6951	CS76215	Pu2-23	49.42	16.36	CZE
248	8364	6958	CS76216	Ra-0	46	3.3	FRA
249	8365	8365	CS76217	Rak-2	49	16	CZE
250	8367	6959	CS76218	Ren-1	48.5	-1.41	FRA
251	8368	6960	CS77211	Ren-11	48.5	-1.41	FRA
252	8370	7524	CS78505	Rmx-A02	42.036	-86.511	USA
253	8371	7525	CS76220	Rmx-A180	42.036	-86.511	USA
254	8374	8374	CS76222	Rsch-4	56.3	34	RUS
255	8379	6961	CS76226	Se-0	38.3333	-3.53333	ESP
256	8381	6963	CS28742	Sorbo	38.35	68.48	TJK
257	8384	6966	CS77266	Sq-1	51.4083	-0.6383	UK
258	8385	6967	CS76230	Sq-8	51.4083	-0.6383	UK
259	8387	8387	CS76231	St-0	59	18	SWE
260	8388	8388	CS78521	Stw-0	52	36	RUS
261	8389	8389	CS76242	Ta-0	49.5	14.5	CZE
262	8392	6970	CS76268	Ts-1	41.7194	2.93056	ESP
263	8393	6971	CS28775	Ts-5	41.7194	2.93056	ESP
264	8395	8395	CS78528	Tu-0	45	7.5	ITA
265	8396	6973	CS76293	Ull2-3	56.0648	13.9707	SWE
266	8398	6975	CS78531	Uod-1	48.3	14.45	AUT
267	8400	6977	CS76297	Van-0	49.3	-123	CAN
268	8404	6979	CS76301	Wei-0	47.25	8.26	SUI
269	8406	6981	CS28828	Ws-2	52.3	30	RUS
270	8407	6982	CS76304	Wt-5	52.3	9.3	GER
271	8408	6983	CS76305	Yo-0	37.45	-119.35	USA
272	8409	6984	CS28844	Zdr-1	49.3853	16.2544	CZE
273	8410	6985	CS76306	Zdr-6	49.3853	16.2544	CZE
274	8420	8420	CS76152	Kelsterbach-4	50.0667	8.5333	GER
275	8426	8426	CS78551	Ull1-1	56.06	13.97	SWE
276	8429	7438	CS76194	N13	61.36	34.15	RUS
277	8430	8430	CS76171	Lisse	52.25	4.5667	NED
278	8610	8610	CS76083	11ME1.32	42.093	-86.359	USA
279	8796	8796	CS76084	11PNA4.101	42.0945	-86.3253	USA
280	9057	9057	CS78615	Vinslov	56.1	13.9167	SWE

Continued on next page.

Table A.2 – continued from previous page

No.	ID_473	ID_250K	ABRC	Native	Latitude	Longitude	Country
281	*aba1*						
282	*lut2*						
283	*npq1*						
284	*npq4*						

Table A.1 – The list of the 92 Cvi-0 x L*er* RIXs lines and inbred line of Cvi-o and L*er*-1 was used in this study. Seeds were provided by Joost Keurentjes, Wageningen University.

No.	Lines
1	CvL-1 x CvL-146
2	CvL-10 x CvL-26
3	CvL-101 x CvL-176
4	CvL-102 x CvL-28
5	CvL-105 x CvL-145
6	CvL-107 x CvL-124
7	CvL-109 x CvL-185
8	CvL-109 x CvL-47
9	CvL-110 x CvL-32
10	CvL-112 x CvL-30
11	CvL-113 x CvL-141
12	CvL-114 x CvL-3
13	CvL-114 x CvL-60
14	CvL-115 x CvL-126
15	CvL-117 x CvL-73
16	CvL-118 x CvL-108
17	CvL-118 x CvL-164
18	CvL-119 x CvL-177
19	CvL-12 x CvL-142
20	CvL-122 x CvL-42
21	CvL-125 x CvL-117
22	CvL-128 x CvL-6
23	CvL-132 x CvL-129
24	CvL-133 x CvL-35
25	CvL-134 x CvL-29
26	CvL-135 x CvL-10
27	CvL-135 x CvL-140
28	CvL-136 x CvL-102
29	CvL-137 x CvL-165
30	CvL-139 x CvL-162
31	CvL-139 x CvL-36
32	CvL-14 x CvL-4
33	CvL-146 x CvL-64
34	CvL-147 x CvL-50
35	CvL-147 x CvL-69

No.	Lines
36	CvL-149 x CvL-165
37	CvL-150 x CvL-37
38	CvL-152 x CvL-42
39	CvL-153 x CvL-108
40	CvL-153 x CvL-20
41	CvL-154 x CvL-144
42	CvL-156 x CvL-166
43	CvL-16 x CvL-4
44	CvL-16 x CvL-66
45	CvL-164 x CvL-7
46	CvL-166 x CvL-25
47	CvL-168 x CvL-22
48	CvL-169 x CvL-175
49	CvL-17 x CvL-21
50	CvL-170 x CvL-24
51	CvL-171 x CvL-143
52	CvL-174 x CvL-34
53	CvL-180 x CvL-157
54	CvL-183 x CvL-118
55	CvL-186 x CvL-27
56	CvL-187 x CvL-190
57	CvL-187 x CvL-69
58	CvL-189 x CvL-133
59	CvL-19 x CvL-173
60	CvL-19 x CvL-67
61	CvL-190 x CvL-176
62	CvL-191 x CvL-31
63	CvL-192 x CvL-189
64	CvL-20 x CvL-138
65	CvL-21 x CvL-22
66	CvL-24 x CvL-171
67	CvL-25 x CvL-9
68	CvL-26 x CvL-74
69	CvL-33 x CvL-58
70	CvL-35 x CvL-120

No.	Lines
71	CvL-38 x CvL-35
72	CvL-39 x CvL-27
73	CvL-40 x CvL-74
74	CvL-41 x CvL-70
75	CvL-43 x CvL-131
76	CvL-44 x CvL-50
77	CvL-45 x CvL-23
78	CvL-46 x CvL-29
79	CvL-48 x CvL-160
80	CvL-49 x CvL-158
81	CvL-5 x CvL-172
82	CvL-5 x CvL-188
83	CvL-51 x CvL-111
84	CvL-51 x CvL-18
85	CvL-54 x CvL-183
86	CvL-55 x CvL-18
87	CvL-59 x CvL-116
88	CvL-6 x CvL-131
89	CvL-61 x CvL-162
90	CvL-63 x CvL-151
91	CvL-7 x CvL-46
92	CvL-8 x CvL-61
93	Ler x Ler
94	Cvi x Ler
95	Ler x Cvi
96	Cvi x Cvi
97	Cvi-0
98	Ler

Table A.3 – The list of the 233 accessions of *Arabidopsis* used in Experiment V.

No.	ID_473	ID_250K	ABRC	Native	Latitude	Longitude	Country
1	66	66	CS76108	CAM-61	48.2667	-4.58333	FRA
2	96	96	CS76158	LAC-5	47.7	6.81667	FRA
3	149	149	CS76163	LDV-58	48.5167	-4.06667	FRA
4	173	173	CS76182	MIB-22	47.3833	5.31667	FRA
5	178	178	CS76183	MIB-28	47.3833	5.31667	FRA
6	259	259	CS76206	PAR-4	46.65	-0.25	FRA
7	260	260	CS76207	PAR-5	46.65	-0.25	FRA
8	281	281	CS76252	TOU-A1-115	46.6667	4.11667	FRA
9	328	328	CS76256	TOU-A1-62	46.6667	4.11667	FRA
10	362	362	CS76259	TOU-C-3	46.6667	4.11667	FRA
11	373	373	CS76261	TOU-H-12	46.6667	4.11667	FRA
12	374	374	CS76262	TOU-H-13	46.6667	4.11667	FRA
13	378	378	CS76263	TOU-I-17	46.6667	4.11667	FRA
14	383	383	CS76266	TOU-J-3	46.6667	4.11667	FRA
15	386	386	CS76267	TOU-K-3	46.6667	4.11667	FRA
16	641	641	CS76165	LI-OF-095	40.7777	-72.9069	USA
17	2274	2274	CS76228	SLSP-30	43.665	-86.496	USA
18	5056	5056	CS76281	UKSE06-192	51.3	0.5	UK
19	5122	5122	CS76283	UKSE06-278	51.3	0.4	UK
20	5158	5158	CS76284	UKSE06-349	51.3	0.4	UK
21	5160	5160	CS76285	UKSE06-351	51.3	0.4	UK
22	5202	5202	CS76286	UKSE06-414	51.3	0.4	UK
23	5606	5606	CS76278	UKNW06-436	54.7	-3.4	UK
24	5742	5742	CS76272	UKID37	51.3	1.1	UK
25	5753	5753	CS76273	UKID48	54.7	-2.7	UK
26	5785	5785	CS76274	UKID80	54.7	-2.9	UK
27	5832	5832	CS76092	App1-16	56.3333	15.9667	SWE
28	5837	5837	CS76099	Bor-1	49.4013	16.2326	CZE
29	5987	5987	CS76122	DraIV 6-16	49.4112	16.2815	CZE
30	6005	6005	CS76123	DraIV 6-35	49.4112	16.2815	CZE
31	6008	6008	CS76124	Duk	49.1	16.2	CZE
32	6016	6016	CS76834	Eds-1	62.9	18.4	SWE
33	6020	6020	CS76132	Fj?1-5	56.06	14.29	SWE
34	6039	6039	CS76143	Hovdala-2	56.1	13.74	SWE
35	6042	6042	CS76174	Lom1-1	56.09	13.9	SWE
36	6096	6096	CS76234	T1060	55.6472	13.2225	SWE
37	6169	6169	CS76243	TAD 01	62.8714	18.3447	SWE
38	6190	6190	CS76248	TDr-3	55.7686	14.1381	SWE
39	6194	6194	CS76249	TDr-8	55.7706	14.1342	SWE
40	6243	6243	CS76251	Tottarp-2	55.95	13.85	SWE

Continued on next page.

Table A.3 – continued from previous page

No.	ID_473	ID_250K	ABRC	Native	Latitude	Longitude	Country
41	6318	6318	CS76269	UduI 1-34	49.2771	16.6314	CZE
42	6449	6449	CS76308	ZdrI 2-25	49.3853	16.2544	CZE
43	6709	8261	CS76096	Bg-2	47.6479	-122.305	USA
44	6727	6727	CS28140	CIBC-2	51.4083	-0.6383	UK
45	6729	6729	CS28141	CIBC-4	51.4083	-0.6383	UK
46	6730	6730	CS28142	CIBC-5	51.4083	-0.6383	UK
47	6810	6810	CS28407	KNO-11	41.2816	-86.621	USA
48	6897	8251	CS76087	Ag-0	45	1.3	FRA
49	6898	8253	CS76091	An-1	51.2167	4.4	BEL
50	6899	8260	CS76094	Bay-0	49	11	GER
51	6904	8269	CS76101	Br-0	49.2	16.6166	CZE
52	6906	8273	CS76106	C24	40.2077	-8.42639	POR
53	6909	8279	CS76113	Col-0	38.3	-92.3	USA
54	6910	8280	CS76114	Ct-1	37.3	15	ITA
55	6911	8281	CS76116	Cvi-0	15.1111	-23.6167	CPV
56	6914	8288	CS76126	Edi-0	56	-3	UK
57	6915	8289	CS76478	Ei-2	50.3	6.3	GER
58	6916	8291	CS76127	Est-1	58.3	25.3	RUS
59	6919	8295	CS76133	Ga-0	50.3	8	GER
60	6923	8308	CS76940	HR-10	51.4083	-0.6383	UK
61	6924	8309	CS76144	HR-5	51.4083	-0.6383	UK
62	6931	8322	CS78461	Kz-9	49.5	73.1	KAZ
63	6932	8324	CS76164	Ler-1	47.984	10.8719	GER
64	6936	8336	CS76179	Lz-0	46	3.3	FRA
65	6937	8339	CS76191	Mrk-0	49	9.3	GER
66	6938	8340	CS76555	Ms-0	55.7522	37.6322	RUS
67	6940	8342	CS76193	Mz-0	50.3	8.3	GER
68	6942	8344	CS76197	Nd-1	50	10	SUI
69	6946	8352	CS76203	Oy-0	60.23	6.13	NOR
70	6958	8364	CS76216	Ra-0	46	3.3	FRA
71	6960	8368	CS77211	Ren-11	48.5	-1.41	FRA
72	6962	8248	CS76227	Shahdara	38.35	68.48	TJK
73	6963	8381	CS28742	Sorbo	38.35	68.48	TJK
74	6966	8384	CS77266	Sq-1	51.4083	-0.6383	UK
75	6967	8385	CS76230	Sq-8	51.4083	-0.6383	UK
76	6970	8392	CS76268	Ts-1	41.7194	2.93056	ESP
77	6971	8393	CS28775	Ts-5	41.7194	2.93056	ESP
78	6973	8396	CS76293	Ull2-3	56.0648	13.9707	SWE
79	6975	8398	CS78531	Uod-1	48.3	14.45	AUT
80	6977	8400	CS76297	Van-0	49.3	-123	CAN

Continued on next page.

Table A.3 – continued from previous page

No.	ID_473	ID_250K	ABRC	Native	Latitude	Longitude	Country
81	6979	8404	CS76301	Wei-0	47.25	8.26	SUI
82	6981	8406	CS28828	Ws-2	52.3	30	RUS
83	6982	8407	CS76304	Wt-5	52.3	9.3	GER
84	6984	8409	CS28844	Zdr-1	49.3853	16.2544	CZE
85	6989	6989	CS28013	Alst-1	54.8	-2.4333	UK
86	6994	6994	CS28049	Ann-1	45.9	6.13028	FRA
87	6996	6996	CS28017	An-2	51.2167	4.4	BEL
88	7000	7000	CS28007	Aa-0	50.9167	9.57073	GER
89	7004	7004	CS28097	Bs-2	47.5	7.5	SUI
90	7013	7013	CS28061	Bd-0	52.4584	13.287	GER
91	7015	7015	CS28079	Bla-1	41.6833	2.8	ESP
92	7021	7021	CS28081	Bla-3	41.6833	2.8	ESP
93	7024	7024	CS28084	Bla-6	41.6833	2.8	ESP
94	7025	7025	CS28078	Bl-1	44.5041	11.3396	ITA
95	7026	7026	CS28091	Boot-1	54.4	-3.2667	UK
96	7028	7028	CS28058	Bch-1	49.5166	9.3166	GER
97	7029	7029	CS28059	Bch-3	49.5166	9.3166	GER
98	7030	7030	CS28060	Bch-4	49.5166	9.3166	GER
99	7031	7031	CS28099	Bsch-0	40.0167	8.6667	GER
100	7032	7032	CS28100	Bsch-2	40.0167	8.6667	GER
101	7044	7044	CS28102	Bu-2	50.5	9.5	GER
102	7062	7062	CS28128	Ca-0	50.2981	8.26607	GER
103	7078	7078	CS28163	Co-2	40.12	-8.25	POR
104	7079	7079	CS28164	Co-3	40.12	-8.25	POR
105	7081	8278	CS78422	Co	40.2077	-8.42639	POR
106	7098	7098	CS28208	Di-1	47	5	FRA
107	7102	7102	CS28210	Do-0	50.7224	8.2372	GER
108	7106	7106	CS28211	Dr-0	51.051	13.7336	GER
109	7109	7109	CS28229	Ema-1	51.3	0.5	UK
110	7110	7110	CS28217	Ede-1	52.0333	5.66667	NED
111	7113	7113	CS28224	Ei-4	50.3	6.3	GER
112	7115	7115	CS28226	Ei-6	50.3	6.3	GER
113	7116	7116	CS28227	Eil-0	51.4599	12.6327	GER
114	7128	7128	CS28243	Est-0	58.3	25.3	RUS
115	7139	7139	CS28252	Fi-1	50.5	8.0167	GER
116	7143	7143	CS28279	Gel-1	51.0167	5.86667	NED
117	7145	7145	CS28277	Ge-1	46.5	6.08	SUI
118	7149	7149	CS28330	Gu-0	50.3	8	GER
119	7151	7151	CS28282	Go-0	51.5338	9.9355	GER
120	7158	7158	CS28326	Gr-5	47	15.5	AUT

Continued on next page.

Table A.3 – continued from previous page

No.	ID_473	ID_250K	ABRC	Native	Latitude	Longitude	Country
121	7163	7163	CS28336	Ha-0	52.3721	9.73569	GER
122	7165	7165	CS28350	Hn-0	51.3472	8.28844	GER
123	7169	7169	CS28345	Hh-0	54.4175	9.88682	GER
124	7176	7176	CS28362	Is-1	50.5	7.5	GER
125	7178	7178	CS28373	Jm-1	49	15	CZE
126	7186	7186	CS28395	Kn-0	54.8969	23.8924	LTU
127	7192	7192	CS28386	Kil-0	55.6395	-5.66364	UK
128	7195	7195	CS28390	Kl-1	50.95	6.9666	GER
129	7199	7199	CS28394	Kl-5	50.95	6.9666	GER
130	7206	7206	CS28420	Kro-0	50.0742	8.96617	GER
131	7210	7210	CS28440	La-1	52.7333	15.2333	POL
132	7227	7227	CS28457	Li-5:2	50.3833	8.0666	GER
133	7228	7228	CS28458	Li-5:3	50.3833	8.0666	GER
134	7229	7229	CS28459	Li-6	50.3833	8.0666	GER
135	7238	7238	CS28471	Ll-1	41.59	2.49	ESP
136	7239	7239	CS28472	Li-2	41.59	2.49	ESP
137	7255	7255	CS28492	Mh-0	50.95	7.5	POL
138	7256	7256	CS28493	Mh-1	50.95	7.5	POL
139	7258	7258	CS28573	Nw-0	50.5	8.5	GER
140	7260	7260	CS28575	Nw-2	50.5	8.5	GER
141	7265	7265	CS28528	Nd-0	50	10	SUI
142	7277	7277	CS28580	Ob-1	50.2	8.5833	GER
143	7280	7280	CS28583	Old-1	53.1667	8.2	GER
144	7282	7282	CS28587	Or-0	50.3827	8.01161	GER
145	7284	7284	CS28849	Ors-2	44.7203	22.3955	ROU
146	7291	7291	CS28595	Pa-2	38.07	13.22	ITA
147	7292	7292	CS28596	Pa-3	38.07	13.22	ITA
148	7297	7297	CS28601	Pf-0	48.5479	9.11033	GER
149	7299	7299	CS28639	Pi-2	47.04	10.51	AUT
150	7300	7300	CS28640	Pla-0	41.5	2.25	ESP
151	7301	7301	CS28641	Pla-1	41.5	2.25	ESP
152	7309	7309	CS28649	Po-1	50.7167	7.1	GER
153	7310	7310	CS28651	Pr-0	50.1448	8.60706	GER
154	7328	7328	CS28731	Sf-2	41.7833	3.03333	ESP
155	7333	7333	CS28729	Sei-0	46.5438	11.5614	ITA
156	7337	7337	CS28739	Si-0	50.8738	8.02341	GER
157	7340	7340	CS28725	Sav-0	49.1833	15.8833	CZE
158	7344	7344	CS28732	Sg-1	47.6667	9.5	GER
159	7351	7351	CS28786	Ty-0	56.4278	-5.23439	UK
160	7352	7352	CS28757	Te-0	60.0585	23.2982	FIN

Continued on next page.

Table A.3 – continued from previous page

No.	ID_473	ID_250K	ABRC	Native	Latitude	Longitude	Country
161	7353	7353	CS28758	Tha-1	52.08	4.3	NED
162	7355	7355	CS28760	Tiv-1	41.96	12.8	ITA
163	7373	7373	CS28780	Tsu-0	34.43	136.31	JPN
164	7376	7376	CS28784	Tu-1	45	7.5	ITA
165	7378	7378	CS28787	Uk-1	48.0333	7.7667	GER
166	7381	7381	CS28790	Uk-4	48.0333	7.7667	GER
167	7382	7382	CS28795	Utrecht	52.0918	5.1145	NED
168	7386	7386	CS28802	Vi-0	50.1946	8.74639	GER
169	7391	7391	CS28809	Wag-4	51.9666	5.6666	NED
170	7392	7392	CS28810	Wag-5	51.9666	5.6666	NED
171	7397	7397	CS28823	Ws	52.3	30	RUS
172	7404	7404	CS28813	Wc-1	52.6	10.0667	GER
173	7405	7405	CS28814	Wc-2	52.6	10.0667	GER
174	7408	7408	CS28833	Wt-3	52.3	9.3	GER
175	7411	7411	CS28822	Wl-0	47.9299	10.8134	GER
176	7413	7413	CS28820	Wil-2	54.6833	25.3167	LTU
177	7418	7418	CS28847	Zu-1	47.3667	8.55	SUI
178	7430	7430	CS28527	Nc-1	48.6167	6.25	FRA
179	7438	8429	CS76194	N13	61.36	34.15	RUS
180	7457	7457	CS28688	RLD-2	56.25	34.3167	RUS
181	7461	8303	CS76897	H55	49	15	CZE
182	7479	7479	CS28610	PHW-10	51.2878	0.0565	UK
183	7483	7483	CS28614	PHW-14	51.2878	0.0565	UK
184	7504	7504	CS28633	PHW-33	52.25	4.5667	NED
185	7507	7507	CS28636	PHW-36	48.6103	2.3086	FRA
186	7508	7508	CS28637	PHW-37	48.6103	2.3086	FRA
187	7519	8350	CS78486	Omo2-3	56.1481	15.8155	SWE
188	7521	8333	CS76177	Lp2-6	49.38	16.81	CZE
189	7522	8338	CS76190	Mr-0	44.15	9.65	ITA
190	8213	8360	CS76214	Pro-0	43.25	-6	ESP
191	8215	8294	CS76129	Fei-0	40.5	-8.32	POR
192	8222	8222	CS76170	Lis-2	56	14.7	SWE
193	8234	8234	CS76138	Gul1-2	56.3	16	SWE
194	8236	8236	CS76146	HSm	49.33	15.76	CZE
195	8241	8241	CS76166	Liarum	55.95	13.85	SWE
196	8242	8242	CS76167	Lillo-1	56.1512	15.7844	SWE
197	8243	8243	CS77173	PHW-2	43.7703	11.2547	ITA
198	8247	8247	CS78396	San-2	56.07	13.74	SWE
199	8256	8256	CS76093	Ba1-2	56.4	12.9	SWE
200	8258	8258	CS78404	Ba4-1	56.4	12.9	SWE

Continued on next page.

Table A.3 – continued from previous page

No.	ID_473	ID_250K	ABRC	Native	Latitude	Longitude	Country
201	8259	8259	CS78405	Ba5-1	56.4	12.9	SWE
202	8264	8264	CS76097	Bla-1	41.6833	2.8	ESP
203	8270	8270	CS78414	Bs-1	47.5	7.5	SUI
204	8271	8271	CS76103	Bu-0	50.5	9.5	GER
205	8274	8274	CS76109	Can-0	29.2144	-13.4811	ESP
206	8296	8296	CS76134	Gd-1	53.5	10.5	GER
207	8304	8304	CS76140	Hi-0	52	5	NED
208	8310	8310	CS76145	Hs-0	52.24	9.44	GER
209	8312	8312	CS28361	Is-0	50.5	7.5	GER
210	8313	8313	CS78454	Jm-0	49	15	CZE
211	8334	8334	CS77056	Lu-1	55.71	13.2	SWE
212	8337	8337	CS76551	Mir-0	44	12.37	ITA
213	8343	8343	CS76195	Na-1	47.5	1.5	FRA
214	8374	8374	CS76222	Rsch-4	56.3	34	RUS
215	8387	8387	CS76231	St-0	59	18	SWE
216	8388	8388	CS78521	Stw-0	52	36	RUS
217	8389	8389	CS76242	Ta-0	49.5	14.5	CZE
218	8395	8395	CS78528	Tu-0	45	7.5	ITA
219	8420	8420	CS76152	Kelsterbach-4	50.0667	8.5333	GER
220	8426	8426	CS78551	Ull1-1	56.06	13.97	SWE
221	8610	8610	CS76083	11ME1.32	42.093	-86.359	USA
222	8796	8796	CS76084	11PNA4.101	42.0945	-86.3253	USA
223	9057	9057	CS78615	Vinslov	56.1	13.9167	SWE

Table A.4 – Details of sequencing primers used in this study. Primers listed here were designed for genotyping of the Knockout lines purpose. Primers for genotyping T-DNA insertions were designed using the T-DNA Primer Design software (http://signal.salk.edu/tdnaprimers.2.html).

Name	Sequence (5′-3′)	Description
At1PSB27-1L	ACGAAAGGATAGGTTGGTTGG	Forward primer for sequencing AT1G03600 inserted gene
At1PSB27-1R	GCTTTTCCGAGAAGAGCTTTC	Reverse primer for AT1G03600 sequencing inserted gene
At1PSB27-2L	TTTCATGCATATTCACCCACC	Forward primer for AT1G03600.1 sequencing inserted gene
At1PSB27-2R	ATCACTGCCGACGTATCTTTG	Reverse primer for AT1G03600.1 sequencing inserted gene
At1LPA19-1L	TGGACGTGGCTAAAAATCATC	Forward primer for AT1G05400.1 sequencing inserted gene
At1LPA19-1R	TCATGACGGCTACAAGGAAAC	Reverse primer for AT1G05400.1 sequencing inserted gene
At4PGR1-1L	CCCATCATGACATTTCTCTTCTC	Forward primer for AT4G03280 sequencing inserted gene
At4PGR1-1R	ATGAGGACGCCATTGTTGTAG	Reverse primer for AT4G03280 sequencing inserted gene
At1LPA19-2L	TAGTCATCTGGAACCGGACAC	Forward primer for AT1G05385.1 sequencing inserted gene
At1LPA19-2R	AACCACGACGATCAAACAAAG	Reverse primer for AT1G05385.1 sequencing inserted gene
At1NQ1-1L	GATCTCACCCATCTCCCTCTC	Forward primer for AT1G03590.1 sequencing inserted gene
At1NQ1-1R	ATACACAACGGATCTGATCGC	Reverse primer for AT1G03590.1 sequencing inserted gene
At1NQ2-1L	TTGCTTGTTTCCTTTCAATCG	Forward primer for AT1G03687 sequencing inserted gene
At1NQ2-1R	CTTTAAACGCTTGAGCATTGC	Reverse primer for AT1G03687 sequencing inserted gene
At1NQ3-1L	CTGCTGCTTCTCTTGACCTTG	Forward primer for AT1G79620 sequencing inserted gene
At1NQ3-1R	AAACAGCCGATAGAGAAAGGC	Reverse primer for AT1G79620 sequencing inserted gene
At4PGR1-2L	AAGGTAGCGTAAGGGACAAGC	Forward primer for AT4G03280 sequencing inserted gene
At4PGR1-2R	ATTGGTGCATAAAGCTTGTGC	Reverse primer for AT4G03280 sequencing inserted gene
At2NQ1-1L	CAACCCATTTCAATCTTCTCG	Forward primer for AT2G21860 sequencing inserted gene
At2NQ1-1R	GGATGAGCTGAAGAGTGATGC	Reverse primer for AT2G21860 sequencing inserted gene
At3APX2-1L	GAAAGGAGTTGTGCTACGTCG	Forward primer for AT3G09640 sequencing inserted gene
At3APX2-1R	GCTGCATCCAGAAACAAAGAC	Reverse primer for AT3G09640 sequencing inserted gene

Table A.5 – Details of GBS library prep protocol developed by Niccy Aitken.

Process	Descriptions
1. Plate Setups	- Extract DNA from plant tissue and allocated into 95 well of each plate and one for negative control.
2. Plate out Sample DNA and adapters	- Quantitate DNA using fluorometry (Qubit) - Mix approx. 500 ng gDNA with 3 μl (0.75ng/ul) PstI adapter working stock. - Spin briefly. Speedy-vac at low temp (I'âĂŹve been using 45deg) until liquid has completely evaporated. - If,DNA is of high conc, and consistent, so that less than $\sim$15 μl of DNA is needed for the library
3. Digest and Ligation	- Ligation should proceed immediately after digestion
- Digestion	1. Make PstI Master Mix - for 2 plates, I usually mix ingredients straight into dispensing trough. 10x NEB CutSmart: 2.0 μl x 200 = 400 PstI-HF: 0.2 μl x 200 = 40 dH_20 17.8 μl x 200 = 3560 Total: 20.0 μl x 200 = 4000 2. Transfer 20 μl of the digest mix with a multichannel pipette to each well 3. cover with film 4. vortex gently 5. spin down 6. incubate at 37 degrees for 2 hrs 7. hold at 4 degrees until ligation
- Ligation	1. Prepare Ligation Master Mix - for 2 plates, I usually mix ingredients straight into dispensing trough. 10x Ligation Buffer: 5.0 μl x 200 = 1000 T4 DNA Ligase: 1.0 μl * x 200 = 200 dH2O: 24.0 μl x 200 = 4680 Total: 30.0 μl x 200 = 6000 Add all of mix to multichannel reservoir 2. With multi-channel pipette, add 30.0 μl of Ligation Mix to each well of the reaction plate 3. cover with film

Continued on next page.

Table A.5 – continued from previous page

Process	Descriptions
	4. 16 degrees for 30 minutes 5. 37 degrees for 2 minutes 6. 16 degrees for 30 minutes 7. 37 degrees for 2 minutes 8. 16 degrees for 30 minutes 9. 37 degrees for 2 minutes 10. 80 degrees for 30 minutes 11. hold at 4 degrees 12. Transfer plate to -20 freezer
4. Purification	1. Purify with Qiagen MinElute 96-well PCR purification kit 2. include the wash step with dH2O 3. for elution, use 23μl 1x TE and pipette up and down 20+ times to elute DNA 4. Remove 10 μ to PCR plate (for the next step) and the remainder (>10 μl) to another plate for backup storage.
Post purification quantitation (optional)	With Qubit Fluorometer, just to get an indication of concentration and that the DNAâĂŹs still there prior to PCR.
5. PCR Amplification	- 50ul PCR for each sample, starting with 10 ul of purified post-ligation product, mix straight into multi-channel reservoir. 1. Prepare PCR Master Mix - Bioline* 2x Taq Master Mix 25 μl x 100 = 2500 x2 = 5000 - PCR primer 1 (10 μM),1.0ul x 100 = 100 x2 = 200 - PCR primer 2 (10 μM),1.0ul x 100 = 100 x2 = 200 - dH_20 13 μl x 100 =,1300 x2 = 2600 2. With a multi-channel pipette, transfer 40ul of the mix to each well of the prepared 10 ul of purified post-ligation product. 3. Run 24-cycle PCR - 72 degrees for 5 mins - 95 degrees for 60s

Continued on next page.

Table A.5 – continued from previous page

Process	Descriptions
	- 95 degrees for 30s - 65 degrees for 30s - 72 degrees for 30s - Repeat above 3 steps 24x** - 72 degrees for 5 mins - hold at 10 degrees ∗ MyTaq HS Mix ∗∗ If there is buckets of DNA (eg 1000 ng as per the original protocol), then 18 cycles is usually enough. If DNA quantity or quality is low, 28 cycles helps a lot.
6.Post purification quantitation	- With Caliper GXII using undiluted PCR product. Calculate concentrations of each individual sample for chosed size range (my current choice is 250-450bp)
7. Pool Samples to make Library	- Pool a variable volume of all samples normalised for equal concentration.
8. Size Fractionation	A. Electrophorese on a 1.5% hi res agarose gel and size select desired range (we do about 250-450bp). Purify with gel purification kit. B. OR using the Caliper XT for size selection. No further purification necessary.

Appendix B

Supplementary Data for Chapter 3

B.1 The chlorophyll fluorescence measuring P1 protocol (one minute 10 seconds of actinic light followed by one minute 30 seconds dark relaxation period).

```
;version August 22, 2012: 3 min
TS=20ms
include default.inc  ;Includes standard options, do not remove it !
include light.inc  ;Includes standard options, do not remove it !
Shutter=1
Sensitivity=46
Act3=0
Act1=100
Act2=100
Super=100

;-----------------------------------------------------------------------------------------------------
;*** Fo Measurement
*****************************************************************************************
;-----------------------------------------------------------------------------------------------------
F0duration = 5s
F0period = 1s
<0,F0period..F0duration>=>mfmsub
;
;Fo definition
<0s>=>checkPoint,"startFo"
<F0duration - F0period>=>checkPoint,"endFo"
;
;-----------------------------------------------------------------------------------------------------
;*** Saturating Pulse & Fm Measurement
*************************************************************************
;-----------------------------------------------------------------------------------------------------
PulseDuration=800ms;#####
a1=F0duration + 2*mfmsub_length;#####
;
<a1>=>SatPulse(PulseDuration)
<a1>=>act1(PulseDuration)
;
<a1>=>mpulse
;
;Fm definition
<a1 + PulseDuration/2>=>checkPoint,"startFm"
<a1 + PulseDuration - mfmsub_length>=>checkPoint,"endFm"
;
;Visual frame definition                                    ## Image shown in pre-processing window
<a1 + PulseDuration/2 + TS>=>checkPoint,"timeVisual"
;
;-----------------------------------------------------------------------------------------------------
;******* Dark Relaxation Measurement
*************************************************************************
;-----------------------------------------------------------------------------------------------------
DarkRelaxation1=17s;#####
b1= a1 + PulseDuration + 2*mfmsub_length;#####
b2=2s;#####
<b1, b1 + 200ms .. b1 + b2>=>mfmsub
<b1 + b2 + 200ms, b1 + 2*b2 .. b1+DarkRelaxation1>=>mfmsub
;
```

```
;-------------------------------------------------------------------------------------------------
;******* Kautsky Effect Measurement ***************************************************
;-------------------------------------------------------------------------------------------------
;
;******* Actinic light Exposure ***********************************
ALPeriod=70s;#####
c1= a1 + PulseDuration + DarkRelaxation1 + mfmsub_length;#####
<c1>=>act1(ALPeriod)
<c1>=>act2(ALPeriod)
;
;*******Fast Kautsky kinetics**************************************
c2=2s;#####
;
<c1 + TS, c1 + TS + 2*TS.. c1+c2>=>mfmsub;
;
;*******Slow Kautsky kinetics**************************************
c3=2s;#####                                          period of slow measurement
;
<c1 + c2 + c3/10, c1 + c2+ c3/5, c1 + c2 + c3/2>=>mfmsub
;
<c1 + c2 + c3, c1 + c2 + 2*c3 .. c1 + ALPeriod>=>mfmsub;
;
;Fp definition
<c1>=>checkPoint,"startFp"
<c1 + c2 + c3>=>checkPoint,"endFp"
;
;-------------------------------------------------------------------------------------------------
;******* Saturating Pulses - Fm' Quenching Analysis ****************************************
;-------------------------------------------------------------------------------------------------
;
;******* Saturating Pulses - Fm_L1 *********************************
f1=c1+<8s>;#####
f11=f1#<mfmsub_length,2*mfmsub_length ..PulseDuration - mfmsub_length>;#####
f11=>mfmsub
f1 + mfmsub_length=>checkPoint,"startFt_L1"
f1 + PulseDuration - mfmsub_length=>checkPoint,"endFt_L1"
;
f2=f1 + PulseDuration;#####
f2=>SatPulse(PulseDuration);
f2=>mpulse
f2+PulseDuration/2=>checkPoint,"startFm_L1"
f2 + PulseDuration - mfmsub_length=>checkPoint,"endFm_L1"
;
;******* Saturating Pulses - Fm_L2 *********************************
f3=c1+<18s>;#####
f31=f3#<mfmsub_length,2*mfmsub_length ..PulseDuration - mfmsub_length>;#####
f31=>mfmsub
f3 + mfmsub_length=>checkPoint,"startFt_L2"
f3 + PulseDuration - mfmsub_length=>checkPoint,"endFt_L2"
;
f4=f3 + PulseDuration;#####
f4=>SatPulse(PulseDuration);
```

```
f4=>mpulse
f4 + PulseDuration/2=>checkPoint,"startFm_L2"
f4 + PulseDuration - mfmsub_length=>checkPoint,"endFm_L2"
;
;******* Saturating Pulses - Fm_L3 **********************************
f5=c1+<28s>;#####
f51=f5#<mfmsub_length,2*mfmsub_length ..PulseDuration - mfmsub_length>;#####
f51=>mfmsub
f5 + mfmsub_length=>checkPoint,"startFt_L3"
f5 + PulseDuration - mfmsub_length=>checkPoint,"endFt_L3"
;
f6=f5 + PulseDuration;#####
f6=>SatPulse(PulseDuration);
f6=>mpulse
f6 + PulseDuration/2=>checkPoint,"startFm_L3"
f6 + PulseDuration - mfmsub_length=>checkPoint,"endFm_L3"
;******* Saturating Pulses - Fm_L4 **********************************
f7=c1+<48s>;#####
f71=f7#<mfmsub_length,2*mfmsub_length ..PulseDuration - mfmsub_length>;#####
f71=>mfmsub
f7 + mfmsub_length=>checkPoint,"startFt_L4"
f7 + PulseDuration - mfmsub_length=>checkPoint,"endFt_L4"
;
f8=f7 + PulseDuration;#####
f8=>SatPulse(PulseDuration);
f8=>mpulse
f8 + PulseDuration/2=>checkPoint,"startFm_L4"
f8 + PulseDuration - mfmsub_length=>checkPoint,"endFm_L4"
;
;******* Saturating Pulses - Fm_Lss **********************************
f9=c1 + <68s>;#####
f91=f9#<mfmsub_length,2*mfmsub_length ..PulseDuration - mfmsub_length>;#####
f91=>mfmsub
f9 + mfmsub_length=>checkPoint,"startFt_Lss"
f9 + PulseDuration - mfmsub_length=>checkPoint,"endFt_Lss"
;
f10=f9 + PulseDuration;#####
f10=>SatPulse(PulseDuration);
f10=>mpulse
f10 + PulseDuration/2=>checkPoint,"startFm_Lss"
f10 + PulseDuration - mfmsub_length=>checkPoint,"endFm_Lss"
;
;-----------------------------------------------------------------------------------------------
;*** Dark relaxation after actinic light period ****************************************
;-----------------------------------------------------------------------------------------------
DarkRelaxation2=100s;#####
h1=c1 + ALPeriod;#####
h2=2*TS;#####
h3=3s;#####
;
;******** Relaxation measurement*************************************
;
```

```
<h1+h2, h1+2*h2, h1+4*h2, h1+8*h2, h1+16*h2>=>mfmsub;
<h1+h3, h1+2*h3..h1+DarkRelaxation2>=>mfmsub
;
;******* Saturating Pulses - Fm_D1 **********************************
g1=h1 + <28s>;#####
g11=g1#<mfmsub_length,2*mfmsub_length ..PulseDuration - mfmsub_length>;#####
g11=>mfmsub
g1 + mfmsub_length=>checkPoint,"startFt_D1"
g1 + PulseDuration - mfmsub_length=>checkPoint,"endFt_D1"
;
g2=g1 + PulseDuration;#####
g2=>SatPulse(PulseDuration)
g2=>act1(PulseDuration)
g2=>mpulse
g2 + PulseDuration/2=>checkPoint,"startFm_D1"
g2 + PulseDuration - mfmsub_length=>checkPoint,"endFm_D1"
;
;******* Saturating Pulses - Fm_D2 **********************************
g3=h1 + <58s>;#####
g31=g3#<mfmsub_length,2*mfmsub_length ..PulseDuration - mfmsub_length>;#####
g31=>mfmsub
g3 + mfmsub_length=>checkPoint,"startFt_D2"
g3 + PulseDuration - mfmsub_length=>checkPoint, "endFt_D2"
;
g4=g3 + PulseDuration;#####
g4=>SatPulse(PulseDuration)
g4=>act1(PulseDuration)
g4=>mpulse
g4 + PulseDuration/2=>checkPoint,"startFm_D2"
g4 + PulseDuration - mfmsub_length=>checkPoint,"endFm_D2"
;
;******* Saturating Pulses - Fm_D3 **********************************
g5=h1+<88s>;#####
g51=g5#<mfmsub_length,2*mfmsub_length ..PulseDuration - mfmsub_length>;#####
g51=>mfmsub
g5 + mfmsub_length=>checkPoint,"startFt_D3"
g5 + PulseDuration - mfmsub_length=>checkPoint,"endFt_D3"
;
g6=g5 + PulseDuration;#####
g6=>SatPulse(PulseDuration)
g6=>act1(PulseDuration)
g6=>mpulse
g6 + PulseDuration/2=>checkPoint,"startFm_D3"
g6 + PulseDuration - mfmsub_length=>checkPoint,"endFm_D3"
;
;END ***************************************************************
```

B.2 The chlorophyll fluorescence measuring P2 protocol (15 minutes of actinic light followed by 5 minutes dark relaxation period).

```
TS=20ms
; Quenching protocol with Actinic1 & Actinic2 : 20 min
; Protocol: Quenching-without-FR1-Lucam.p modified by ZB for ANU
;version September 27, 2012
;high-resolution CCD
;
include default.inc  ;Includes standard options, do not remove it !
include light.inc  ;Includes standard options, do not remove it !
Shutter=0
Sensitivity=50
Act1=100
Act2=100
Super=100

;-------------------------------------------------------------------------------------------------------
;*** Fo Measurement ************************************************************
;-------------------------------------------------------------------------------------------------------
F0duration = 5s
F0period = 1s
<0,F0period..F0duration>=>mfmsub
;
;Fo definition
<0s>=>checkPoint,"startFo"
<F0duration - F0period>=>checkPoint,"endFo"
;
;-------------------------------------------------------------------------------------------------------
;*** Saturating Pulse & Fm Measurement *************************************************
;-------------------------------------------------------------------------------------------------------
PulseDuration=800ms;#####
a1=F0duration + 2*mfmsub_length;#####
;
<a1>=>SatPulse(PulseDuration)
<a1>=>act1(PulseDuration)
<a1>=>act2(PulseDuration)
;
<a1>=>mpulse
;
;Fm definition
<a1 + mfmsub_length>=>checkPoint,"startFm"
<a1 + PulseDuration - mfmsub_length>=>checkPoint,"endFm"
;
;Visual frame definition                                    ## Image shown in pre-processing window
<a1 + PulseDuration/2 + TS>=>checkPoint,"timeVisual"
;
;-------------------------------------------------------------------------------------------------------
;******* Dark Relaxation Measurement *****************************************************
;-------------------------------------------------------------------------------------------------------
DarkRelaxation1=17s;#####
b1= a1 + PulseDuration + 2*mfmsub_length;#####
b2=2s;#####
<b1, b1 + 200ms .. b1 + b2>=>mfmsub
<b1 + b2 + 200ms, b1 + 2*b2 .. b1+DarkRelaxation1>=>mfmsub
;
;-------------------------------------------------------------------------------------------------------
```

```
;******* Kautsky Effect Measurement
************************************************************
;-------------------------------------------------------------------------------------------------
;
;******* Actinic light Exposure ************************************
ALPeriod=900s;#####
c1= a1 + PulseDuration + DarkRelaxation1 + mfmsub_length;#####
<c1>=>act1(ALPeriod)
<c1>=>act2(ALPeriod)
;
;*******Fast Kautsky kinetics*************************************
c2=3s;#####
;
<c1 + TS, c1 + TS + mfmsub_length.. c1+c2>=>mfmsub;
;
;*******Slow Kautsky kinetics*************************************
c3=4s;#####                                          period of slow measurement
;
<c1 + c2 + c3/10, c1 + c2+ c3/5, c1 + c2 + c3/2>=>mfmsub
;
<c1 + c2 + c3, c1 + c2 + c3 +12s .. c1 + ALPeriod>=>mfmsub;
;
;Fp definition
<c1>=>checkPoint,"startFp"
<c1 + c2 + c3>=>checkPoint,"endFp"
;
;-------------------------------------------------------------------------------------------------
;******* Saturating Pulses - Fm' Quenching Analysis***********************************
;-------------------------------------------------------------------------------------------------
;
;******* Saturating Pulses - Fm_L1 **********************************
f1=c1+<58s>;#####
f11=f1#<mfmsub_length,2*mfmsub_length ..PulseDuration - mfmsub_length>;#####
f11=>mfmsub
f1 + mfmsub_length=>checkPoint,"startFt_L1"
f1 + PulseDuration - mfmsub_length=>checkPoint,"endFt_L1"
;
f2=f1 + PulseDuration;#####
f2=>SatPulse(PulseDuration);
f2=>mpulse
f2+PulseDuration/2=>checkPoint,"startFm_L1"
f2 + PulseDuration - mfmsub_length=>checkPoint,"endFm_L1"
;
;******* Saturating Pulses - Fm_L2 **********************************
f3=c1+<118s>;#####
f31=f3#<mfmsub_length,2*mfmsub_length ..PulseDuration - mfmsub_length>;#####
f31=>mfmsub
f3 + mfmsub_length=>checkPoint,"startFt_L2"
f3 + PulseDuration - mfmsub_length=>checkPoint,"endFt_L2"
;
f4=f3 + PulseDuration;#####
f4=>SatPulse(PulseDuration);
f4=>mpulse
f4 + PulseDuration/2=>checkPoint,"startFm_L2"
```

```
f4 + PulseDuration - mfmsub_length=>checkPoint,"endFm_L2"
;
;******* Saturating Pulses - Fm_L3 **********************************
f5=c1+<178s>;#####
f51=f5#<mfmsub_length,2*mfmsub_length ..PulseDuration - mfmsub_length>;#####
f51=>mfmsub
f5 + mfmsub_length=>checkPoint,"startFt_L3"
f5 + PulseDuration - mfmsub_length=>checkPoint,"endFt_L3"
;
f6=f5 + PulseDuration;#####
f6=>SatPulse(PulseDuration);
f6=>mpulse
f6 + PulseDuration/2=>checkPoint,"startFm_L3"
f6 + PulseDuration - mfmsub_length=>checkPoint,"endFm_L3"
;
;******* Saturating Pulses - Fm_L4 **********************************
f7=c1+<238s>;#####
f71=f7#<mfmsub_length,2*mfmsub_length ..PulseDuration - mfmsub_length>;#####
f71=>mfmsub
f7 + mfmsub_length=>checkPoint,"startFt_L4"
f7 + PulseDuration - mfmsub_length=>checkPoint,"endFt_L4"
;
f8=f7 + PulseDuration;#####
f8=>SatPulse(PulseDuration);
f8=>mpulse
f8 + PulseDuration/2=>checkPoint,"startFm_L4"
f8 + PulseDuration - mfmsub_length=>checkPoint,"endFm_L4"
;
;******* Saturating Pulses - Fm_L5 **********************************
f9=c1+<298s>;#####
f91=f9#<mfmsub_length,2*mfmsub_length ..PulseDuration - mfmsub_length>;#####
f91=>mfmsub
f9 + mfmsub_length=>checkPoint,"startFt_L5"
f9 + PulseDuration - mfmsub_length=>checkPoint,"endFt_L5"
;
f10=f9 + PulseDuration;#####
f10=>SatPulse(PulseDuration);
f10=>mpulse
f10 + PulseDuration/2=>checkPoint,"startFm_L5"
f10 + PulseDuration - mfmsub_length=>checkPoint,"endFm_L5"
;
;******* Saturating Pulses - Fm_L6 **********************************
f11=c1+<358s>;#####
f111=f11#<mfmsub_length,2*mfmsub_length ..PulseDuration - mfmsub_length>;#####
f111=>mfmsub
f11 + mfmsub_length=>checkPoint,"startFt_L6"
f11 + PulseDuration - mfmsub_length=>checkPoint,"endFt_L6"
;
f12=f11 + PulseDuration;#####
f12=>SatPulse(PulseDuration);
f12=>mpulse
f12 + PulseDuration/2=>checkPoint,"startFm_L6"
f12 + PulseDuration - mfmsub_length=>checkPoint,"endFm_L6"
;
```

```
;******* Saturating Pulses - Fm_L7 **********************************
f13=c1+<418s>;#####
f131=f13#<mfmsub_length,2*mfmsub_length ..PulseDuration - mfmsub_length>;#####
f131=>mfmsub
f13 + mfmsub_length=>checkPoint,"startFt_L7"
f13 + PulseDuration - mfmsub_length=>checkPoint,"endFt_L7"
;
f14=f13 + PulseDuration;#####
f14=>SatPulse(PulseDuration);
f14=>mpulse
f14 + PulseDuration/2=>checkPoint,"startFm_L7"
f14 + PulseDuration - mfmsub_length=>checkPoint,"endFm_L7"
;
;******* Saturating Pulses - Fm_L8 **********************************
f15=c1+<478s>;#####
f151=f15#<mfmsub_length,2*mfmsub_length ..PulseDuration - mfmsub_length>;#####
f151=>mfmsub
f15 + mfmsub_length=>checkPoint,"startFt_L8"
f15 + PulseDuration - mfmsub_length=>checkPoint,"endFt_L8"
;
f16=f15 + PulseDuration;#####
f16=>SatPulse(PulseDuration);
f16=>mpulse
f16 + PulseDuration/2=>checkPoint,"startFm_L8"
f16 + PulseDuration - mfmsub_length=>checkPoint,"endFm_L8"
;
;******* Saturating Pulses - Fm_L9 **********************************
f17=c1+<538s>;#####
f171=f17#<mfmsub_length,2*mfmsub_length ..PulseDuration - mfmsub_length>;#####
f171=>mfmsub
f17 + mfmsub_length=>checkPoint,"startFt_L9"
f17 + PulseDuration - mfmsub_length=>checkPoint,"endFt_L9"
;
f18=f17 + PulseDuration;#####
f18=>SatPulse(PulseDuration);
f18=>mpulse
f18 + PulseDuration/2=>checkPoint,"startFm_L9"
f18 + PulseDuration - mfmsub_length=>checkPoint,"endFm_L9"
;
;******* Saturating Pulses - Fm_L10 **********************************
f19=c1+<598s>;#####
f191=f19#<mfmsub_length,2*mfmsub_length ..PulseDuration - mfmsub_length>;#####
f191=>mfmsub
f19 + mfmsub_length=>checkPoint,"startFt_L10"
f19 + PulseDuration - mfmsub_length=>checkPoint,"endFt_L10"
;
f20=f19 + PulseDuration;#####
f20=>SatPulse(PulseDuration);
f20=>mpulse
f20 + PulseDuration/2=>checkPoint,"startFm_L10"
f20 + PulseDuration - mfmsub_length=>checkPoint,"endFm_L10"
;
;******* Saturating Pulses - Fm_L11 **********************************
f21=c1+<658s>;#####
```

```
f211=f21#<mfmsub_length,2*mfmsub_length ..PulseDuration - mfmsub_length>;#####
f211=>mfmsub
f21 + mfmsub_length=>checkPoint,"startFt_L11"
f21 + PulseDuration - mfmsub_length=>checkPoint,"endFt_L11"
;
f22=f21 + PulseDuration;#####
f22=>SatPulse(PulseDuration);
f22=>mpulse
f22 + PulseDuration/2=>checkPoint,"startFm_L11"
f22 + PulseDuration - mfmsub_length=>checkPoint,"endFm_L11"
;
;******* Saturating Pulses - Fm_L12 **********************************
f23=c1+<718s>;#####
f231=f23#<mfmsub_length,2*mfmsub_length ..PulseDuration - mfmsub_length>;#####
f231=>mfmsub
f23 + mfmsub_length=>checkPoint,"startFt_L12"
f23 + PulseDuration - mfmsub_length=>checkPoint,"endFt_L12"
;
f24=f23 + PulseDuration;#####
f24=>SatPulse(PulseDuration);
f24=>mpulse
f24 + PulseDuration/2=>checkPoint,"startFm_L12"
f24 + PulseDuration - mfmsub_length=>checkPoint,"endFm_L12"
;
;******* Saturating Pulses - Fm_L13 **********************************
f25=c1+<778s>;#####
f251=f25#<mfmsub_length,2*mfmsub_length ..PulseDuration - mfmsub_length>;#####
f251=>mfmsub
f25 + mfmsub_length=>checkPoint,"startFt_L13"
f25 + PulseDuration - mfmsub_length=>checkPoint,"endFt_L13"
;
f26=f25 + PulseDuration;#####
f26=>SatPulse(PulseDuration);
f26=>mpulse
f26 + PulseDuration/2=>checkPoint,"startFm_L13"
f26 + PulseDuration - mfmsub_length=>checkPoint,"endFm_L13"
;
;******* Saturating Pulses - Fm_L14 **********************************
f27=c1+<838s>;#####
f271=f27#<mfmsub_length,2*mfmsub_length ..PulseDuration - mfmsub_length>;#####
f271=>mfmsub
f27 + mfmsub_length=>checkPoint,"startFt_L14"
f27 + PulseDuration - mfmsub_length=>checkPoint,"endFt_L14"
;
f28=f27 + PulseDuration;#####
f28=>SatPulse(PulseDuration);
f28=>mpulse
f28 + PulseDuration/2=>checkPoint,"startFm_L14"
f28 + PulseDuration - mfmsub_length=>checkPoint,"endFm_L14"
;
;******* Saturating Pulses - Fm_L15 **********************************
f29=c1+<898s>;#####
f291=f29#<mfmsub_length,2*mfmsub_length ..PulseDuration - mfmsub_length>;#####
f291=>mfmsub
```

```
f29 + mfmsub_length=>checkPoint,"startFt_Lss"
f29 + PulseDuration - mfmsub_length=>checkPoint,"endFt_Lss"
;
f30=f29 + PulseDuration;#####
f30=>SatPulse(PulseDuration);
f30=>mpulse
f30 + PulseDuration/2=>checkPoint,"startFm_Lss"
f30 + PulseDuration - mfmsub_length=>checkPoint,"endFm_Lss"
;
;-------------------------------------------------------------------------------------------------------
;*** Dark relaxation after actinic light period ****************************************
;-------------------------------------------------------------------------------------------------------
DarkRelaxation2=300s;#####
h=c1 + ALPeriod +mfmsub_length;#####
;
;******** Relaxation measurement*************************************
;
<h, h+DarkRelaxation2/10..h+DarkRelaxation2>=>mfmsub
;
;******* Saturating Pulses - Fm_D1 **********************************
g1=h + <98s>;#####
g11=g1#<mfmsub_length,2*mfmsub_length ..PulseDuration - mfmsub_length>;#####
g11=>mfmsub
g1 + mfmsub_length=>checkPoint,"startFt_D1"
g1 + PulseDuration - mfmsub_length=>checkPoint,"endFt_D1"
;
g2=g1 + PulseDuration;#####
g2=>SatPulse(PulseDuration)
g2=>act1(PulseDuration)
g2=>act2(PulseDuration)
g2=>mpulse
g2 + PulseDuration/2=>checkPoint,"startFm_D1"
g2 + PulseDuration - mfmsub_length=>checkPoint,"endFm_D1"
;
;******* Saturating Pulses - Fm_D2 **********************************
g3=h + <198s>;#####
g31=g3#<mfmsub_length,2*mfmsub_length ..PulseDuration - mfmsub_length>;#####
g31=>mfmsub
g3 + mfmsub_length=>checkPoint,"startFt_D2"
g3 + PulseDuration - mfmsub_length=>checkPoint, "endFt_D2"
;
g4=g3 + PulseDuration;#####
g4=>SatPulse(PulseDuration)
g4=>act1(PulseDuration)
g4=>act2(PulseDuration)
g4=>mpulse
g4 + PulseDuration/2=>checkPoint,"startFm_D2"
g4 + PulseDuration - mfmsub_length=>checkPoint,"endFm_D2"
;
;******* Saturating Pulses - Fm_D3 **********************************
g5=h+<298s>;#####
g51=g5#<mfmsub_length,2*mfmsub_length ..PulseDuration - mfmsub_length>;#####
g51=>mfmsub
g5 + mfmsub_length=>checkPoint,"startFt_D3"
```

```
g5 + PulseDuration - mfmsub_length=>checkPoint,"endFt_D3"
;
g6=g5 + PulseDuration;#####
g6=>SatPulse(PulseDuration)
g6=>act1(PulseDuration)
g6=>act2(PulseDuration)
g6=>mpulse
g6 + PulseDuration/2=>checkPoint,"startFm_D3"
g6 + PulseDuration - mfmsub_length=>checkPoint,"endFm_D3"
;
;END ************************************************************
```

B.3 The chlorophyll fluorescence measuring P3 protocol (eight minutes of actinic light followed by three minutes dark relaxation period).

```
TS=40ms
; Quenching protocol with Actinic1 & Actinic2 8mins + dark 3 mins
; Protocol: Quenching-without-FR1-Lucam.p modified by Keng
;version Nove0ber 30, 2012
;high-resolution CCD
;
include default.inc  ;Includes standard options, do not remove it !
include light.inc  ;Includes standard options, do not remove it !
Shutter=0
Sensitivity=50
Act1=100
Act2=100
Super=100

;-------------------------------------------------------------------------------------------------
;*** Fo Measurement ************************************************************
;-------------------------------------------------------------------------------------------------
F0duration = 5s
F0period = 1s
<0,F0period..F0duration>=>mfmsub
;
;Fo definition
<0s>=>checkPoint,"startFo"
<F0duration - F0period>=>checkPoint,"endFo"
;
;-------------------------------------------------------------------------------------------------
;*** Saturating Pulse & Fm Measurement ***************************************************
;-------------------------------------------------------------------------------------------------
PulseDuration=800ms;#####
a1=F0duration + 2*mfmsub_length;#####
;
<a1>=>SatPulse(PulseDuration)
<a1>=>act1(PulseDuration)
<a1>=>act2(PulseDuration)
;
<a1>=>mpulse
;
;Fm definition
<a1 + mfmsub_length>=>checkPoint,"startFm"
<a1 + PulseDuration - mfmsub_length>=>checkPoint,"endFm"
;
;Visual frame definition                                    ## Image shown in pre-processing window
<a1 + PulseDuration/2 + TS>=>checkPoint,"timeVisual"
;-------------------------------------------------------------------------------------------------
;******* Dark Relaxation Measurement *********************************************
;-------------------------------------------------------------------------------------------------
DarkRelaxation1=17s;#####
b1= a1 + PulseDuration + 2*mfmsub_length;#####
b2=2s;#####
<b1, b1 + 200ms .. b1 + b2>=>mfmsub
<b1 + b2 + 200ms, b1 + 2*b2 .. b1+DarkRelaxation1>=>mfmsub
;
;-------------------------------------------------------------------------------------------------
```

```
;******* Kautsky Effect Measurement ********************************************
;-------------------------------------------------------------------------------------------------
;
;******* Actinic light Exposure ***********************************
ALPeriod=450s;#####
c1= a1 + PulseDuration + DarkRelaxation1 + mfmsub_length;#####
<c1>=>act1(ALPeriod)
<c1>=>act2(ALPeriod)
;
;*******Fast Kautsky kinetics**************************************
c2=3s;#####
;
<c1 + TS, c1 + TS + mfmsub_length.. c1+c2>=>mfmsub;
;
;*******Slow Kautsky kinetics**************************************
c3=4s;#####                                          period of slow measurement
;
<c1 + c2 + c3/10, c1 + c2+ c3/5, c1 + c2 + c3/2>=>mfmsub
;
<c1 + c2 + c3, c1 + c2 + c3 +12s .. c1 + ALPeriod>=>mfmsub;
;
;Fp definition
<c1>=>checkPoint,"startFp"
<c1 + c2 + c3>=>checkPoint,"endFp"
;
;-------------------------------------------------------------------------------------------------
;******* Saturating Pulses - Fm' Quenching Analysis ************************************
;-------------------------------------------------------------------------------------------------
;
;******* Saturating Pulses - Fm_L1 *********************************
f1=c1+<18s>;#####
f11=f1#<mfmsub_length,2*mfmsub_length ..PulseDuration - mfmsub_length>;#####
f11=>mfmsub
f1 + mfmsub_length=>checkPoint,"startFt_L1"
f1 + PulseDuration - mfmsub_length=>checkPoint,"endFt_L1"
;
f2=f1 + PulseDuration;#####
f2=>SatPulse(PulseDuration);
f2=>mpulse
f2+PulseDuration/2=>checkPoint,"startFm_L1"
f2 + PulseDuration - mfmsub_length=>checkPoint,"endFm_L1"
;
;******* Saturating Pulses - Fm_L2 *********************************
f3=c1+<38s>;#####
f31=f3#<mfmsub_length,2*mfmsub_length ..PulseDuration - mfmsub_length>;#####
f31=>mfmsub
f3 + mfmsub_length=>checkPoint,"startFt_L2"
f3 + PulseDuration - mfmsub_length=>checkPoint,"endFt_L2"
;
f4=f3 + PulseDuration;#####
f4=>SatPulse(PulseDuration);
f4=>mpulse
f4 + PulseDuration/2=>checkPoint,"startFm_L2"
```

```
f4 + PulseDuration - mfmsub_length=>checkPoint,"endFm_L2"
;
;******* Saturating Pulses - Fm_L3 **********************************
f5=c1+<58s>;#####
f51=f5#<mfmsub_length,2*mfmsub_length ..PulseDuration - mfmsub_length>;#####
f51=>mfmsub
f5 + mfmsub_length=>checkPoint,"startFt_L3"
f5 + PulseDuration - mfmsub_length=>checkPoint,"endFt_L3"
;
f6=f5 + PulseDuration;#####
f6=>SatPulse(PulseDuration);
f6=>mpulse
f6 + PulseDuration/2=>checkPoint,"startFm_L3"
f6 + PulseDuration - mfmsub_length=>checkPoint,"endFm_L3"
;
;******* Saturating Pulses - Fm_L4 **********************************
f7=c1+<78s>;#####
f71=f7#<mfmsub_length,2*mfmsub_length ..PulseDuration - mfmsub_length>;#####
f71=>mfmsub
f7 + mfmsub_length=>checkPoint,"startFt_L4"
f7 + PulseDuration - mfmsub_length=>checkPoint,"endFt_L4"
;
f8=f7 + PulseDuration;#####
f8=>SatPulse(PulseDuration);
f8=>mpulse
f8 + PulseDuration/2=>checkPoint,"startFm_L4"
f8 + PulseDuration - mfmsub_length=>checkPoint,"endFm_L4"
;
;******* Saturating Pulses - Fm_L5 **********************************
f9=c1+<98s>;#####
f91=f9#<mfmsub_length,2*mfmsub_length ..PulseDuration - mfmsub_length>;#####
f91=>mfmsub
f9 + mfmsub_length=>checkPoint,"startFt_L5"
f9 + PulseDuration - mfmsub_length=>checkPoint,"endFt_L5"
;
f10=f9 + PulseDuration;#####
f10=>SatPulse(PulseDuration);
f10=>mpulse
f10 + PulseDuration/2=>checkPoint,"startFm_L5"
f10 + PulseDuration - mfmsub_length=>checkPoint,"endFm_L5"
;
;******* Saturating Pulses - Fm_L6 **********************************
f11=c1+<118s>;#####
f111=f11#<mfmsub_length,2*mfmsub_length ..PulseDuration - mfmsub_length>;#####
f111=>mfmsub
f11 + mfmsub_length=>checkPoint,"startFt_L6"
f11 + PulseDuration - mfmsub_length=>checkPoint,"endFt_L6"
;
f12=f11 + PulseDuration;#####
f12=>SatPulse(PulseDuration);
f12=>mpulse
f12 + PulseDuration/2=>checkPoint,"startFm_L6"
f12 + PulseDuration - mfmsub_length=>checkPoint,"endFm_L6"
```

```
;
;******* Saturating Pulses - Fm_L7 **********************************
f13=c1+<148s>;#####
f131=f13#<mfmsub_length,2*mfmsub_length ..PulseDuration - mfmsub_length>;#####
f131=>mfmsub
f13 + mfmsub_length=>checkPoint,"startFt_L7"
f13 + PulseDuration - mfmsub_length=>checkPoint,"endFt_L7"
;
f14=f13 + PulseDuration;#####
f14=>SatPulse(PulseDuration);
f14=>mpulse
f14 + PulseDuration/2=>checkPoint,"startFm_L7"
f14 + PulseDuration - mfmsub_length=>checkPoint,"endFm_L7"
;
;******* Saturating Pulses - Fm_L8 **********************************
f15=c1+<178s>;#####
f151=f15#<mfmsub_length,2*mfmsub_length ..PulseDuration - mfmsub_length>;#####
f151=>mfmsub
f15 + mfmsub_length=>checkPoint,"startFt_L8"
f15 + PulseDuration - mfmsub_length=>checkPoint,"endFt_L8"
;f16=f15 + PulseDuration;#####
f16=>SatPulse(PulseDuration);
f16=>mpulse
f16 + PulseDuration/2=>checkPoint,"startFm_L8"
f16 + PulseDuration - mfmsub_length=>checkPoint,"endFm_L8"
;
;******* Saturating Pulses - Fm_L9 **********************************
f17=c1+<238s>;#####
f171=f17#<mfmsub_length,2*mfmsub_length ..PulseDuration - mfmsub_length>;#####
f171=>mfmsub
f17 + mfmsub_length=>checkPoint,"startFt_L9"
f17 + PulseDuration - mfmsub_length=>checkPoint,"endFt_L9"
;
f18=f17 + PulseDuration;#####
f18=>SatPulse(PulseDuration);
f18=>mpulse
f18 + PulseDuration/2=>checkPoint,"startFm_L9"
f18 + PulseDuration - mfmsub_length=>checkPoint,"endFm_L9"
;
;******* Saturating Pulses - Fm_L10 **********************************
f19=c1+<298s>;#####
f191=f19#<mfmsub_length,2*mfmsub_length ..PulseDuration - mfmsub_length>;#####
f191=>mfmsub
f19 + mfmsub_length=>checkPoint,"startFt_L10"
f19 + PulseDuration - mfmsub_length=>checkPoint,"endFt_L10"
;
f20=f19 + PulseDuration;#####
f20=>SatPulse(PulseDuration);
f20=>mpulse
f20 + PulseDuration/2=>checkPoint,"startFm_L10"
f20 + PulseDuration - mfmsub_length=>checkPoint,"endFm_L10"
;
;******* Saturating Pulses - Fm_L11 **********************************
```

```
f21=c1+<358s>;#####
f211=f21#<mfmsub_length,2*mfmsub_length ..PulseDuration - mfmsub_length>;#####
f211=>mfmsub
f21 + mfmsub_length=>checkPoint,"startFt_L11"
f21 + PulseDuration - mfmsub_length=>checkPoint,"endFt_L11"
;
f22=f21 + PulseDuration;#####
f22=>SatPulse(PulseDuration);
f22=>mpulse
f22 + PulseDuration/2=>checkPoint,"startFm_L11"
f22 + PulseDuration - mfmsub_length=>checkPoint,"endFm_L11"
;
;******* Saturating Pulses - Fm_L12 **********************************
f23=c1+<448s>;#####
f231=f23#<mfmsub_length,2*mfmsub_length ..PulseDuration - mfmsub_length>;#####
f231=>mfmsub
f23 + mfmsub_length=>checkPoint,"startFt_Lss"
f23 + PulseDuration - mfmsub_length=>checkPoint,"endFt_Lss"
;
f24=f23 + PulseDuration;#####
f24=>SatPulse(PulseDuration);
f24=>mpulse
f24 + PulseDuration/2=>checkPoint,"startFm_Lss"
f24 + PulseDuration - mfmsub_length=>checkPoint,"endFm_Lss"
;
;-------------------------------------------------------------------------------------------------------
;*** Dark relaxation after actinic light period ****************************************
;-------------------------------------------------------------------------------------------------------
DarkRelaxation2=180s;#####
h=c1 + ALPeriod +mfmsub_length;#####
;
;******** Relaxation measurement*************************************
;
<h, h+DarkRelaxation2/10..h+DarkRelaxation2>=>mfmsub
;
;******* Saturating Pulses - Fm_D1 **********************************
g1=h + <28s>;#####
g11=g1#<mfmsub_length,2*mfmsub_length ..PulseDuration - mfmsub_length>;#####
g11=>mfmsub
g1 + mfmsub_length=>checkPoint,"startFt_D1"
g1 + PulseDuration - mfmsub_length=>checkPoint,"endFt_D1"
;g2=g1 + PulseDuration;#####
g2=>SatPulse(PulseDuration)
g2=>act1(PulseDuration)
g2=>act2(PulseDuration)
g2=>mpulse
g2 + PulseDuration/2=>checkPoint,"startFm_D1"
g2 + PulseDuration - mfmsub_length=>checkPoint,"endFm_D1"
;
;******* Saturating Pulses - Fm_D2 **********************************
g3=h + <58s>;#####
g31=g3#<mfmsub_length,2*mfmsub_length ..PulseDuration - mfmsub_length>;#####
g31=>mfmsub
```

```
g3 + mfmsub_length=>checkPoint,"startFt_D2"
g3 + PulseDuration - mfmsub_length=>checkPoint, "endFt_D2"
;
g4=g3 + PulseDuration;#####
g4=>SatPulse(PulseDuration)
g4=>act1(PulseDuration)
g4=>act2(PulseDuration)
g4=>mpulse
g4 + PulseDuration/2=>checkPoint,"startFm_D2"
g4 + PulseDuration - mfmsub_length=>checkPoint,"endFm_D2"
;
;******* Saturating Pulses - Fm_D3 **********************************
g5=h+<118s>;#####
g51=g5#<mfmsub_length,2*mfmsub_length ..PulseDuration - mfmsub_length>;#####
g51=>mfmsub
g5 + mfmsub_length=>checkPoint,"startFt_D3"
g5 + PulseDuration - mfmsub_length=>checkPoint,"endFt_D3"
;
g6=g5 + PulseDuration;#####
g6=>SatPulse(PulseDuration)
g6=>act1(PulseDuration)
g6=>act2(PulseDuration)
g6=>mpulse
g6 + PulseDuration/2=>checkPoint,"startFm_D3"
g6 + PulseDuration - mfmsub_length=>checkPoint,"endFm_D3"
;
;******* Saturating Pulses - Fm_D4 **********************************
g7=h+<178s>;#####
g71=g5#<mfmsub_length,2*mfmsub_length ..PulseDuration - mfmsub_length>;#####
g71=>mfmsub
g7 + mfmsub_length=>checkPoint,"startFt_D4"
g7 + PulseDuration - mfmsub_length=>checkPoint,"endFt_D4"
;
g8=g7 + PulseDuration;#####
g8=>SatPulse(PulseDuration)
g8=>act1(PulseDuration)
g8=>act2(PulseDuration)
g8=>mpulse
g8 + PulseDuration/2=>checkPoint,"startFm_D4"
g8 + PulseDuration - mfmsub_length=>checkPoint,"endFm_D4"
;
;END ***************************************************************
-----------------------------------------------------
```

B.4 Supplementary Figure for Chapter 3

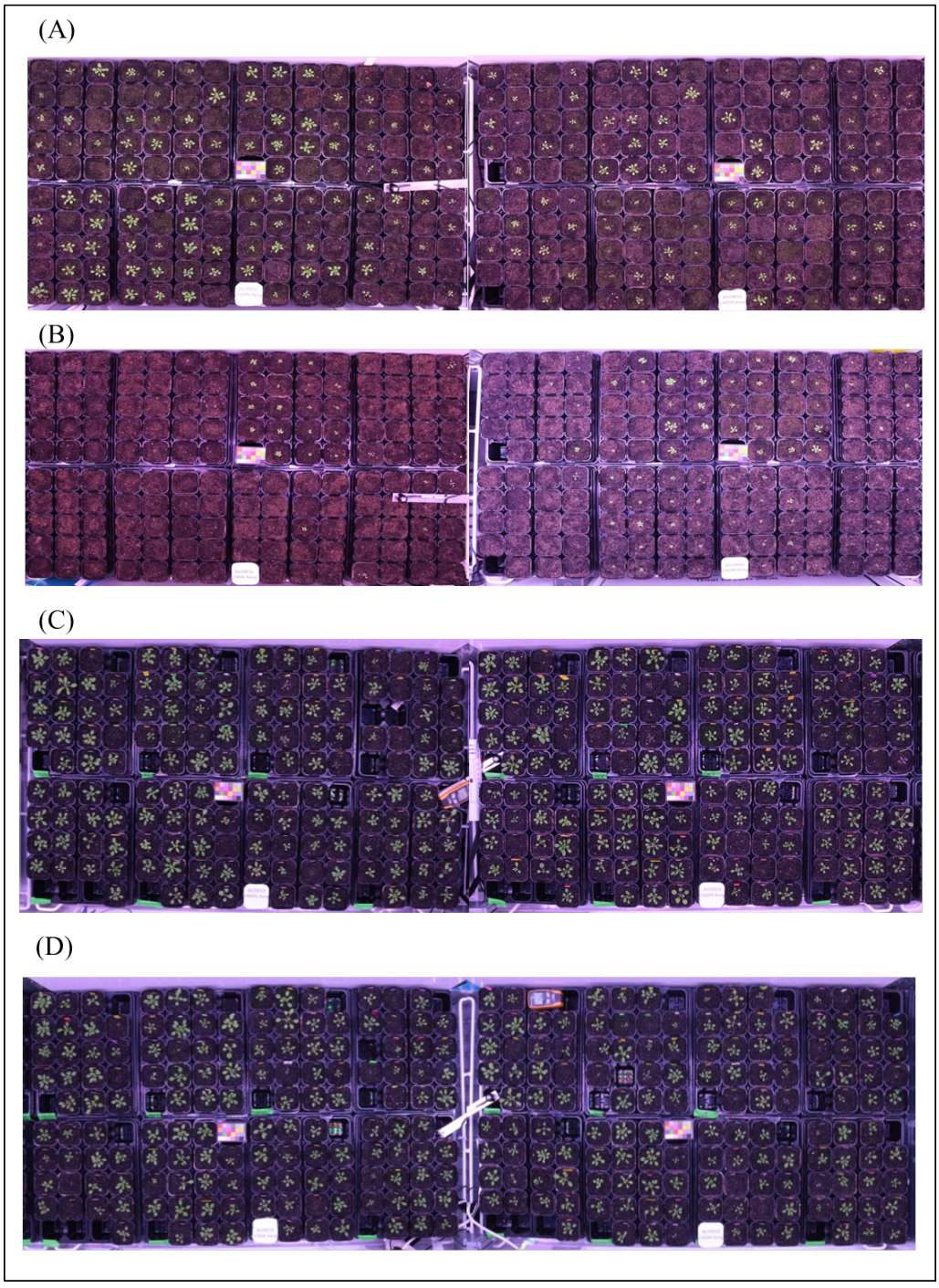

Figure B.1 – An overview snapshot of *Arabidopsis* natural accessions grown under Coastal (A), Inland (B) simulated spring season, and Coastal (C), Inland (D) simulated autumn season. The percentage of survival plants was higher under Coastal condition in both spring and autumn. However, when comparing the overall survival rate between spring and autumn, plants grow under typical autumn season has a higher percentage of survival.

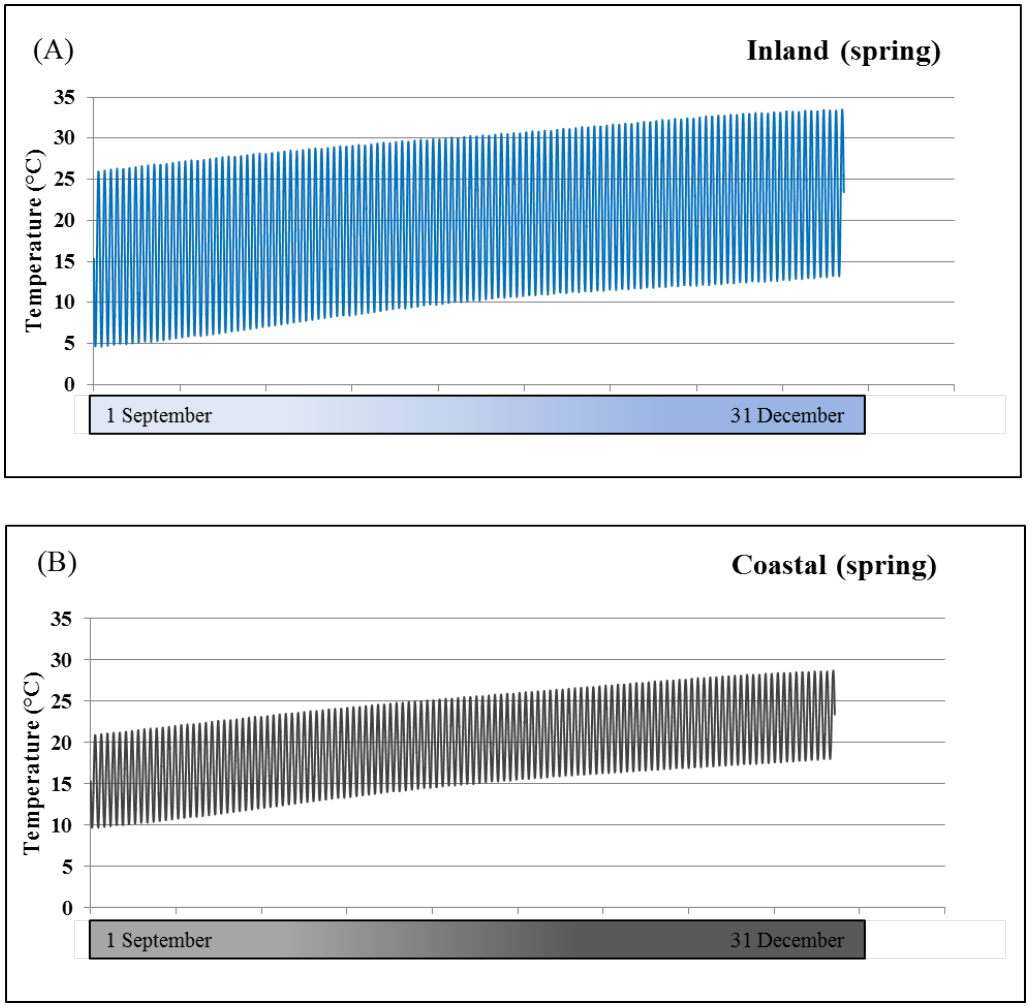

Figure B.2 – Controlled temperature plot using SolarCal software in typical spring season (program started on 1 September and end on 31 December). (A) represents seasonal change in temperature of Inland condition, and (B) represents seasonal change in temperature of Coastal condition. Under Coastal condition, the differences in temperature during the day was around 10 °C, in comparison to 15 °C difference under Inland condition. Therefore, in the Inland condition, plants were experiencing low temperature at seedling stage (around 5 °C), while it was warmer in the Coastal condition (around 10 °C).

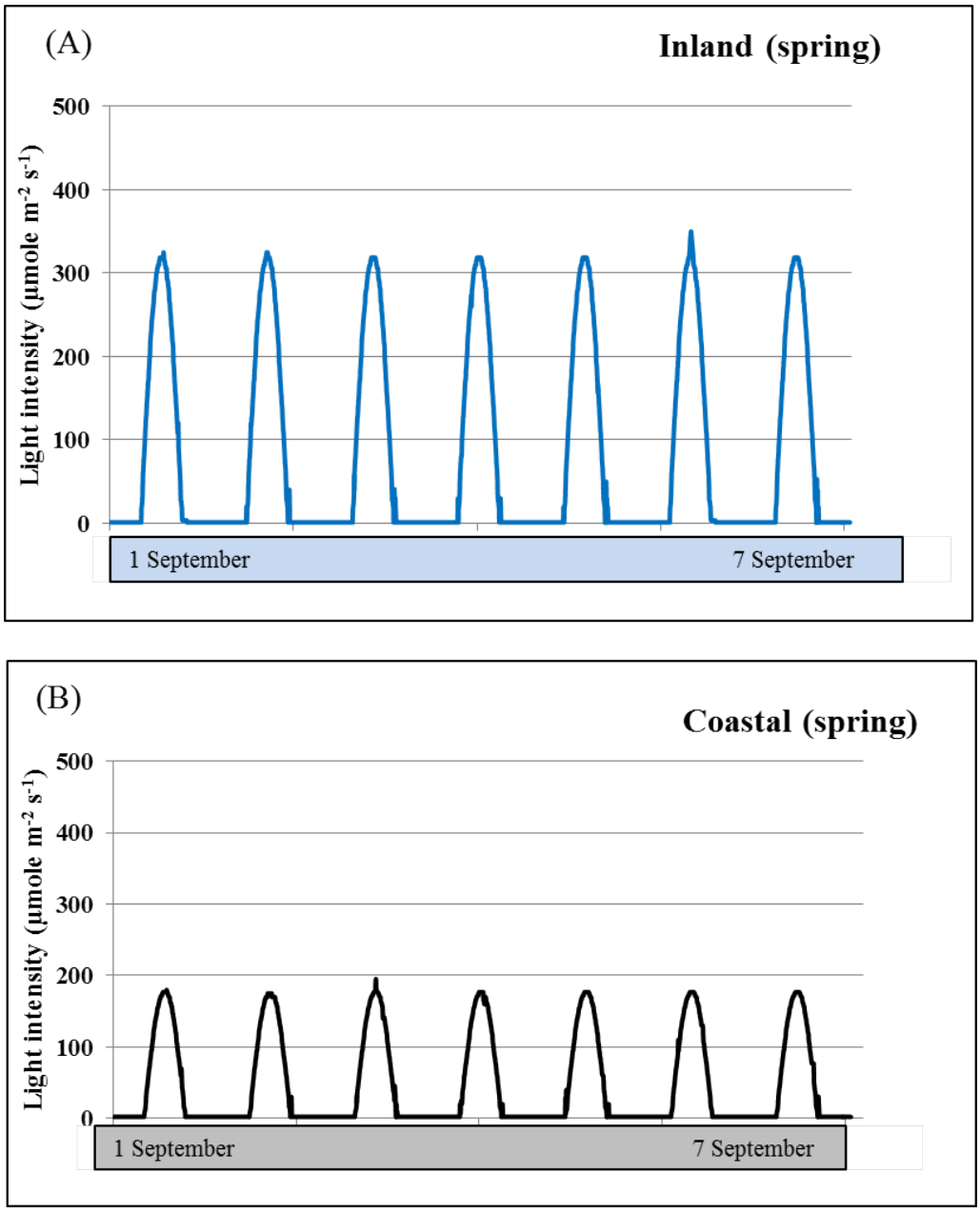

Figure B.3 – Controlled light intensity graphs using SolarCal software in typical spring season during the first seven day period of the experiment. (A) represents light intensity of Inland condition (maximum at 350 μmol m^{-2} s^{-1}), and (B) represents light intensity of Coastal condition (maximum at 160 μmol m^{-2} s^{-1}).

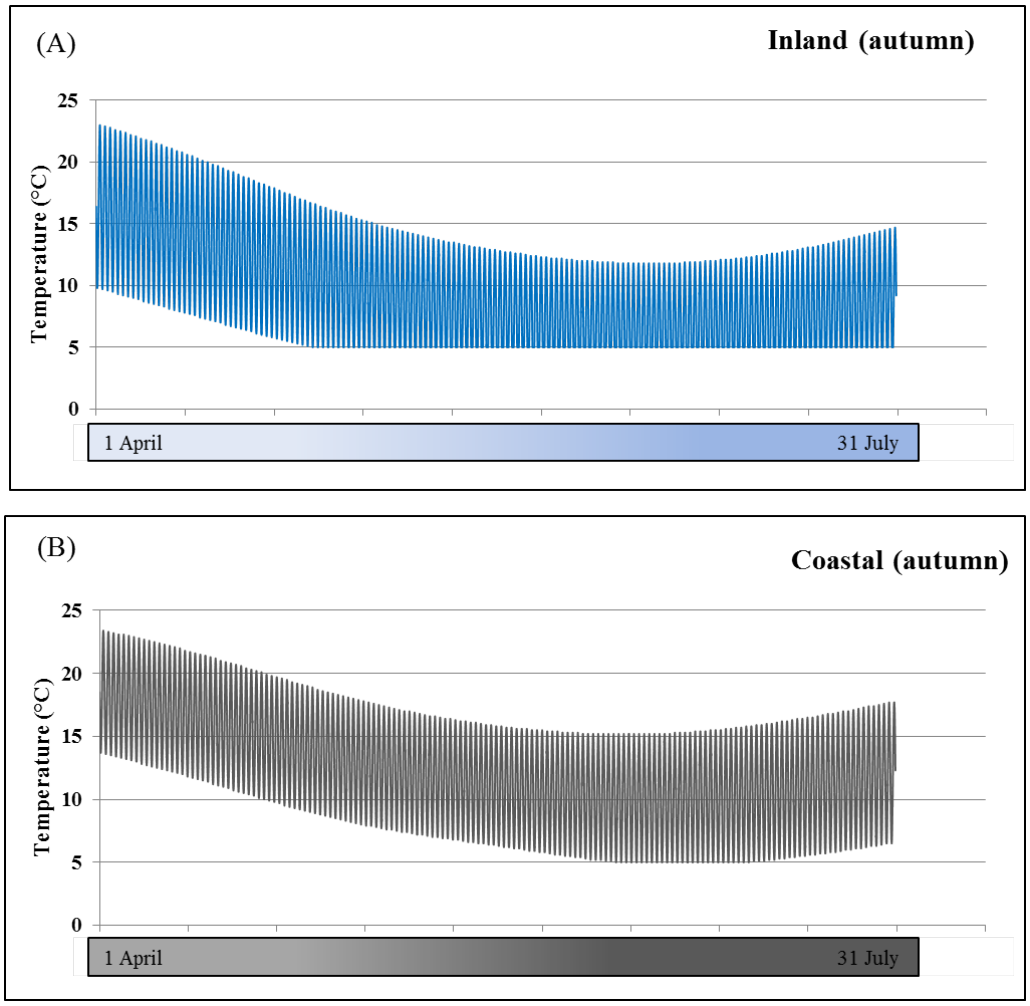

Figure B.4 – Controlled temperature plot using SolarCal software in typical autumn season (program started on 1 April and end on 31 July). (A) represents seasonal change in temperature of Inland condition, and (B) represents seasonal change in temperature of Coastal condition. Under Coastal condition, the differences in temperature during the day is around 10 °C, while it was around 15 °C difference under Inland condition. Temperature reached 5 °C after 30 days in the Inland condition, while it takes around 60 days for Coastal condition.

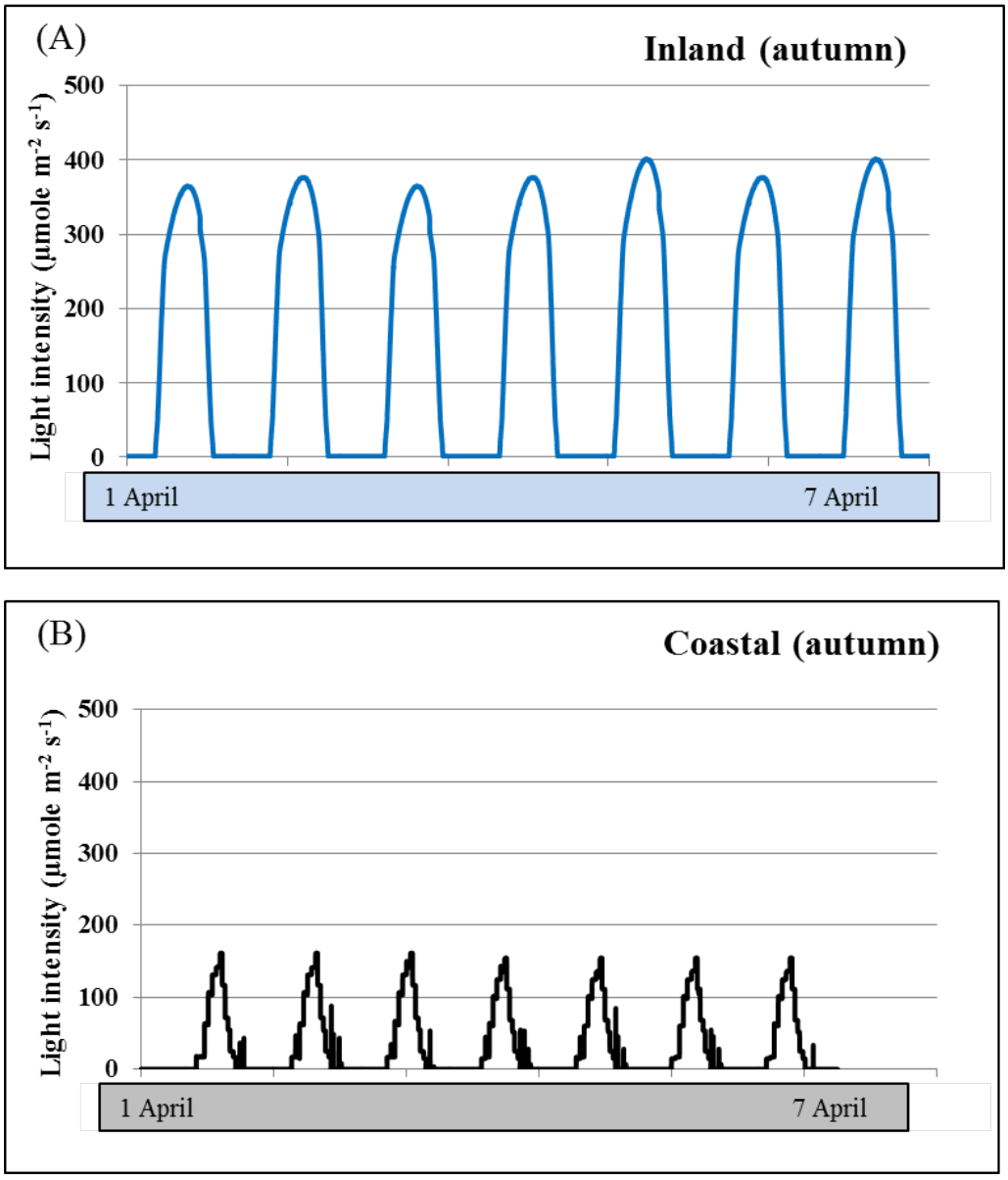

Figure B.5 – Controlled light intensity graphs using SolarCal software in typical autumn season during the first seven day period. (A) represents light intensity of Inland condition (maximum at 400 μmol m^{-2} s^{-1}), and (B) represents light intensity of Coastal condition (maximum at 160 μmol m^{-2} s^{-1}).

Appendix C

Supplementary Data for Chapter 4

Table C.1 – Summary of QTL and candidate genes list of the Cvi-0 x L*er* RIXs population from across five growing conditions.

QTL	Chr	Markers	Position	Candidate genes		Description
				AGI	Location	
RIX-QTL1-1	1	CRY2	1.18	ERF14: AT1G04370	1175177-1175578	encodes a member of the ERF (ethylene response factor) subfamily B-3 of ERF/AP2 transcription factor family.
				AT1G04380	k1176921-117840	Encodes a protein similar to a 2-oxoglutarate-dependent dioxygenase.Involved in oxidation-reduction process
				AT1G04390	1179363-118370	BTB/POZ domain-containing protein. Involved in biological process
				CRY2:AT1G04400	1185550-1188517	Blue light receptor mediating blue-light regulated cotyledon expansion and flowering time. Involved in blue-light induced stomatal opening.
				AT1G04410	k1189078-1191412	Involved in carbohydrate metabolic process, malate metabolic process, response to cadmium ion, response to cytokinin, response to salt stress, response to zinc ion, tricarboxylic acid cycle
				AT1G04420	1191608-1193884	Involved in oxidation-reduction process.
		AXR-1	1.5	AT1G05160	1487378-1490947	Involved in brassinosteroid biosynthetic process, brassinosteroid homeostasis, gibberellin biosynthetic process, multicellular organismal development, oxidation-reduction process, sterol metabolic process
				AXR1: AT1G05180	1498114-1501824k	Response to cytokinin. Involved in DNA repair, auxin-activated signaling pathway, leaf morphogenesis
				emb2394: AT1G05190	1502344-1503830	Involved in translation, embryo development ending in seed dormancy
				GLR3.4: AT1G05200	k1504960-1509152	Involved in calcium ion transport, response to light stimulus
				AT1G05210	1510404-1511683k	Unknown
		HH.335C	3.11	PHYA: AT1G09570	3095256-3100357	Light-labile cytoplasmic red/far-red light photoreceptor involved in the regulation of photomorphogenesis.

Continued on next page.

Table C.1 – continued from previous page

QTL	Chr	Markers	Position	Candidate genes		Description
				AGI	Location	
RIX-QTL1-2	1	EC.66C	5.96	UBP1B: AT1G17370	5951542-5955037	Involved in stress granule formation and mRNA processing
				JAZ5: AT1G17380	5955488-5957212	Jasmonate-zim-domain protein 5 (JAZ5); Involved in defense response, negative regulation of nucleic acid-templated transcription, regulation of defense response
		GD.86L	6.53	AT1G18900	6528984-6532614	Pentatricopeptide repeat (PPR) superfamily protein
				AT1G18910	k6532559-6538145k	Zinc ion binding;zinc ion binding; function in: zinc ion binding
		GH.160L	7.85	AT1G22190	7835782-7837288	The gene encodes a putative transcription factor belongings to the abiotic stress-associated DREB A-6 clade.
				AT1G22200	7837591-7840788	Endoplasmic reticulum vesicle transporter protein; function in: molecularfunction unknown
				TPPC: AT1G22210	7841518-7844056	Haloacid dehalogenase-like hydrolase (HAD) superfamily protein; involved in: trehalose biosynthetic process, metabolic process
				AT1G22230	7849861-7851122	Unknown protein; located in: chloroplast
RIX-QTL2-1	2	FD.85C	9.42	AT2G22125	9406263-9414518	Encodes a protein involved in cell elongation in root and anther filaments. Mutants have greater cell volumes in root tissues and have additive phenotypes with other cell expansion
				EME1B: AT2G22140	9414839-9418668	Forms a complex with MUS81 that functions as endonuclease in DNA recombination and repair processes.
				PLAT2: AT2G22170	9426849-9427817	Lipase/lipooxygenase, PLAT/LH2 family protein; functions in: molecular function unknown
				TPPE: AT2G22190	9433765-9436544	Involved in trehalose biosynthetic process
		GB.150L	9.97	AT2G23420	9971701-9975192	Functions in nicotinate phosphoribosyltransferase activity;involved in: pyridine nucleotide biosynthetic process

Continued on next page.

Table C.1 – continued from previous page

QTL	Chr	Markers	Position	Candidate genes		Description
				AGI	Location	
				ICK1:AT2G23430	9976746-9978021	Encodes a cyclin-dependent kinase inhibitor protein that functions as a negative regulator of cell division and promoter of endoreduplication.Involved in lateral root morphogenesis, leaf development.
				AT2G23440	9979405-9979819	Unknown function
				AT2G23450	k9988754-9991695	Protein kinase superfamily protein
RIX-QTL2-2	2	MSAT2.22	19.63	CRR6: AT2G47910	19614698-19615769	Encodes a chloroplast thylakoid membrane protein. Required for the assembly/accumulation of the NAD(P)H dehydrogenase complex of the photosynthetic electron transport chain.
				AT2G47960	19625614-19629183	Unknown function
				AT2G47970	19629474-19631138	Unknown function
RIX-QTL3-1	3	DF.77C	0.25	AT3G01650	k242011-245268	Involved in auxin metabolic process, cytokinin metabolic process, negative regulationof response to water deprivation
				AT3G01710	259639-261840	Unknown function
		GB.120C	1.35	ZDS: AT3G04870	1342608-1346387	Involved in the biosynthesis of carotenes and xanthophylls, reduces zeta-carotene to lycopene.
				DRT102: AT3G04880	1346273-1347377k	Involved in DNA repair, carbohydrate metabolic process, photoreactive repair, response to UV, response to cold
				AT3G04890	1347646-1349202	Unknown function
				AT3G04910	1354742-1358160	Serine/threonine protein kinase, whose transcription is regulated by circadian rhythm.
RIX-QTL3-2	3	GH.226C	7.38	PSBTN: AT3G21055	7376635-7377186	Encodes photosystem II 5 kD protein subunit PSII-T. Involved in photosynthesis
				NADK1: AT3G21070	7380191-7383980	Involved in NAD metabolic process, NADP biosynthetic process, phosphorylation, pyridine nucleotide biosynthetic process
		GC.83C	8.34	LSH4: AT3G23290	8326825-8328132	LIGHT SENSITIVE HYPOCOTYLS 4 (LSH4);
				AT3G23300	8333025-8336146	Unknown function
				AT3G23330	8347200-8349347	Tetratricopeptide repeat (TPR)-like superfamily protein

Continued on next page.

Table C.1 – continued from previous page

QTL	Chr	Markers	Position	Candidate genes		Description
				AGI	Location	
		GD.318C	8.96	AT3G24530	8945425-8947938	Involved in protein metabolic process
				AT3G24570	8966521-8968657	Unknown function
				AT3G24570	8966642-8968640	Unknown function
				AT3G24590	8970672-8972168	Encodes a signal peptidase Plsp1, involved in protein maturation, proteolysis, signal peptide processing, thylakoid membrane organization
		AD.92L	9.8	GAPA: AT3G26650	9795071-9797045	Encodes one of the two subunits forming the photosynthetic glyceraldehyde-3-phosphate dehydrogenase (GAPDH)
				LBD24: AT3G26660	9797129-9797620	Unknown function
				AT3G26680	9801214-9803792	Involved in a SNM-dependent recombinational repair process of oxidatively induced DNA damage.
				CCB1: AT3G26710	9813371-9814750	Unknown function, involved in cytochrome b6f complex assembly
		BF.148C	10.6	AT3G28320	10581704-10583000	Protein of unknown function (DUF677)
RIX-QTL3-3	3	HH.440L	15.11	AT3G43140	k15112431-15112845	Transposable element gene
		BF.128C	15.75	AT3G43890	15741468-15743453	Cysteine/Histidine-rich C1 domain family protein; functions in: zinc ion binding; involved in: biological process unknown
				DCL3: AT3G43920	15753548-15760859	Involved in RNA processing, defense response
				AT3G43930	15760897-15763330	Unknown function
		HH.117C	16.57	AT3G45210	16557273-16557970	Protein of unknown function, DUF584
				APAP1: AT3G45230	16569051-16569827	Encodes the arabinogalactan protein core of plant cell wall proteoglycan that contains arabinogalactan and cell wall matrix glycan pectin and/or xylan domains.
			17.64	AT3G47850	17654072-17656013	Unknown function

Continued on next page.

Table C.1 – continued from previous page

QTL	Chr	Markers	Position	Candidate genes		Description
				AGI	Location	
				CHL: AT3G47860	17656670-17658316	Encodes a chloroplastic lipocalin AtCHL. Located in thylakoid lumen. Involved in the protection of thylakoidal membrane lipids against reactive oxygen species, especially singlet oxygen, produced upon excess light.
RIX-QTL3-4	3	BH.109L	22.93	HB-12: AT3G61890	k22914154-22915325	Involved in multicellular organism development, response to abscisic acid, response to osmotic stress, response to salt stress, response to virus, response to water deprivation, transcription, DNA-templated
				AT3G61950	k22939546-22941451	Functions in: DNA binding, sequence-specific DNA binding transcription factor activity; involved in: regulation of transcription
		HH.90L	23.25	AT3G62860	23239446-23242251	alpha/beta-Hydrolases superfamily protein; functions in catalytic activity
				APG3: AT3G62910	k23257554-23260427	Encodes a plastid-localized ribosome release factor 1 that is essential in chloroplast development. Pale green, albino mutant seedlings arrest early in seedling development.
RIX-QTL4-1	4	T7M24	2.63	AT4G05136	2649683-2649898	Unknown function
RIX-QTL5-1	5	EC.198L	2.5	AT5G07800	2486576-2489296	Flavin-binding monooxygenase family protein; involved in: oxidation reduction
				AT5G07890	2517381-2519992	Unknown function
		BH.180C	2.76	CI51: AT5G08530	2759317-2761875	Involved in oxidation reduction, mitochondrial electron transport
				AT5G08535	2762029-2763432	Unknown function
				AT5G08540	2763823-2765734	Unknown function
RIX-QTL5-2	5	DF.231C	5.63	AT5G17140	5637830-5638273	Unknown function
RIX-QTL5-3	5	GH.473C	7.21	AT5G21222	7208643-7213894	protein kinase family
		GH.121L	8.06	PAE9: AT5G23870	8045844-8050175	Encodes a pectin acetylesterase that removes cell wall acetate associated with pectin formation in Arabidopsis leaves.
				AT5G23890	8058689-8063201	Unknown function

Continued on next page.

Table C.1 – continued from previous page

QTL	Chr	Markers	Position	Candidate genes		Description
				AGI	Location	
				AT5G23903	8066419-8067096	Unknown function
		HH.480C	9.06	AT5G25950	9057793-905996	Unknown function
				AT5G25960	9062917-9065011	Unknown function

Appendix D

Supplementary Data for Chapter 5

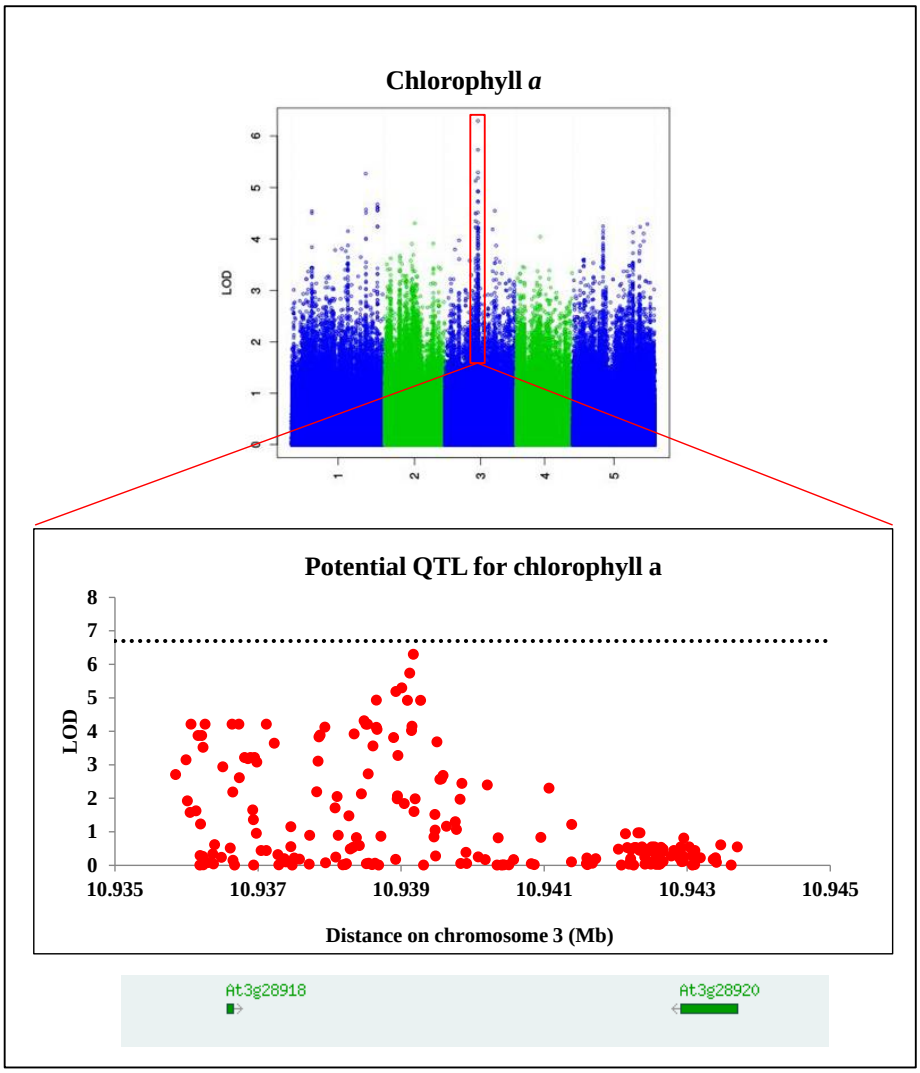

Figure D.1 – Manhattan plots of GWAS results showing the potential QTL for chlorophyll *a* trait from Experiment V. The expansion of 20kb window and the candidate genes nearby from the highest peak.

Table D.1 – Showing the potential QTLs for leaf area trait from Experiment IV. The expansion of 20kb window and the candidate genes nearby from the highest peak.

QTL	Chr	snp region	Candidate genes		Description
			Gene name:AGI	Location	
LA-QTL1	1	2_16744849	AT2G40081	16735002-16735115	unknown protein
		2_16745468	**LHCB4.3**: AT2G40100	16745653-16746627	Lhcb4:3 protein (Lhcb4.3, light harvesting complex of photosystem II)
			AT2G40110	16747940-16749512	Yippee family putative zinc-binding protein
			AT2G40113	16750035-16751084	Pollen Ole e 1 allergen and extensin family protein; FUNCTIONS IN: molecular_function unknown
			AT2G40116	16751714-1675453	Phosphoinositide-specific phospholipase C family protein; FUNCTIONS IN: phospholipase C activity
			AT2G40120	16754939-16757592	Protein kinase superfamily protein; FUNCTIONS IN: protein serine/threonine kinase activity
LA-QTL4	4	4_13091298	**ACD1-LIKE**: AT4G25650	13080901-13083197	Similar to ACD1. Leaves of antisense ACD1-like plants turn yellow in darkness like wild-type whereas antisense ACD1 plants remain dark after five days of dark treatment.
			AT4G25660	13083407-13085188	PPPDE putative thiol peptidase family protein
			AT4G25670	13085198-1308638	unknown protein
			AT4G25690	13090209-13091797	unknown protein
			AT4G25700	13093934-13095935	Converts beta-carotene to zeaxanthin via cryptoxanthin.
			AT4G25707	13097640-13097762	This gene encodes a small protein and has either evidence of transcription or purifying selection.
LA-QTL5	5	5_24474120	**RGF1**: AT5G60810	24466531-24467179	Encodes a root meristem growth factor (RGF).
		5_24478009	AT5G60820	24469587-24470895	RING/U-box superfamily protein; FUNCTIONS IN: zinc ion binding
			bZIP70: AT5G60830	24472639-24473319	FUNCTIONS IN: DNA binding, sequence-specific DNA binding transcription factor activity; INVOLVED IN: regulation of transcription
			AT5G60840	24473319-24474491	unknown protein

Table D.2 – Summary of QTL and candidate genes listed based on single trait GWAS analyses for chlorophyll a under given growth conditions (coastal and inland) (www.arabidopsis.org).

QTL	Chromosome	snp region	Candidate genes		Description
			Gene name:AGI	Location	
Chl-QTL1	3	10,939,172	AT3G28918	10932966-10933058	unknown protein; LOCATED IN: endomembrane system
			ATHB34: AT3G28920	10940446-10941833	homeobox protein 34 (HB34); FUNCTIONS IN: DNA binding, sequence-specific DNA binding transcription factor activity; INVOLVED IN: regulation of transcription

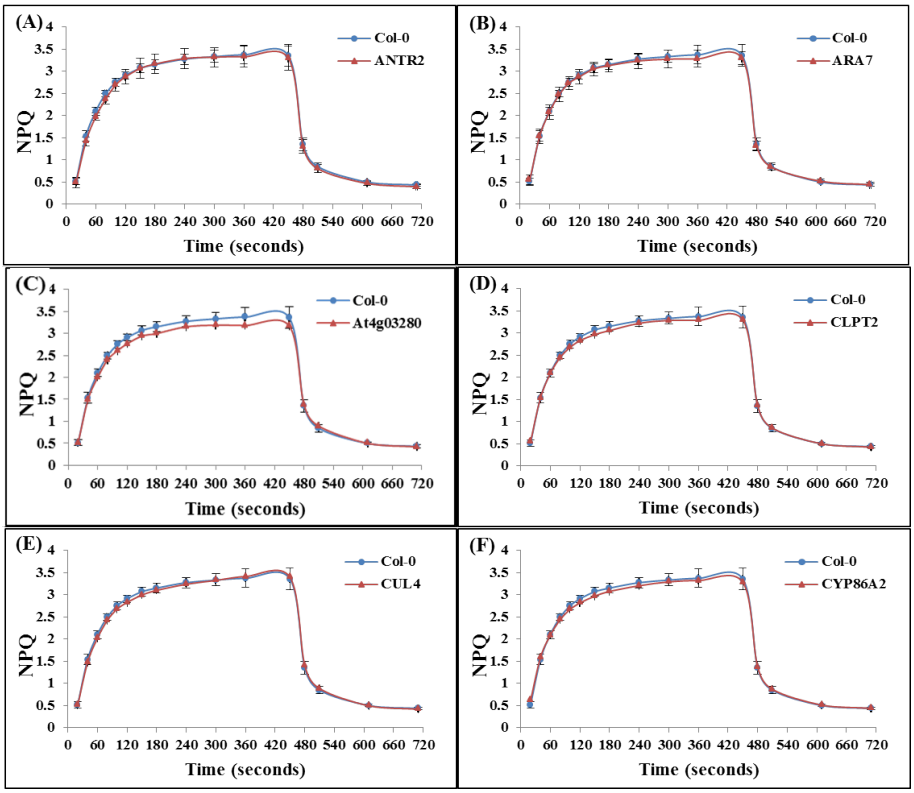

Figure D.2 – NPQ kinetics of 6 knockout lines screening compared to Col-0 plants under coastal condition. Blue lines represent the NPQ kinetic of Col-0 plants (n=5), and red lines represent knockout lines (n=5). A, B, C, and D represented NPQ kinetic of ANTR2, ARA7, At4g03280, CLPT2, CUL4, and CYP86A2 respectively. The data are mean ±SD.

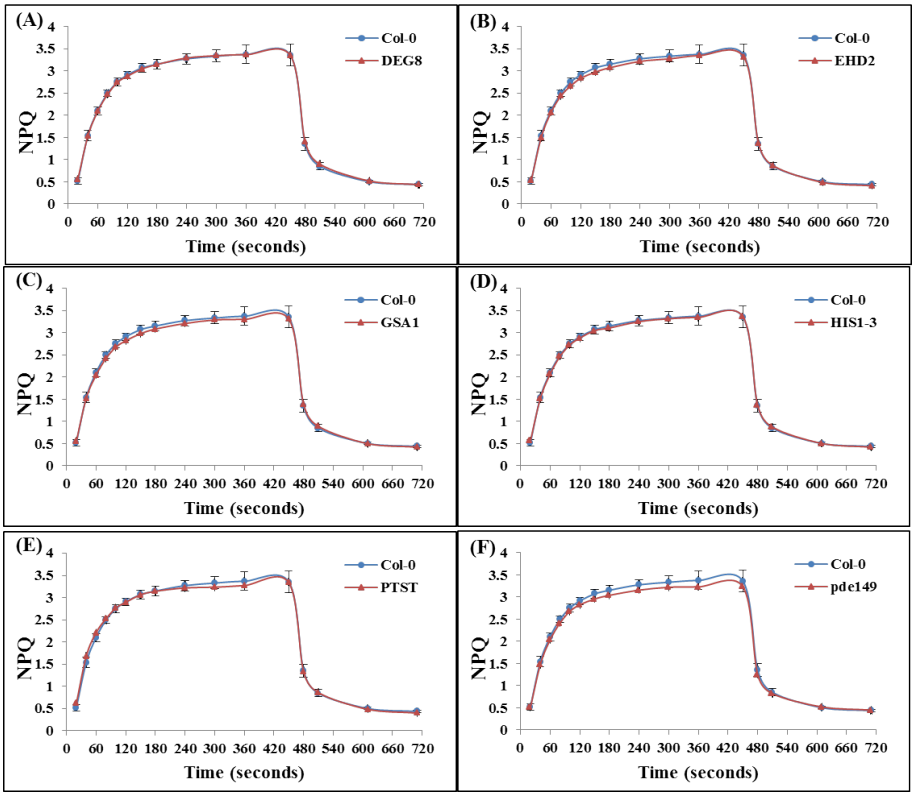

Figure D.3 – NPQ kinetics of 6 knockout lines screening compared to Col-0 plants under coastal condition. Blue lines represent the NPQ kinetic of Col-0 plants (n=5), and red lines represent knockout lines (n=5). A, B, C, and D represented NPQ kinetic of EDG8, EHD2, GSA1, HIS1-3, PTST, and PDE149 respectively. The data are mean ±SD.

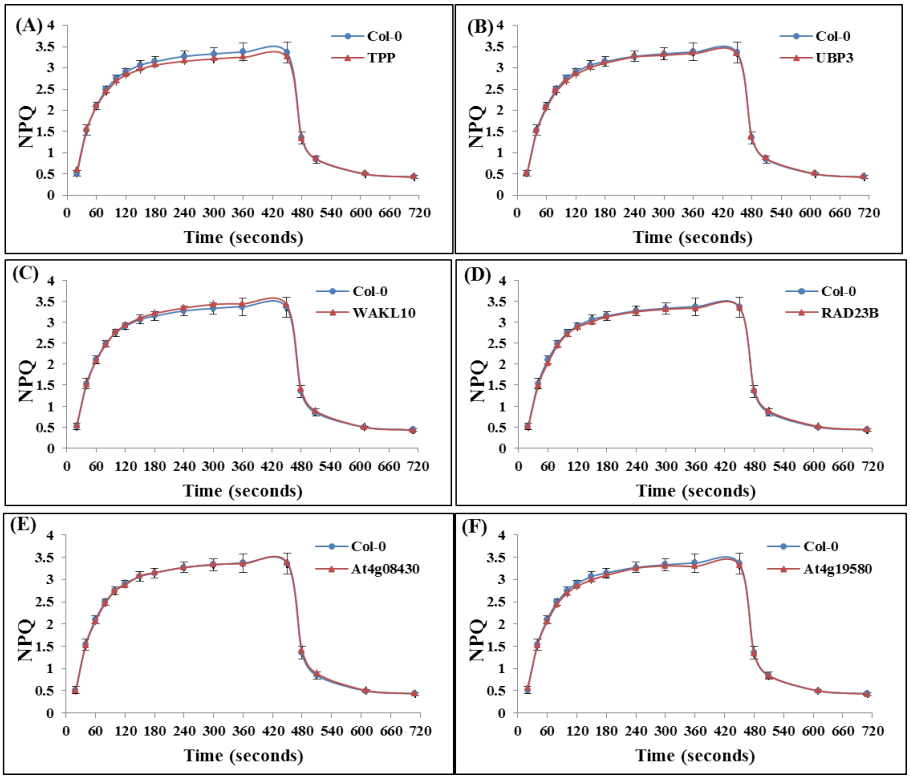

Figure D.4 – NPQ kinetics of 6 knockout lines screening compared to Col-0 plants under coastal condition. Blue lines represent the NPQ kinetic of Col-0 plants (n=5), and red lines represent knockout lines (n=5). A, B, C, and D represented NPQ kinetic of TPP, UBP3, WAKL10, RAD23B, At1g08430, and At4g19580 respectively. The data are mean ±SD.

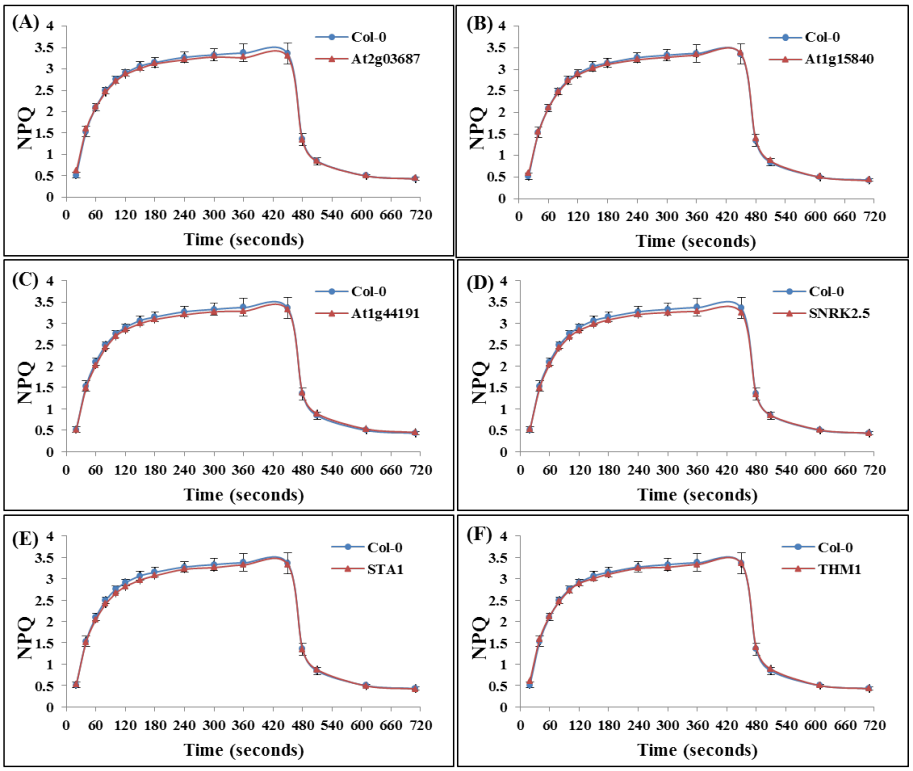

Figure D.5 – NPQ kinetics of 7 knockout lines screening compared to Col-0 plants under coastal condition. Blue lines represent the NPQ kinetic of Col-0 plants (n=5), and red lines represent knockout lines (n=5). A, B, C, and D represented NPQ kinetic of At2g03687, At1g15840, At1g44191, SNRK2.5, STA1, and THM1 respectively. The data are mean ±SD.

Table D.3 – Summary of motifs identification of high and low NPQ sequence at *PsbS* promoter. Motifs that marked in red colour are presented different motif position found at promoter region between Col-0, high and low accessions.

No.	Motif	Sequence	Function
1	3-AF1 binding site	AAGAGATATTT	light responsive element
2	A-box	CCGTCC	cis-acting regulatory element
3	AAGAA-motif	GAAAGAA	?
4	ABRE	TACGGTC	cis-acting element involved in the abscisic acid responsiveness
5	ACE	ACGTGGA	cis-acting element involved in light responsiveness
6	AE-box	AGAAACAT	part of a module for light response
7	ARE	TGGTTT	cis-acting regulatory element essential for the anaerobic induction
8	ATCT-motif	AATCTAATCT	part of a conserved DNA module involved in light responsiveness
9	AuxRE	TGTCTCAATAAG	part of an auxin-responsive element
10	Box I	TTTCAAA	light responsive element
11	Box-W1	TTGACC	fungal elicitor responsive element
12	CAAT-box	CCAAT	common cis-acting element in promoter and enhancer regions
13	CCGTCC-box	CCGTCC	cis-acting regulatory element related to meristem specific activation
14	CGTCA-motif	CGTCA	cis-acting regulatory element involved in the MeJA-responsiveness
15	G-box	CACGTC	cis-acting regulatory element involved in light responsiveness
16	GATA-motif	AAGATAAGATT	part of a light responsive element
17	GAG-motif	AGAGAGT	part of a light responsive element
18	HSE	AAAAAATTTC	cis-acting element involved in heat stress responsiveness
19	LTR	CCGAAA	cis-acting element involved in low-temperature responsiveness
20	MRE	AACCTAA	MYB binding site involved in light responsiveness
21	O2-site	GATGACATGA	cis-acting regulatory element involved in zein metabolism regulation
22	P-box	CCTTTTG	gibberellin-responsive element
23	Skn-1_motif	GTCAT	cis-acting regulatory element required for endosperm expression
24	Sp1	CC(G/A)CCC CC(G/A)CCC GGGCGG	light responsive element
25	TATA-box	TATA	core promoter element around -30 of transcription start
		TACAAAA	core promoter element around -30 of transcription start
26	TC-rich repeats	GTTTTCTTAC ATTTTCTTCA	cis-acting element involved in defense and stress responsiveness
27	TCA-element	GAGAAGAATA	cis-acting element involved in salicylic acid responsiveness
28	TCCC-motif	TCTCCCT	part of a light responsive element
29	TGA-element	AACGAC	auxin-responsive element
30	W box	TTGACC	?

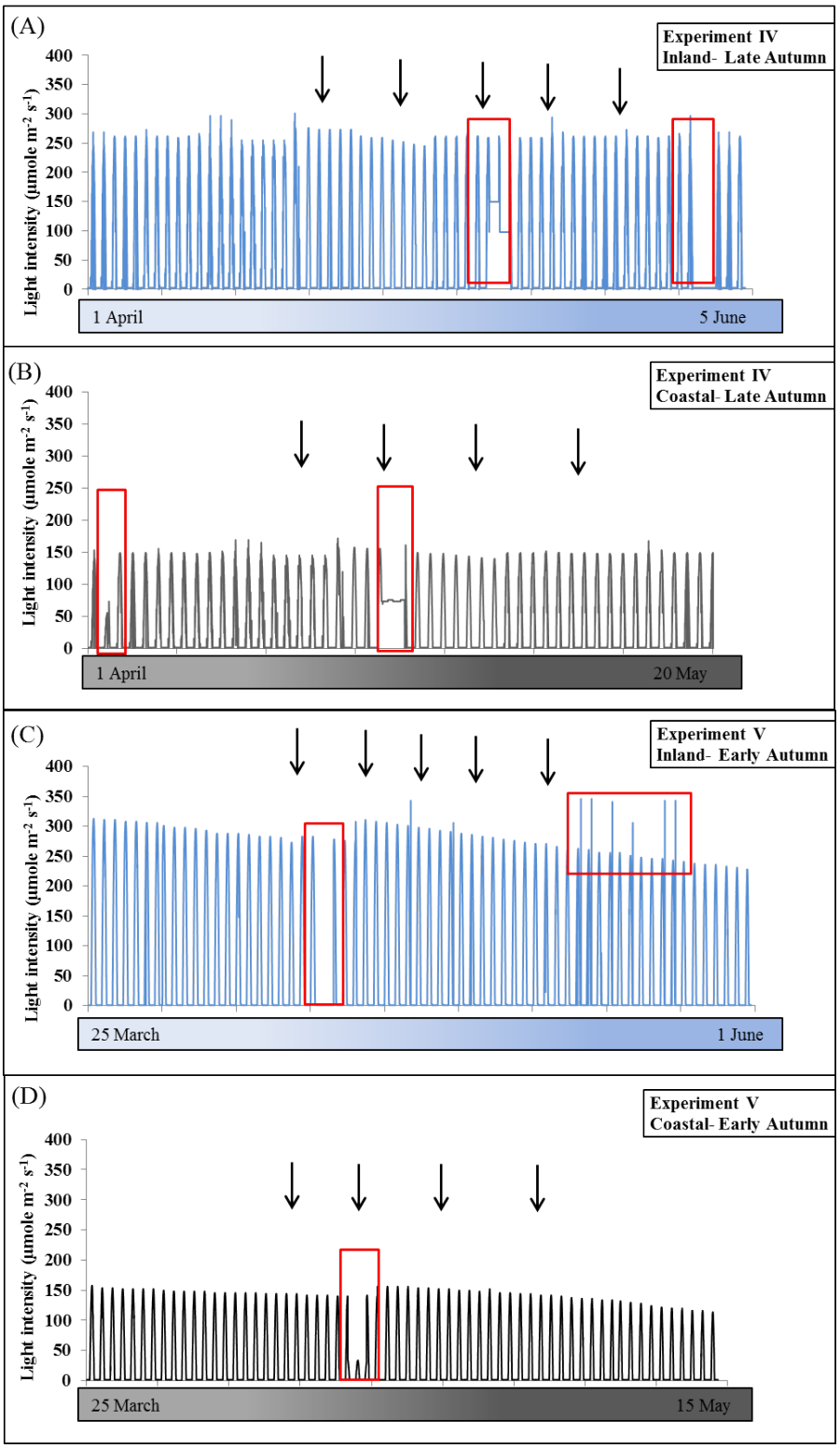

Figure D.6 – Showing weather controlled using SolarCal software in typical autumn season (program started on 1 April for the experiment IV and started on 25 March for the experiment V). Graphs showed seasonal change in light intensity of inland condition (A) and coastal condition (B) of the experiment IV, and the seasonal change in light intensity of the experiment V for inland (C) and coastal (D). The graphs showed the unstable of controlled conditions in both experiments which might affect plant growth and development.

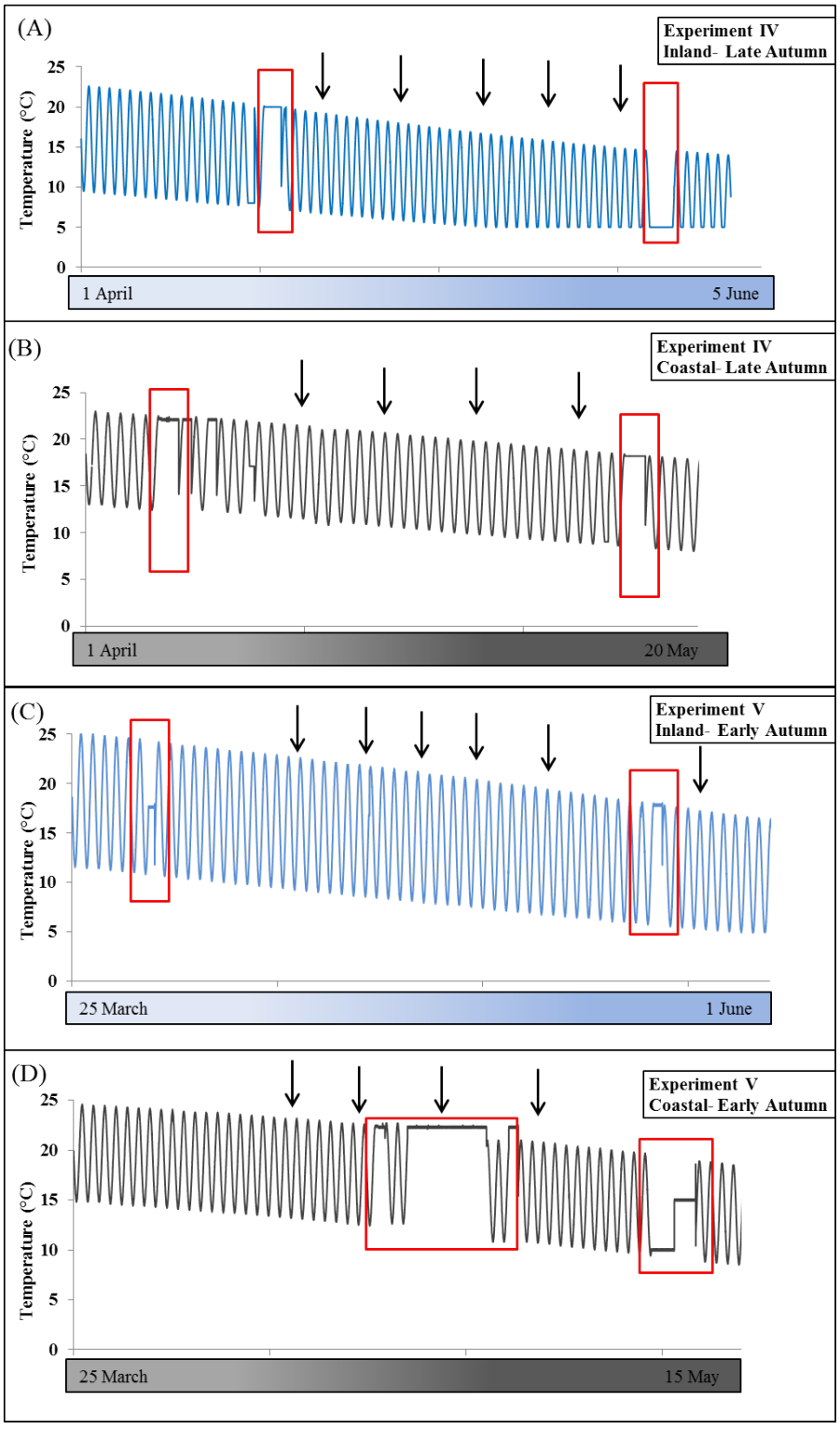

Figure D.7 – Showing weather controlled using SolarCal software simulated autumn season (program started on 1 April for Experiment IV and started on 25 March for Experiment V). Graphs showed seasonal change in temperature of inland condition (A) and coastal condition (B) of Experiment IV, and the seasonal change in temperature of Experiment V for inland (C) and coastal (D). The graphs showed the instability of controlled conditions in both experiments which might affect plant growth and development.

Figure D.8 – Enlarge amino acid change at the SNPs peaks: non-synonymous amino acids (red) and synonymous amino acids (green). Data was generated using from online software: http://signal.salk.edu/atg1001/3.0/gebrowser.php.

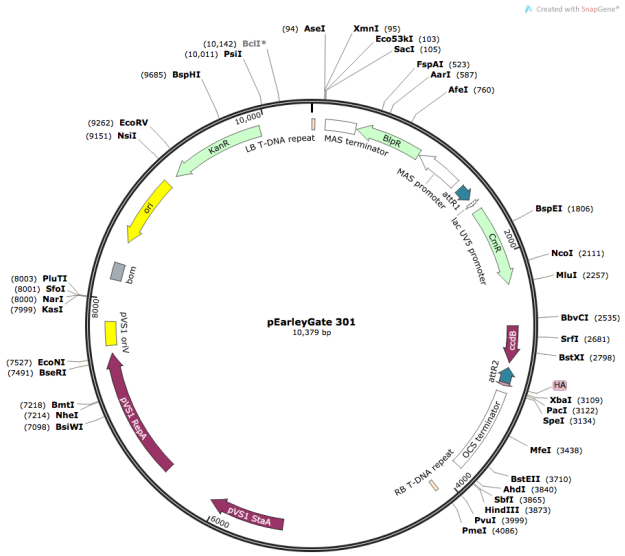


```
1     gattttatgtaatatttttttttaaaaggtatattgatgtgagttgcccaaaaaaagaagaaggtgtgattgatgtgaaattgttttcaaaataggggtt
101   taatgtatgtacatataattaaaattaaaatgaaagtttatgatatttaaatattatatgtccattttgaatatatatgatgattgttcaattgatacaa
201   tttaaattacaaaataatgaacttttagtagaagacaatgttttgtgtttaaagtcgtaactttaatgagactcatagaaagaaaacaaatatgcctaaa
301   cccgcttgtcatgatgtgagatgaggtgttagtgtccaaagttcaaacacgtcttttcatcgagaaaactaatttaaacacgaaaaattattcctttctgag
401   tgttgtgcgagtatttgtagtttcaaatgtttttactcgattcaagtttttaccgtccctaactattttaaggttataagcgggtgcggttgcggttac
501   gggagtttgcggaaacgggcgatcacggttttaagcgttatcaagcattttgaacgactggttgagcgtttgataataggtgcgtttgcgggagttttat
601   gactgataaaccagccggtgcgatagtaattaaataaaaaataaccaaaatgaatataatattattactattaaaagaaataaaaatacaatatattagaa
701   aaattgattttctgaccaaataaaaatacaatatatcatctcgtccgacgaaaatgattttctaatcgagaaaacaaatcgaaacatgtattcaatcaaaa
801   aactcaaaagaatacaaaatataaaataaaacaatgatgccatgaaatagtcaaagaattacactagctaatgagtgaataaaatgatagatgatacttat
901   gtttgattcttgattttgattttcatcggatgccataattgagagaatagagttacaatatattgattagggttttctaataaaaataagatatataaaa
1001  gattagattatttttaattatagtgatttagggtttgggtggaaaccacaattatttttaattaactaaaaatagattatttttttattttttaatctaaccgc
1101  taccgcccgcaaccgcaaacgcttgcgggaaggagctttgaaaattggcaattttgagcggtccaaagcgatatctagcggtttctatgattggttcca
1201  atcgctaataaccgctaccaaccgcaaacgctgcgtttatgggtggtagagggagaaccaatcagcccttaacaaaaccgaaaaaactaaagatttgaac
1301  ctaagtgtcgaagattctttcggaccagtctttaccactagactacctaacaaatacgaaaatatgaagccaaaattgtttttatactatttgcgaccgt
1401  aagtttgggtttagcccgcttgtgtttgtgcccggctctggctatattaaaaaagaattagatatttttcaaatataatatttttttacaaaatatgtaat
1501  tgatgtgaatttttttcaatataggtgttcttatttatatacatattataaaaaaaattaagccatttcgtttttgtaatatctaatgtaccagttccatt
1601  agtatgtactttgctagtataacataccctttgacgtgaatcttccatgagtatgtttctttagtgttgaccagacacaattcatttaaatcagtacat
1701  aaattggatttttagttccaaaatatgattttcttgaaagaaatattttatatttttattagaaagagttattagttcgtcataaatggttctttgaatat
1801  gacatttatttttgttttttttgtttactgtctaaataagtataacttttaaaaagtgtatctaaatttttttaaaaactattatattgatagattttatttttt
1901  ctccacaaaaacgttatctccagttcaccacatagagagcatggaaaggacaattgggagacgtggacgcactttaagcccatcactagatttcccttat
2001  atcttttaatctcttcacttccacaacacaacacaaaacacatcactgatccttctctcatcctcagaaagaATGGCTCAAACCATGCTGCTTACTTCAG
2101  GCGTCACCGCCGGCCATTTTTTGAGGAACAAGAGCCCTTTGGCTCAGCCCAAAGTTCACCATCTCTTCCTCTCTGGAAACTCTCCGGTTGCTCTACCATC
2201  TAGGAGACAATCATTCGTTCCTCTCGCTCTCTTCAAACCCAAAACCAAAGCTGCTCCTAAAAAGgttttcacatactctttacttgtcccacaaggaaca
2301  tttcttgtgtgtttgatggtaatgttaagattttcatatacattttagGTTGAGAAGCCGAAGAGCAAGGTTGAGGATGGCATCTTTGGAACGTCTGGTG
2401  GGATAGGTTTCACAAAGGCGAATGAGCTATTCGTTGGTCGTGTTGCTATGATCGGTTTCGCTgtaagtcccctctctgagatacaccgaacttatcttcca
2501  agaaagaagctttatatgaaagttgtttctatgcatagGCATCGTTGCTTGGTGAGGCGTTGACGGGAAAAGGGATATTAGCTCAGCTAAATCTGGA
2601  GACAGGGATACCGATTTACGAAGCAGAGCCATTGCTTCTCTTCTTCATCTTGTTCACTCTGTTGGGAGCCATTGGAGCTCTCGGAGACAGAGGAAAATTC
2701  GTCGACGATCCTCCCACCGGGCTCGAGAAAGCCGTCATTCCTCCCGGCAAAAACGTCCGATCTGCTCTCGGTCTCAAAGAACAAGGTATCTCTCAACATT
2801  TCTATTTCTATCTTTGTTACAATGACATTGCTCTGAACAACCAATGCAAATAAtataacctgatagagtactatagtaactagtataactgaattggcct
2901  aagtgtagtgtccggatcggctttatgtttatttatcgttatcctaagatacaaatgtgagacaaaagatactagcatggaacttcaatctccaaaaat
3001  aatctctaaatgtttatttatttatcgttggcctgatagattatttatcgttatcaatttctatcttttt
```

Sequences are highlight in colours indicated SNPs polymorphism altered from Col-0

Figure D.9 – Vector map and sequence of high NPQ construct (Vector map was generated from www.snapgene.com).

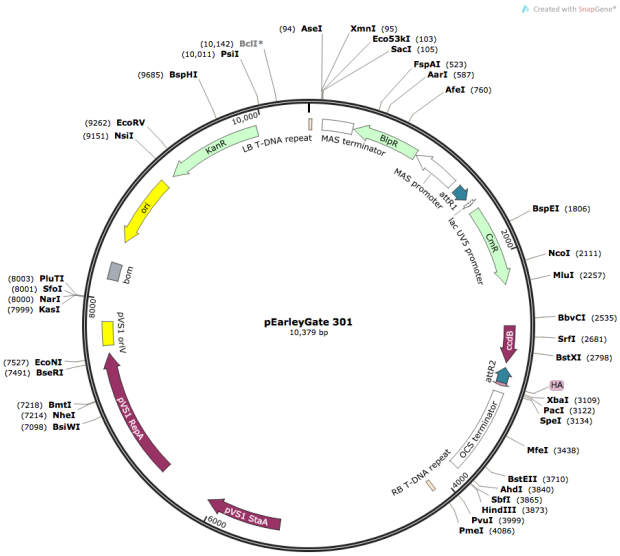


```
1    gattttatgtaatatttttttttaaaaggtatattgatgtgagttgcccaaaaaaagaagaaggtgtgattgatgtgaaattgttttcaaaataggggtt
101  taatgtatgtacatataattaaaattaaaatgaaagtttatgatatttaaatattatatgtccatttgaatatatatgatgattgttcaattgatacaa
201  tttaaattacaaaataatgaacttttagtagaagacaatgttttgtgtttaaattataacttaatgagactcatagaaagaaaacaaatatgcctaaa
301  cccgcttgtcatgatgtgagatgaggtgttcgtgtccaaagttcaaacacgtctctcatcgagaaaactaattaaacaccaaaaattattcctttctgag
401  tgttgtgcgagtatttgtagtttcaaatgtttttactcgattcaagtttttaccgtccctaactatttaaggttataagcgggtgcggttgcggttac
501  gggagtttgcggaaacgggcgatcacggtttaagcgttatcaagcattttgaacgactggttgagcgtttgataataggtgcgtttgcgggagttttat
601  gactgataaaccagccggtgcgatagtaattaaataaaaaataaccaaaataaatatatattactattaaaagaaataaaaatataatattagaa
701  aaattgattttctgaccaaatataaaatacaatatatcatctcgtccgactaaaacattttctaatcgagaaaacaaatcgaaacatgtattcaatcaaaa
801  aactcaaaagaatacaaaatataaaatataaaacaatgatgccatgaaatagtcaaagaattacactagctaatgagtgaataaaatgatagatgatacttat
901  gtttgattcttgattttgattttcatcggatgccataattgagagaatagagttacaatatattgattagggttttctaataaaaataagatatataaaa
1001 gattagattattttaattatagtgattagggtttgggtggaaaccacaattattttaattaactaaaaagagattatttttttattttttaatctaaccgc
1101 taccgcccgcaaccgcaaacgcttgcgggaaggagctttgaaaattggcgatttgagcggtccaaagcgatatctagcggtttctatgattggttcca
1201 atcgctaataaccgctaccaaccgcaaacgctgcgtttatgggtggtagagggagaaccaatcagcccttaacaaaaccgaaaaaactaaagatttgaac
1301 ctaagtgtcgaagattctttcggaccagtctttaccactagactacctaacaaatacgaaaatatgaagccaaaattgtttttatactatttgcgaccgt
1401 aagtttgggtttagcccgcttgtgtttgtgccggctctggctatattaaaaaagaattagatatttttcaaatataatatttttttacaaaatatgtaat
1501 tgatgtgaatttttttcaatataggtgttcttagttatatacatattatatgaaaaaattaagccatttcgtttttgtaatatctaatgtaccagttccatt
1601 agtatgtactttgctagtataacatacccttttgacgtgaatcttctatgagtatgtttctttagttttgaccagacacaattcatttacatcaatacat
1701 aaattggattttagttccaaaatatgattttcttgaaagaaatattttatatttttattagaaggagttattagttttgtcataaatggttctttgaatat
1801 gacatttatttttgttttttttgtttactgtctaaataagtataacttttaaaaagtgtatctaaatttttttaaaaactattatattgatagatttatttttt
1901 ctccacaaaaacgttatctccagttcaccacatagagagtatggaaaggacaattgggagacgtggacgcactttaagcccatcaatagatttcccttat
2001 atcttttaatctcttcacttccacaacacaacacaaaacacatcactgatccttctctcatcctcagaaagaATGGCTCAAACCATGCTGCTTACTTCAG
2101 GCGTCACCGCCGGCCATTTTTTGAGGAACAAGAGCCCTTTGGCTCAGCCCAAAGTTCACCATCTCTTCCTCTCTGGAAACTCTCCGGTTGCACTACCATC
2201 TAGGAGACAATCATTCGTTCCTCTCGCTCTCTTCAAACCCAAAACCAAAGCTGCTCCTAAAAAGgttttcacatactctttacttgtcccacaaggaaca
2301 tttcttgtgtgtttgatggtaatgttaagattttcatatacattttagGTTGAGAAGCCGAAGAGCAAGGTTGAGGATGGCATCTTTGGAACGTCTGGTG
2401 GGATGGGTTTCACAAAGGCGAATGAGCTATTCGTTGGTCGTGTTGCTATGATCGGTTTCGCTgtaagtcccctctatgaaatacactaacttatcttcca
2501 agaaagaagctttagtatgaaagctgtgtttctatgcatagGCATCGTTGCTTGGTGAGGCGTTGACGGGAAAAGGGATATTAGCTCAGCTGAATCTGGA
2601 GACAGGGATACCGATTTACGAAGCAGAGCCATTGCTTCTCTTCTTCATCTTGTTCACTCTGTTGGGAGCCATTGGAGCTCTCGGAGACAGAGGAAAATTC
2701 GTCGACGATCCTCCCACCGGGCTCGAGAAAGCCGTCATTCCTCCCGGCAAAAACGTCCGATCTGCCCTCGGTCTCAAAGAACAAGGTATCTCTCAACATT
2801 TCTATTTCTATCTTTGTTACAATGACATTGCTCTGAACAACCAATGCAAATAAtataacctgatagagtactatagtaactagtataactgaattggcct
2901 aagtgtagtgtccggatcggctttatgtttatttatcgttatcctaagatacaaatgtgagacaaaagatactagcatggaactgtcaatctccaaaaat
3001 aatctctaaatgtttatttatttatcgttggcctgatagattatttatcgttatcaatttctatctttttt
```

Sequences are highlight in colours indicated SNPs polymorphism altered from Col-0

Figure D.10 – Vector map and sequence of low NPQ construct (Vector Map was generated from www.snapgene.com).

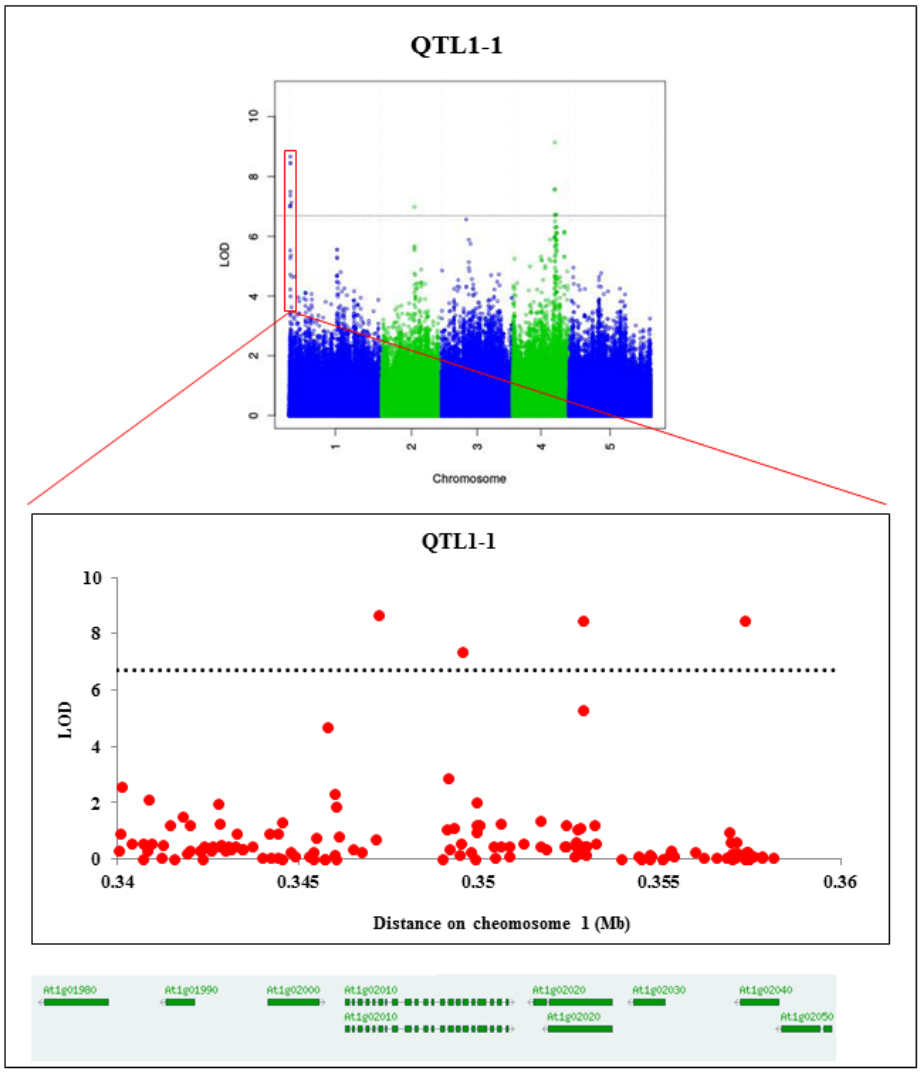

Figure D.11 – Manhattan plots of GWAS results for NPQ showing the potential candidate genes within 20kb window of QTL1-1.

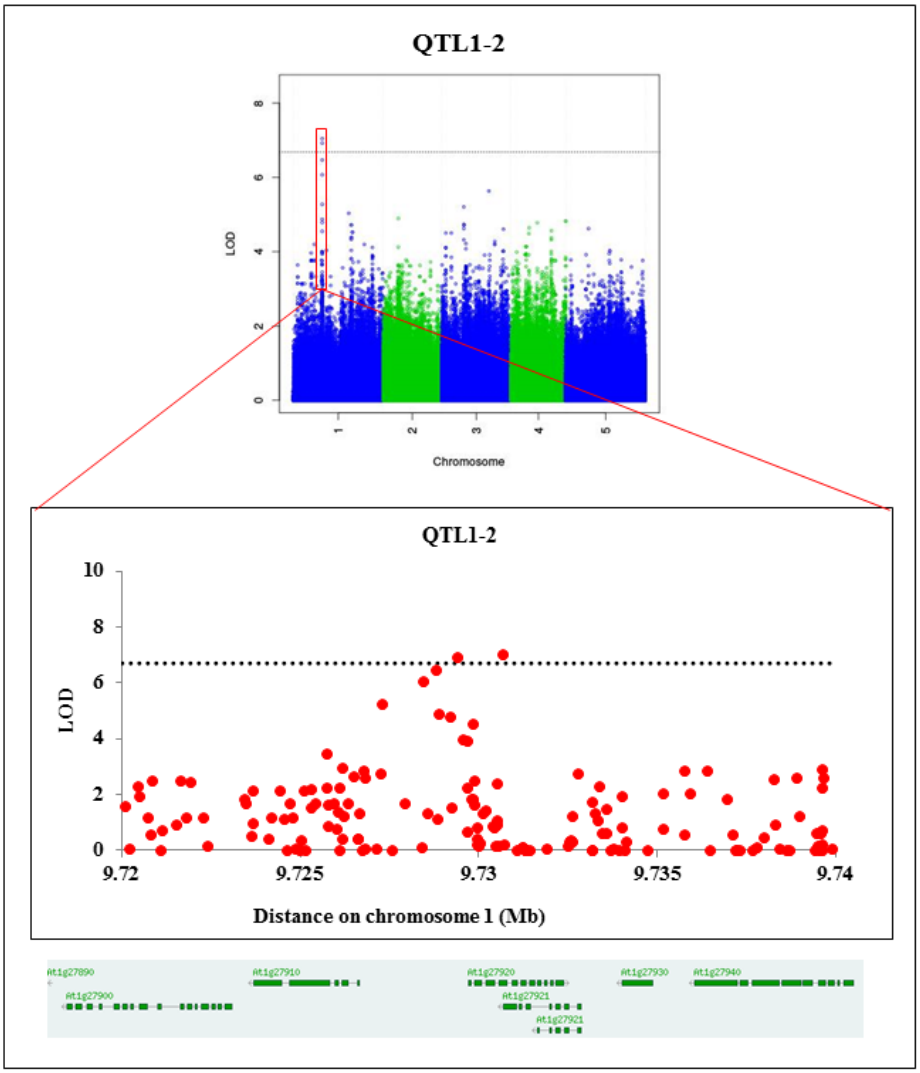

Figure D.12 – Manhattan plots of GWAS results for NPQ showing the potential candidate genes within 20kb window of QTL1-2.

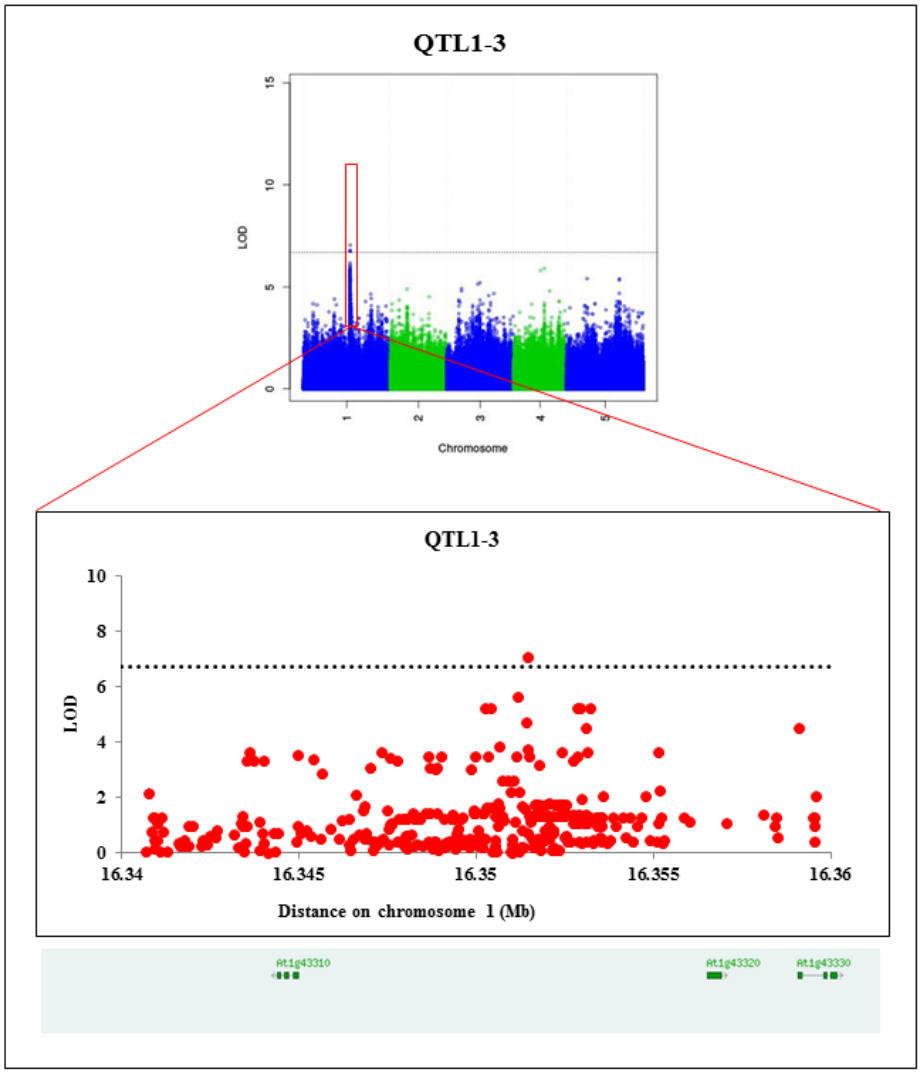

Figure D.13 – Manhattan plots of GWAS results for NPQ showing the potential candidate genes within 20kb window of QTL1-3.

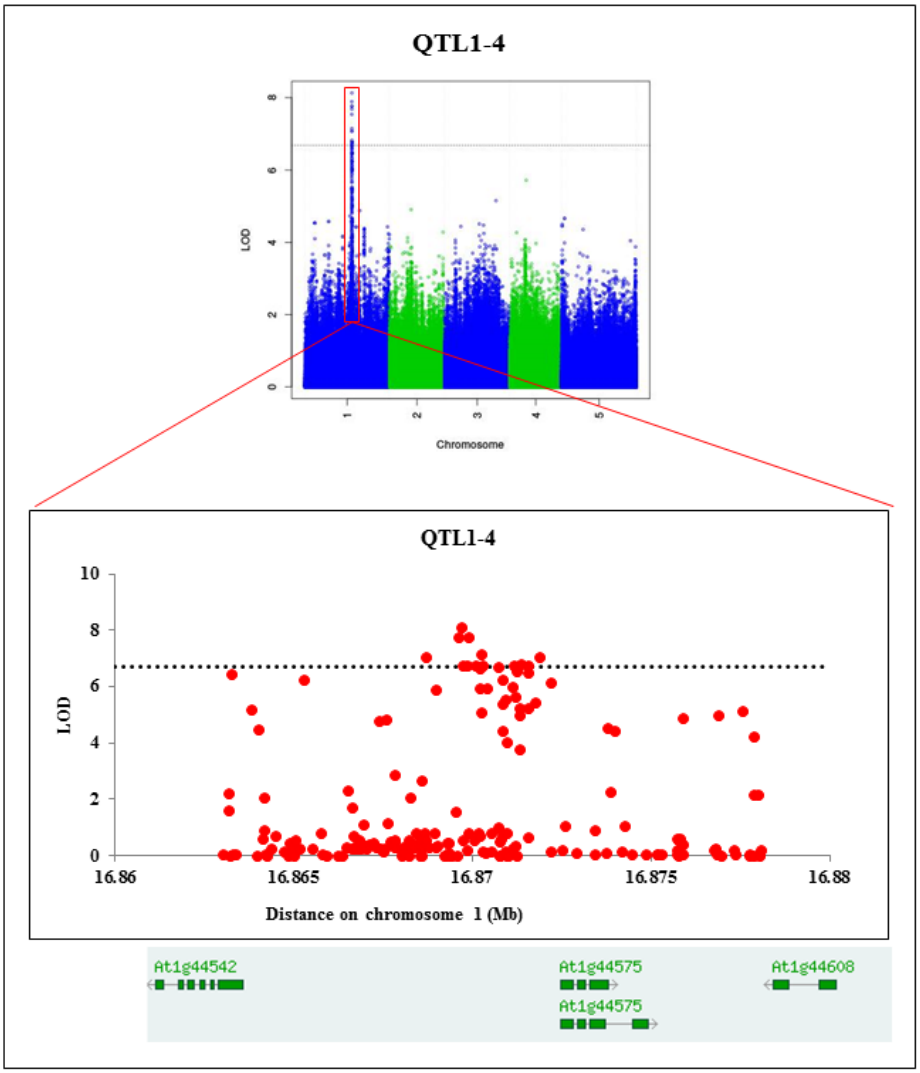

Figure D.14 – Manhattan plots of GWAS results for NPQ showing the potential candidate genes within 20kb window of QTL1-4.

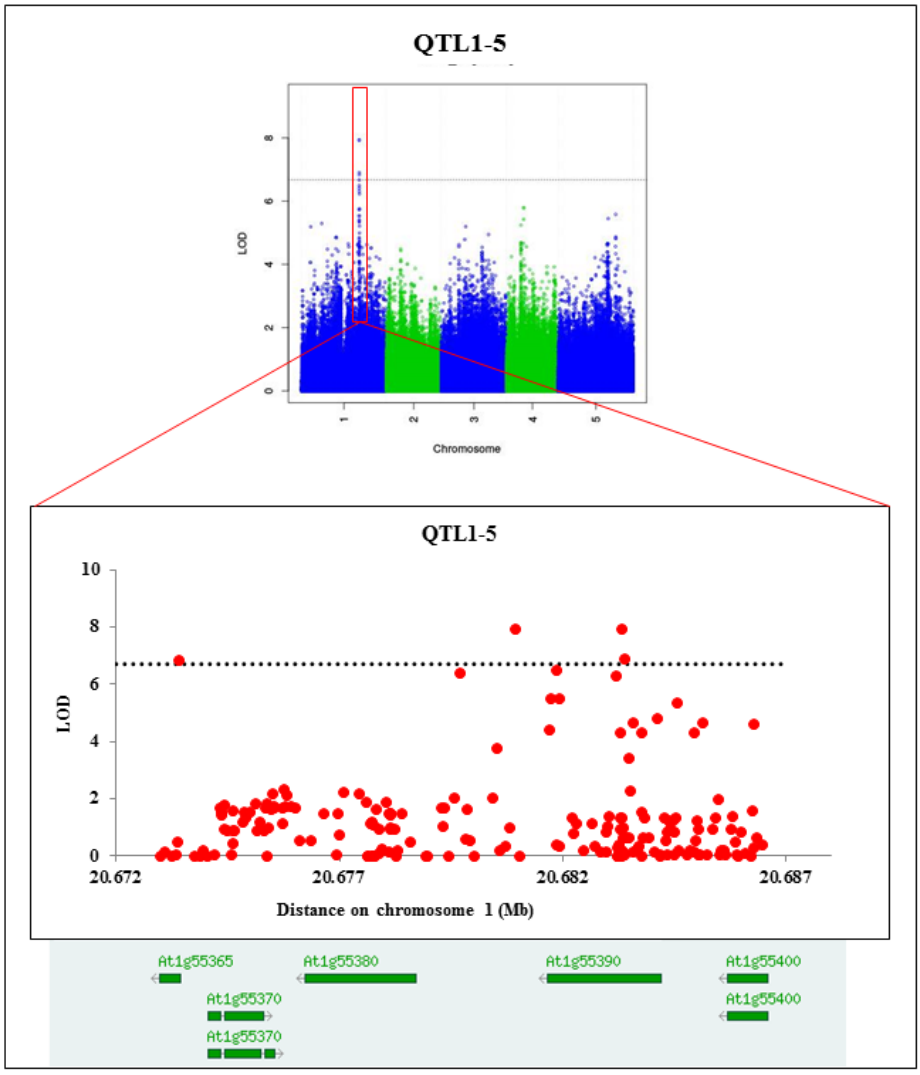

Figure D.15 – Manhattan plots of GWAS results for NPQ showing the potential candidate genes within 20kb window of QTL1-5.

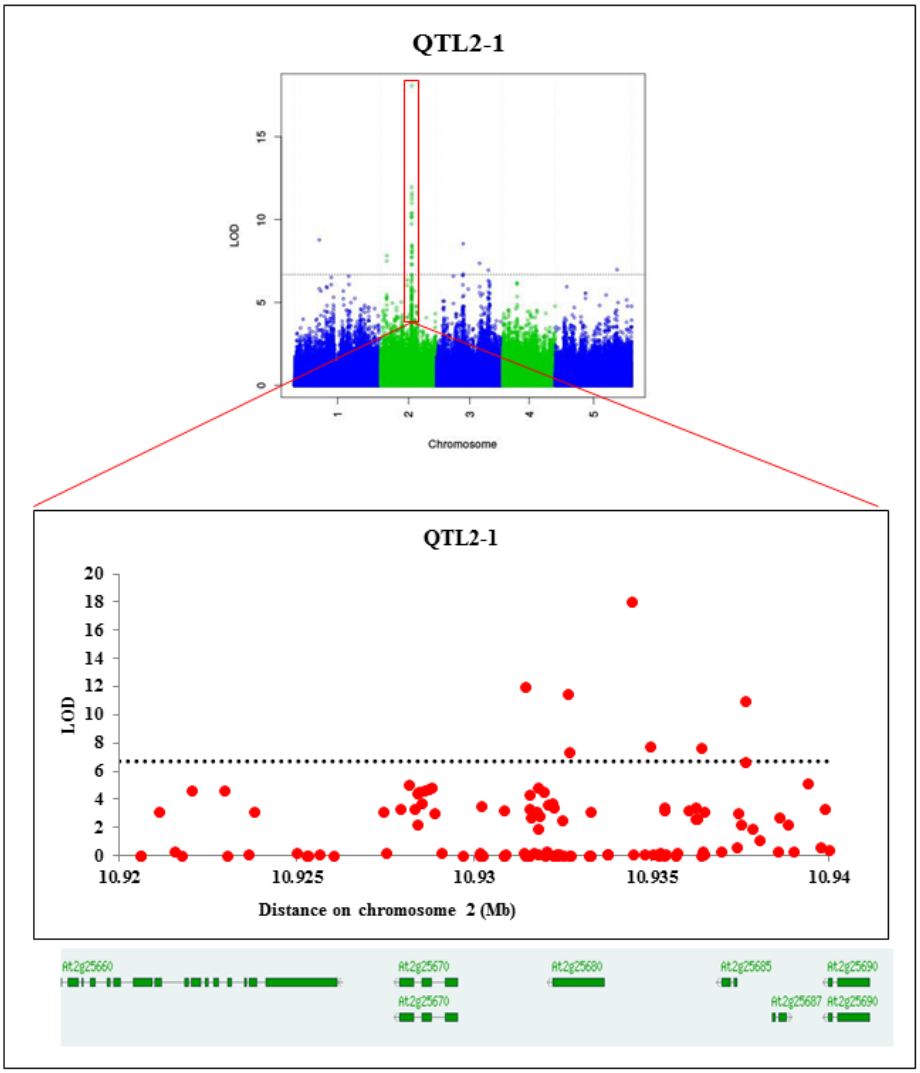

Figure D.16 – Manhattan plots of GWAS results for NPQ showing the potential candidate genes within 20kb window of QTL2-1.

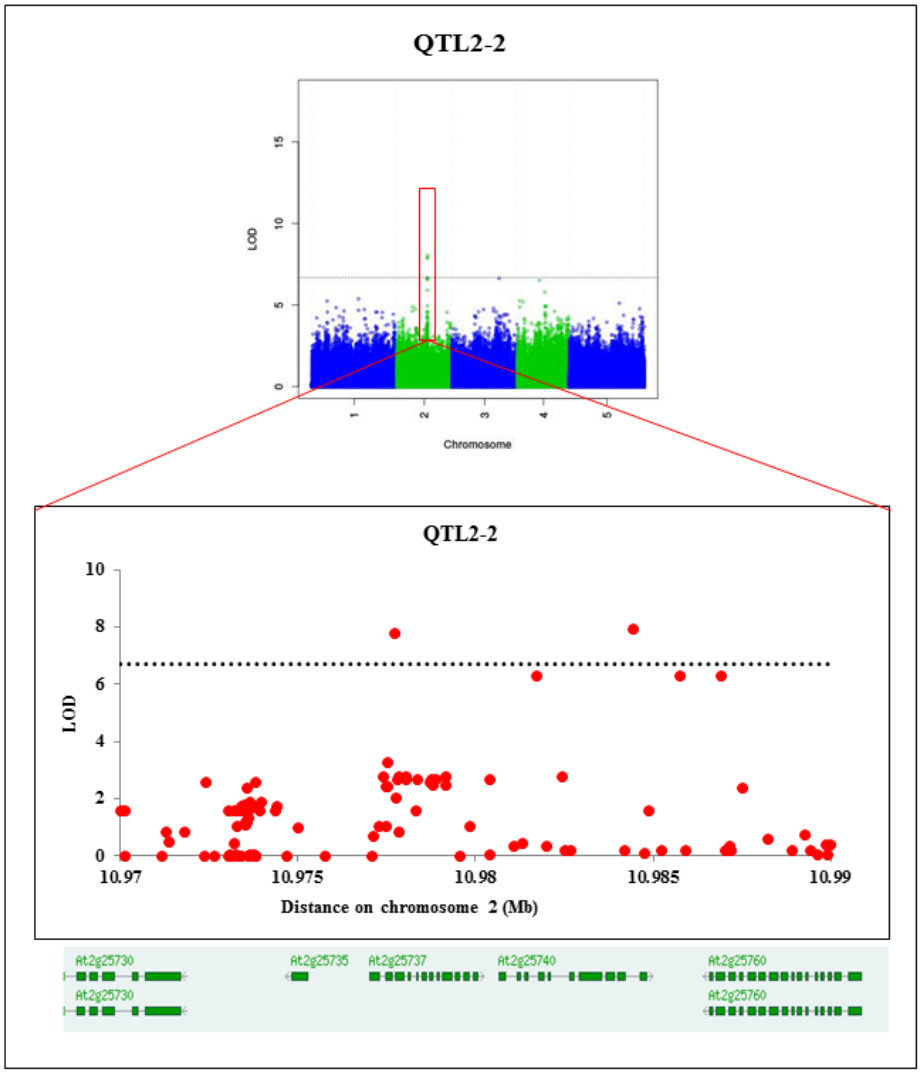

Figure D.17 – Manhattan plots of GWAS results for NPQ showing the potential candidate genes within 20kb window of QTL2-2.

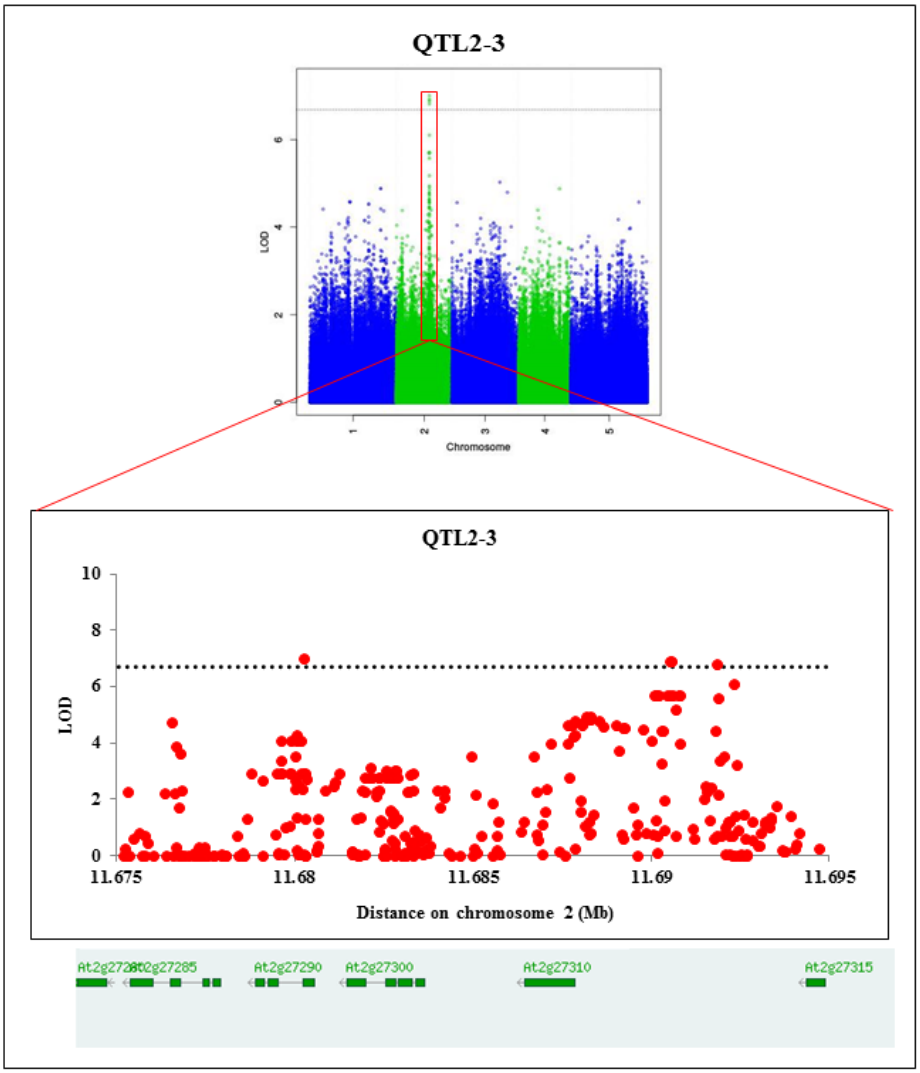

Figure D.18 – Manhattan plots of GWAS results for NPQ showing the potential candidate genes within 20kb window of QTL2-3.

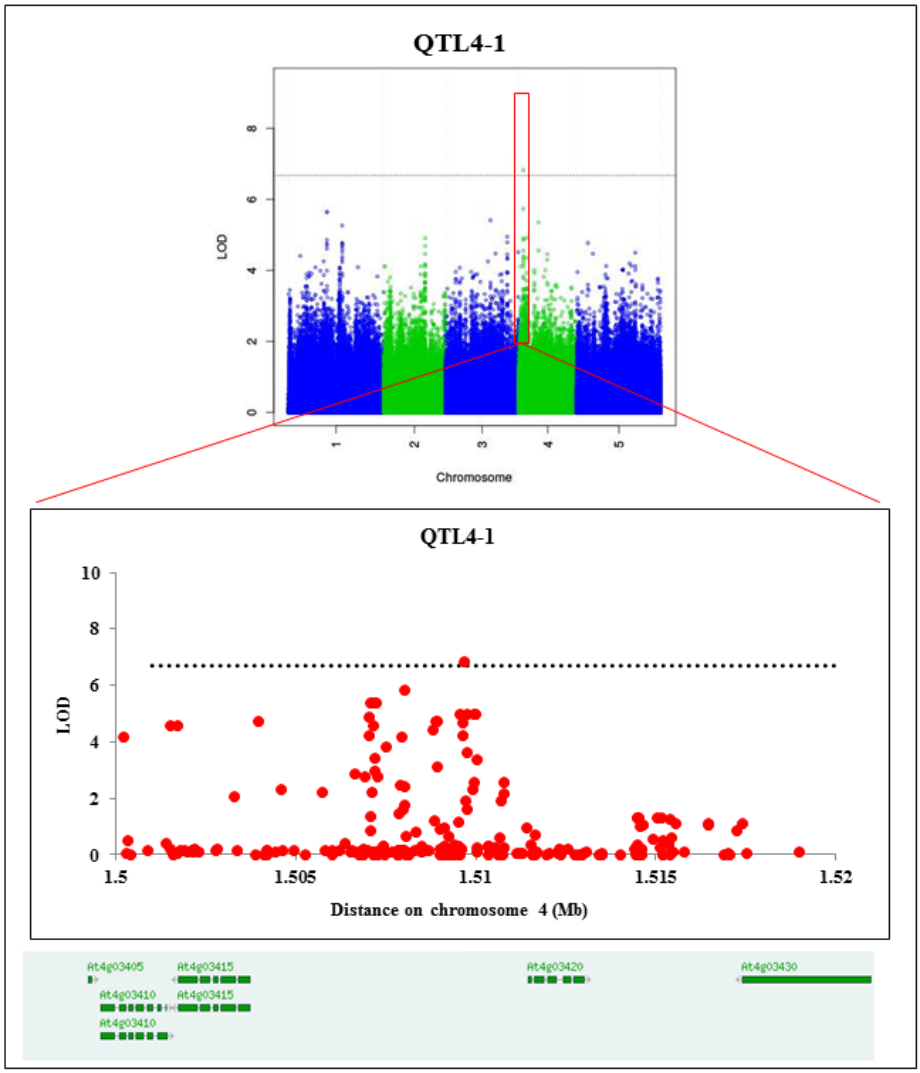

Figure D.19 – Manhattan plots of GWAS results for NPQ showing the potential candidate genes within 20kb window of QTL4-1.

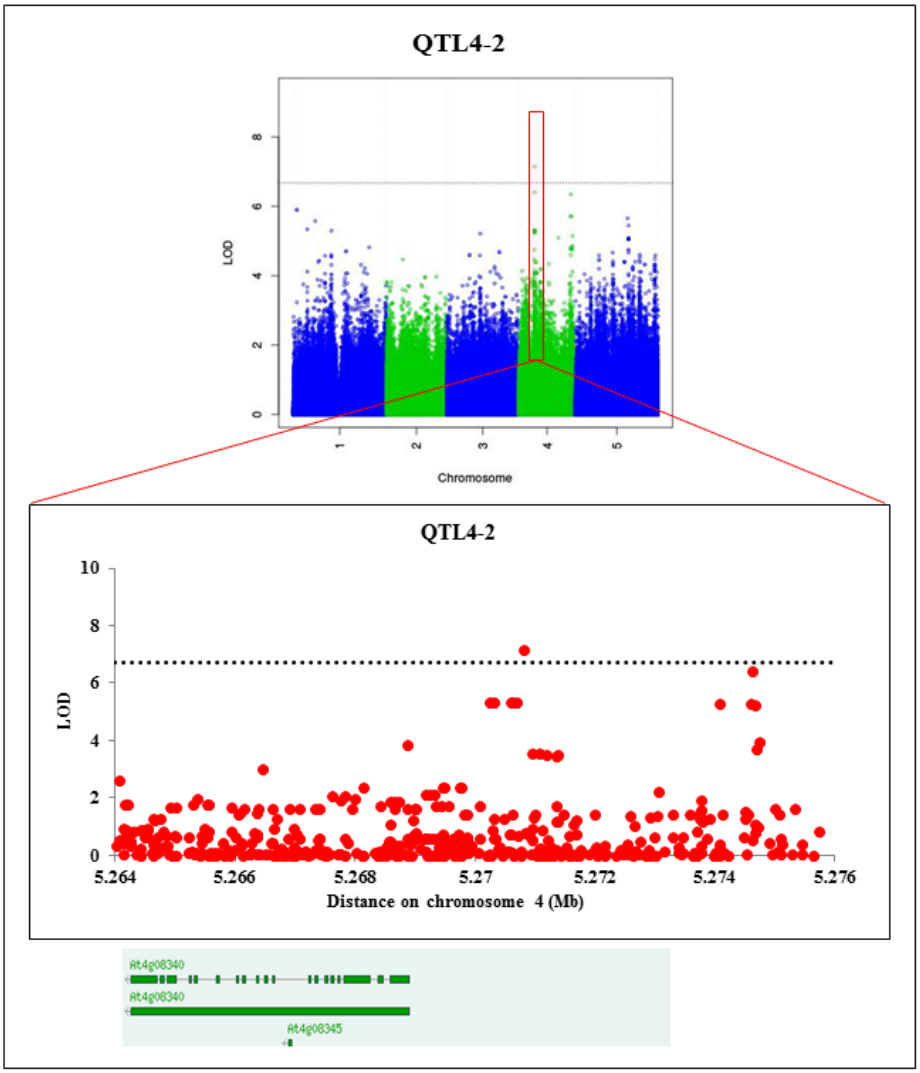

Figure D.20 – Manhattan plots of GWAS results for NPQ showing the potential candidate genes within 20kb window of QTL4-2.

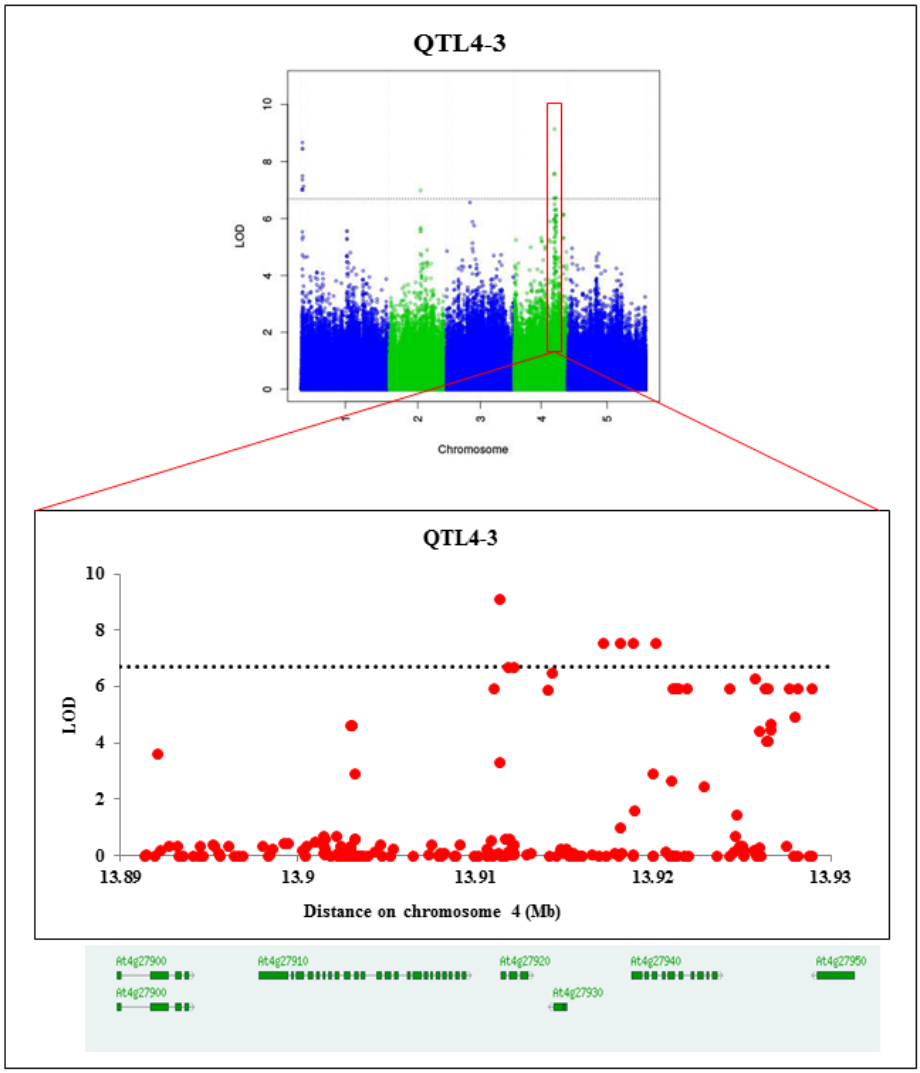

Figure D.21 – Manhattan plots of GWAS results for NPQ showing the potential candidate genes within 20kb window of QTL4-3.

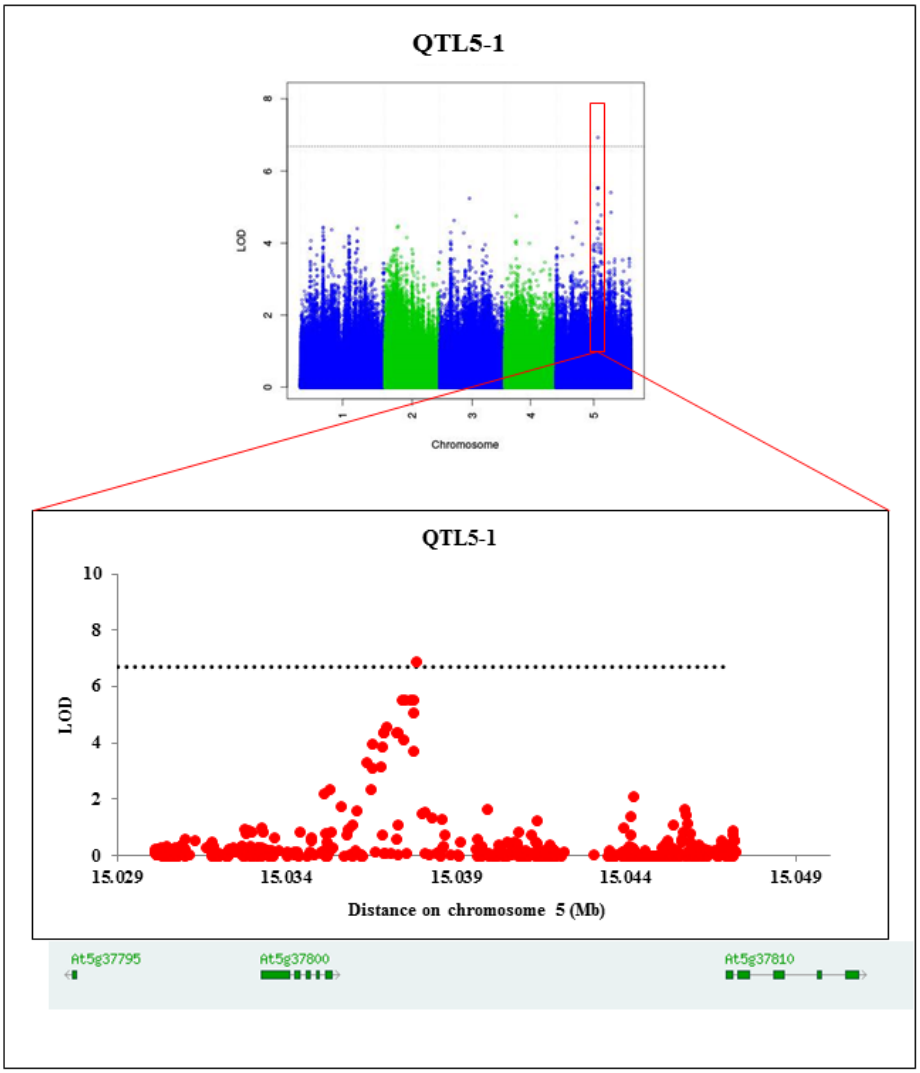

Figure D.22 – Manhattan plots of GWAS results for NPQ showing the potential candidate genes within 20kb window of QTL5-1.

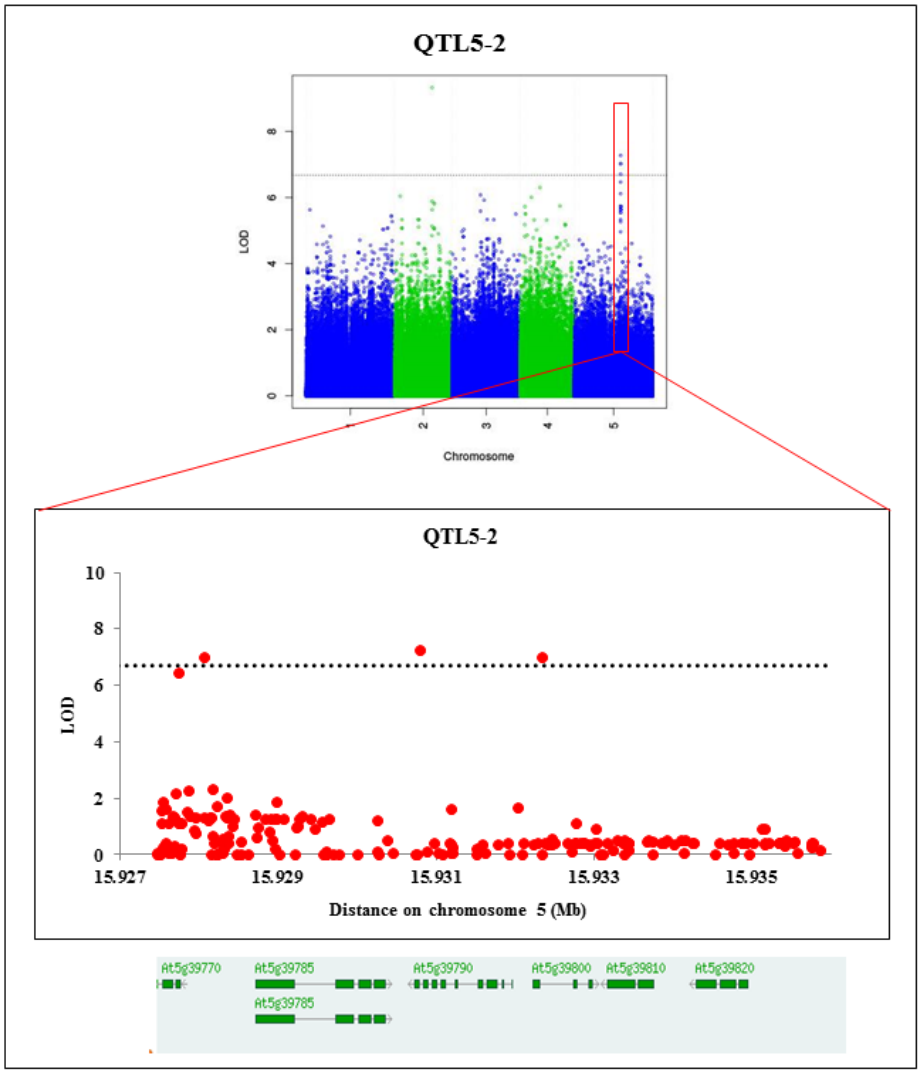

Figure D.23 – Manhattan plots of GWAS results for NPQ showing the potential candidate genes within 20kb window of QTL5-2.

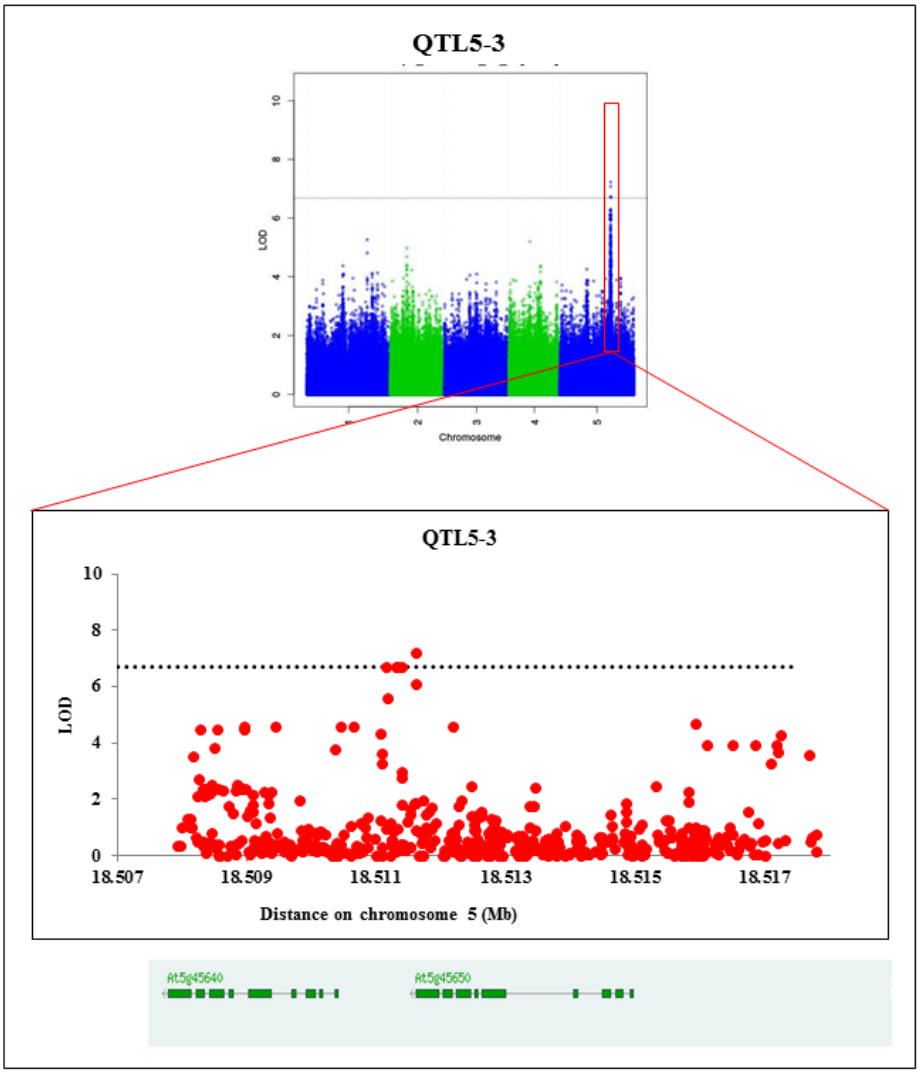

Figure D.24 – Manhattan plots of GWAS results for NPQ showing the potential candidate genes within 20kb window of QTL5-3.

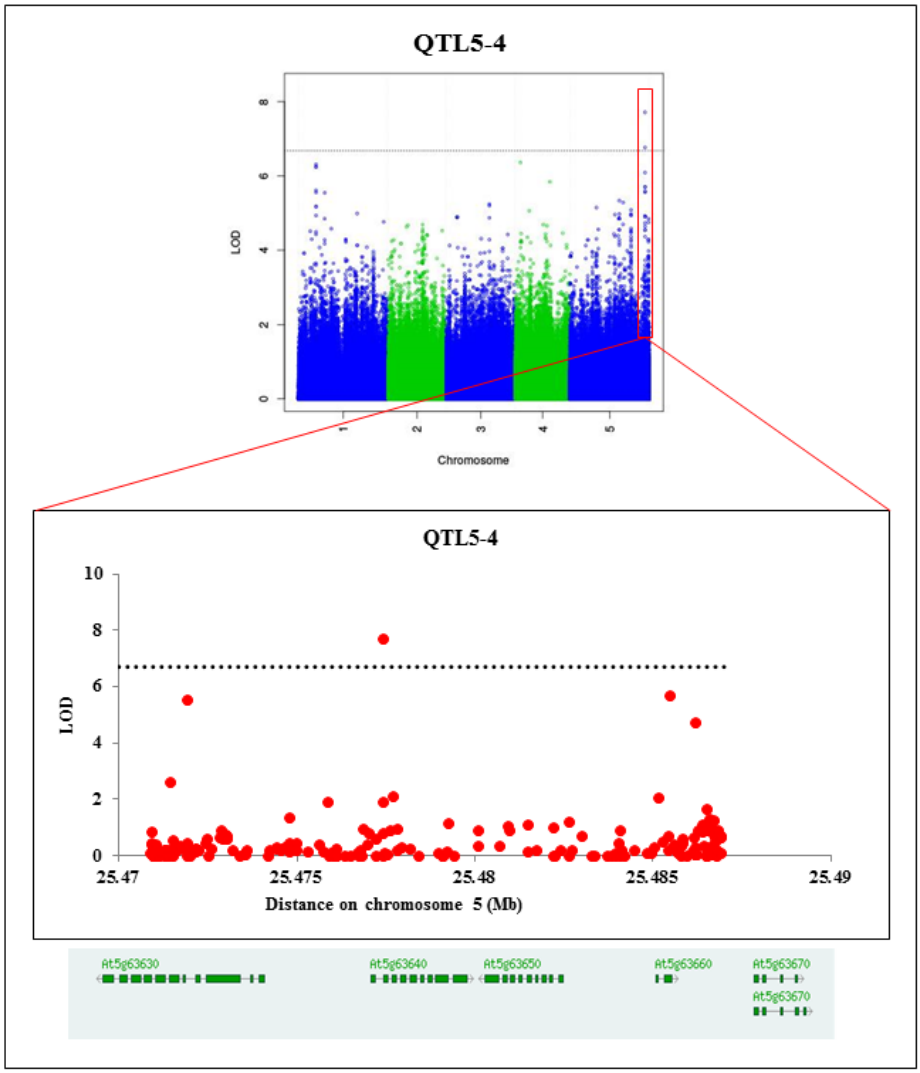

Figure D.25 – Manhattan plots of GWAS results for NPQ showing the potential candidate genes within 20kb window of QTL5-4.

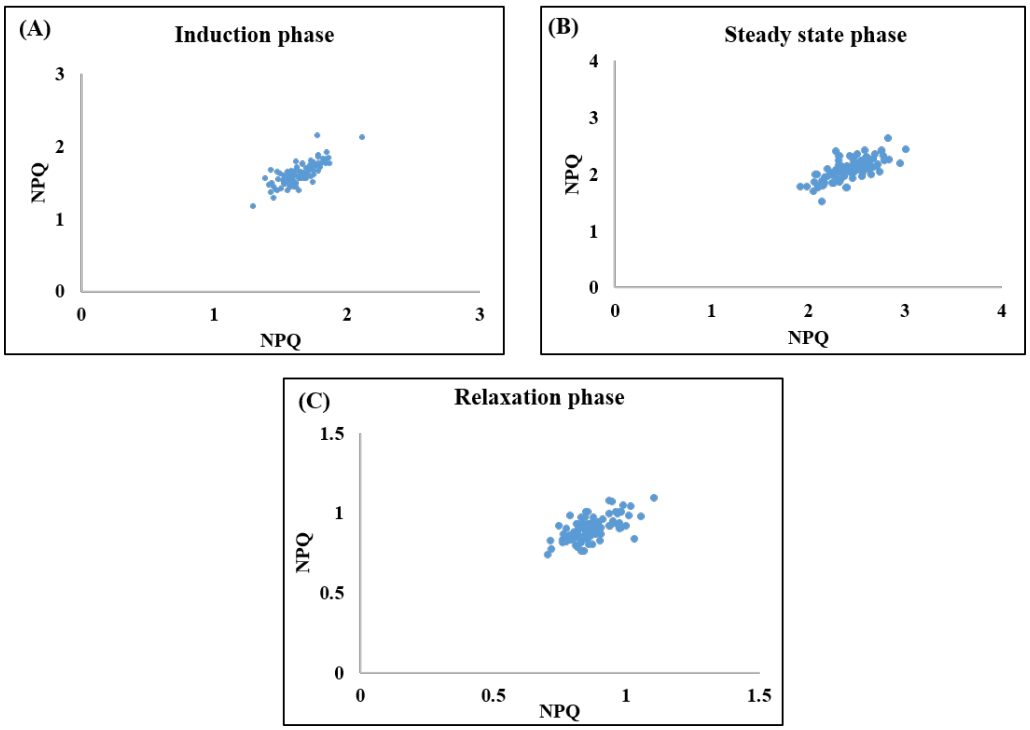

Figure D.26 – Plots show the degree of reproducibility of NPQ traits (induction phase (A), steady state phase (B), and relaxation phase (C)) in independent experiments. NPQ values of two replicates plant grown coastal condition of one experiment (x-axis) and another experiment (y-axis) at 32 day of age.

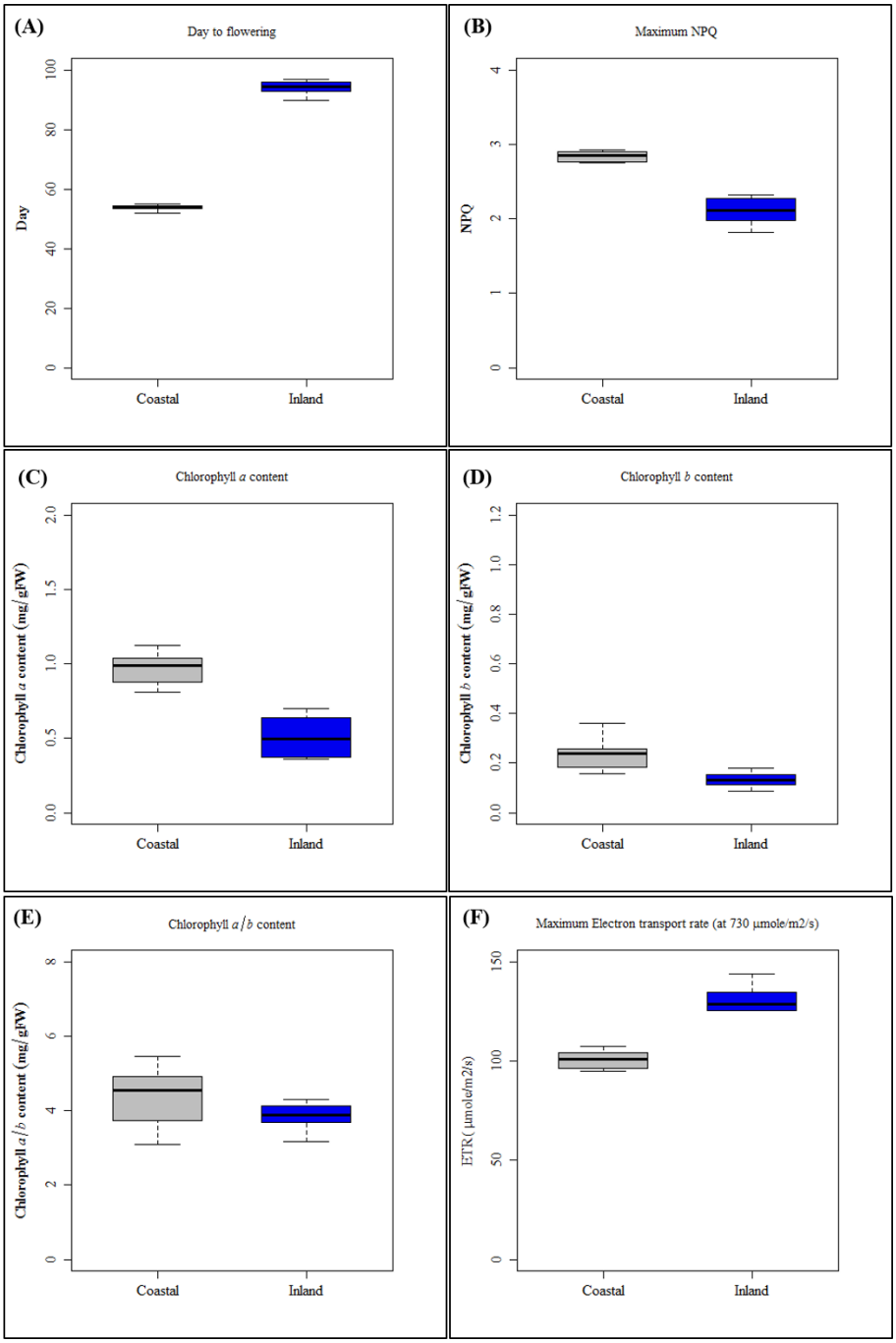

Figure D.27 – Plots show the distribution of Col-0 replicated (n=8) grown under Coastal and Inland Early Autumn of day to flowering (A), maximum NPQ (B), chlorophyll *a* (C), chlorophyll *b* (D), chlorophyll *a/b* (E), and ETR (F).

Table D.4 – Summary of NPQ QTL and candidate genes based on GWAS analyses under coastal and inland of Experiment IV and V (www.arabidopsis.org).

QTL	Chr	Region	No.	Candidate genes		Description	Selection criteria			
				Gene	Location		A	B	C	D
QTL1-1	1	347,233	1	AT1G01980	340172-341999	Member of Reticuline oxidase-like family				
			2	AT1G01990	343166-344341	unknown protein				
			3	AT1G02000	345812-347592	UDP-D-glucuronate 4-epimerase				
			4	SEC1A: AT1G02010	347891-352480	member of KEULE Gene Family				
			5	AT1G02020	352637-354969	nitroreductase family protein; FUNCTIONS IN: oxidoreductase activity, acting on NADH or NADPH, nitrogenous group as acceptor				
			6	AT1G02030	355321-357258	C2H2-like zinc finger protein; FUNCTIONS IN: sequence-specific DNA binding transcription factor activity, zinc ion binding, nucleic acid binding; INVOLVED IN: regulation of transcription				
			7	AT1G02040	358104-359078	C2H2-type zinc finger family protein; FUNCTIONS IN: sequence-specific DNA binding transcription factor activity, zinc ion binding, nucleic acid binding				
			8	LAP6: AT1G02050	359117-360518	LESS ADHESIVE POLLEN 6 (LAP6); FUNCTIONS IN: transferase activity, transferring acyl groups other than amino-acyl groups, catalytic activity, acyltransferase activity; INVOLVED IN: phenylpropanoid biosynthetic process				
QTL1-2	1	9,729,376	9	AT1G27900	9715453-9720568	RNA helicase family protein; FUNCTIONS IN: in 7 functions; INVOLVED IN: biological_process unknown				
			10	PUB45: AT1G27910	9720736-9724714	Encodes a protein containing a UND, a U-box, and an ARM domain.				
			11	MAP65-8: AT1G27920	9726948-9729848	microtubule-associated protein 65-8 (MAP65-8)				
			12	AT1G27921	9728124-9730331	Potential natural antisense gene, locus overlaps with AT1G27920				
			13	AT1G27930	9731260-9732719	Function unknown. Interacts with eIF3.				
			14	ABCB13: AT1G27940	9733597-9738129	P-glycoprotein 13 (PGP13); FUNCTIONS IN: ATPase activity, coupled to transmembrane movement of substances				
QTL1-3	1	16,351,441	15	AT1G43310	16345974-16346475	Nucleotide-sugar transporter family protein; FUNCTIONS IN: molecular_function unknown; INVOLVED IN: biological_process unknown; LOCATED IN: chloroplast				

Continued on next page.

Table D.4 – continued from previous page

QTL	Chr	Region	No.	Candidate genes		Description	Selection criteria			
				Gene	Location		A	B	C	D
			16	AT1G43320	16356762-16357118	unknown protein; FUNCTIONS IN: molecular_function unknown; INVOLVED IN: biological_process unknown				
			17	AT1G43330	16359029-16360023	Homeodomain-like superfamily protein; CONTAINS InterPro DOMAIN/s				
QTL1-4	1	16,858,769	18	AT1G44191	16,814,879- 16,872,210	Encodes a ECA1 gametogenesis related family protein				
			19	CYCLASE3: AT1G44542	16,864,970-16,866,605	Cyclase family protein; functions in: molecular function unknown				
			20	NPQ4: AT1G44575	16,871,696 - 16,873,383	Encoding PSII-S (CP22), Involved in NPQ, Mutant has a normal violaxanthin cycle but has a limited capacity of quenching singlet excited chlorophylls and is tolerant to lipid peroxidation.				
			21	AT1G44608	16,875,119-16,876,258	Unknown protein				
QTL1-5	1	20,680,932	22	AT1G55365	20,673,983-20,674,363	Protein of Unknown function ; involved in: biological process unknown				
			23	NDF5: AT1G55370	20,674,783-20,676,351	NDH-dependent cyclic electron flow 5 (NDF5); functions in: carbohydrate binding, catalytic activity; INVOLVED IN: positive regulation of gene expression, photosynthetic electron transport in photosystem I				
			24	AT1G55380	20,676,622-20,678,607	Cysteine/Histidine-rich C1 domain family protein. INVOLVED IN: oxidation-reduction process				
			25	AT1G55390	20,680,876-20,683,043	Cysteine/Histidine-rich C1 domain family protein. INVOLVED IN: oxidation-reduction process				
			26	AT1G55400	20,684,233-20,684,965	similar to unknown protein [Arabidopsis thaliana] (TAIR:AT5G27590.1)				
QTL2-1	2	10,934,450	27	emb2410: AT2G25660	10916203-10927390	embryo defective 2410 (emb2410); FUNCTIONS IN: molecular_function unknown; INVOLVED IN: embryo development ending in seed dormancy;				
			28	AT2G25670	10928664-10931057	BEST Arabidopsis thaliana protein match is: copper ion binding (TAIR:AT4G32610.1)				
			29	MOT1: AT2G25680	10933061-10934551	Encodes a high-affinity molybdate transporter. Mutant has reduced concentrations of molybdate in roots and shoots, and reduced shoot and root length when growing on Mo-limited medium.				

Continued on next page.

Table D.4 – continued from previous page

QTL	Chr	Region	No.	Candidate genes		Description	Selection criteria			
				Gene	Location		A	B	C	D
			30	SCRL17: AT2G25685	10937678-10938081	Encodes a member of a family of small, secreted, cysteine rich proteins with sequence similarity to SCR (S locus cysteine-rich protein).				
			31	AT2G25687	10939037-10939418	Encodes a defensin-like (DEFL) family protein.				
QTL2-2	2	10,984,417	32	AT2G25730	10956301-10972927	unknown protein; LOCATED IN: cellular_component unknown				
			33	AT2G25735	10975060-10975759	unknown protein				
			34	AT2G25737	10976936-10979900	Sulfite exporter TauE/SafE family protein; LOCATED IN: endomembrane system, integral to membrane				
			35	AT2G25740	10980122-10983945	ATP-dependent protease La (LON) domain protein; FUNCTIONS IN: ATP-dependent peptidase activity				
			36	AT2G25760	10984808-10988924	Protein kinase family protein; FUNCTIONS IN: protein serine/threonine kinase activity, protein kinase activity				
QTL2-3	2	11,680,235	37	AT2G27280	11673826-11675613	Coiled-coil domain-containing protein 55 (DUF2040)				
			38	AT2G27285	11675960-11678118	Coiled-coil domain-containing protein 55 (DUF2040)				
			39	AT2G27290	11678400-11679797	Protein of unknown function (DUF1279); FUNCTIONS IN: molecular_function unknown				
			40	NTL8: AT2G27300	11680417-11681955	NTM1-like 8 (NTL8); CONTAINS InterPro DOMAIN/s				
			41	AT2G27310	11683862-11684967	F-box family protein; BEST Arabidopsis thaliana protein match is: F-box family protein (TAIR:AT2G36090.1)				
			42	AT2G27315	11689591-11689953	Protein of unknown function (DUF1278); CONTAINS InterPro DOMAIN/s				
QTL4-1	4	1,509,645	43	AT4G03410	1501168-1503561	Peroxisomal membrane 22 kDa (Mpv17/PMP22) family protein; FUNCTIONS IN: molecular_function unknown				
			44	PP2C52: AT4G03415	1503573-1505855	Encodes a myristoylated 2C-type protein phosphatase that interacts with AGB1 and is localized to the plasma membrane.				
			45	AT4G03420	1511839-1514030	Protein of unknown function (DUF789)				
			46	STA1: AT4G03430	1517134-1520563	Encodes a nuclear protein similar to the human U5 small ribonucleoprotein-associated 102-kD protein and to the yeast pre-mRNA splicing factors Prp1p and Prp6p.				
QTL4-2	4	5,270,810	47	AT4G08340	5264215-5271148	similar to Ulp1 protease family protein [Arabidopsis thaliana] (TAIR:AT1G35770.1)				

Continued on next page.

Table D.4 – continued from previous page

QTL	Chr	Region	No.	Candidate genes		Description	Selection criteria			
				Gene	Location		A	B	C	D
			48	AT4G08345	5268128-5268213	similar to Ulp1 protease family protein [Brassica oleracea] (GB:ABD64941.1)				
QTL4-3	4	13,911,309	49	AT4G27900	13890644-13892995	CCT motif family protein; FUNCTIONS IN: molecular_function unknown				
			50	SDG16: AT4G27910	13894694-13900474	SET domain protein 16 (SDG16); FUNCTIONS IN: zinc ion binding				
			51	PYL10: AT4G27920	13901220-13901970	Encodes a member of the PYR (pyrabactin resistance)/PYL(PYR1-like)/RCAR (regulatory components of ABA receptor) family proteins with 14 members.				
			52	AT4G27930	13902635-13902978	unknown protein				
			53	MTM1: AT4G27940	13904474-13907245	manganese tracking factor for mitochondrial SOD2 (MTM1); FUNCTIONS IN: binding; INVOLVED IN: transport, mitochondrial transport				
			54	CRF4: AT4G27950	13909569-13910859	encodes a member of the ERF (ethylene response factor) subfamily B-5 of ERF/AP2 transcription factor family.				
QTL5-1	5	15,037,793	55	AT5G37795	15032508-15032581	tRNA-Asn (anticodon: GTT)				
			56	RSL1: AT5G37800	15036197-15037574	RHD SIX-LIKE 1 (RSL1); FUNCTIONS IN: DNA binding, sequence-specific DNA binding transcription factor activity; INVOLVED IN: regulation of transcription				
			57	NIP4;1: AT5G37810	15045232-15047807	NOD26-like intrinsic protein 4;1 (NIP4;1); FUNCTIONS IN: water channel activity; INVOLVED IN: transport, transmembrane				
QTL5-2	5	15,930,795	58	AT5G39770	15919241-15927549	Represents a non-function pseudogene homologous to AtMSU81 (At4g30870).				
			59	AT5G39785	15929188-15932276	FUNCTIONS IN: structural constituent of ribosome; INVOLVED IN: translation; LOCATED IN: ribosome				
			60	PTST: AT5G39790	15932714-15935261	Encodes a chloroplast localized protein that is involved in protein translocation and starch metabolism.				
			61	AT5G39800	15935464-15937132	Mitochondrial ribosomal protein L27; CONTAINS InterPro DOMAIN/s: Ribosomal protein L27/L41				
			62	AGL98: AT5G39810	15937278-15938344	AGAMOUS-like 98 (AGL98); FUNCTIONS IN: sequence-specific DNA binding transcription factor activity; INVOLVED IN: regulation of transcription				

Continued on next page.

Table D.4 – continued from previous page

QTL	Chr	Region	No.	Candidate genes		Description	Selection criteria			
				Gene	Location		A	B	C	D
			63	NAC094: AT5G39820	15939300-15940491	NAC domain containing protein 94 (NAC094); FUNCTIONS IN: sequence-specific DNA binding transcription factor activity; INVOLVED IN: multicellular organismal development, regulation of transcription				
QTL5-3	5	18,511,604	64	AT5G45640	18507489-18511616	Subtilisin-like serine endopeptidase family protein; FUNCTIONS IN: identical protein binding, serine-type endopeptidase activity				
			65	AT5G45650	18513431-18518868	subtilase family protein; FUNCTIONS IN: identical protein binding, serine-type endopeptidase activity				
QTL5-4	5	25,477,423	66	AT5G63630	25472598-25476511	P-loop containing nucleoside triphosphate hydrolases superfamily protein; FUNCTIONS IN: helicase activity, ATP binding				
			67	AT5G63640	25477678-25481489	ENTH/VHS/GAT family protein; FUNCTIONS IN: protein transporter activity				
			68	SNRK2.5: AT5G63650	25481517-25483719	encodes a member of SNF1-related protein kinases (SnRK2) whose activity is activated by ionic (salt) and non-ionic (mannitol) osmotic stress.				
			69	PDF2.5: AT5G63660	25485692-25486062	Predicted to encode a PR (pathogenesis-related) protein.				
			70	SPT42: AT5G63670	25487927-25489389	SPT4 homolog 2 (SPT42); FUNCTIONS IN: positive transcription elongation factor activity, zinc ion binding				

Bibliography

1001 Genome Consortium (2016), 1,135 Genomes Reveal the Global Pattern of Polymorphism in Arabidopsis thaliana. *Cell* 166: 1–11.

Al-Shehbaz, I.a. and O'Kane, S.L. (2002), Taxonomy and Phylogeny of Arabidopsis (Brassicaceae). *The Arabidopsis Book* 6(1): 1.

Alboresi, A., Dall'osto, L., Aprile, A., Carillo, P., Roncaglia, E., Cattivelli, L. and Bassi, R. (2011), Reactive oxygen species and transcript analysis upon excess light treatment in wild-type Arabidopsis thaliana vs a photosensitive mutant lacking zeaxanthin and lutein. *BMC plant biology* 11(1): 62.

Allen, J.F. and Forsberg, J. (2001), Molecular recognition in thylakoid structure and function. *Trends in Plant Science* 6(7): 317–326.

Alonso-blanco, C., Aarts, M.G.M., Bentsink, L., Keurentjes, J.J.B. and Reymond, M. (2009), What Has Natural Variation Taught Us about Plant Development , Physiology , and Adaptation ? *The Plant Cell* 21(July): 1877–1896.

Alter, P., Dreissen, A., Luo, F.L. and Matsubara, S. (2012), Acclimatory responses of Arabidopsis to fluctuating light environment: Comparison of different sunfleck regimes and accessions. *Photosynthesis Research* 113(1-3): 221–237.

Asada, K. (2006), Production and scavenging of reactive oxygen species in chloroplasts and their functions. *Plant physiology* 141(2): 391–396.

Athanasiou, K., Dyson, B.C., Webster, R.E. and Johnson, G.N. (2010), Dynamic Acclimation of Photosynthesis Increases Plant Fitness in Changing Environments. *Plant Physiology* 152(1): 366–373.

Atwell, S., Huang, Y.S., Vilhjálmsson, B.J., Willems, G., Li, Y., Meng, D., Platt, A., Tarone, A.M., Hu, T.T., Muliyati, N.W., Zhang, X., Amer, M.A., Baxter, I., Chory, J., Dean, C., Debieu, M., Meaux, J.D., Joseph, R., Faure, N., Kniskern,

J.M., Jones, J.D.G., Michael, T., Roux, F., Salt, D.E., Tang, C., Todesco, M. and Traw, M.B. (2010), Genome-wide association study of 107 phenotypes in a common set of Arabidopsis thaliana inbred lines. *Nature* 465(7298): 627–631.

Bailey, S., Horton, P. and Walters, R.G. (2004), Acclimation of Arabidopsis thaliana to the light environment: The relationship between photosynthetic function and chloroplast composition. *Planta* 218(5): 793–802.

Bailey, S., Walters, R.G., Jansson, S. and Horton, P. (2001), Acclimation of Arabidopsis thaliana to the light environment: The existence of separate low light and high light responses. *Planta* 213(5): 794–801.

Baker, N.R. (2008), Chlorophyll fluorescence: a probe of photosynthesis in vivo. *Annual review of plant biology* 59: 89–113.

Balasubramanian, S., Schwartz, C., Singh, A., Warthmann, N., Kim, M.C., Maloof, J.N., Loudet, O., Trainer, G.T., Dabi, T., Borevitz, J.O., Chory, J. and Weigel, D. (2009), QTL mapping in new Arabidopsis thaliana advanced intercross-recombinant inbred lines. *PLoS ONE* 4(2): 1–8.

Ballottari, M., Dall'Osto, L., Morosinotto, T. and Bassi, R. (2007), Contrasting behavior of higher plant photosystem I and II antenna systems during acclimation. *Journal of Biological Chemistry* 282(12): 8947–8958.

Bellafiore, S., Barneche, F., Peltier, G. and Rochaix, J.D. (2005), State transitions and light adaptation require chloroplast thylakoid protein kinase STN7. *Nature* 433(7028): 892–895.

Bentsink, L., Hanson, J., Hanhart, C.J., Blankestijn-de Vries, H., Coltrane, C., Keizer, P., El-Lithy, M., Alonso-Blanco, C., de Andrés, M.T., Reymond, M., van Eeuwijk, F., Smeekens, S. and Koornneef, M. (2010), Natural variation for seed dormancy in Arabidopsis is regulated by additive genetic and molecular pathways. *Pnas* 107(9): 4264–4269.

Bergelson, J. and Roux, F. (2010), Towards identifying genes underlying ecologically relevant traits in Arabidopsis thaliana. *Nature reviews. Genetics* 11(12): 867–879.

Betterle, N., Ballottari, M., Zorzan, S., Bianchi, S.D., Cazzaniga, S., Osto, L.D., Morosinotto, T. and Bassi, R. (2009), Light-induced Dissociation of an Antenna

Hetero-oligomer Is Needed for Non-photochemical Quenching Induction âŰą. *The Journal of Biological Chemistry* 284(22): 15255–15266.

Bianchi, S.D., Betterle, N., Kouril, R., Cazzaniga, S., Boekema, E., Bassi, R. and Dall'osto, L. (2011), Arabidopsis Mutants Deleted in the Light-Harvesting Protein Lhcb4 Have a Disrupted Photosystem II Macrostructure and Are Defective in Photoprotection. *The Plant cell* 23(7): 2659–2679.

Björkman, O. (1987), Photon yield of O2 evolution and chloropgyll fluorescence characteristics at 77 K among vascular plant of diverse origin. *Planta* 170: 489–504.

Blankenship, R.E. (2002), *Molecular Mechanisms of Photosynthesis*, volume 4. Blackwell Science, Malden, MA.

Borevitz, J.O., Maloof, J.N., Lutes, J., Dabi, T., Redfern, J.L., Trainer, G.T., Werner, J.D., Asami, T., Berry, C.C., Weigel, D. and Chory, J. (2002), Quantitative trait loci controlling light and hormone response in two accessions of Arabidopsis thaliana. *Genetics* 160(2): 683–696.

Botto, J.F., Alonso-Blanco, C., Garzarón, I., Sánchez, R.a. and Casal, J.J. (2003), The Cape Verde Islands allele of cryptochrome 2 enhances cotyledon unfolding in the absence of blue light in Arabidopsis. *Plant physiology* 133(December): 1547–1556.

Brachi, B., Morris, G.P. and Borevitz, J.O. (2011), Genome-wide association studies in plants: the missing heritability is in the field. *Genome biology* 12(10): 232.

Broman, K.W. (2005), The genomes of recombinant inbred lines. *Genetics* 169(2): 1133–1146.

Brown, T.B., Cheng, R., Sirault, X.R.R., Rungrat, T., Murray, K.D., Trtilek, M., Furbank, R.T., Badger, M., Pogson, B.J. and Borevitz, J.O. (2014), TraitCapture: Genomic and environment modelling of plant phenomic data. *Current Opinion in Plant Biology* 18(1): 73–79.

Butler, W.L. (1978), Energy distribution in the photochemical apparatus of photosynthesis. *Annu. Rev. Plant. Physiol* 29: 345–378.

Cardol, P., Alric, J., Girard-Bascou, J., Franck, F., Wollman, F.A. and Finazzi, G. (2009), Impaired respiration discloses the physiological significance of state

transitions in Chlamydomonas. *Proceedings of the National Academy of Sciences of the United States of America* 106(37): 15979–15984.

Cavanagh, C., Morell, M., Mackay, I. and Powell, W. (2008), From mutations to MAGIC: resources for gene discovery, validation and delivery in crop plants. *Current Opinion in Plant Biology* 11(2): 215–221.

Cheng, R., Abney, M., Palmer, A.a. and Skol, A.D. (2011), QTLRel: an R Package for Genome-wide Association Studies in which Relatedness is a Concern. *BMC genetics* 12(1): 66.

Cheng, R., Borevitz, J. and Doerge, R.W. (2013), Selecting informative traits for multivariate quantitative trait locus mapping helps to gain optimal power. *Genetics* 195(3): 683–691.

Clarke, J.D. (2009), Cetyltrimethyl ammonium bromide (CTAB) DNA miniprep for plant DNA isolation. *Cold Spring Harbor Protocols* 4(3): 5177–5179.

Cookson, S.J. and Granier, C. (2006), A dynamic analysis of the shade-induced plasticity in Arabidopsis thaliana rosette leaf development reveals new components of the shade-adaptative response. *Annals of Botany* 97(3): 443–452.

Crouchman, S., Ruban, A. and Horton, P. (2006), PsbS enhances nonphotochemical fluorescence quenching in the absence of zeaxanthin. *FEBS Letters* 580(8): 2053–2058.

Dall'Osto, L., Cazzaniga, S., Wada, M. and Bassi, R. (2014), On the origin of a slowly reversible fluorescence decay component in the Arabidopsis npq4 mutant. *Philosophical transactions of the Royal Society of London. Series B, Biological sciences* 369(1640): 20130221.

Demmig-Adams, B. and Adams, W. (1996), The role of xanthophyll cycle carotenoids in protection of photosynthesis. *Trends in Plant Science* 1: 21–26.

Demmig-Adams, B., Stewart, J.J. and Adams III, W. (2014), Non-photochemical quenching and energy dissipation in plants, algae and cyanobacteria. *In Advances in Photosynthesis and Respiration 40*, chapter Chloroplas, Springer Dordrecht Heidelberg New York London.

Eberhard, S., Finazzi, G. and Wollman, F.A. (2008), The dynamics of photosynthesis. *Annual review of genetics* 42: 463–515.

El-Assal, S.D., Alonso-Blanco, C., Peeters, a.J., Raz, V. and Koornneef, M. (). *Nature genetics* (4): 435–440.

El-Lithy, M.E., Rodrigues, G.C., Van Rensen, J.J.S., Snel, J.F.H., Dassen, H.J.H.A., Koornneef, M., Jansen, M.A.K., Aarts, M.G.M. and Vreugdenhil, D. (2005), Altered photosynthetic performance of a natural Arabidopsis accession is associated with atrazine resistance. *Journal of Experimental Botany* 56(416): 1625–1634.

Elshire, R.J., Glaubitz, J.C., Sun, Q., Poland, J.A., Kawamoto, K., Buckler, E.S. and Mitchell, S.E. (2011), A robust, simple genotyping-by-sequencing (GBS) approach for high diversity species. *PLoS ONE* 6(5): 1–10.

Essemine, J., Govindachary, S., Joly, D., Ammar, S., Bouzid, S. and Carpentier, R. (2012), Biochimica et Biophysica Acta Effect of moderate and high light on photosystem II function in Arabidopsis thaliana depleted in digalactosyldiacylglycerol âŸĘ. *BBA - Bioenergetics* 1817(8): 1367–1373.

Filiault, D.L. and Maloof, J.N. (2012), A genome-wide association study identifies variants underlying the arabidopsis thaliana shade avoidance response. *PLoS Genetics* 8(3).

Finazzi, G., Johnson, G.N., Dall'Osto, L., Joliot, P., Wollman, F.A. and Bassi, R. (2004), A zeaxanthin-independent nonphotochemical quenching mechanism localized in the photosystem II core complex. *Proceedings of the National Academy of Sciences of the United States of America* 101(33): 12375–12380.

Foyer, C.H., Neukermans, J., Queval, G., Noctor, G. and Harbinson, J. (2012), Photosynthetic control of electron transport and the regulation of gene expression. *Journal of Experimental Botany* 63(4): 1637–1661.

García-Plazaola, J.I., Esteban, R., Fernández-Marín, B., Kranner, I. and Porcar-Castell, A. (2012), Thermal energy dissipation and xanthophyll cycles beyond the Arabidopsis model. *Photosynthesis Research* 113(1-3): 89–103.

Gechev, T.S., Van Breusegem, F., Stone, J.M., Denev, I. and Laloi, C. (2006), Reactive oxygen species as signals that modulate plant stress responses and programmed cell death. *BioEssays* 28(11): 1091–1101.

Gibson, G. (2012), Rare and common variants: twenty arguments. *Nature Reviews Genetics* 13(2): 135–145.

Golan, T., Müller-Moulé, P. and Niyogi, K.K. (2006), Photoprotection mutants of Arabidopsis thaliana acclimate to high light by increasing photosynthesis and specific antioxidants. *Plant, Cell and Environment* 29(5): 879–887.

GonZalez-Pérez, S., Gutiérrez, J., García-García, F., Osuna, D., Dopazo, J., Lorenzo, O., Revuelta, J.L. and Arellano, J.B. (2011), Early Transcriptional Defense Responses in Arabidopsis Cell Suspension Culture under 156(July): 1439–1456.

Govindjee (1995), Sixty-three Years Sine Kautsky: Chlorophyll a fluorescence. *Journal of pharmaceutical sciences* 22: 131–160.

Graßes, T., Pesaresi, P., Schiavon, F., Varotto, C., Salamini, F., Jahns, P. and Leister, D. (2002), The role of ΔpH-dependent dissipation of excitation energy in protecting photosystem II against light-induced damage in Arabidopsis thaliana. *Plant Physiology and Biochemistry* 40(1): 41–49.

Green, B.R. and Durnford, D.G. (1996), the Chlorophyll-Carotenoid Proteins of Oxygenic Photosynthesis. *Annual Review of Plant Physiology and Plant Molecular Biology* 47(1): 685–714.

Halliday, K.J., Salter, M.G., Thingnaes, E. and Whitelam, G.C. (2003), Phytochrome control of flowering is temperature sensitive and correlates with expression of the floral integrator FT. *Plant Journal* 33(5): 875–885.

Harvaux, M. and Kloppstech, K. (2001), The protective functions of carotenoid and flavonoid pigments against excess visible radiation at chilling temperature investigated in Arabidopsis npq and tt mutants. *Planta* 213: 953–966.

Havaux, M., Bonfils, J.p., Lutz, C. and Niyogi, K.K. (2000), Photodamage of the Photosynthetic Apparatus and Its Dependence on the Leaf Developmental Stage in the. *Society* 124(September): 273–284.

Havaux, M. and Niyogi, K.K. (1999), The violaxanthin cycle protects plants from photooxidative damage by more than one mechanism. *Proceedings of the National Academy of Sciences of the United States of America* 96(15): 8762–8767.

Hendrickson, L., Förster, B., Furbank, R.T. and Chow, W.S. (2004), Processes contributing to photoprotection of grapevine leaves illuminated at low temperature. *Physiol. Plant.* 121(2): 272–281.

Heyneke, E., Luschin-Ebengreuth, N., Krajcer, I., Wolkinger, V., Müller, M. and

Zechmann, B. (2013), Dynamic compartment specific changes in glutathione and ascorbate levels in Arabidopsis plants exposed to different light intensities. *BMC Plant Biology* 13: 104–123.

Horton, M.W., Hancock, A.M., Huang, Y.S., Toomajian, C., Atwell, S., Auton, A., Muliyati, N.W., Platt, A., Sperone, F.G., Vilhjálmsson, B.J., Nordborg, M., Borevitz, J.O. and Bergelson, J. (2012), Genome-wide patterns of genetic variation in worldwide Arabidopsis thaliana accessions from the RegMap panel. *Nature genetics* 44(2): 212–6.

Hossain, M.A., Teixeira, J.a. and Fujita, M. (2011), Glyoxalase System and Reactive Oxygen Species Detoxification System in Plant Abiotic Stress Response and Tolerance : An Intimate Relationship. *Abiotic Stress in Plants - Mechanisms and Adaptations* : 235–266.

Huang, X., Wei, X., Sang, T., Zhao, Q., Feng, Q., Zhao, Y., Li, C., Zhu, C., Lu, T., Zhang, Z., Li, M., Fan, D., Guo, Y., Wang, A., Wang, L., Deng, L., Li, W.W., Lu, Y., Weng, Q., Liu, K., Huang, T., Zhou, T., Jing, Y., Li, W.W., Lin, Z., Buckler, E.S., Qian, Q., Zhang, Q.F., Li, J. and Han, B. (2010), Genome-wide association studies of 14 agronomic traits in rice landraces. *Nature genetics* 42(11): 961–967.

Ihnken, S., Kromkamp, J.C. and Beardall, J. (2011), Photoacclimation in Dunaliella tertiolecta reveals a unique NPQ pattern upon exposure to irradiance. *Photosynthesis Research* 110(2): 123–137.

Ishida, S., Takabayashi, A., Ishikawa, N., Hano, Y., Endo, T. and Sato, F. (2009), A novel nuclear-encoded protein, NDH-dependent cyclic electron flow 5, is essential for the accumulation of chloroplast NAD(P)H dehydrogenase complexes. *Plant and Cell Physiology* 50(2): 383–393.

Jacoby, W.G. (2000), Loess: A nonparametric, graphical tool for depicting relationships between variables. *Electoral Studies* 19(4): 577–613.

Johansson Jänkänpää, H. (2011), *Stress Responses of Arabidopsis Plants with a Varying Level of Non- photochemical Quenching*. KBC, Umeå University, Umeå, Sweden.

Johansson Jänkänpää, H., Frenkel, M., Zulfugarov, I., Reichelt, M., Krieger-Liszkay, A., Mishra, Y., Gershenzon, J., Moen, J., Lee, C.H. and Jansson, S. (2013), Non-Photochemical Quenching Capacity in Arabidopsis thaliana Affects Herbivore Behaviour. *PLoS ONE* 8(1).

Johnson, G.N., Young, A.J., Scholes, J.D. and Horton, P. (1993), The dissipation of excess excitation energy in British plant species. *Plant, cell and environment* 16(1993): 673–679.

Johnson, M.P., Davison, P.A., Ruban, A.V. and Horton, P. (2008), The xanthophyll cycle pool size controls the kinetics of non-photochemical quenching in Arabidopsis thaliana. *FEBS Letters* 582(2): 262–266.

Johnson, M.P., Perez-Bueno, M.L., Zia, A., Horton, P. and Ruban, A.V. (2009), The Zeaxanthin-Independent and Zeaxanthin-Dependent qE Components of Nonphotochemical Quenching Involve Common Conformational Changes within the Photosystem II Antenna in Arabidopsis. *Plant Physiology* 149(2): 1061–1075.

Johnson, M.P. and Ruban, A.V. (2010), Arabidopsis plants lacking PsbS protein possess photoprotective energy dissipation. *Plant Journal* 61(2): 283–289.

Johnson, M.P. and Ruban, A.V. (2011), Restoration of rapidly reversible photoprotective energy dissipation in the absence of PsbS protein by enhanced ΔpH. *Journal of Biological Chemistry* 286(22): 19973–19981.

Joliot, P.a. and Finazzi, G. (2010), Proton equilibration in the chloroplast modulates multiphasic kinetics of nonphotochemical quenching of fluorescence in plants. *Proceedings of the National Academy of Sciences of the United States of America* 107: 12728–12733.

Jung, H.s. and Niyogi, K.K. (2009), Quantitative genetic analysis of thermal dissipation in Arabidopsis. *Plant Physiology* 150(2): 977–86.

Karp, G. (2009), *Cell and Molecular Biology: Concepts and Experiments. 6th ed.* John-Wiley and Sons Limited.

Keurentjes, J.J.B., Bentsink, L., Alonso-Blanco, C., Hanhart, C.J., Vries, H.B.D., Effgen, S., Vreugdenhil, D. and Koornneef, M. (2007), Development of a near-isogenic line population of Arabidopsis thaliana and comparison of mapping power with a recombinant inbred line population. *Genetics* 175(2): 891–905.

Khanna-Chopra, R. (2012), Leaf senescence and abiotic stresses share reactive oxygen species-mediated chloroplast degradation. *Protoplasma* 249(3): 469–481.

Kim, E.H., Li, X.P., Razeghifard, R., Anderson, J.M., Niyogi, K.K., Pogson, B.J. and Chow, W.S. (2009), The multiple roles of light-harvesting chlorophyll

a/b-protein complexes define structure and optimize function of Arabidopsis chloroplasts: A study using two chlorophyll b-less mutants. *Biochimica et Biophysica Acta - Bioenergetics* 1787(8): 973–984.

Koornneef, M., Alonso-Blanco, C. and Vreugdenhil, D. (2004), Naturally occurring genetic variation in Arabidopsis thaliana. *Annual Review of Plant Biology* 55(1): 141–172.

Korte, A. and Farlow, A. (2013), The advantages and limitations of trait analysis with GWAS: a review. *Plant methods* 9(1): 29.

Kover, P.X., Valdar, W., Trakalo, J., Scarcelli, N., Ehrenreich, I.M., Purugganan, M.D., Durrant, C. and Mott, R. (2009), A multiparent advanced generation inter-cross to fine-map quantitative traits in Arabidopsis thaliana. *PLoS Genetics* 5(7).

Krause, G. (1991), Chlorophyll fluorescence and photosynthesis : The Basics. *Annual Review of Plant Physiology and Plant Molecular Biology* 42: 313–349.

Krinsky, N. (1971), *Function in Caroteniods*. Birkhauser, Basel.

Kulheim, C., Agren, J. and Jansson, S. (2002), Rapid Regulation of Light Harvesting and Plant Fitness in the Field. *Science* 297(5578): 91–93.

Kump, K.L., Bradbury, P.J., Wisser, R.J., Buckler, E.S., Belcher, A.R., Oropeza-Rosas, M.a., Zwonitzer, J.C., Kresovich, S., McMullen, M.D., Ware, D., Balint-Kurti, P.J. and Holland, J.B. (2011), Genome-wide association study of quantitative resistance to southern leaf blight in the maize nested association mapping population. *Nature Genetics* 43(2): 163–168.

Lambrev, P.H., Nilkens, M., Miloslavina, Y., Jahns, P. and Holzwarth, A.R. (2010), Kinetic and spectral resolution of multiple nonphotochemical quenching components in Arabidopsis leaves. *Plant physiology* 152(3): 1611–1624.

Li, B., Suzuki, J.I. and Hara, T. (1998), Latitudinal variation in plant size and relative growth rate in Arabidopsis thaliana. *Oecologia* 115(3): 293–301.

Li, X.P., Björkman, O., Shih, C., Grossman, A.R., Rosenquist, M., Jansson, S. and Niyogi, K.K. (2000), A pigment-binding protein essential for regulation of photosynthetic light harvesting. *Nature* 403(6768): 391–5.

Li, X.P., Gilmore, A.M., Caffarri, S., Bassi, R., Golan, T., Kramer, D. and Niyogi,

K.K. (2004), Regulation of photosynthetic light harvesting involves intrathylakoid lumen pH sensing by the PsbS protein. *Journal of Biological Chemistry* 279(22): 22866–22874.

Li, X.P., Muller-Moule, P., Gilmore, A.M. and Niyogi, K.K. (2002), PsbS-dependent enhancement of feedback de-excitation protects photosystem II from photoinhibition. *Proceedings of the National Academy of Sciences of the United States of America* 99(23): 15222–15227.

Li, Y., Cheng, R., Spokas, K.A., Palmer, A.A. and Borevitz, J.O. (2014), Genetic variation for life history sensitivity to seasonal warming in Arabidopsis thaliana. *Genetics* 196(2): 569–577.

Li, Y., Huang, Y., Bergelson, J., Nordborg, M. and Borevitz, J.O. (2010), Association mapping of local climate-sensitive quantitative trait loci in Arabidopsis thaliana. *Proceedings of the National Academy of Sciences* 107(49): 21199–21204.

Li, Z., Ahn, T.K., Avenson, T.J., Ballottari, M., Cruz, J.a., Kramer, D.M., Bassi, R., Fleming, G.R., Keasling, J.D. and Niyogi, K.K. (2009), Lutein accumulation in the absence of zeaxanthin restores nonphotochemical quenching in the Arabidopsis thaliana npq1 mutant. *The Plant cell* 21(6): 1798–1812.

Ling, Q., Huang, W. and Jarvis, P. (2011), Use of a SPAD-502 meter to measure leaf chlorophyll concentration in Arabidopsis thaliana. *Photosynthesis Research* 107(2): 209–214.

Loudet, O., Chaillou, S., Camilleri, C., Bouchez, D. and Daniel-Vedele, F. (2002), Bay-0 x Shahdara recombinant inbred line population: A powerful tool for the genetic dissection of complex traits in Arabidopsis. *Theoretical and Applied Genetics* 104(6-7): 1173–1184.

Lu, Y. (2016), Identification and Roles of Photosystem II Assembly, Stability, and Repair Factors in Arabidopsis. *Frontiers in Plant Science* 7(February): 168.

Ma, Y.Z., Holt, N.E., Li, X.P., Niyogi, K.K. and Fleming, G.R. (2003), Evidence for direct carotenoid involvement in the regulation of photosynthetic light harvesting. *Proceedings of the National Academy of Sciences of the United States of America* 100(8): 4377–4382.

Maruta, T., Noshi, M., Tanouchi, A., Tamoi, M., Yabuta, Y., Yoshimura, K., Ishikawa, T. and Shigeoka, S. (2012), H 2O 2-triggered retrograde signaling

from chloroplasts to nucleus plays specific role in response to stress. *Journal of Biological Chemistry* 287(15): 11717–11729.

Mathis, P., Butler, W.L. and Satoh, K. (1979), Carotenoid Triplet State and Chlorophyll Fluorescence Quenching in Chloroplasts and Subchloroplast Particles. *Photochemistry and Photobiology* 30(5): 603–614.

Matsubara, S., Förster, B., Waterman, M., Robinson, S.a., Pogson, B.J., Gunning, B. and Osmond, B. (2012), From ecophysiology to phenomics: some implications of photoprotection and shade-sun acclimation in situ for dynamics of thylakoids in vitro. *Philosophical transactions of the Royal Society of London. Series B, Biological sciences* 367(1608): 3503–14.

Matsubara, S., Krause, G.H., Aranda, J., Virgo, A., Beisel, K.G., Jahns, P. and Winter, K. (2009), Sun-shade patterns of leaf carotenoid composition in 86 species of neotropical forest plants. *Functional Plant Biology* 36(1): 20–36.

Maxwell, K. and Johnson, G.N. (2000), Chlorophyll fluorescence–a practical guide. *Journal of experimental botany* 51(345): 659–668.

Meijón, M., Satbhai, S.B., Tsuchimatsu, T. and Busch, W. (2014), Genome-wide association study using cellular traits identifies a new regulator of root development in Arabidopsis. *Nature genetics* 46(1): 77–81.

Mhamdi, A., Queval, G., Chaouch, S., Vanderauwera, S., Van Breusegem, F. and Noctor, G. (2010), Catalase function in plants: A focus on Arabidopsis mutants as stress-mimic models. *Journal of Experimental Botany* 61(15): 4197–4220.

Mishra, Y., Johansson Jänkänpää, H., Kiss, A.Z., Funk, C., Schröder, W.P. and Jansson, S. (2012), Arabidopsis plants grown in the field and climate chambers significantly differ in leaf morphology and photosystem components. *BMC Plant Biology* 12(1): 6.

Mittler, R. and Blumwald, E. (2015), The roles of ROS and ABA in systemic acquired acclimation. *The Plant cell* 27(1): 64–70.

Miyaji, T., Kuromori, T., Takeuchi, Y., Yamaji, N., Yokosho, K., Shimazawa, A., Sugimoto, E., Omote, H., Ma, J.F., Shinozaki, K. and Moriyama, Y. (2015), AtPHT4;4 is a chloroplast-localized ascorbate transporter in Arabidopsis. *Nature communications* 6(5928): 1–11.

Müller, P., Li, X.P. and Niyogi, K.K. (2001), Non-photochemical quenching. A response to excess light energy. *Plant physiology* 125(4): 1558–1566.

Munekage, Y., Hojo, M., Meurer, J., Endo, T., Tasaka, M. and Shikanai, T. (2002), PGR5 is involved in cyclic electron flow around photosystem I and is essential for photoprotection in Arabidopsis. *Cell* 110(3): 361–371.

Munekage, Y., Takeda, S., Endo, T., Jahns, P., Hashimoto, T. and Shikanai, T. (2001), Cytochrome b6f mutation specifically affects thermal dissipation of absorbed light energy in Arabidopsis. *Plant Journal* 28(3): 351–359.

Murchie, E.H. and Niyogi, K.K. (2011), Manipulation of photoprotection to improve plant photosynthesis. *Plant physiology* 155(1): 86–92.

Nilkens, M., Kress, E., Lambrev, P., Miloslavina, Y., Müller, M., Holzwarth, A.R. and Jahns, P. (2010), Identification of a slowly inducible zeaxanthin-dependent component of non-photochemical quenching of chlorophyll fluorescence generated under steady-state conditions in Arabidopsis. *Biochimica et Biophysica Acta - Bioenergetics* 1797(4): 466–475.

Niyogi, K. (1999), Photoprotection revisited: genetic and molecular approaches. *Annu. Rev. Plant. Physiol. Plant. Mol. BioL* 50: 333–359.

Niyogi, K.K. (1998), Arabidopsis Mutants Define a Central Role for the Xanthophyll Cycle in the Regulation of Photosynthetic Energy Conversion. *the Plant Cell Online* 10(7): 1121–1134.

Niyogi, K.K., Li, X.P., Rosenberg, V. and Jung, H.S. (2005), Is PsbS the site of non-photochemical quenching in photosynthesis? *Journal of Experimental Botany* 56(411): 375–382.

Niyogi, K.K., Shih, C., Soon Chow, W., Pogson, B.J., Dellapenna, D. and Björkman, O. (2001), Photoprotection in a zeaxanthin- and lutein-deficient double mutant of Arabidopsis. *Photosynthesis research* 67(1-2): 139–45.

Nordborg, M., Hu, T.T., Ishino, Y., Jhaveri, J., Toomajian, C., Zheng, H., Bakker, E., Calabrese, P., Gladstone, J., Goyal, R., Jakobsson, M., Kim, S., Morozov, Y., Padhukasahasram, B., Plagnol, V., Rosenberg, N.A., Shah, C., Wall, J.D., Wang, J., Zhao, K., Kalbfleisch, T., Schulz, V., Kreitman, M. and Bergelson, J. (2005), The pattern of polymorphism in Arabidopsis thaliana. *PLoS Biology* 3(7): 1289–1299.

Osmond, C.B., Ramus, J., Levavasseur, G., Franklin, L.A. and Henley, W.J. (1993), Fluorescence quenching during photosynthesis and photoinhibition of Ulva rotundata blid. *Planta* 190(1): 97–106.

Peng, L. and Shikanai, T. (2011), Supercomplex formation with photosystem I is required for the stabilization of the chloroplast NADH dehydrogenase-like complex in Arabidopsis. *Plant physiology* 155(4): 1629–39.

Pérez-Pérez, J.M., Serrano-Cartagena, J. and Micol, J.L. (2002), Genetic analysis of natural variations in the architecture of Arabidopsis thaliana vegetative leaves. *Genetics* 162(2): 893–915.

Pigliucci, M. (2002), Ecology and evolutionary biology of Arabidopsis. *The Arabidopsis book / American Society of Plant Biologists* 1(1): e0003.

Pogson, B.J., Niyogi, K.K., Björkman, O. and DellaPenna, D. (1998), Altered xanthophyll compositions adversely affect chlorophyll accumulation and nonphotochemical quenching in Arabidopsis mutants. *Proceedings of the National Academy of Sciences of the United States of America* 95(22): 13324–13329.

Porra, R.J. (2002), The chequered history of the development and use of simultaneous equations for the accurate determination of chlorophylls a and b. *Photosynthesis Research* 73(1-3): 149–156.

Price, A.L., Patterson, N.J., Plenge, R.M., Weinblatt, M.E., Shadick, N.A. and Reich, D. (2006), Principal components analysis corrects for stratification in genome-wide association studies. *Nat Genet* 38(8): 904–909.

Ramel, F., Sulmon, C., Bogard, M., Couée, I. and Gouesbet, G. (2009), Differential patterns of reactive oxygen species and antioxidative mechanisms during atrazine injury and sucrose-induced tolerance in Arabidopsis thaliana plantlets. *BMC plant biology* 9: 28.

Ritchie, R.J. (2006), Consistent sets of spectrophotometric chlorophyll equations for acetone, methanol and ethanol solvents. *Photosynthesis Research* 89(1): 27–41.

Roach, T. and Krieger-Liszkay, A. (2012), The role of the PsbS protein in the protection of photosystems i and II against high light in Arabidopsis thaliana. *Biochimica et Biophysica Acta - Bioenergetics* 1817(12): 2158–2165.

Rockman, M.V. and Kruglyak, L. (2008), Breeding designs for recombinant inbred advanced intercross lines. *Genetics* 179(2): 1069–1078.

Rooijen, R.V., Aarts, M.G.M. and Harbinson, J. (2015), Natural genetic variation for acclimation of photosynthetic light use efficiency to growth irradiance in Arabidopsis. *Plant physiology* 167(4): 1412–29.

Ruban, A.V. and Horton, P. (1995), Regulation of non-photochemical quenching of chlorophyll fluorescence in plants. *Australian Journal of Plant Physiology* 22(2): 221–230.

Ruban, A.V. and Murchie, E.H. (2012), Assessing the photoprotective effectiveness of non-photochemical chlorophyll fluorescence quenching: A new approach. *Biochimica et Biophysica Acta - Bioenergetics* 1817(7): 977–982.

Salomé, P.A., Bomblies, K., Laitinen, R.A.E., Yant, L., Mott, R. and Weigel, D. (2011), Genetic architecture of flowering-time variation in Arabidopsis thaliana. *Genetics* 188(2): 421–433.

Schöttler, M.a. and Tóth, S.Z. (2014), Photosynthetic complex stoichiometry dynamics in higher plants: environmental acclimation and photosynthetic flux control. *Frontiers in plant science* 5(MAY): 188.

Sener, M.K., Jolley, C., Ben-Shem, A., Fromme, P., Nelson, N., Croce, R. and Schulten, K. (2005), Comparison of the light-harvesting networks of plant and cyanobacterial photosystem I. *Biophysical journal* 89(3): 1630–1642.

Sestak, Z. (1999), Chlorophyll fluorescence kinetic depends on age of leaves and plants. *In The Chloroplast: From Molecular Biology to Biotechnology*, Kluwer Academic Publishers, pp. 291–296.

Sgherri, C.L.M., Pinzino, C. and Navari-Izzo, F. (1996), Sunflower seedlings subjected to increasing stress by water deficit: Changes in O2 âĂć- production related to the composition of thylakoid membranes. *Physiologia Plantarum* 96(3): 446–452.

Sharma, P., Jha, A.B., Dubey, R.S. and Pessarakli, M. (2012), Reactive Oxygen Species, Oxidative Damage, and Antioxidative Defense Mechanism in Plants under Stressful Conditions. *Journal of Botany* 2012: 1–26.

Shindo, C., Bernasconi, G. and Hardtke, C.S. (2007), Natural genetic variation in arabidopsis: Tools, traits and prospects for evolutionary ecology. *Annals of Botany* 99(6): 1043–1054.

Shumbe, L., Chevalier, A., Legeret, B., Taconnat, L., Monnet, F. and Havaux, M.

(2016), Singlet Oxygen-Induced Cell Death in Arabidopsis under High Light Stress is Controlled by OXI1 Kinase. *Plant physiology* 170(March): 1757–1771.

Somerville, C. and Koornneef, M. (2002), A fortunate choice: the history of Arabidopsis as a model plant. *Nature reviews. Genetics* 3(11): 883–889.

Stemke, J.A. and Santiago, L.S. (2011), Consequences of light absorptance in calculating electron transport rate of desert and succulent plants. *Photosynthetica* 49(2): 195–200.

Stewart, J.J., Adams, W.W., Cohu, C.M., Polutchko, S.K., Lombardi, E.M. and Demmig-Adams, B. (2015), Differences in light-harvesting, acclimation to growth-light environment, and leaf structural development between Swedish and Italian ecotypes of Arabidopsis thaliana. *Planta* 242(6): 1277–1290.

Suorsa, M., Järvi, S., Grieco, M., Nurmi, M., Pietrzykowska, M., Rantala, M., Kangasjärvi, S., Paakkarinen, V., Tikkanen, M., Jansson, S. and Aro, E.M. (2012), PROTON GRADIENT REGULATION5 is essential for proper acclimation of Arabidopsis photosystem I to naturally and artificially fluctuating light conditions. *The Plant cell* 24(7): 2934–48.

Svistoonoff, S., Creff, A., Reymond, M., Sigoillot-Claude, C., Ricaud, L., Blanchet, A., Nussaume, L. and Desnos, T. (2007), Root tip contact with low-phosphate media reprograms plant root architecture. *Nature genetics* 39(6): 792–796.

Takahashi, S. and Badger, M.R. (2011), Photoprotection in plants: A new light on photosystem II damage. *Trends in Plant Science* 16(1): 53–60.

Takahashi, S. and Murata, N. (2008), How do environmental stresses accelerate photoinhibition? *Trends in Plant Science* 13(4): 178–182.

Teng, S., Rognoni, S., Bentsink, L. and Smeekens, S. (2008), The Arabidopsis GSQ5/DOG1 Cvi allele is induced by the ABA-mediated sugar signalling pathway, and enhances sugar sensitivity by stimulating ABI4 expression. *Plant Journal* 55(3): 372–381.

The Arabidopsis Genome Initiative (2000), Analysis of the genome sequence of the flowering plant Arabidopsis thaliana. *Nature* 408(6814): 796–815.

Thines, B.C., Youn, Y., Duarte, M.I. and Harmon, F.G. (2014), The time of day

effects of warm temperature on flowering time involve PIF4 and PIF5. *Journal of Experimental Botany* 65(4): 1141–1151.

Tikkanen, M., Grieco, M., Kangasjärvi, S. and Aro, E.M. (2010), Thylakoid Protein Phosphorylation in Higher Plant Chloroplasts Optimizes Electron Transfer under Fluctuating Light. *Plant Physiology* 152(2): 723–735.

Tikkanen, M., Piippo, M., Suorsa, M., Sirpiö, S., Paula, M., Vainonen, J., Vener, A., Allahverdiyeva, Y. and Aro, E.M. (2006), State transitions revisited - A buffering system for dynamic low light acclimation of Arabidopsis. *Plant Molecular Biology* 62(4-5): 779–793.

Tripathy, B.C. and Oelmüller, R. (2012), Reactive oxygen species generation and signaling in plants. *Plant Signaling & Behavior* 7(12): 1621–1633.

Trontin, C., Tisné, S., Bach, L. and Loudet, O. (2011), What does Arabidopsis natural variation teach us (and does not teach us) about adaptation in plants? *Current Opinion in Plant Biology* 14(3): 225–231.

Tsukaya, H. (2005), Leaf shape: Genetic controls and environmental factors. *International Journal of Developmental Biology* 49(5-6): 547–555.

Turan, S. (2012), Light Acclimation in Plants : Photoinhibition and Photoprotection. *Advances in bioresearch* 3(1): 90–94.

Umate, P. (2010), Genome-wide analysis of the family of light-harvesting chlorophyll a/b-binding proteins in Arabidopsis and rice. *Plant signaling & behavior* 5(12): 1537–42.

Visscher, P.M., Hill, W.G. and Wray, N.R. (2008), Heritability in the genomics era âĂŤ concepts and misconceptions. *Nature Reviews Genetics* 9(4): 255–266.

Walters, R.G. (2005), Towards an understanding of photosynthetic acclimation. *Journal of Experimental Botany* 56(411): 435–447.

Warren, C.R. (2008), Rapid Measurement of Chlorophylls with a Microplate Reader. *Journal of Plant Nutrition* 31(7): 1321–1332.

Weigel, D. (2012), Natural Variation in Arabidopsis: From Molecular Genetics to Ecological Genomics. *Plant Physiology* 158(1): 2–22.

Weigel, D. and Mott, R. (2009), The 1001 genomes project for Arabidopsis thaliana. *Genome biology* 10(5): 107.

Williams, R.W., Gu, J., Qi, S. and Lu, L. (2001), The genetic structure of recombinant inbred mice: high-resolution consensus maps for complex trait analysis. *Genome biology* 2: RESEARCH0046.

Willig, A., Shapiguzov, A., Goldschmidt-Clermont, M. and Rochaix, J.D. (2011), The phosphorylation status of the chloroplast protein kinase STN7 of Arabidopsis affects its turnover. *Plant physiology* 157(4): 2102–7.

Wingler, A., Marès, M. and Pourtau, N. (2004), Spatial patterns and metabolic regulation of photosynthetic parameters during leaf senescence. *New Phytologist* 161: 781–789.

Wintermans, P.C.A., Bakker, P.A.H.M. and Pieterse, C.M.J. (2016), Natural genetic variation in Arabidopsis for responsiveness to plant growth-promoting rhizobacteria. *Plant Molecular Biology* 90(6): 623–634.

Wituszynska, W. and Karpinski, S. (2013), Programmed Cell Death as a Response to High Light, UV and Drought Stress in Plants. *Abiotic Stress - Plant Responses and Applications in Agriculture* .

Wolyn, D.J., Borevitz, J.O., Loudet, O., Schwartz, C., Maloof, J., Ecker, J.R., Berry, C.C. and Chory, J. (2004), Light-response quantitative trait loci identified with composite interval and eXtreme array mapping in Arabidopsis thaliana. *Genetics* 167(2): 907–917.

Woo, N.S., Badger, M.R. and Pogson, B.J. (2008), A rapid, non-invasive procedure for quantitative assessment of drought survival using chlorophyll fluorescence. *Plant methods* 4: 27.

Xu, Y.H., Liu, R., Yan, L., Liu, Z.Q., Jiang, S.C., Shen, Y.Y., Wang, X.F. and Zhang, D.P. (2012), Light-harvesting chlorophyll a/b-binding proteins are required for stomatal response to abscisic acid in Arabidopsis. *Journal of Experimental Botany* 63(3): 1095–1106.

Young, A.J. (1993), *Occurrence and distribution of carotenoids in photosynthesic systems*. Chapman & Hall, London.

Zaks, J., Amarnath, K., Kramer, D.M., Niyogi, K.K. and Fleming, G.R. (2012), A kinetic model of rapidly reversible nonphotochemical quenching. *Proceedings of the National Academy of Sciences* 109(39): 15757–15762.

Zhang, X., Hause, R.J. and Borevitz, J.O. (2012), Natural Genetic Variation for

Growth and Development Revealed by High-Throughput Phenotyping in Arabidopsis thaliana. *G3 (Bethesda, Md.)* 2(1): 29–34.

Zhao, K., Tung, C.W., Eizenga, G.C., Wright, M.H., Ali, M.L., Price, A.H., Norton, G.J., Islam, M.R., Reynolds, A., Mezey, J., McClung, A.M., Bustamante, C.D. and McCouch, S.R. (2011), Genome-wide association mapping reveals a rich genetic architecture of complex traits in Oryza sativa. *Nat Commun* 2: 467.

Zou, F., Gelfond, J.A.L., Airey, D.C., Lu, L., Manly, K.F., Williams, R.W. and Threadgill, D.W. (2005), Quantitative trait locus analysis using recombinant inbred intercrosses: Theoretical and empirical considerations. *Genetics* 170(3): 1299–1311.